Characterization of novel interaction partners of the *Yersinia enterocolitica* effector protein YopM and their role in macrophage cytokine expression

Dissertation zur Erlangung der Würde des Doktorgrades

an der Fakultät für Mathematik, Informatik und Naturwissenschaften

Fachbereich Biologie

der Universität Hamburg

vorgelegt von

Marie Schnapp

Hamburg, 2016

Die vorliegende Arbeit wurde von Januar 2014 bis August 2016 unter Anleitung von Prof. Dr. med. Martin Aepfelbacher am Institut für Medizinische Mikrobiologie, Virologie und Hygiene des Universitätsklinikums Hamburg-Eppendorf erstellt.

Dissertation zur Erlangung des Doktorgrades
im Fachbereich Biologie
der Universität Hamburg
vorgelegt von
Diplom-Biologin Marie Schnapp
aus Bielefeld

Dissertationsgutachter:	Prof. Dr. med. Martin Aepfelbacher
	Prof. Dr. rer. nat. Wolfgang Streit
Disputationsgutachter:	Prof. Dr. med. Martin Aepfelbacher
	Prof. Dr. rer. nat. Wolfgang Streit
	Prof. Dr. rer. nat. Julia Kehr
Tag der Disputation	02.12.2016

II Summary

YopM is one of the most important effector proteins translocated into host cells by pathogenic *Yersinia* spp. *(Y. pestis*, *Y. pseudotuberculosis, Y. enterocolitica*). Previously YopM has been demonstrated to contribute to *Yersinia* virulence by suppressing the host immune response, particularly through modulation of cytokine production. The cellular mechanisms contributing to this phenotype have largely remained unknown. Since YopM enters the nucleus of *Yersinia* infected cells, it has been speculated, that it directly regulates the transcription of cytokines in the nucleus. In this doctoral work this could be confirmed for the YopM from *Yersinia enterocolitica* WA314. Moreover the mechanism could be attributed to YopM's eukaryotic interaction partners. The DEAD-box helicase DDX3 was verified as a novel partner of YopM and identified as its nuclear exporter. YopM not only utilizes the nuclear export function of DDX3 to exit the nucleus, it also uses the DDX3 mediated export to regulate its intranuclear quantities. Intranuclear YopM influenced the nuclear activation state of the ribosomal S6 kinase RSK, which is another eukaryotic interaction partner of YopM. This enhanced RSK phosphorylation in turn stimulated cytokine production e.g. interleukin 10 (IL-10) expression. Within this study also the cooperation of YopM and YopP, another *Yersinia* effector, were analyzed in *Yersinia* infected primary human macrophages. With immunoprecipitation- and pulldown-experiments the interface region of YopM and DDX3 could be ascribed to the N-terminus of DDX3 and the leucin rich repeat region of YopM. Moreover, the data indicated that YopM forms a ternary complex with RSK and DDX3. By employing a CRM1 inhibitor (Leptomycin B (LMB)) or preforming DDX3 knockdown we could abrogate the DDX3/CRM1 mediated nuclear export. Both treatments induced nuclear YopM accumulation and nuclear RSK phosphorylation without altering the RSK distribution in cytosol and nucleus. This indicated that YopM directly influences the phosphorylation of nuclear RSK. RNAseq analysis of *Yersinia* infected human macrophages revealed that YopM upregulates the anti-inflammatory cytokine IL-10 and several other cytokine genes. C-terminal truncated YopM fails to bind to RSK. By employing a mutant *Yersinia* strain translocating a C-terminally truncated version of YopM, it was shown that the interaction of YopM with RSK controls expression of IL-10 and TNF. Based on those findings, we concluded that YopM can influence the gene transcription of different cytokines by its stimulating effect on RSK phosphorylation. Further we assume that the DDX3/CRM1 mediated nuclear shuttling of YopM can fine tune the amount of phosphorylated nuclear RSK and thereby control cytokine transcription. YopP is next to YopM the other *Yersinia* effector, which affects cytokine transcription. With infection experiments the cooperation of YopM and YopP was investigated. In the presence of YopP, YopM acted as an antagonist of YopP, i.e. it upregulated IL-10, IL-6 and IL-1β expression in *Yersinia* infected macrophages. In the absence of YopP, YopM reversed it function and downregulated the expression of IL- 10, IL-6 and IL-1β in the infected macrophages. Thus, YopM appears to cooperate with YopP in modulation of cytokine production by macrophages. Thereby YopM's actions depend on the context of the infection, i.e. whether YopP is active or not.

III Zusammenfassung

YopM ist eines der wichtigsten Effektorproteine, die von pathogenen *Yersinia* spp. (*pestis, pseudotuberculosis*, *enterocolitica*) in die Wirtzelle transloziert werden. Es wird vermutet, dass YopM zur Etablierung der Infektion beiträgt, indem es in die Zytokinproduktion des Wirtes eingreift und dessen natürliche Immunantwort unterdrückt. Die zellulären Mechanismen, die zu diesem Phenotyp führen, sind bis dato weitgehend unbekannt. Durch die nukleäre Lokalisation von YopM wird aber vermutet, dass das Effektorprotein evtl. die Transkription von Zytokinen moduliert. Dieses konnte im Rahmen dieser Arbeit für YopM aus *Y. enterocolitica* WA314 bestätigt werden. Außerdem zeigen unsere Ergebnisse, dass dieser Prozess von YopMs Interaktionspartnern in der Wirtszelle abhängig ist. Die „DEAD-box" Helikase DDX3 wurde als neuer Interaktionspartner von YopM verifiziert und als nukleärer Export-Faktor von YopM identifiziert. Über Immunpräzipitationen und GST-pulldown-Experimente wurde die Interaktion zwischen YopM und DDX3 gezeigt, sowie die Interaktionsdomänen auf den N-terminalen Bereich von DDX3 und die Kernregion von YopM eingrenzt. Weitere Interaktionsstudien verdeutlichten das YopM zusammen mit RSK und DDX3 einen ternären Komplex bildet. Blockierung des DDX3 vermittelten Kernexports führte zu einer Steigerung von nukleären YopM. Gleichzeitig wurde eine gesteigerte Phosphorylierung der ribosomalen S6 Kinase (RSK), einem bekannten Interaktionspartner von YopM, im Kern beobachtet. Diese gesteigerte Phosphorylierung wurde stark vermindert, wenn C-terminal trunkiertes YopM, welches kein RSK mehr bindet, in HEK293 Zellen exprimiert wurde. *Yersinia*-Infektionsversuche, durchgeführt in primären humanen Makrophagen einhergehend mit Transkriptionsanalysen (RT-PCR), zeigten, dass YopM auf transkriptioneller Ebene die Expression des anti-inflammatorischen Zytokins Interleukin 10 (IL-10) stimuliert. Dass die IL-10 Regulation in *Yersinia*-infizierten Makrophagen von der YopM/RSK Interaktion abhängig ist, zeigten Versuche mit einem Stamm, der trunkiertes YopM tranzloziert. RSK fungiert in seiner phosphorylierten Form unter anderem als Transkriptionsaktivator. YopM zeigte einen direkten Einfluss auf die RSK Phosphorylierung im Kern. Vermutlich nutzt YopM den DDX3-abhängigen nukleären-cytoplasmatischen Transfer um über den Phosphorylierungsstatus von RSK die IL-10-Transkription im Wirt zu regulieren. Neben IL-10 modulierte YopM die Transkription weiterer Zytokine wie z.B. TNF, IL-6 und IL-1β. Obwohl diese Regulation nicht immer RSK-abhängig war, scheint YopM im Allgemeinen die Transkription von Zytokinen zu regulieren und damit zu einer erfolgreichen bakteriellen Infektion beizutragen. Neben YopM ist YopP ein weiteres *Yersinia* Effektorprotein, welches bekannt dafür ist, die Immunantwort des Wirtes zu modulieren. Weitere Infektionsversuche mit YopM-, YopP- and YopP/YopM-defizienten *Yersinia*–Stämmen, zeigten in Transkriptionsanalysen das YopP die Transkription vieler Zytokine im Gegensatz zu YopM hemmt. In Abwesenheit von beiden Effektorproteinen wurde dieser antagonistische Effekt zum Teil in einen synergistischen Effekt umgewandelt. Diese Daten verdeutlichen, dass im Kontext einer Infektion nicht nur YopM die Immunantwort des Wirtes moduliert, sondern ein komplexes Zusammenspiel der Effektoren zu einer erfolgreichen Yersinien-Infektion führt.

IV Introduction

1. The genus *Yersinia*

*Yersinia*e are gram- negative, rod-shaped and facultative anaerobe bacteria that belong to the family of *Enterobacteriaceae.* In 1894, Alexandre Yersin and Shibasaburo Kitasato first described the bacterium causing bulbonic and pneumonic plague, later referred to as *Yersinina pestis* (Bibel & Chen 1976). Seventeen *Yersinia* species of the genus had been defined by now, among them the following three human pathogens: *Yersinia pestis* , *Yersinia enterocolitica* and *Yersinia pseudotuberculosis* (Wölke et al. 2011). *Y. pestis*, the causal agent of plague is commonly known to be transmitted from rodents to humans via the rat flea. Today infections are more likely transmitted from the contact of infected or dead rodents and the invasion of the bacteria through a skin injury. Once in the organism, the bacteria manifests in the lymph nodes where it replicates. From there it is able to invade the bloodstream and can reach different organs (Kayser et al. 2001). In rare occasions the infection progresses to pneumonia leading to a person-to-person transmission via droplet infection (Perry & Fetherston 1997). In contrast, *Y. enterocolitica* and *Y.pseudotuberculosis* are foodborne pathogens that can be found in diverse environment, for example ground, soil, plants and insects. Humans get infected through the oral fecal route by ingestion of contaminated food or water. Additionally *Y. enterocolitica* is known to infect mammals such like wildlife and farm animals. Hence, it is not surprising that the frequent outbreaks of *Y. enterocolitica* have had their origin in infected, undercooked pork meat (Bottone 1997; Grahek-Ogden et al. 2007). On contrary the most common reservoirs for *Y. pseudotuberculosis* are carrots and lettuce (Jalava et al. 2006). In general both enteric *Yersinia* species cause yersiniosis with various gut-associated symptoms (e.g., enteritis, ileitis, diarrhea, and mesenteric lymphadenitis). Only in very rare cases they can lead to systemic infections and induce extra-intestinal sequelae like erythema nodosum and reactive arthritis (Koornhof et al. 1999). Once in the intestine *Yersinia* produce adhesins and invasins to attach to and invade M- cells overlaying the Peyer's patches (PP) (Isberg & Barnes 2001; Schulte et al. 2000). From the M-cells the bacteria invade the follicle-associated epithelium (FAE) of the Peyer's patches, which are a part of the gut-associated lymphoid tissue. Mouse infection experiments with *Y. enterocolitica* revealed destruction of, the follicle-associated epithelium and parts of the PP within five to seven days of infection (Autenrieth & Flrschlng 1996). From the PP *Y. enterocolitica* disseminate ,via the lymphatics and blood vessels, in the mesenteric lymph nodes (MSN) and other extra-intestinal tissues like liver and spleen (Cornelis & Wolf-Watz 1997). Within the tissue the bacteria replicates and forms micro-colonies in which they appear to be resistant to phagocytosis by

macrophages and neutrophils. Additionally pathogenic *Yersinia* is able to modulate the immune response of these cells by activating its plasmid encoded virulence machinery comprising of a type three secretion system (TTSS) and several bacterial effector proteins (Yops). The effectors are translocated in the host cytoplasm via the TTSS and each manipulates the host immune response to favor bacterial survival (Viboud & Bliska 2005). The infection routes of the three human pathogenic *Yersinina spp*. are summarized in Figure 1 (Section IV, 1.1.).

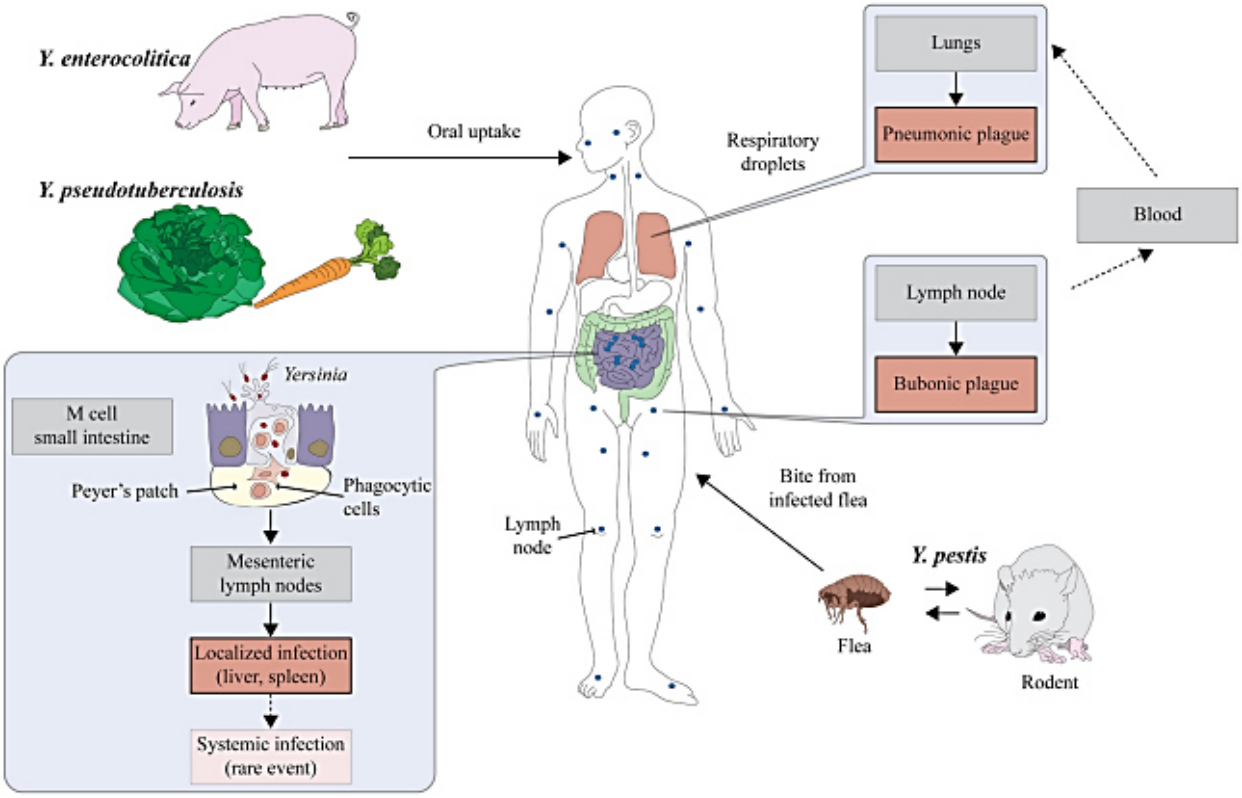

Figure 1: Overview of life-cycle and pathogenesis of the human pathogenic *Yersinia* species.
The enteropathogenic *Yersinia* species *Y.enterocolitica* and *Y.pseudotuberculosis* are associated with meat (mainly pork) and lettuce/vegetables. They are ingested via contaminated food and enter the lymphatic system through the M cells in the small intestine and from there establish infection. The main reservoirs of *Y.pestis* are rodents. Transmission of the bacteria to humans occurs through the bite of an infected flea resulting in bubonic plague. Pneumonic plague is developed when *Y.pestis* reaches the lung and is transmitted via respiratory droplets (Heroven & Dersch 2014)

1.2. Infection strategies of *Yersinia*: chromosomal and plasmid mediated virulence

Yersinia species sustain infection via a repertoire of chromosomal or virulence plasmid (pYV) encoded proteins. Mouse infection experiments with plasmid cured (P-) *Y. enterocolitica*- and *Y. pseudotuberculosis*-strains revealed that genes encoded on the plasmid are not mandatory for the bacterium to attach and invade the host but to establish and sustain the infection. Time course experiments demonstrated that the plasmid cured strains are

diminished after several days of infection whereas the P+ strains replicate within infected tissues (Pujol & Bliska 2005; Viboud & Bliska 2005). Although, the virulence plasmid encoded proteins seem to be mandatory to sustain infection, early studies showed that their expression within the bacteria is not sufficient to cause disease (Heesemann et al. 1984; Heesemann & Laufs 1983). Next to the Yops, the chromosomal encoded virulence proteins are necessary to achieve full virulence. Several of them are adhesins such like invasin and ail (Attachment invasion locus). Adhesins are bacterial outer membrane proteins which act at different times and stages of infection. Their ability to bind a variety of host molecules such as collagen, fibronectin, laminin and β1-integrins make them essential for the bacterial invasion into epithelial cells (Isberg et al. 1987; Clark et al. 1998; Forman et al. 2008; Miller et al. 2001; Miller et al. 1990; Mikula et al. 2012). Especially invasin is crucial to facilitate effective translocation of the bacteria across the epithelial barrier via binding β1-integrins. Next to contributing to the successful bacterial invasion Ail also mediates resistance to complement killing and thereby ensures the survival of intracellular bacteria (Bliska & Falkow 1992). Additionally, its ability to bind collagen contributes to establish symptoms of a systemic *Yersinia spp*. infection such as reactive arthritis and erythema nodosum (Cover & Aber 1989). Both ail and invasin expression is temperature sensitive regulated. Whereas ail was shown to be preferentially expressed at 30 to 37°C (Pierson & Falkow 1993; Bliska & Falkow 1992), the invasin expression is limited at high temperatures (Simonet & Falkow 1992) and regulated by the chromosomally encoded transcriptional regulator rovA (Revell & Miller 2000). RovA mutant strains showed an reduced inflammatory response when colonizing the PP and showed defects in the ability to colonize the MLN (Revell & Miller 2001). Besides adhesins and their regulators the *Yersinia* chromosome harbors genes encoding the Yst toxin, the gene set encoding flagellum-proteins (Straley & Perry 1995) and the High Pathogenicity Island (HPI). The latter mentioned HPI is mostly found in the highly infectious strains and encodes an iron- uptake system essential for systemic *Yersinia* infection (Heesemann et al., 1993; Carniel et al. 1996). Both chromosomal and pYV encoded proteins have an additive effect in establishing *Yersinia* virulence. Both chromosomal encoded invasin and the virulence plasmid encoded adhesin YadA for example are critical for colonization of the Peyer's patches after oral inoculation for both enteric *Yersinia* species (Pepe et al. 1995; Marra & Isberg 1997; Heise & Dersch 2006). All known adhesins of *Yersinia* spp., whether chromosomal or plasmid encoded, help to establish a tight cell contact between bacteria and host cell. Upon this contact pYV encoded proteins are expressed. The type three secretion system (TTSS) assembles and the different *Yersinia* effector proteins (Yops) are translocated in the host cell to interfere with the host immune response (Michiels & Cornelis 1991; Bliska et al. 1993; Straley et al. 1993; Mota & Cornelis

2005; Felek & Krukonis 2008; Tsang et al. 2010; Tsang et al. 2013; Mikula et al. 2012; Paczosa et al. 2014). The TTSS is a multiprotein complex, which is structural and evolutionary similar to the flagellum. Its basal body punctures the two gram negative bacterial membranes and encompasses several proteins. This multiprotein complex creates the basis to build the needle. The needle can have a length up to 600 Å (60 nm) and is the building bridge between bacteria and host cell. A schematic overview of the TTSS is depicted in Figure 2 (Section IV, 1.2). Through the needle structure the six *Yersinia* effector proteins (YopT, YopE, YopO, YopH, YopP, YopM) are injected into the host cell cytoplasm. Before effector translocation, YopB and YopD introduce pores into the cell membrane of the host (Dewoody et al. 2013). Once in the host, the effectors manipulate signaling to maintain bacterial survival. It was shown that the Yop-TTSS-system functions to counteract several key innate defense mechanisms of phagocytes, which ultimately delays development of an adaptive immune response (Brubaker 2003; G. R. Cornelis 2002). The concreate manipulations induced by the individual effector will be described in the following.

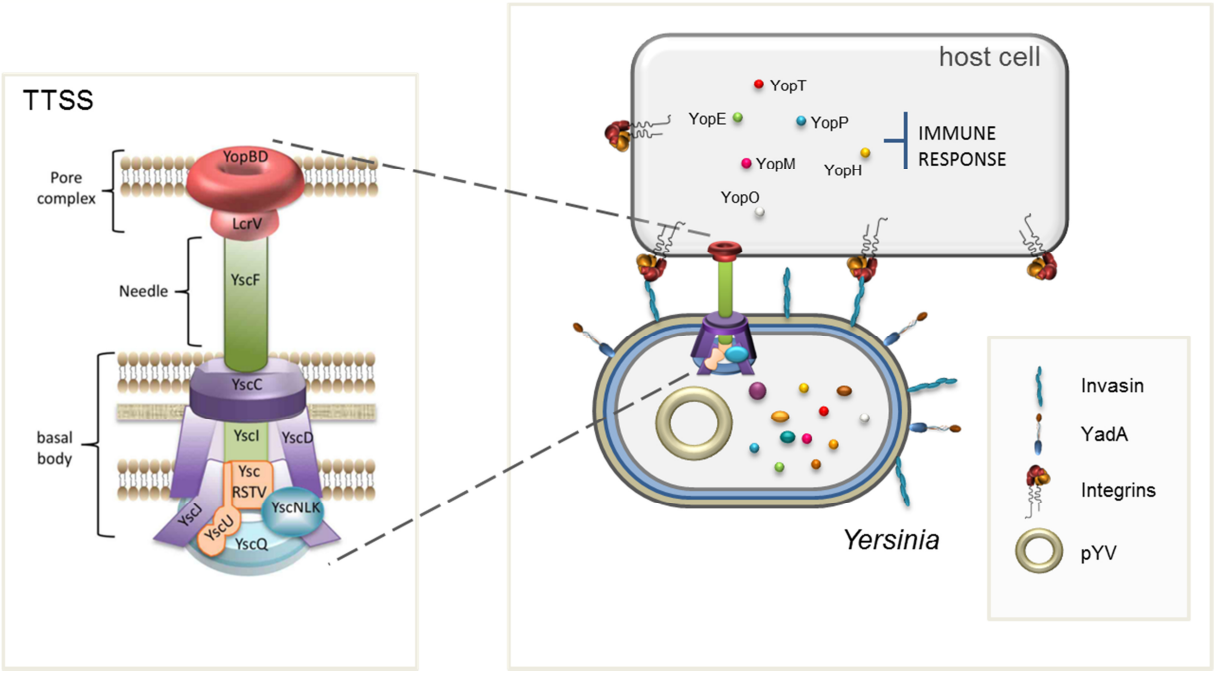

Figure 2: The Yop-TTSS system.
Bacterial Invasin binds to the eukaryotic β1- integrins to achieve host cell contact. Upon cell contact the *Yersinia* virulence piasmid (pYV) encoded adhesin YadA and the proteins for the Type three secretion system (TTSS) as well as the *Yersinia* outer proteins (Yops) are expressed. In the following assembly of the needle structure takes place. Proteins building the basal body, the needle and the pore are indicated in the shematic overview of the TTSS (left) (Dewoody et al. 2013). Through the needle and the pore the Yops are now translocated in the host cell cytoplasm (right). Within the host the different Yops manipulate the host immune system to sustain bacterial survival.

1.3. The *Yersinia* effector proteins (Yops) and their mechanisms to manipulate the host to establish and sustain infection

The six translocated immunoregulatory effectors of *Y. enterocolitica* are: YopT, YopE, YopO, YopH, YopP and YopM. In the following their structural features and their physiological functions within *Yersinia* infected cells are summarized.

1.3.1. YopE, YopT and YopO

The three effectors YopE, YopT and YopO belong to a family of bacterial toxins that target Rho GTPases (Barbieri et al. 2002). Rho GTPases itself are small regulatory GTP binding proteins that control rearranging of the cytoskeleton. The most studied GTPases are RhoA, Rac1, and Cdc42. RhoA influences stress fiber formation, Rac1 the structure of lamellopodia and Cdc42 of filopodia (Viboud & Bliska 2005). Furthermore Rho GTPases were shown to influence cell polarity, microtubule dynamics, membrane transport pathways and transcription factor activity (Etienne-Manneville & Hall 2002). Rho GTPase activity is controlled by the GDP-GTP exchange which is promoted by guanine nucleotide exchange factors (GEF). Whereas GTPase activating proteins (GAPs) promote the hydrolysis from GTP to GDP and results in the inactive GDP bound state of Rho GTPases. GDP dissociation inhibitors (GDIs) are a third group of Rho GTPase manipulators. They inhibit the binding of Rho GTPases to the cell membrane. YopE, YopO and YopT function in a similar manner as Rho GTPase manipulators in order to sustain bacterial survival in the host.

- **YopE**

YopE functions as a GAP. Despite sequence homology it is structural similar to eukaryotic GAPs and therefore is able to inactivate Rho-GTPases by hydrolyzing GTP to GDP (Black & Bliska 2000; Von Pawel-Rammingen et al. 2000; Andor et al. 2001; Scheffzek et al. 1998; Evdokimov et al. 2002; Roppenser et al. 2009). The Rho GTPase inactivation leads to rearranging of the cytoskeleton and results in minimized phagocytosis of the *Yersiniae* (Aepfelbacher & Heesemann 2001). Next to rearranging the cytoskeleton YopE was found to inhibit caspase-1,which plays a role in inflammasome reassembly and is involved in IL-1β production (Schotte et al. 2004). By repressing the production of the proinflammatory cytokine IL-1β, YopE manipulates the initiate and adaptive immune response of the host additionally to prevent phagocytosis.

- **YopT**

YopT from *Y. enterocolitica* is a Cysteinprotease, which preferentially binds GTPases such like RhoA, Rac1 and CDC42 and functions like a GDI. The protein cleaves the Geranylgeranyl-cysteine residue which anchors the GTPases to the membrane (Shao et al.

2002; Shao et al. 2003). Abrogation of the connection between GTPase and the membrane leads to deactivation of GTPases and thereby prevents phagocytosis of *Yersinia* by macrophages or neutrophils (Grosdent et al. 2002; Zumbihl et al. 1999). Further, YopT is able to reorganize the actin cytoskeleton at the phagocytic cup and podosomal adhesion structures, resulting in disordered chemotaxis of macrophages, which in consequence are not able to sense the bacteria (Aepfelbacher 2004).

- **YopO**

YopO is a multi-domain protein with an N-terminal serine/threonine kinase and a C-terminal GTPase interaction site. The N-terminal domain is important for the secretion of the protein via the TTSS and facilitates binding to the cell membrane (Dukuzumuremyi et al. 2000; Galyov et al. 1993; Håkansson et al. 1996). The C-terminal GTPase interaction site additionally interacts with actin (Juris et al. 2000; Dukuzumuremyi et al. 2000). YpkA, the equivalent of YopO in *Y. pseudotuberculosis,* was shown to be first activated when translocated in the host and bound to actin. In YopO from *Y. enterocolitica* two separate G-actin binding sites, one as well in the N-terminal kinase region and one in the C-terminal guanine nucleotide dissociation inhibitor-like region (aa, aa 441-729), were identified and shown to be mandatory for its activation (Trasak et al. 2007). Once activated auto-phosphorylation of YopO takes place and results in phosphorylation of substrates such as myelin basic protein (MBP) and histones which leads to rounding of the infected cells (Trasak et al. 2007; Juris et al. 2000). Further YopO is shown to inhibit the YadA-dependent phagocytosis of *Yersinia* spp. (Trasak et al. 2007). Morover *Yersinia* protein kinase A (YpKA), the YopO homologue in *Y. pseudotuberculosis*, is described to prevent stress fiber formation in cells by its interference with the GDP/GTP exchange (Prehna et al. 2006; Dukuzumuremyi et al. 2000; Barz et al. 2000). Next to modifications of the cytoskeleton YopO is suspected to contribute to the lethality of *Y. pestis* by causing the extensive bleeding observed in *Y. pestis* infected patients. The kinase domain of YopO was found to inhibit Gαq-signaling whose silencing causes intensified bleeding and defects in thrombocyte activating (Laskowski-Arce & Orth 2007).

1.3.2. YopH: A Protein Tyrosine Phosphatase

The 50kDA protein YopH is one of the most potent tyrosine phosphatases known (Guan & Dixon 1990; Phan et al. 2003; Sun et al. 2003). In neutrophils YopH blocks Ca^{2+} signaling and thereby abrogates degranulation, which consequently leads to bacterial survival (Persson et al. 1999). To sustain bacterial infection YopH also blocks immediate recognition of the host cell by antagonizing the signaling cascade induced in the host when bacteria bind to the β1-integrin receptors via invasin. In this process YopH is primarily found to

dephosphorylate proteins of the focal adhesion complex. Such like p130Cas, focal adhesion kinase (Fak), Paxillin, Fyn-binding protein (FyB) and SKAP-HOM (Guy R. Cornelis 2002; Viboud & Bliska 2005; Aepfelbacher 2004). Dephosphorylating of p130Cas by YopH for example results in inhibition of phagocytose by detachment of actin structures including the focal adhesion (Evdokimov et al. 2001; Andersson et al. 1996). Moreover YopH is found to prevent T-cell activation (Yao et al. 1999), the production of the chemoattractant protein 1 produced by macrophages (Sauvonnet, Lambermont, et al. 2002) and T-cell activation (Sauvonnet, Garcia-sanz, et al. 2002).

1.3.3. YopP/ YopJ: A Acetyltransferase that inhibits MAPK- and NF-κB- signaling pathways

YopP (*Y. enterocolitica*) /YopJ (*Y pestis, Y. pseudotuberculosis*) is a 33 kDa protein, which potent inhibits the mitogen activated protein kinase (MAPK) pathway and the NF-κB signaling within the host cell (Monack et al. 1997; Ruckdeschel et al. 1997; Schesser et al. 1998; Orth et al. 1999; Denecker et al. 2002). Both signaling cascades lead to production of pro-inflammatory cytokines, i.e. tumor necrosis factor alpha (TNF-α) (in macrophages), interleukin 8 (IL-8) (epithelial and endothelial cells) and interleukin 6 (IL-6) (endothelial cells). Interference of YopP with the NF-κB (nuclear factor kappa-light-chain-enhancer of activated B-cells) activating IKK (inhibitor of nuclear factor kappa-B kinase)-complex and other activators of the MAPK pathway mediate repression of the mentioned cytokines (Monack et al. 1997; Ruckdeschel et al. 1997; Schesser et al. 1998; Orth et al. 1999; Denecker et al. 2002). Based on the finding that overexpression of YopJ enriches de-ubiquitination und de-sumolation (Orth et al. 2000; Viboud & Bliska 2005), it at first was assumed that YopP/YopJ might act as a cysteine protease, which silences signaling complexes that are associated with MAPK and NF-κB activation by de-ubiquitination (Orth et al. 2000). However, more recent studies provide evidence that YopP rather acts as an acetyltransferase. The transfer of acetyl-residues to serine or threonine of IKK-β and MAPKKs block the phospho-mediated activation and thereby the production of pro-inflammatory cytokines (Mittal et al. 2006; Mukherjee et al. 2006, Trosky et al. 2008). Additionally YopP effectively triggers apoptosis to maintain bacterial infection. The initiation of apoptosis by *Yersinia* infection specifically involves TLR4 (toll like receptor 4) signaling. Experiments with murine macrophages defective for MyD88 (Myeloid differentiation primary response gene 88) or TRIF (Toll/IL-1R domain-containing adapter inducing interferon-β) revealed that TRIF, but not MyD88, is manipulated by the bacteria to induce apoptosis. Next to apoptosis this YopP mediated manipulation can also provide protection against *Yersinia*-mediated cell death (Ruckdeschel et al. 2001; Sing et al. 2005; Reithmeier-Rost et al. 2007; Pouliot et al. 2007; Auerbuch & Isberg 2007; Zhang et al. 2005; Ruckdeschel et al. 2004) .

1.3.4. YopM: A leucine rich repeat protein which greatly contributes to the virulence of pathogenic *Yersinia* spp.

YopM is a leucine rich protein which isoforms are variable in size (Guy R Cornelis 2002). The size differences are caused by the varying numbers of leucine-rich-repeats (LRRs). The YopM of *Yersina pseudotuberculosis* YPIII pIB1 for example harbors 15 LRRs (~46 kDa) (McCoy et al. 2010) similar to the YopM of *Y. pestis* KIM5 (46.2-kDa) (Kerschen et al. 2004). In contrast to these YopM from *Y. enterocolitica* WA314 (type 0:8) possesses 5 additional LRRs resulting in a higher molecular weight (~57 kDa) (Oberhettinger et al. 2011). Next to structural characteristics not much is known about YopMs physiological functions. Mouse infection experiments with pathogenic *Yersinia* clearly revealed a major role of YopM in maintaining virulence but the cellular mechanisms contributing to this phenotype are still largely unknown (Leung et al. 1990). In contrast to all others previously described translocated *Yersinia* effectors (YopE, YopT, YopO, YopH, YopP*)* no cellular function could be assigned to YopM so far. In the following the structural features and known physiological properties of YopM from*Y. enterocolitica* and *Y.pestis* will be described more detailed.

1.3.4.1. Structural features of YopM

YopM from *Y. pestis* 195/P was the first YopM crystallized. The structural analysis revealed a flat horseshoe like structure formed by 15 tandem copies of leucine-rich repeats residues (a G. Evdokimov et al. 2001; a G. Evdokimov et al. 2000). In general, LRRs are highly conserved structures. The N-terminus consist of two alpha helices, which are supposed to be important for the right assembly of the LRRs (Kobe & Deisenhofer 1995). The alpha helical structure is followed by the conserved LRR region, which comprises of repetitive β-sheet forming the characteristic helical like structure (Bella et al. 2008). C-terminal the LRR proteins are flanked by an unstructured but conserved C-terminus including a capping motif to protect the hydrophobic LRR containing core of the protein (Kobe & Deisenhofer 1995). Functional varieties of LRR containing proteins are mostly caused by binding to various proteins in the cell (Kobe & Deisenhofer 1994). The concave site of the LRR structure was found to be important for binding eukaryotic partners (Uff et al. 2002; Kim et al. 2007). The bacterial LRR protein Internalin of *Listeria monocytogenes* interacts for example with the eukaryontic protein E-Cadherin (Schubert et al. 2002). Additional YopM from *Y. pestis* was shown to associate with α-thrombin through its LRRs 4–9 and 6–9 (Hines et al. 2001; Skrzypek & Straley 1996). YopM from *Y. enterocolitica* WA314 was shown to associate with the DEAD-box helicase 3 (DDX3). Structural analysis of this YopM isoform (aa 34 to 481 enclosing the alpha helices and all 20 LRR) revealed a dimer in solution (Rumm 2014; Berneking et al. 2016). The monomeric structure of *Y. enterocolitica* YopM is highly similar to the structure of the *Yersina pestis* 195/P YopM: When comparing both monomeric structures

an dislocation of 16 Å could be observed in the backbone of *Y. enterocolitica* WA314 YopM (Rumm 2014). Interestingly, the smallest symmetric unit within the crystal of *Y. pestis* YopM was a tetramer comprising of two identical dimers. Each dimer is built by two YopM monomers, which interact via its C-termini. On these C-termini another tail-to-tail dimer connects creating a hollow cylinder (Evdokimov et al. 2001). Strikingly, the complex of *Y. enterocolitica* YopM did not show such a structure in the crystal. Instead one molecule in the asymmetric unit associated with the other via the C-terminal LRR 20 (residues 461-481) through interacting with its internal LRRs 14-17 (residues 342-422). Two of such identical dimers build in fact a tetramer, which forms a hollow structure unlike a cylinder (Berneking et al. 2016; Rumm 2014) (Section IV, 1.3.4.1., Figure 3). The structural differences between YopM from *Y. pestis* and *Y. enterocolitica* are most likely reasoned by the extra LRR of *Y. enterocolitica,* which lead to a different bending of the LRR backbone. The physiological consequences of these different structural features are so far unknown. Moreover nothing is known yet about how YopMs interaction with any of its known eukaryotic binding partners, the ribosomal S6 Kinase (RSK) or Protein Kinase C-Related Kinase (PKN/PRK) (Hentschke et al. 2010; McDonald et al. 2003), is organized on the structural level.

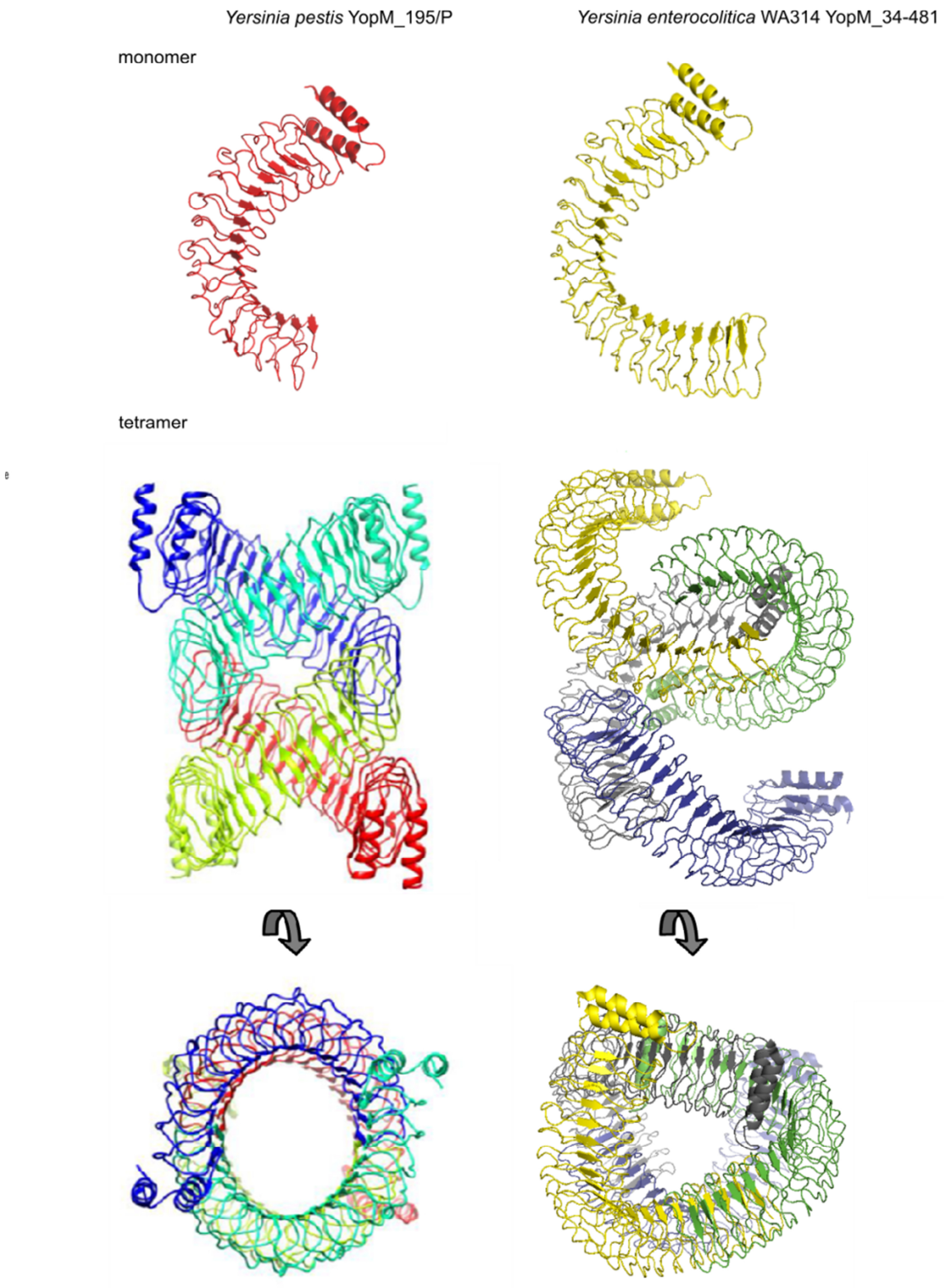

Figure 3: Comparison of YopM from *Y. pestis* 195/P and *Y. enterocolitica* WA314.
Monomeric and tetrameric structure from either YopM_195/P from *Y.pestis* (PDB code 1jl5) (Evdokimov et al. 2001) or YopM_34-418 from *Y. enterocolitica* WA314 (PDB code 4OW2, Rumm 2014; Berneking et al. 2016). Both proteins are illustrated in ribbon representation constructed with PyMol (Schrödinger LLC, USA). The asymmetric unit of *Y.enterocolitica* YopM contains four molecules equivalent to two biological assemblies each represented by a dimer. YopM molecules of one dimer are colored in yellow and green and of the other dimer in light grey and blue. Modified figure from the dissertation of Andreas Rumm (Rumm 2014).

1.3.4.2. Physiological functions of YopM

Mouse experiments with wild type *Y. pestis or* YopM deficient strains clearly indicate that YopM plays a major role in mouse virulence of *Yersiniae* (Leung et al. 1990; Kerschen et al. 2004). Accordingly, it was hypothesized that YopM facilitates its virulence by counteracting against the acute inflammatory response of the host. The mechanisms which contributes to that effect in vivo is subject of extensive research. Within the host YopM was shown to be ubiquitous abundant. Unlike the other translocated effectors proteins, it traffics to the nucleus of infected cells (Skrzypek et al. 1998; Skrzypek et al. 2003; Scharnert et al. 2013; Benabdillah et al. 2004). Neither a clear mechanism for the nuclear import nor the nuclear export could be identified so far. For *Y. pestis* a vesicular mechanism is proposed by which YopM reaches the peripheral region of the nucleus 3-4h post infection (Skrzypek et al. 1998). Additionally LRR 1–3 and the C-terminus of YopM had been demonstrated to act as nuclear signal motifs in yeast. It was shown that the C-terminal domain of YopM has the property to convey a reporter protein to the nucleus of mammalian cells (Benabdillah et al. 2004), although no homologies to known nuclear localization sequences (NLS) could be acknowledged within this C-terminal domain of YopM (Skrzypek et al. 1998). So far no importin could be identified to assist YopM to cross the nuclear envelope. Given the example of the YopM homologue IpaH9.8, a Shigella effector possessing E3 ligase activity, which was shown to migrate in the nucleus dependent on the microtubule network (Toyotome et al. 2001), it is assumed that YopM eventually enters the nucleus by a novel mechanism (Benabdillah et al. 2004). However, nuclear localization of YopM let to the assumption that it might alter gene expression. Nucleotide microarray experiments with *Y. enterocolitica* infected mouse macrophages did not reveal any YopM- regulated genes under stringent statistical criteria (Hoffmann et al. 2004). Another study on transcriptome alterations in *Y. enterocolitica* infected PU5-1.8 mouse macrophages demonstrated that the majority of *Y. enterocolitica* YopM regulated genes are related to cell cycle control and cell growth instead immune regulation. Three genes involved in DNA maintenance were found to be downregulated by YopM as well as transcription factor B-myb which is a cell cycle regulator. Trio and P52rIpk, suspected to regulate cell growth, were also identified to be downregulated by YopM (Sauvonnet, Garcia-sanz, et al. 2002). A more recent study with recombinant purified YopM from *Y. enterocolitica* O8 strain, functioning as a cell penetrating peptide, revealed a significantly mRNA reduction of TNF, IL-12p35, IL-15 and IL-18 in HS60 LPS treated macrophages when incubated with YopM (Rüter et al. 2010; Höfling et al. 2014). In mouse infection experiments similar genes had been found to be downregulated by *Y.pestis* YopM. In addition to TNF, IL-12, IL-15 and IL-18, IL-1β were identified to be YopM depended downregulated whereas no effect could be observed for the *Y. pestis* YopM on IL-4 and IL-10 regulation (Kerschen et al. 2004). This stands in contrast to the YopM dependent upregulation of IL-10 and IL-18, in the sera of mice infected with *Y. pseudotuberculosis*. Next

to upregulation of IL-10 and IL-18, IFN-γ was found to be downregulated by YopM (McPhee et al. 2010). Irrespective of YopM`s characteristic to interfere with the expression and production of immunoregulatory cytokines, YopM is described to interact with the two serine-threonine kinases RSK and PKN. Interaction induces sustained RSK activation by interfering with its dephosphorylation (Hentschke et al. 2010; McDonald et al. 2003). Phosphorylated RSK is proposed to phosphorylate PKN (McDonald et al. 2003): Only in the presence of YopM the ternary complex comprising YopM, RSK and PKN is formed. Since PKN is not a physiological RSK substrate, it can be stated that YopM brings together the two eukaryotic kinases (McDonald et al, Hentschke et al. 2010). So far no in vivo effects resulting from this interaction are known. Mouse infection experiments revealed a RSK and PKN dependent IL-10 regulation (McPhee et al. 2010; McPhee et al. 2012). In contrast transcriptional regulation of TNF-α is induced by YopM independent of the interaction of YopM and RSK (Höfling et al. 2014). A recent study identified caspase-1 as a new interaction partner of YopM. Caspase-1 is attacked by different bacteria to block pyroptosis, an inherently inflammatory program of cell death directed by the activation of caspase-1, within the infected host (Bergsbaken et al. 2009) The host controls the activation of caspase-1 by NOD-like receptors (NLRs) signaling. The cytosolic receptor detects pathogen-associated molecular patterns (PAMPs) and triggers an initiate response to the invading pathogen by forming multi-protein complexes called inflammasomes. This inflammasomes trigger caspase activity and the process of pyroptosis (Saxena & Yeretssian 2014). Caspase-1 activation is typically accompanied by processing caspase-1 into p20 and p10 subunits. It was shown that YopM of *Y. pestis* inhibits the recruitment of procaspase-1 to the NLRP3 (nucleotide-binding domain, leucine-rich-containing family, pyrin domain-containing-3) proinflammasome and thereby inhibits inflammasome assembly (LaRock & Cookson 2012). Moreover active caspase-1 is required to process pro– IL- 1β to IL-1β. Thus, the IL-1β production is diminished in the presence of YopM because of its inhibitory effects on caspase-1 activation (LaRock and Cookson 2012, Chung et al. 2014). One study identified the scaffolding protein IQGAP1 (IQ Motif Containing GTPase Activating Protein 1) as a new interaction partner of *Y.pestis* YopM (Chung et al. 2014). They suggest that IQGAP1 is important for activation of the NLRP3 inflammasome in macrophages during *Yersinia* infection but is dispensable for other NLRP3-dependent stimuli that lead to Caspase-1 activation (Chung et al. 2014). In their proposed model of caspase inhibition via IQGAP they hypothesize that the interaction of YopM and IQGAP1 depends on YopMs interaction with RSK. Our laboratory could exclude a general inhibitory effect of *Y. enterocolitica* YopM on caspase-1 inhibition (Rumm 2014). Known features of YopM´s physiological functions are summarized in Figure 4 (Section IV, 1.3.4.2.).

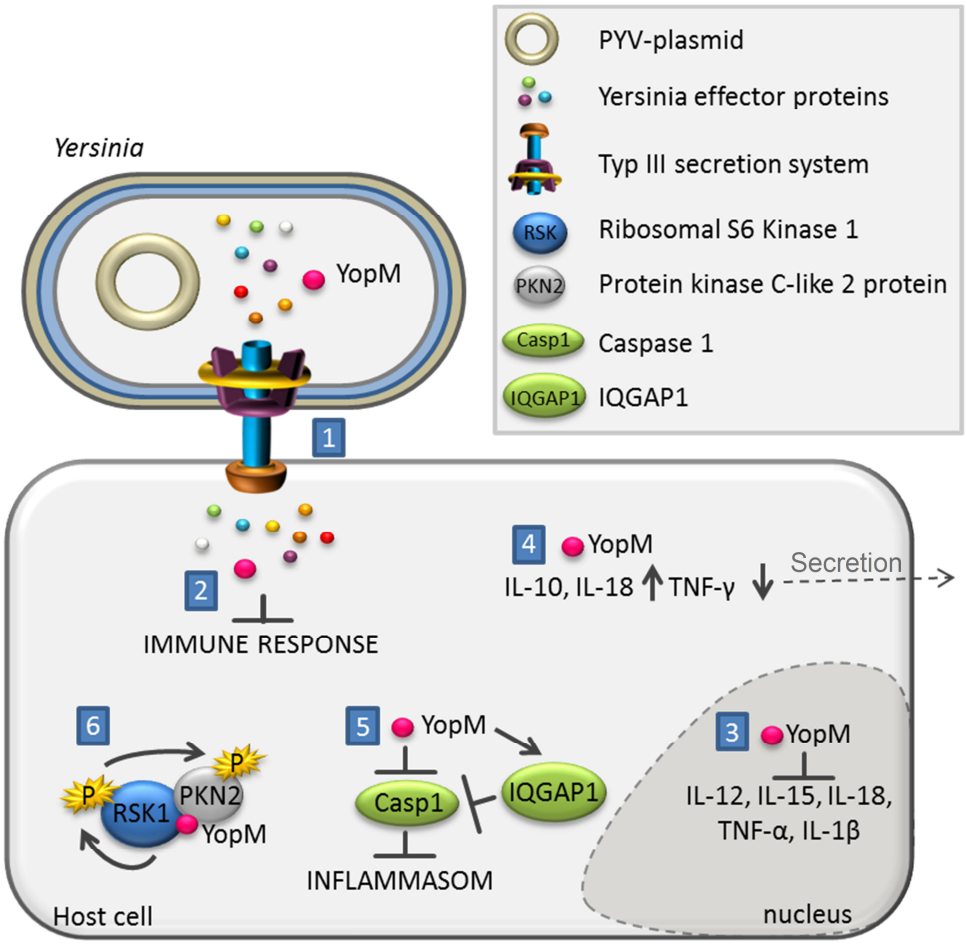

Figure 4: Known features of YopM.
YopM is translocated in the host cell via the type three secretion system (1). The effectors and the proteins for the type three secretion apparatus are encoded on the PYV virulence plasmid of *Yersinia*. Once in the host YopM was shown to contribute to the suppression of its inflammatory response upon infection (2). YopM translocate to the nucleus of cells and mediates gene regulation. YopM decreases the expression of IL-12, IL-15, IL-18 and IL-1β (3). Mouse infection models revealed a YopM dependent upregulation of IL-10 and IL-18, whereas the pro-inflammatory cytokine TNF-γ was found to be downregulated (4). YopM inhibits Caspase 1 via interaction with IQGAP to repress the inflammasome activity and IL-1β secretion (5). Complex formation of YopM with the two cellular kinases RSK and PKN had been shown accompanied by a YopM dependent phosphorylation of both proteins (6).

2. Known interaction partners of YopM

2.1. The ribosomal S6 Kinase (RSK) and its physiological functions

RSK was first discovered in 1985 as intracellular kinase activity which phosphorylates ribosomal protein S6 (Erikson & Maller 1985). Three years later the desired protein kinase, named p90rsk or ribosomal S6 kinase (RSK), could be purified from cellular extracts (Jones et al. 1988). Homologous of the 85–90 kDa kinase could be found in various species such as mouse, chicken, rat, *Drosophila melanogaster* and *C. elegans*. In humans four isoforms exist. Isoform 1-3 are highly expressed in a variety of human tissues (Zeniou et al. 2002).

RSK4 is in contrast to isoform 1-3 lower expressed and restricted to brain, heart, cerebellum, kidney tissue and skeletal muscle in mice (Dümmler et al. 2005). However, the structure of all RSK isoforms is similar. They comprise of two kinase domains which are N- and C-terminal located and connected by a linker region. This structure is enclosed by a short N- and C-terminus. The N-terminal kinase domain (NTKD; aa 68 to 323) is responsible for substrate phosphorylation, whereas the C-terminal kinase domain (CTKD; aa 422 to 675) mediates the auto phosphorylation of RSK. Throughout the molecule six conserved phosphorylation sites were identified. Four of them (Ser-221, Ser-363, Ser-380 and Thr-573) are crucial for RSK activation, whereas no function could be assigned to Thr 359 and Ser 732 (Dalby et al. 1998, Bjørbæk, Zhao, and Moller 1995; Frödin and Gammeltoft 1999). Phosphorylation and thereby activation of RSK is initiated by association of extracellular signal-regulated kinase (ERK). ERK binds to RSK via its C-terminal located docking motif, the so called D-domain (Roux et al. 2003) which appear to fit the KIM (kinase interaction motif) consensus sequence (Romeo et al. 2012). ERK itself is part of the extracellular signal mitogen-activated protein kinase (MAPK) cascade which is activated by growth factors, neurotransmitter and hormones. MAPK cascades are initiated by small GTP binding proteins, for instance Ras (Kyriakis et al 1992). Ras interacts with the adaptor protein Raf, which passes the signal to a MAPK kinase (MAPKK), in this case MEK. Phosphorylated MEK activates ERK and ERK itself triggers the activation of RSK by binding to the mentioned D-domain/KIM (Street & Wt 2006). Next to the MAPK cascade, the Jun kinases and p38 MAPKs can lead to ERK activation. They are activated by extracellular signals related to cellular stress, like UV radiation, reactive oxygen species (ROS), heat shock and TNF-α production. Therefore they are also known as stress activated protein kinases. However, docking of activated ERK leads to phosphorylation of RSK on threonine residue 573 (Thr 573), which leads to activation of the C-terminal kinase domain (CTKD) of RSK. The activated CTKD triggers autophosphorylation of the serine residues 380 within the linker-region of RSK. This autophosphorylation is mandatory to create a docking site for 3′-phosphoinositide-dependent kinase-1 (PDK1), a constitutively active Ser/Thr kinase. PDK1 binding induces phosphorylation of RSK residue serine 221 (Ser 221) within the N- terminal kinase domain (NTKD) and thereby completes RSK activation. Fully activated RSK autophosphorylates serine residue 794 (Ser 794) (Romeo et al. 2012) and several nuclear an cytoplasmic substrates in the cell. The latter mentioned process leads to regulation of diverse cellular processes like cell growth, proliferation, survival, motility translational- and transcriptional regulation (Anjum & Blenis 2008; Schröder et al. 2008; Romeo et al. 2012; Chen et al. 1992). The activation cascade of RSK is summarized in Figure 5 (Section IV, 2.1.). A transcription factor regulated by RSK is the cAMP response element binding protein

(CREB). CREB controls early gene transcription upon its phosphorylation on serine 133 (Ser 133) which is facilitated by RSK (Ginty et al. 1994; Xing et al. 1996). Despite CREB, activated RSK was identified to bind and enhance the function of the transcriptional co-activators CREB-binding protein (CBP) and p300 (Nakajima et al. 1996). By interacting with these two molecules, which regulate complex formation of the transcription machinery, RSK indirect regulates transcription of all genes controlled by the transcription factors that associate with CBP. CBP and p300 associated transcription factors are CREB, FOS, JUN, STAT, MyoD, E2F, NF-κB and steroid receptors (Anjum & Blenis 2008). The family of FOS transcription factors comprises c-Fos, which is stabilized by C-terminal phosphorylation mediated by RSK. Genes involved in inflammatory processes, such as proliferation and apoptosis are suspected to be regulated via RSK by controlling the NF κB transcriptional factor. Activation of NF-κB is dependent on dissociation of IKBα (NF-kappa-B inhibitor alpha). RSK may influence this process by phosphorylating at least one residue within IKBα. Once phosphorylated IKBα is degraded and NF-κB can enter the nucleus where it activates its targets genes e.g. Interferon gamma (INF-γ), interleukins such as IL-1α/β; IL-6, IL-12β and TNF (Ghoda et al. 1997). Next to transcriptional regulation RSK coordinates the translation initiation processes and thereby influences gene expression and protein synthesis. It was found to act upon translation initiation factor eIF4b which is from importance for reassembling the translation initiation machinery (Shahbazian et al. 2006). Post-translational modifications as well as inactivation of pro-apoptotic protein BAD (Bcl-2-associated death promoter protein) are RSK mediated regulations which promote cell survival (Anjum et al. 2005). Thus, RSK is a multiplayer, involved in many fundamental processes, within the cell. Therefore it is not surprising that defects in RSK signaling had been linked to several diseases such as cancer (Clark et al. 2005; Chen et al. 1996) or the Coffin-Lowry syndrome (Yang et al. 2004). Additionally RSK was described to be target of viral manipulation. The vaccina virus HIV-1 and ORF45 of Kaposi's sarcoma-associated herpesvirus were shown to activate RSK to their advantage (Andrade et al. 2004; Hetzer et al. 2007; Kuang et al. 2008).

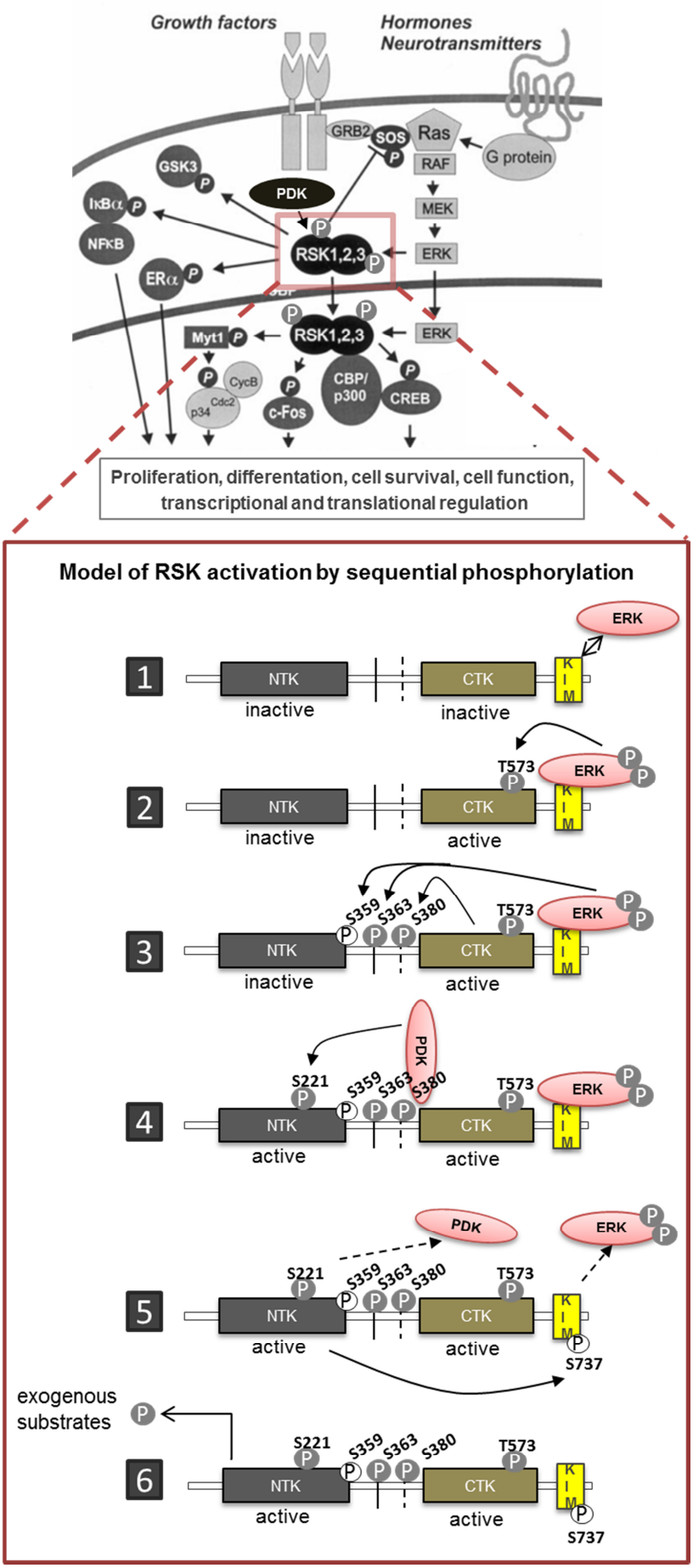

Figure 5: Model of RSK activation by sequential phosphorylation and its role in signal transduction. Celluar cascade which leads to RSK activation within the cell (top). The extracellular kinase ERK is activated via an extracellular signal mitogen-activated protein kinase (MAPK) cascade, which itself is activated by growth factors, neurotransmitter and hormones. Once activated all MAPK cascades have in common that they are initiated by a small GTP binding protein such like Ras in the ERK cascade. From there the signal is transmitted to an adaptor protein, here RAF which passes the signal to the so called MAPK kinase (MAPKK) here MEK. MEK activates the extracellular regulated kinase ERK itself which triggers the activation of RSK by binding to the so called docking domain (D domain/KIM). Docking of activated ERK leads to sequential phosphorylation of RSK. ERK induces phosphorylation of Thr-573, resulting in activation of the C-terminal kinase domain (CTKD), which results in auto-phosphorylation of the Ser-380 within the linker-region of RSK. Thr-359 and Ser-363 within the linker-region might also be phosphorylated by ERK. Nevertheless the auto-phosphorylated RSK on S380 is mandatory to create a docking site for 3′-phosphoinositide-dependent kinase-1 (PDK1), a constitutively active Ser/Thr kinase. PDK1 binding is accompanied with phosphorylation of the Ser-221 within the N-terminal kinase domain (NTK) of RSK and hereby completes activation of RSK. Fully activated RSK was shown to phosphorylate Ser-794 which in some cases results in dislocation of ERK. More importantly, fully activated RSK was shown to phosphorylate several substrates throughout the cell (depicted on the bottom) and thereby regulate diverse cellular processes like cell growth, proliferation survival and motility, translational and transcriptional regulation. The schema is modified from (Frödin & Gammeltoft 1999; Romeo et al. 2012).

2.2. The Protein Kinase C-Related Kinase (PKN/PRK)

In 1984 a protein with serine threonine kinase activity had been detected in cytoplasmic rat liver extracts (Gabrielli et al. 1984). Later it turned out to be the protein kinase C-related kinase (PKN) which cDNA was first cloned in 1994 from a human hippocampal cDNA library (Mukai & Ono 1994). In mammals three different isoforms of these kinases are described: PKNα/PAK1/PRK1, PKNβ, PRK2/PAK2 and PKNγ. All of them are ubiquitous expressed in tissues and throughout cells. Depending on the physiological state of the cell the different PKN isoforms can preferentially localize either in the nucleus or cytosol of the cell. PKNα for example is mainly cytosolic in various cultured cells such as NIH3T3, rat-1, and HeLa cells under normal growing conditions. However, stress such as heat shock or serum deprivation induced nuclear translocation of PKNα (Mukai et al. 1996). Structural analysis of all three isoforms revealed that next to the C-terminal serine /threonine kinase domain, the protein has an antiparallel coiled-coil ACC domain and a C2-like region which are conserved among PKN family members. The ACC domain consists of three homologous stretches which can form an antiparallel coiled-coil fold (ACC finger). That region mediates the binding of PKN to small GTPases like RhoA and other proteins associating with PKN (Maesaki et al. 1999; Takahashi et al. 1999).The C2-like domain is located between the ACC domain and the N-terminal kinase domain and has auto inhibitory functions. Activation of PKN is not fully understood so far. Studies identify a phosphorylation activity of PKN after Rho or Rac binding. One proposed mechanism is that binding of RhoA to the ACC region leads to unmasking of another region which blocks the kinase activity and therefore results in phosphorylation activity of PKN. PKN belongs, like RSK, to the AGC family of kinases, which in general have a functional and a catalytic domain (Pearce et al. 2010). Therefore it is proposed that PKN is Rho dependent activated via phosphoinositide-dependent protein kinase 1 (PDK1). On the other hand PKN modulates the function of its activators (small GTPases and PDK1). GTPase activity and PDK1 function was inhibited or altered in the presence of PKN (Shibata et al. 1996, Mukai 2003). In regards of its known eukaryotic interaction partners, i.e. small GTPases, PKN is suspected to play a role in the re-organization of the cytoskeleton (Vincent & Settleman 1997; Dong et al. 2000) and modulating cell-cell adhesions (Calautti et al. 2002). Expression of active PKN and Rho in 3T3 cells let to transcriptional activation of c-fos serum response element (SRE) (Mukai 2003) indicating that PKN can as well influence gene expression. Next to transcriptional regulation PKN is described to phosphorylate the translation initiation factor eIF4E (Mukai 2003; Lee et al. 2000). Moreover PKN cleavage, catalyzed by caspase-3 or related proteases; was demonstrated to be pro-apoptotic (Takahashi et al. 1998). Thus, PKN is a protein with various functions. Next to its interaction with small GTPases and PDK, all PKN

isoforms had been found in a ternary complex with the bacterial effector protein YopM together with the serine threonine kinase RSK (McDonald et al. 2003; Hentschke et al. 2010). Activation of PKN by RSK upon its own phosphorylation via YopM, was proposed but not proven so far (McDonald et al. 2003).

2.3. The DEAD-box helicase 3 (DDX3)

The DEAD-box helicase three (DDX3) belongs to the family of DEAD-box-RNA helicases, which possess a conserved DEAD (D-E-A-D: Asp-Glu-Ala-Asp) motif, eponymous for the family. In 1997 the two homologue proteins DDX3X (DBX) and DDX3Y (DBY), located on X or Y chromosomes, were first identified and thereafter found to be existent in various species from yeast to human (Lahn and Page, 1997; Park et al., 1998; Kim et al., 2001). Whereas DDX3X is ubiquitous expressed in all tissues, DDX3 expression is restricted to male germline tissue and consequently suspected to play a role in male fertility (Ditton et al. 2004). DDX3X however has been demonstrated to have gene regulatory and cell cycle controlling functions. Moreover it is involved in all aspects of RNA metabolism such as RNA splicing, mRNA export, transcriptional and translational regulation, RNA decay and ribosome biogenesis (Rocak & Linder 2004). This RNA modulating processes facilitated by RNA helicases are mediated by hydrolysis of NTP (ATP, AMP). Corresponding NTP binding motifs are found in a wide variety of helicases and are named Walker A and B motifs (motifs I and II in SF1 and SF2) (Rayment et al. 1996; Walker et al. 1982). Both motifs can be found throughout the DDX3 molecule which in general is composed of two domains (domain one/ domain two) (Caruthers & McKay 2002; Singleton et al. 2007). Within these domains seven conserved sequences are determined additional to the Walker A and B motif to build the conserved helicase core of DDX3: Ia; Ib, III, IV V, Q and VI (Linder 2006). The Q-motif and the Walker A-motifs were shown to be involved in NTP binding whereas III and possibly VI hydrolyze bound NTP. The other four domains (Ia; Ib, IV, V) are involved in RNA and intramolecular interaction. In contrast to the conserved helicase- core are the N- and C-termini of DEAD-box helicases much more divergent and are thought to confer functional specificity of individual DEAD-box helicases (Rocak & Linder 2004). Crystallization of the DDX3 domain 1 and 2 with bound AMP revealed that the individual domains 1 and 2 comprise of five β-strands surrounded by five α-helices (Högbom et al. 2007). A schematic overview of DDX3 and organization of its kinase motifs are given in Figure 6 (Section IV, 2.3.). In vivo DDX3 is known to influence gene expression on all regulatory levels and to thereby direct diverse cellular processes. Its interaction with several transcriptional promotors results in modulation of diverse protein levels. For example decreases DDX3 by promotor interaction the adhesion molecule E-Cadherin (Botlagunta et al. 2008) or enhances INF-β (Soulat et al. 2008). The yeast homolog Ded1b of human DDX3 is suspected to regulate mRNA splicing since it was

found to interact with the spliceosome and export-competent messenger ribonucleoprotein particles (mRNPs) (Schröder 2010). However, involvement of DDX3 in shuttling mature RNA from the nucleus to the cytoplasm was demonstrated for human DDX3. DDX3 itself is known to exit the nucleus via the export protein CRM1 (exportin chromosome region maintenance 1) and the tip associated protein (TAP) (Yedavalli et al. 2004; Schröder et al. 2008). CRM1 exports proteins with nuclear export sequence (NES), whereas TAP mainly transfers RNA from the nucleus to the cytosol. Nevertheless DDX3 and CRM1 association enables HIV to export its spliced/unspliced mRNA in the cytoplasm. The HIV rev protein, which itself binds RNA, associates with DDX3 and exits the nucleus together with DDX3 and CRM1 (Yedavalli et al. 2004). Depletion experiments with TAP resulted in nuclear enrichment of DDX3. This suggests that DDX3 is transferred from the cytosol to the nucleus via the TAP-mediated pathway as well (Lai et al. 2008). In the cytoplasm DDX3 interacts with several translation initiation factors. Association with eiF4E leads to translation of mRNA containing structured 5´ untranslated regions (Lai et al. 2008; Shih et al. 2012; Soto-Rifo et al. 2012). Interaction of DDX3 and eIf3 initiate the assembly of the ribosome and might be the main mechanism by which DDX3 regulates protein translation (Lee et al. 2008; Geissler et al. 2012; Ariumi 2014). Next to gene-regulatory processes, DDX3 is known to regulate cell cycle control, proliferation and apoptosis. Cell cycle arrest is mediated by its interaction with Cyclin D1. E-Cadherin promotor suppression via DDX3 results in increased cell migration and metastasis in breast cancer cells indicating that DDX3 can be a cancerogen (Botlagunta et al. 2008). On the contrary DDX3 was also reported to function as a tumor suppressor e.g. in hepatocellular carcinoma and non-small-cell lung cancer (Chao et al. 2006; Ariumi 2014)Similar to its ambivalent role in tumor genesis, DDX3 can be a suppressor or activator of apoptosis. On one hand it was found to prevent apoptotic signaling by capping dead receptors, on the other hand its association with p53 upon DNA damage results in apoptosis (Sun et al. 2013). DDX3´s diverse roles, in a variety of regulatory processes indicate that it is most likely one of the major a key players within the cell. Accordingly, DDX3 is also known to be a prime target of various viral manipulations. Besides HIV, which exploits DDX3 to shuttle its mRNA out of the nucleus, at least four other different viruses were shown to interfere with DDX3 to abrogate or promote its regulatory function in their favors (Schröder 2010). INF -β production by DDX3 is induced by Toll-like receptors or RIG-like helicases (RLH) receptor activation. Upon activation by viral nucleic acids or RNAs in the cytoplasm of cells both signaling cascades lead to TBK1 (Tank binding kinase 1) and IKKb activation which downstream phosphorylate DDX3. Subsequently, DDX3 phosphorylates IRF3 (Interferon regulatory factor 3), which upon activation and dimerization travels to the nucleus and enhances transcription of NFκ-B regulated genes, including INF-β. The poxvirus K7 was shown to interfere with this

DDX3 mediated activation of IRF3 (Schröder et al. 2008). Besides being targeted to guaranty virus survival DDX3 can function antiviral. It was demonstrated diminish Hepatitis B virus replication (Owsianka and Patel 1999,H. Wang, Kim, and Ryu 2009). Recently also bacterial effector proteins where found to exploit the functions of DDX3. The *Y. enterocolitica* effector protein YopM was identified to interact with DDX3 and to utilize its functions to exit the nucleus. This DDX3 mediated nucleo-cytoplasmatic fine tuning of nuclear YopM is thought to have positive effects on transcriptional regulation of cytokines (Berneking et al. 2016).

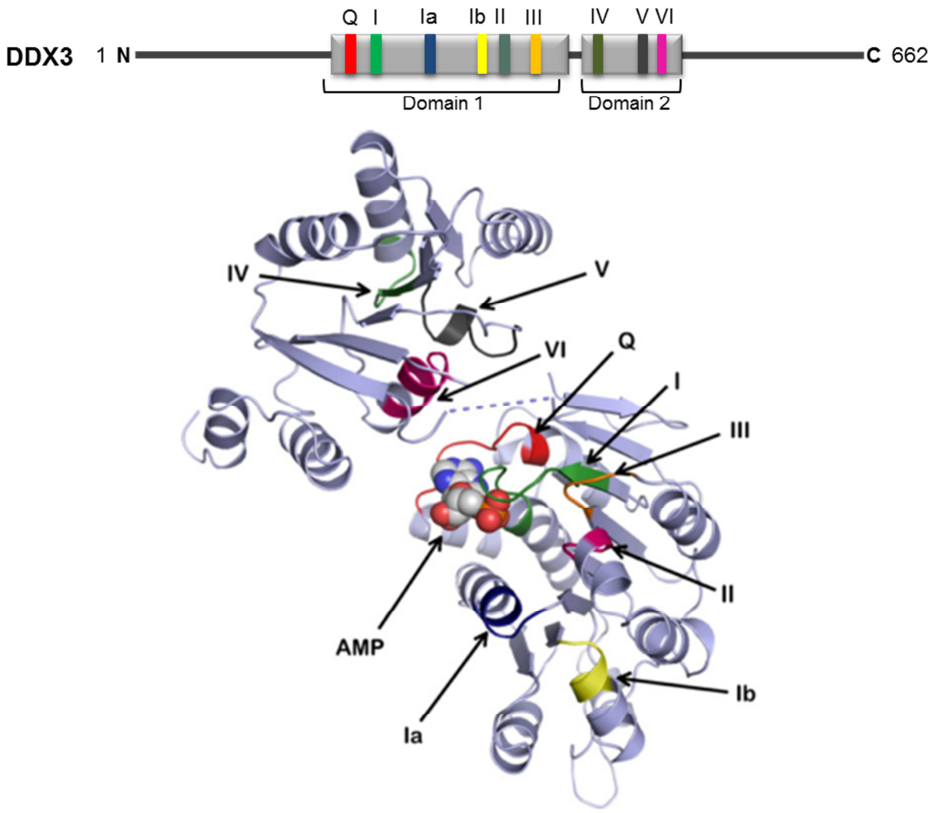

Figure 6: Overall structure of DDX3.
Schematic overview of DDX3 with the two domains and the 9 conserved consensus motifs indicated(modified from Bol, Xie, and Raman 2015) and the structure of the two crystalized DDX3 domains together with AMP in which the 9 motifs are specified as well.The disordered part of the sequence connecting the two domains is represented by a broken line (Högbom et al. 2007):

3. Host immune regulation

3.1. Host immune modulations by the *Yersinia* effectors YopM and YopP/YopJ

The release of cytokines is part of the inflammatory response of cells upon bacterial infection, thus pathogens try to dampen these immediate immune response of the host. Several studies described the importance of tumor necrosis factor alpha (TNF-α), gamma interferon (IFN-γ), and interleukin-12 (IL-12) in *Yersinia* infections (Autenrieth et al. 1994; Autenrieth & Heesemann 1992; Bohn & Autenrieth 1996; Nakajima & Brubaker 1993). Real time PCR (RT-PCR) experiments with a recombinant purified YopM of *Y. enterocolitica* 8081 as a cell penetrating peptide (CPP) demonstrated immunoregulatory properties of YopM as well. The experiments showed that YopM is able to efficiently downregulate the transcription of pro-inflammatory cytokines such as tumor necrosis factor-α (TNF-α) and interleukins (12, 15, 18) in HS60 cells (Höfling et al. 2014 , Rüter et al. 2010). Moreover a YopM dependent increase of the anti-inflammatory cytokine IL-10 had been reported on the transcriptional and translational level in *Yersinia* infected mice or macrophages (McPhee et al. 2012; McPhee et al. 2010; Berneking et al. 2016). Further influencing inflammasome formation and regulating pyroptosis as well as IL-1β and IL-18 production in cells was shown to be one way of *Yersinia* effectors YopM and YopP to sustain infection (Lilo et al. 2008; Philip et al. 2014; Weng et al. 2014, LaRock & Cookson 2012, Chung et al. 2014). Nevertheless neither the mechanisms nor the regulation of all these cytokines targeted by the *Yersinia* effectors are known in detail. One exception is the TNF response, which is mainly regulated by YopP (Nakajima & Brubaker 1993; Ruckdeschel et al. 1997). YopP inhibits the MAPK activation by interfering with ERK1/2, p38 and c-Jun NH_2-terminal kinase (JNK) (Boland & Cornelis 1998; Ruckdeschel et al. 1998). Further YopP interferes with Caspase-8 via RIP kinase to induce cell death and cleaves caspase-1 to regulate immune signaling trough the cytokine IL-1β (Lilo et al. 2008; Philip et al. 2014; Weng et al. 2014). Inhibition of the IL-1β production was recently also attributed to YopM by inhibiting Caspase -1 activity in the host cell by an IQGAP dependent mechanism (LaRock & Cookson 2012) ,Chung et al. 2014). Inhibition of caspase-1 blocks the maturation of IL-1β and IL-18 and the induction of pyroptosis, which is a form of hyper inflammatory programmed cell death to counter bacterial replication and clear infected immune cells (Sahoo et al. 2011; Lamkanfi & Dixit 2011). Although to block this host initiated regulation most likely is important for pathogenic *Yersinia* the ability to interfere with caspase-1 was only demonstrated for the YopM of *Y. pseudotuberculosis* and *pestis* (LaRock & Cookson 2012; Chung et al. 2014) but not for the YopM of *Y. enterocolitica* (Rumm 2014), which indicates that different YopM isoforms might trigger different immune regulations within the infected host. Another example for this is the YopM dependent regulation of IL-10. *Y. enterocolitica or Y. pseudotuberculosis* infected macrophages or mice

revealed a YopM dependent increase of the protein (McPhee et al. 2010; McPhee et al. 2012; Berneking et al. 2016). Transcriptional-analysis on the other hand documented that the IL-10 expression was not regulated by YopM from *Y.pestis* (Kerschen et al. 2004) or *Y. enterocolitica* 8081 (Rüter et al. 2010). Recent studies state an interplay of the most extensive studied factors YopM and YopP in caspase-1 activation (Schoberle et al. 2016; Ratner et al. 2016). YopM and YopJ of *Y. pseudotuberculosis* are able to take over each other's function on caspase-1 activation. Once YopM is lacking YopJ inhibits IL-1β production (Schoberle et al. 2016). *Y. pestis* strains lacking both effectors highly attenuated infection, whereas strains lacking one of the effectors either YopM or YopP are able to induce lethality. The same could be observed for bacterial distribution in liver and spleen of infected mice (Ratner et al. 2016).

3. 2. IL-10 transcriptional regulation: JAK-STAT- and innate immune receptor – signaling

IL-10 and tumor growth factor-β (TGF-β) are the two major anti-inflammatory cytokines known (Gru 2005). IL-10 protein was demonstrated to be upregulated by YopM in *Y. pseudotuberculosis* infected mice (McPhee, Mena, and Bliska 2010, McPhee et al. 2012). RNAseq analysis of *Y enterocolitica* infected macrophages revealed a YopM dependent enhancement of IL-10 transcripts accordingly (Berneking et al. 2016). IL-10 signaling is regulated by the JAK (Janus kinase) -STAT (signal transducer and activator of transcription) pathway, which is known as one of the important signaling pathways downstream of cytokine-receptor interactions (Imada & Leonard 2000; Stark & Darnell 2012). Binding of IL-10 to its membrane-spanning receptors leads to activation of the JAK and STAT. In the case of IL-10, STAT3 is the key activator of transcription (Williams et al. 2004). Upon IL-10 receptor activation the receptor-associated Janus tyrosine kinases, JAK1 and Tyk2, provide a temporary docking site for STAT3. STAT3 binds to that site and is in turn tyrosine-phosphorylated by the receptor-associated JAKs. Phosphorylated STAT3 dimerizes and translocate to the nucleus. Nuclear STAT3-dimers bind to STAT-binding elements (SBE) in the promoters of various IL-10-responsive genes (Donnelly et al. 1999; Yoshimura et al. 2007). One of these genes is the Suppressor of Cytokine Signaling-3 (SOCS3) (Berlato et al. 2002) which was shown to mediate the anti-inflammatory effects of IL-10 in human macrophages by interfering with the Toll-like receptor signaling. SOC3 signaling induces a negative feedback loop and represses expression of NF-κB regulated genes, i.e. TNF, IL-6 and IL-1β (Williams et al. 2004; Berlato et al. 2002; Murray 2006; Jenkins 2014). It was proposed that STAT1 and STAT3 are employed by various cytokines to manipulate Pattern recognition receptors (PRRs). PRR comprise several families of innate immune receptors e.g Toll-like-receptors (TLRs), NOD-like receptors (NLRs), and RIG-I- like receptors (RLRs),

which are known to sensor bacterial/viral DNA in infected host cells by microbial-derived pathogen-associated molecular patterns (PAMPs) to induce inflammatory response. Additionally host-derived endogenous danger-associated molecular patterns (DAMPs) can trigger the inflammatory response (Jenkins 2014). A classical Pathogen –associated molecular pattern (PAMP) is for example LPS, which binds to Toll-like-receptors and induces inflammatory reaction by activating Myd88- (Myeloid differentiation primary response gene 88) dependent and independent signaling cascades. The adaptor proteins Myd88 and TIRAP (Toll-Interleukin-1-Receptor (TIR) Domain Containing Adaptor Protein) mediate signaling via IRAK 1/4 (Interleukin-1 receptor-associated kinase 1/4) to TRAF6 (TNF receptor associated factor), which seem to be important to activate early NF-κB and MAPKs (Sweet & Hume 1996; Akira & Takeda 2004). This signaling cascade also seems to be employed for producing IL-10 upon TLR stimuli. It was shown to result in MAP-kinase activity leading to the activation of its diverse transcription factors and thereby to gene regulation. A schematic overwiev of transcriptional regulation of cytokines and pattern recognition receptors (PRRs) and their influence on each other by autocrine feedback loops are depicted in Figure 7 (Section IV, 3.2.).

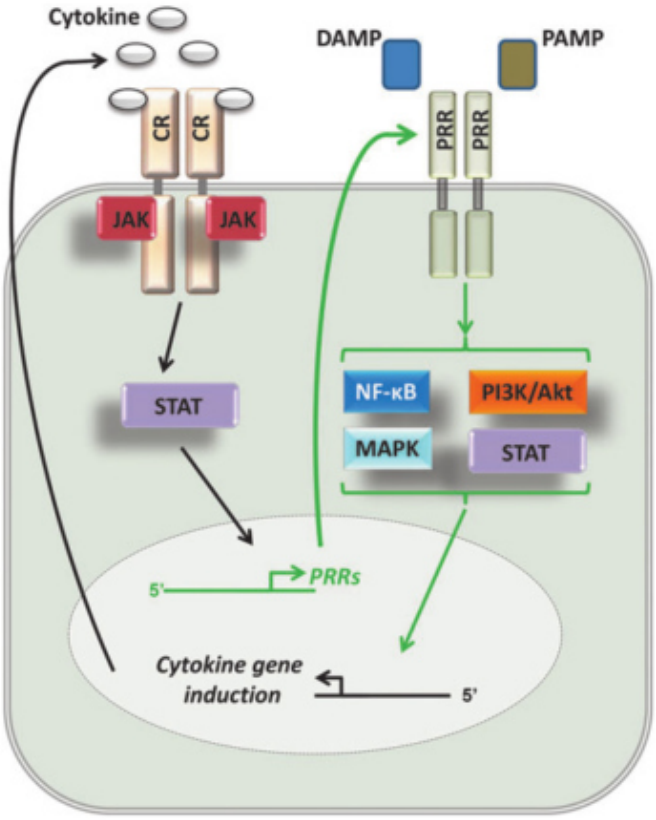

Figure 7: Schematic overview of bi-directional transcription regulation of cytokines and pattern recognition receptors (PRRs).
Upon binding of pathogen-associated molecular patterns (PAMPs) or danger-associated molecular patterns (DAMPs), numerous pattern recognition receptors (PRR) driven signaling cascades are activated. One of it is the nuclear factor-kappaB (NF-κB) transcriptional signaling cascade which leads to the induction of cytokine gene expression (e.g., interleukin-6 family cytokines). Cytokines are then secreted from the cell and bind to their specific cytokine receptors (CR) in an autocrine (shown) or paracrine manner. This for example in the case of IL-10 can lead to activation of the JAK-STAT pathway, which in turn influence PRRs (eg, Toll-like receptors, NOD-like receptors). Green and black arrows depict PRR- and cytokine related events, respectively (Jenkins 2014).

4. Aim of the study

Even though, a lot of attempts had been made to elucidate the mechanisms which contributes to the immunosuppressive role of YopM, it is still unknown. Whereas YopM from *Y. pestis* and Y *pseudotuberculosis* had been shown to interact with caspase 1 (Chung et al. 2014; LaRock & Cookson 2012), experiments performed in our lab with YopM from *Y. enterocolitica* WA314 did not show this inhibitory effect on caspase-1 (Rumm 2014). The outcomes of gene expression analysis, to solve YopM´s line of action, are highly diverse. Depending on the YopM isoform or the techniques used to analyze gene expression, either genes involved in cell growth and cell cycle control were identified or immuneregulatory genes such like TNF and diverse interleukins. The interaction of YopM with RSK and PKN on the contrary has been stated for many YopM isoforms (McDonald et al. 2003; McPhee et al. 2010; Höfling et al. 2014). But so far, this interaction could neither be connected to an in vivo-function of YopM, nor to any downstream-targets from RSK, although YopM was shown to enhance RSK phosphorylation(Hentschke et al. 2010). Thus, YopM is still one of the effectors whose mode of action within the cell remains largely unknown, but is from great interest because it critically contributes to *Yersinia* infection (Leung et al. 1990; Kerschen et al. 2004). With this study, we wanted to better understand YopM´s immuneregulatory role and the cellular mechanisms which contribute to it. For this purpose, we investigated the interaction between YopM with its eukaryontic interaction partners PKN, RSK and DDX3. Thereby we especially focused on the DDX3, which was identified as a new *Y. enterocolitica* interaction partner by Moritz Hentschke. With interaction studies we verified and characterized the biochemical interaction of YopM and DDX3 and studied complex formation together with the other known interaction partner of YopM, RSK and PKN. We further investigated physiological functions of DDX3 which might be manipulated by YopM to draw conclusion towards the in vivo role of YopM.

V Material and Methods

1. Material

1.1. Equipment

Table 1: Equipment

Device	Typ, Manufacturer
Agarose gel electrophoresis	Agarose gel chamber: Roth, Karlsruhe; Germany
Accu -Jet	Accu-jet pro, Brand, Wertheim, Germany
Blotting chamber	OWL Hep-1,Thermo scientifc, Rockford, Ilinois, USA
Centrifuge	Sorvall RC-5B, Thermo Sientific; 5417R and 5810R, Eppendorf, Hamburg, Germany; biofuge pico, Heraeus instruments, Hanau, Germany; Sigma 3-18K, Sigma-Aldrich, St. Louis, Missouri,USA
Cell counting chamber	Neubauer-cell counting chamber, Hartenstein, Würzburg, Germany
Cell culture incubators	CB Series, Binder, Tuttlingen, Germany
Clean bench	Herasafe, Thermo Scientific, Rockford,USA
Developer for X-ray films	Curix 60, Agfa, Mortsel, Beligum
Film Cassette	Hartenstein, Würzburg, Germany
Electoporator	Gene Pulser II electroporator with Puls controller Plus, Biorad
Freezing Container	5100-0001 Cryo 1°C “Mr. Frosty“, Nalgene Scientific, Rockford, USA
Freezer	-80°C: HERA freeze, Heraeus, Kendro Laboratory, Hanau, Germany; -20°C: comfort, Liebherr-International AG, Bulle, Swiss
Fridge	4 -8 °C, Liebherr Premium, Liebherr-International AG, Bulle, Swiss
Microscope	Microscop SZX12 with Kamera DP10 , Olympus, Japan
Microwave	900W, Panasonic, Kadoma/Osaka, Japan
NanoDrop® ND-1000	PeqLab, Erlangen, Germany
pH-Meter	Seven easy, Mettler-Toledo, Giessen, Germany
Photometer	Ultrospec 3100 pro, Amersham/GE healthcare Europe, Munich, Germany
Pipettes	2, 10, 100, 200, 1000 µl, Research Plus, Eppendorf, Hamburg, Germany

Device	Typ, Manufacturer
Power supplies	Biorad power pac universal, Biorad power PC 200, Biorad, Hercules, Californien, USA
Real Time PCR System	Lightcycler 480, Roche Diagnostics, Risch, Swiss
Scanner	CanoScan 4400F, Canon, Amsterdam, Netherland
SDS-PAGE electrophoresis cell	SDS-PAGE: Mini-Protean II Biorad, Munich, Germany
Shaking incubator	Certomat BS-1, Sartorius, Göttingen, Germany
Sonifier	Digital Sonifier 250-D, Branson, Danbury, USA
Thermoblock	DRI-Block DB3 Techne, Bibby Scientific Limited, Staffordshire, UK
Thermocycler	Eppendorf MasterCycler EP S system, Eppendorf, Hamburg, Germany
Transilluminator	Vilber Lourmat, ETX, Eberhardzell, Germany
UV-Transilluminator and Detector	ChemiDoc XRS, Biorad, Hercules,Californien, USA
Vortex	REAX Topo, Heidolph Instruments, Schwabach, Germany
Water bath	Typ 1013, Gesellschaft für Labortechnik, Burgwedel, Germany
Weighing scale	440-47N, Kern, Balingen-Frommern, Germany

1.2. Disposables

Table 2: Disposables

Device	Typ, Manufacturer
A/G Plus-Agarose beads	A/G Plus-Agarose ;Santa Cruz biotechnology, Dallas, Texas, USA
Bottle-top sterile filter units	Vacuum filtration system, capacity 500 ml, pore size 0.2 µm, Nalgene**,** Rochester, NY, USA or Stericup™ filtration system, capacity 1000 ml, pore size 0.22 µl, Merck Millipore, Massachusetts, USA
Calmodulin binding protein	Calmodulin Sepharose 4B, GE healthcare Life Sciences, Little Chalfront, UK
Coverslips	12 mm diameter, round, Hartenstein, Würzburg, Germany
Cell culture dishes	100mm, 150mm, Sarstedt, Nümbrecht, Germany
Cell culture flasks	T-75, Sarstedt, Nümbrecht, Germany

Device	Typ, Manufacturer
Cryo tubes	1.6 ml Sarstedt, Nürnbrecht, Germany
Disposable needles	0.40x 20 mm ,0.55x 25mm, 0.6x 25 mm STERICAN disposable needles, B.Braun, Melsungen Germany
Disposable cuvettes	1.5 ml, 12.5x 12.5x 45mm, BRAND GmbH + CO KG,Wertheim, Germany
Disposable inoculation loop	Sterile , 10 µl,Sarstedt, Nürnbrecht , Germany
Electroporation cuvettes with 1mm Electrode gap	PeqLab Biotechnologie GmbH; Erlangen, Germany
Flag-sepharose	Anti-Flag® M2 Affinity Gel, Sigma Aldrich,St Louis, Missouri, USA
Glass pasteur pipettes	230 mm, Heinz Herenz Medical and Laboratory Supplies, Hamburg, Germany
Gluthathione Sepharose	Gluthathione Sepharose™ 4B, GE Healthcare Life Sciences, Little Chalfront, UK
Multiwell plates	6- / 12-well, Sarstedt, Nümbrecht, Germany
Multiwell plate, 96 wells for RT-PCR	LightCycler 480 Multiwell Plate 96, white, Roche Diagnostics, Risch, Swiss
Object slides	76x 26 mm, Karl Hecht, Sondheim, Germany
Parafilm M	Bemis®, Pechiney Plastic Packaging, Neenah, Wisconsin, USA
Pipette tips	Sterile Biosphere filter tips and non-sterile 10, 200, 1000 µl, Sarstedt, Nümbrecht, Germany
Plastic syringe	sterile, 2 ml, 5 ml, 10 ml, 20 ml, B. Braun, Melsungen, Germany
PVDF Membrane	Immobilion-P, 0,45 µm pore size, Millipore, Billerica, Massachusetts, USA
Reaction tubes	0.2 ml, Biozym Scientific, Hessisch Odendorf, Germany 0.5 ml, 1.5 ml, 2 ml, Sarstedt, Nürnbrecht , Germany 15 ml, 50 ml Centrifuge Tubes, CELLSTAR, Greiner Bio-One, Kremsmuenster, Austria
Scalpels	Sterile, B. Braun, Melsungen , Germany
Serological pipettes	Sterile 2, 5, 10, 25 ml, Sarstedt, Nümbrecht, Germany
Streptavidin binding protein	Streptavidin Sepharose High Performance, GE Healthcare Life Sciences, Little Chalfront, UK
Syringe sterile filters	SFCA 0.2 µm, Thermo Scientific/Nalgene, Rockford, Illinois, USA

Device	Typ, Manufacturer
Whatman filter paper	190 g/m^2, Biorad, Hercules, Californien; USA
X-ray film	Super RX, Fuji medical X-ray film, Fujifilm, Tokyo, Japan
µ MACS Protein A/G beads	MACS, Milteny Biotec GmbH, Bergisch Gladbach, Germany
µ Macs Columns	MACS, Milteny Biotec GmbH, Bergisch Gladbach, Germany
µ Macs Columns separation column 25LE	MACS, Milteny Biotec GmbH, Bergisch Gladbach, Germany
CD 14 Microbeads, human	MACS, Milteny Biotec GmbH, Bergisch Gladbach, Germany

1.3. Kits, enzymes, agents and inhibitors

Table 3: Kits, enzymes and agents

Kit, enzyme, agent	Provider, Manufacturer
Acutase, Enzyme Cell Detachement Medium	eBioscience, San Diego; Califiornia, USA
BioRad Protein Assay	BioRad, Munich, Germany
Digitionin	Sigma-Aldrich, St Louis, USA
DNase, RNase-Free DNase Set	Qiagen, Hilden, Germany
FastAP™ (Alkalische Phosphatase)	Fermentas, St. Leon-Rot, Germany
FastDigest® restriction enzymes	Fermentas, St. Leon-Rot, Germany
Gel extraction and purification kit Nucleo Spin Extract II Kit	Macherey-Nagel, Düren, Germany
iScript cDNA Synthesis Kit	Bio-Rad Hercules, California, USA
Lipofectamine® siMax, RNA transfection agent	Life Technologies, Carlsbad, California, USA
Nucleospin Extract II Kit	Macherey-Nagel, Düren, Germany
5 Prime PCR Extender System	5 Prime, Hamburg, Germany
Plasmid Midi Kit	Qiagen, Hilden, Germany
QIAprep spin Miniprep Kit	Qiagen, Hilden, Germany
RNeasy Mini Kit	Qiagen, Hilden, Germany
SuperSignal West Femto/ Pico detection	Thermo Scientific, Rockford ,USA
T4 DNA Ligase	Roche, Mannheim Germany
TaqMan Fast Advanced Master mix	Applied Biosystems, Carlsbad, California, USA
TaqMan Primer and Probe mix	Life Technologies, Carlsbad, California; USA
Transfection reagent polyethylenimine (pei), linear	Polysience Inc, Pennsylvania, USA

Kit, enzyme, agent	Provider, Manufacturer
Trypsin 0.05 %, 0,53 mM EDTA x 4 Na with phenol red	Invitrogen/Life Technologies
ZR Plasmid Miniprep – Classic Kit	Zymo Research, Irvine, USA

1.4. Inhibitors

Table 4: Inhibitors

Inhibitor	Provider, Manufacturer	Working concentration
Leptomycin B (LMB)	Sigma-Aldrich, Missouri, USA	25 nM
Phosstop (Phosphatase Inhibitor)	Roche Diagnostics, Risch, Swiss	1x
Complete (Protease inhibitor)	Roche Diagnostics, Risch, Swiss	1x

1.5. Growth media, additives, antibiotics

Media were sterilized by autoclaving for 20 min, 121 °C, and 1.4 bar. Supplements, which could not be autoclaved, were sterile filtered.

Table 5: Bacterial growth medium

Media	Composition	
LB-Medium (*lysogenic broth*), pH 7.5		
	10 g/l	Tryptone
	5 g/l	Yeast extract
	5 g/l	NaCl
		ad 1000 ml H_2O
Super Optimal broth with Catabolite repression (SOC)		
	20 g/l	Tryptone
	5 g/l	Yeast extract
	0.5 g/l	NaCl
	0.186 g /l	KCl
		ad 1000 ml ddH_20 adjust to pH 7, autoclave separately afterwards supplement with
	$MgCl_2$ (end concentration 20 Mm, sterile filtered)	
	Glucose (end concentration 20 mM, sterile filtered)	

Table 6: Cell culture medium and additives

Product	Additives		Provider, Manufacturer
Dulbeco's Modified Eagle Medium (DMEM) +Glutamax			Gibco, Carlsbad, Californien, USA
	10 % (v/v)	Fetal calf serum (FCS)	Gibco, Carlsbad, USA

Product	Additives		Provider, Manufacturer
	1 % (v/v)	Penicillin/Streptomycin	Gibco, Carlsbad,USA
Roswell Park Memorial Institute (RPMI) Medium 1640 + Glutamax			Gibco, Carlsbad,USA
	10 % (v/v)	Fetal calf serum (FCS)	Gibco, Carlsbad,USA
	1 % (v/v)	Penicillin/Streptomycin	Gibco, Carlsbad,USA
RPMI Medium 1640 + Glutamax for cultivation of Human peripheral blood monocytes			Gibco, Carlsbad,USA
	20 % (v/v)	autologous serum	
	1 % (v/v)	Penicillin/Streptomycin	Gibco, Carlsbad,USA

Table 7: Antibiotics for selection

Antibiotics	Dissolvent	Working concentration	Provider, Manufacturer
Ampicillin	ddH_2O	100 µg/ml	Sigma-Aldrich, St. Louis, USA
Kanamycin	ddH_2O	50 µg/ml	Sigma-Aldrich, St. Louis, USA
Chloramphenicol	EtOH	20 µg/ml	Roth, Karlsruhe, Germany
Gentamycin	ddH_2O	100 µg/ml	Roth, Karlsruhe, Germany
Nalidixic acid	1M NaOH	100 µg/ml	Sigma-Aldrich, St. Louis, USA
Spectinomycin	ddH_2O	50 µg/ml	Sigma-Aldrich, St. Louis, USA

1.6. Chemicals and buffers

Chemicals were obtained from Amersham/GE Healthcare, Munich (Germany), BD Biosciences, Heidelberg (Germany), Invitrogen/Life Technologies, Carlsbad (USA), Roche, Mannheim (Germany), Biozyme, Oldendorf (Germany), Dianova, Hamburg (Germany), Fermentas, St. Leon-Rot (Germany), Merck, Darmstadt (Germany), PAA, Pasching (Austria), PromoCell, Heidelberg (Germany), Roth, Karlsruhe (Germany) and Sigma-Aldrich, St. Louis (USA). Buffers were autoclaved for 20 min at 121 °C and 1.4 bar or sterile filtered.

Table 8: Buffer

Buffer	Concentration	Composition
Coomassie staining solution	0.1 % (w/v)	Coomassie Brilliant Blue R-250
	25 % (w/v)	Methanol
	10 % (w/v)	Glacial acetic acid
	ddH_2O	
Coomassie destain solution	25 % (w/v)	Methanol
	10 % (w/v)	Acetic acid
	ddH_2O	
PBS (10x)	137 mM	NaCl
	2.7 mM	KCl

Buffer	Concentration	Composition
	14.4 g	Na_2HPO_4
	2.3 mM	KH_2PO_4
	ddH_2O	adjust to pH 7.4 with NaOH
Cell lysis buffer	1x	PBS supplemented with:
	1 %	TritonX-100
	1x	Complete Protease Inhibitor
	1x	Phosstop Phosphatase Inhibitor
<u>SDS-PAGE</u>		
Resolving buffer	1.5 M	Tris-HCl
	0.1 % (w/v)	SDS
	ddH_2O	adjust to pH 8.8
Stacking buffer	0.5 M	Tris-HCl
	0.1 % (w/v)	SDS
	ddH_2O	adjust to pH 6.8
SDS-PAGE sample buffer (4x)	1 M	Tris
	250 mM	SDS
	20 % (w/v)	Glycerol
	4 %	β-Mercaptoethanol
	0.2 %	Bromphenolblau
	ddH_2O	adjust to pH 6.8
SDS-PAGE running buffer	25 mM	Tris
	192 mM	Glycine
	0.1 % (w/v)	SDS
	ddH_2O	
<u>Western blot</u>		
Blotting buffer	150 mM	Tris
	25 mM	Glycine
	20 % (v/v)	Methanol
	ddH_2O	
TBS (10x)	20 mM	Tris
	150 mM	NaCl
	ddH_2O	adjust to pH7.4
TBS-Tween (TBS-T)	1x	TBS, pH 7.4
	0.3 % (v/v)	Tween20

Buffer	Concentration	Composition
Electrophorese		
TAE (50x)	40 mM	Tris-Acetat pH 8.3
	10 mM	EDTA
	ddH_2O	adjust to pH 7.4
Buffer for preparation of chemical competent bacteria		
TFB1 (4°C)	30 mM	KAc
	50 mM	$MnCl_2$
	100 mM	RbCl
	10 mM	$CaCl_2$
	15 % (w/v)	Glycerol
	ddH_2O	adjust to pH 5.8
TFB2 (4°C)	10 mM	MOPS, pH 7.0
	10 mM	RbCl
	75 mM	$CaCl_2$
	15 % (w/v)	Glycerol
	ddH_2O	adjust to pH 6.8
Buffer for $CaCl_2$ Transfection		
Hepes	0.28 M	NaCl
	0.05 M	Hepes ((4-(2-hydroxyethyl)-1-piperazineethanesulfonic acid)
	1.5 mM	Na_2HPO_4
	ddH_2O	adjust to pH 7.05-7.12 (optimal pH 7.08), sterile filter
$CaCl_2$ Solution for transfection	2.5M	$CaCl_2$ in ddH_2O, sterile filter
Buffer for cell fractination		
Cell Lysis Buffer	1x	TBS, pH 7.4
	1.3%	Digitonin
	1x	Complete Proteaseinhibitor
	1x	Phosstop Phosphataseinhibitor
Nuclear Lysis Buffer	1x	TBS, pH 7.4
	0.5 %	NP-40
	1x	Complete Proteaseinhibitor
	1x	Phosstop Phosphataseinhibitor

1.7. Protein and DNA ladders

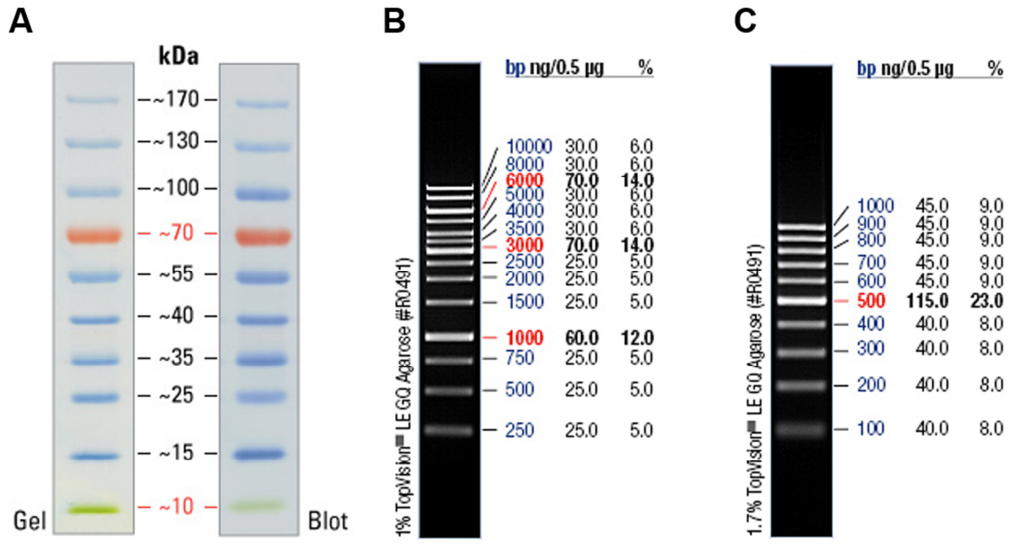

Figure 8: Protein and DNA ladders.
A) PageRuler Prestained Protein Ladder (Thermo Scientific, Rockford, USA). **B)** Quickload 100 bp DNA Ladder (New England Biolabs, Ipswich, USA) C GeneRuler 1 kb DNA Ladder (Thermo Scientific, Rockford, USA).

1.8. siRNA

Table 9 :siRNA sequence

Target	Name	Sequence (5' → 3')	Manufacturer
control	siRNA/siCtrl	Pool of 4 unspecific siRNAs without target gene	Dharmacon, Lafayette, Louisiana, USA
DDX3	siDDX3	ACAUUGAGCUUACUCGUUA	Thermo Scientific, Rockford, Illinois, USA

1.9. Bacterial strains and eukaryotic cells

1.9.1. Bacterial strains

1.9.1.1. *Escherichia coli* strains

Table 10: *Escherichia coli* strains

Strain	Characteristics	Reference
E. coli DH5α	*F-endA1 glnV44 thi-1 recA1 relA1 gyrA96 deoR nupG Φ80dlacZΔM15 Δ(lacZYA-argF)U169, hsdR17 (rK-mK+), λ-*	(Taylor et al. 1993)
E. coli Top10	*F- mcrA Δ(mrr-hsdRMS-mcrBC) Φ80lacZΔ139 Δ(ara-leu)7697 galE15 galK16 rpsL(Str^R) endA1λ$^-$*	(Grant et al. 1990)
E. coli BL21	*F- ompT gal dcm lon hsdSB(rB- mB-) λ*	(Moffatt & Studier 1987)

1.9.1.2. *Yersinia enterocolitica* strains

Table 11: *Y. enterocolitica* strains

Strains	Characteristics	Resistence	Reference
WA314	*Y. enterocolitica* serotype O:8, clinical isolate, pYVO8+,	Nal	(Heesemann & Laufs 1983)
WA-C	Plasmidless derivate of WA314	Nal	(Heesemann & Laufs 1983)
WA314ΔYopM	Derivative of the *Yersinia* WA314 harbouring the virulence plasmid pYVO8 , in which the YopM gene had been replaced by a kanamycin resistance cassette from pUC4k	Kana	(Trülzsch et al. 2004)
WA314ΔYopP	Derivative of the *Yersinia* WA314 in which the YopP gene was replaced by a Chloramphenicol resistance	Chlor	this study, constructed by the lab of Klaus Ruckdeschel
WA314ΔYopM/YopP	Derivative of the *Yersinia* WA314 which lacks both effector proteins YopM and YopP	Kana, Chlor	this study, constructed by the lab of Klaus Ruckdeschel
WA314ΔYopM(pYopM-SBP-CBP)	WA314ΔYopM strain complemented with the plasmid pACYC184 harboring YopM-SBP-CBP	Kana, Chlor	(Hentschke et al. 2010)
WA314ΔYopM(pYopM)	WA314ΔYopM complemented with YopM in pACYC184	Kana, Chlor	(Trülzsch et al. 2004)
WA314ΔYopE(pYopE-SBP-CBP)	WA314ΔYopE strain complemented with the DNA construct YopE-SBP-CBP in pACYC184		this study, constructed by Bernd Roppenser
WA-C(pTTSS)	Virulence plasmid cured *Y. enterocolitica* strain WA-C harbouring the plasmid pTTSS encoding the TTSS secretion/translocation apparatus of WA314 but no Yop effector genes	Spec	(Heesemann & Laufs 1983; Trülzsch et al. 2003)
WA-C(pTTSS+YopM)	WA-C(pTTSS) complemented with YopM in pACYC184	Spec, Chlor	(Trülzsch et al. 2003)
WA314ΔYopM (pYopM_1-481)	WA314ΔYopM complemented with YopM_1-481 in pACYC184	Kana, Chlor	this study

1.9.2. Eukaryotic cells

Table 12: Eukaryotic cells

Cells	Characteristics	Reference
HEK293	Human Embryonic Kidney 293 (HEK293) cells, the cell line was initiated by the transformation and culturing of normal HEK cells with sheared adenovirus 5 DNA. The transformation resulted in the incorporation of approximately 4.5 kilobases from the viral genome into human chromosome 19 of the HEK cells.	(Graham et al. 1977), ordered from American Type Culture Collection (ATCC), Manassas, Virginia, USA, (ATCC# CRL-11268)
J774A.1	Immortal mouse macrophage cell line J774 derived from a tumour in a female BALB/c mouse.	Ordered from ATCC,VA, USA, (ATCC# TIB-67)
Human peripheral blood monocytes	Isolated monocytes were cultured for 6-9 days until differentiated into macrophages	Self-made isolation (Kopp et al. 2006) from buffy coats, which were provided by Frank Bentzien, University Medical Center Eppendorf, Hamburg, Germany

1.10. Plasmids

1.10.1. Prokaryotic expression plasmids

Plasmids were transformed into electro competent *Yersinia* strains, in this case both plasmids were used to recomplement the *Y. enterocolitica* WA314 strain lacking YopM (WA314ΔYopM). Primers used for amplification are listed inTable 13.

Table 13: Prokaryotic expression constructs

Insert	Vector	Description	Origin
YopM-SBP-CBP	modified pACYC184	YopM without Stop Codon but an additional *NotI* side was cloned in pACYC184. The tandem-affinity-tag containing the Calmodulin-Binding-Peptide (CBP) and the Streptavidin-Binding-Peptide (SBP) were derived from the commercially available pNTAP-vector from the Interplay™ Tandem Affinity Purification system (Stratagene) and modified to be cloned into the pACYC184 vector via the new *Not*I and *Xba*I site. The resulting vector harbored a CBP-SBP C-terminally tagged YopM.	(Hentschke et al. 2010)
YopM-1-481	modified pACYC184 (Hentschke et al. 2010)	YopM_1-481 was first amplified with the primer YopM –F-hind and YopM_481-XHOI-rev from the YopM-SBP- CBP and subcloned into the pCS2+MT vector for amplification in *E.coli*. From there the C-terminal truncated YopM was derived via *HindIII* and *XbaI* and subsequently cloned into the modified pACYC184 YopM-SBP-CBP vector via these restriction sites resulting in a vector expressing C-terminal truncated YopM without SBP-CBP tag.	(Berneking et al. 2016)

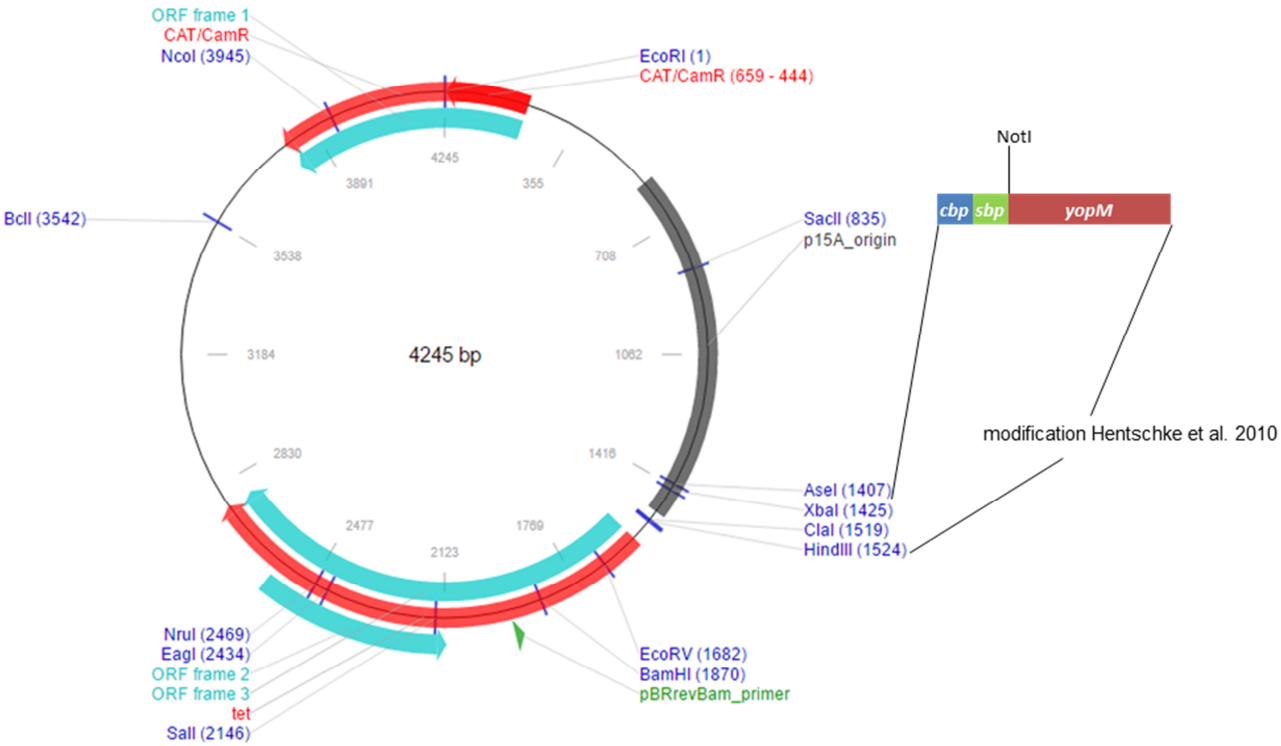

Figure 9: Vectormap of pACYC184 with modifications.
pACYC184 map was derived from the adgene database (https://www.addgene.org/vector-database/1679/) vector modification as described by Moritz Hentschke (Hentschke et al 2010) are indicated.

1.10.2. Eukaryontic expression constructs

Following vectors were transfected in eukaryotic cells to achieve expression of the inserted proteins. For the expression of most proteins either the pCS2+MT (XB-VEC-12442480) or the pCDNA3.1 (+) vector (Invitrogen/Life technologies, Thermo Fisher Scientific, Waltham, USA) was used. For expression in eukaryotic cells, YopM constructs were amplified via PCR from virulence plasmid pYVa127/90 (accession NC_004564.1). HA-DDX3 constructs were amplified from human cDNA (accession NM_001356). Primers used for amplification are listed in Table 15.

Table 14: Eukaryotic expression constructs

Insert	Vector	Description	Origin
myc-YopM	pCS2+MT	YopM was amplified from virulence plasmid pYVa127 with YopM-NCOI-for and YopM-XHOI-rev and cloned into pCS2+MT	(Berneking et al. 2016)
GST-YopM	pEBG-2T vector (Dettori et al. 2009)	YopM was derived from the myc-YopM construct via restriction sites *BamHI* and *NotI* and ligated into the pEBG-2T	(Berneking et al. 2016)
myc-YopM_1-481	pCS2+MT	YopM was amplified from myc-YopM with YopM-NCOI-for and YopM_481-XHOI-rev and cloned via these sides.	(Berneking et al. 2016)

Insert	Vector	Description	Origin
myc-YopM_34-481	pCS2+MT	YopM was amplified from myc-YopM with YopM-34_NCOI-for and YopM_481-XHOI-rev and cloned via these sides.	This study
DDX3_1-662 - flag	pCDNA3.1 +	DDX3 was amplified with DDX3-for and DDX3-flag-BAMHI-rev and cloned via restriction sites *HindIII* and *BamHI*	Berneking et al. 2016)
DDX3-HA	pCDNA3.1 +	DDX3 was amplified with DDX3-HINDIII-for and DDX3_662-HA-BAMHI-rev	Berneking et al. 2016)
DDX3-HA aa418-662	pCDNA3.1 +	DDX3 was amplified with DDX3_418-602-for and DDX3_662-HA-BAMHI-rev and cloned via restriction sites *HindII*I and *BamHI*	Berneking et al. 2016)
DDX3-HA aa1-418	pCDNA3.1 +	DDX3 was amplified with DDX3-HINDIII-for and DDX3_1-418-HA-BAMHIrev cloned via restriction sites *HindIII* and *BamHI*	Berneking et al. 2016)
HA-RSK	pKH3-human RSK1(Addgene plasmid 13841)	HA-tagged RSK1	(Richards et al. 2001)
Flag-PKN	n.d.	Flag-tagged PKN1	(Takahashi et al. 1998)
GFP	pEGFP-C3	GFP expression vector, used as a transfection control	Clontech/Takara, California, USA

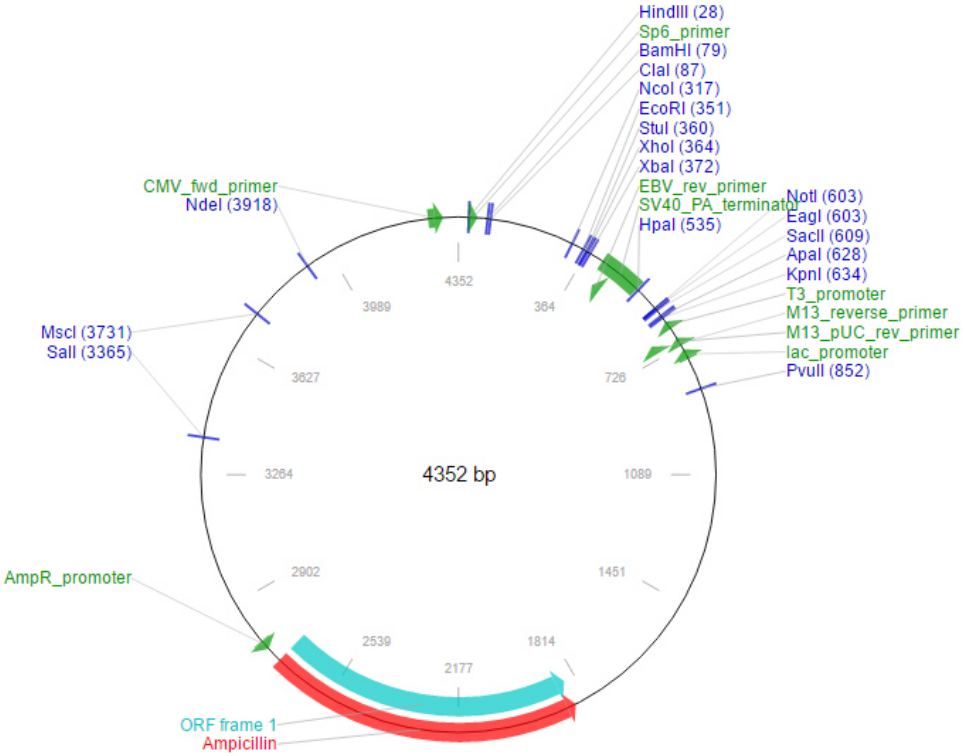

Figure 10: Vector map of pCS2+MT.
The vector map pCS2+MT (CXB-VEC-12442480), was derived from the adgene database (https://www.addgene.org/vector-database/2296/)

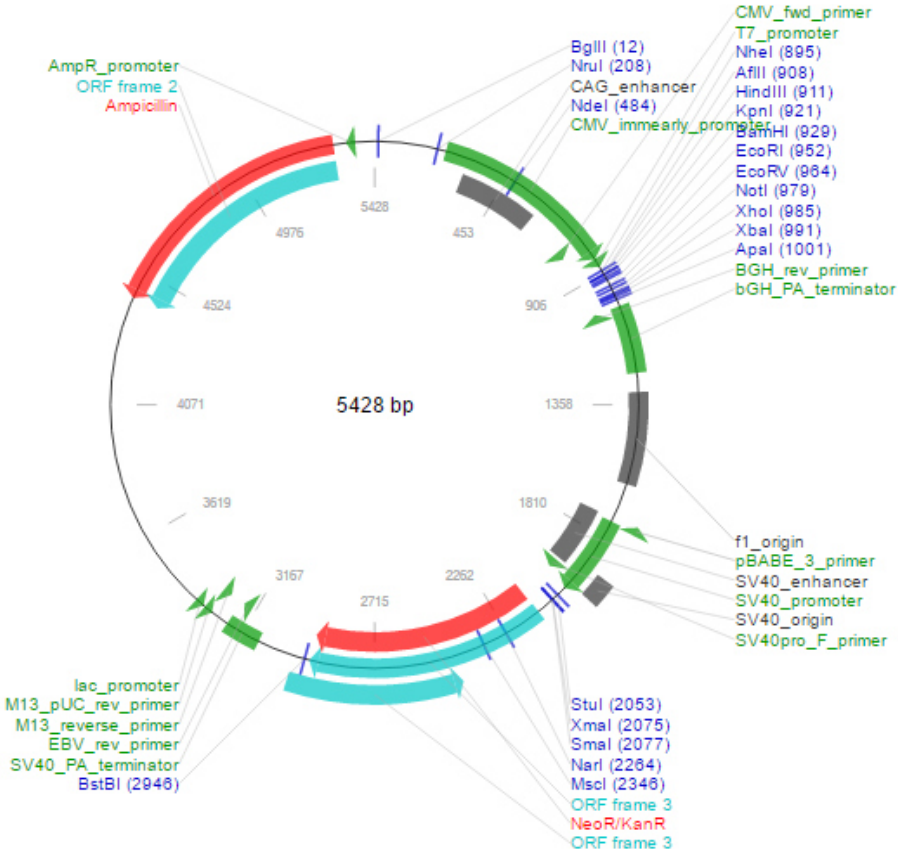

Figure 11: Vector map of pCDNA3.1 (+).
Vector map of pCDNA3.1(+) was derived from the adgene database (https://www.addgene.org/vector-database/2093

1.11. Primer

Table 15: Primer name and sequences

Name	Sequence 5´-3´
YopM –F-hind	GTCAAAGCTTATGTATGGTTTTGTTTGCAATGAA
YopM_481-XHOI-rev	GTCACTCGAGCTAGTCCATCCGAAGATC
YopM-NCOI-for	ACCATGGTTATGTTTATAATCCAAG
YopM-XHOI-rev	GTCAAAGCTTATGTATGGTTTTGTGGTCAATGAA
YopM-34_NCOI-for	ACCATGGTTATGAAATCTAAGACTGAATATTATA
DDX3-for	CAAGCTTACCATGAGTCATGTGGCAGTG
DDX3-HINDIII-for	CAAGCTTATGAGTCATGTGGCAGTGGAAAAT
DDX3-flag-BAMHI-rev	AGGATCCTCACTTATCGTCGTCATCCTTGTAATCCAT GTTACCCCACCAGTCAACC
DDX3_418-602-for	CAAGCTTACCATGGTAGTTTGGGTGGAAGA
DDX3_662-HA-BAMHI-rev	AGGATCCTCAAGCGTAATCTGGAACATCGTATG GGTACATGTTACCCCACCAGTCAACC
DDX3_1-418-HA-BAMHIrev	GGATCCTCAAGCGTAATCTGGAACATCGTATGG GTACATTTTCTGTGTGATGTTTTCAGAGGT

1.12. Antibodies

Rabbit anti-YopE and -anti-YopM polyclonal antiserum was a gift from Jürgen Heesemann (LMU, München, Germany) (Heesemann & Laufs 1983; Jacobi et al. 1998). Rat anti-YopM monoclonal antibody (9552) was produced by employing the YopM gene from *Y. enterocolitica* WA314 and derived YopM recombinant protein as specified recently (Koch-Nolte et al. 2005). Commercially available antibodies used in this study are: Monoclonal mouse anti-DDX3 antibody (Santa Cruz Biotechnology), polyclonal rabbit anti-DDX3 antibody (Bethyl laboratories), monoclonal anti-RSK (C-21) antibody (Santa Cruz Biotechnology), polyclonal goat anti-PKN (C-19) antibody (Santa Cruz Biotechnology), monoclonal rabbit anti-GST antibody (Invitrogen), monoclonal mouse anti-GST antibody(Novus Biologicals, Littleton, USA), monoclonal rabbit Lamin A/C antibody (Cell Signaling), monoclonal mouse anti-flag antibody (Sigma-Aldrich), polyclonal rabbit myc-tag antibody (Cell Signaling), monoclonal rat anti-HA antibody (Santa Cruz Biotechnology),polyclonal rabbit anti-phospho-S380RSK antibody (Cell Signaling), polyclonal rabbit anti-phospho-S221RSK antibody (R&D systems), polyclonal rabbit anti-GAPDH antibody (Sigma-Aldrich), monoclonal mousel anti-actin antibody (Millipore) monoclonal mouse anti-myc antibody (Cell Signaling). Secondary antibodies for Western blot were horseradish peroxidase- linked sheep anti-mouse IgG (GE Healthcare), donkey anti-rabbit IgG F(AB´)2 (Amersham Biosiences), -anti-goat IgG (Santa Cruz Biotechnology) and -anti-rabbit IgG (Cell signaling) and goat anti-rat IgG (GE Healthcare).

Table 16: Antibodies and working concentrations

1st Antibody	Dilutions	Solvent	2nd Antibody	Dilution	Solvent
polyclonal rabbit anti-YopE	1:1000	TBS-T 5% milk	rabbit	1:10000	TBS-T 5% milk
polyclonal rabbit anti YopM	1:3000	TBS-T 5% milk	rabbit	1: 10000	TBS-T 5% milk
monoclonal rat anti-YopM (9552)	1:1000	TBS-T 5% milk	rat	1: 5000	TBS-T 5% milk
monoclonal mouse anti-DDX3 (Santa Cruz)	1:1000	TBS-T 5% milk	mouse	1:10000	TBS-T 5% milk
polyclonal rabbit anti-DDX3 (Bethyl laboratories)	1:1000	TBS-T 5% milk	rabbit	1:10000	TBS-T 5% milk
monoclonal rabbit anti-RSK1(C-21) (Santa Cruz)	1:1000	TBS-T 5% milk	rabbit	1:10000	TBS-T 5% milk
polyclonal goat anti-PKN1 (C-19) (Santa Cruz)	1:1000	TBS-T 5% milk	goat	1:10000 or less	TBS-T 5% milk
monoclonal rabbit anti-GST (Invitrogen)	1:1000	TBS-T 5% milk	rabbit	1:10000	TBS-T 5% milk
monoclonal mouse anti-GST (Novus Biologicals)	1:1000	TBS-T 5% milk	mouse	1:10000	TBS-T 5% milk
monoclonal rabbit anti-Lamin A/C (Cell Signaling)	1:1000	TBS-T 5% milk or TBS-T only	rabbit	1:10000	TBS-T 5% milk or TBS-T only
polyclonal rabbit anti-myc-tag (Cell Signaling)	1:1000	TBS-T 5% milk	rabbit	1:10000	TBS-T 5% milk
monoclonal mouse anti-flag (Sigma-Aldrich)	1:1000	TBS-T 5% milk	mouse	1:10000 or 1:5000	TBS-T 5% milk
monoclonal rat anti-HA (Santa Cruz)	1:1000	TBS-T 5% milk	rat	1: 10000	TBS-T 5% milk
polyclonal rabbit anti-phospho-S380RSK (Cell Signaling)	1:1000	TBS-T 5% milk or TBS-T only	rabbit	1:10000	TBS-T 5% milk or TBS-T only
polyclonal rabbit anti-phospho-S221RSK) (R&D systems)	1:2000	TBS-T 5% milk or TBS-T only	rabbit	1:10000	TBS-T 5% milk or TBS-T only
polyclonal anti-GAPDH (Sigma-Aldrich)	1:2000	TBS-T 5% milk	rabbit	1:10000	TBS-T 5% milk
monoclonal mouse anti-actin (Millipore)	1:2000	TBS-T 5% milk	mouse	1:10000	TBS-T 5% milk
monoclonal mouse anti-myc (Cell Signaling)	1:2000	TBS-T 5% milk	mouse	1:10000	TBS-T 5% milk

1.13. Software and databases

Table 17: Software and databases

Software	Provider
Adobe Photoshop CS5	Adobe Systems GmbH, Munich, Germany
ImageJ analysis software Version 1.43u	National Institute of Health, NIH. https://imagej.nih.gov/ij/
Excel software	Microsoft, Redmond, Washington, USA

Software	Provider
GraphPad Prism 5	GraphPad Software, San Diego, California USA, www.graphpad.com
NCBI data bank	www.ncbi.nlm.nih.gov
PDB Protein data bank	http://www.rcsb.org/pdb/home/home.do
Roche LightCycler® 480 software; Software release 1.5.1.62	Roche Diagnostics, Risch, Swiss
CLC Genomics Workbench	CLC bio, a QIAGEN Company, Aarhus, Denmark

2. Methods

All experiments performed in this study were done in safety level 2 (S2) laboratories.

2.1. Microbiological methods

2.1.1. Cultivation of bacteria

Yersinia spp used for infection experiments were grown in liquid culture. 4 ml LB –media containing the suitable antibiotics were inoculated with material from glycerol stocks or with bacteria freshly plated. The culture was grown overnight in a shaking incubator at 27 °C. To obtain single colonies e.g. for inoculation of cultures, bacteria had been grown on solid media. Either they were streaked out with a sterile inoculation loop, from liquid or glycerol cultures or distributed on agar-plates employing sterile glas pearls. The latter were often employed for growing transformed bacteria. *E.coli* had been treated the same as *Yersinia spp*. except for the incubation temperature. *E.coli* cultures were grown overnight at 37 °C whereas *Yersinia spp*. were incubated at 27 °C overnight.

2.1.2. Conservation of bacteria

Glycerol stocks were prepared for long term storage of bacteria. For this purpose LB medium containing 40 % (w/v) glycerol was mixed with the same amount of liquid bacterial culture in which the bacteria should be ideally in their exponential growth phase (OD_{600} = 0.3-0.6). The mixture was then frozen in liquid nitrogen and transferred to -80 °C for long time storage.

2.1.3. Preparation of chemical- and electro competent bacteria and tansformation

Transformation is a process of horizontal gene transfer by which bacteria take up foreign genetic material from the environment. Once in the bacteria the foreign DNA is mostly degraded, if it is non bacterial. If it has bacterial origin, it can be integrated in the bacterial chromosome or may co-exist as a plasmid next to chromosomal DNA. In both cases the encoded genes can be expressed within the DNA accepting bacteria. Naturally not all bacteria are capable of taking up exogenous DNA. But it is possible to make them artificially competent and use the principle of transformation for molecular biology purposes such as

protein expression. The two ways to make bacteria artificially competent is either with chemical- or electric- impulses.

2.1.3.1. Preparation and transformation of chemical competent *E.coli*

Within cloning processes chemical competent *E.coli* are often employed to produce multiple copies of desired foreign plasmids. To achieve uptake of the foreign DNA by transformation the bacteria need to be artificially competent. Excess of Ca^{2+} ions manipulate the permeability of the bacterial membrane and increase the capacity of the bacteria to take up environmental DNA. To achieve chemical competence 300 ml LB-medium (in one liter flask) was inoculated with a preparatory culture of the desired *E.coli* strain (e.g DH5α, Top10) and grown to an optical density 600 nm between OD_{600} =0.3 and 0.5. To achieve high transformation rates the bacteria are pelleted in their exponential phase (OD_{600} = 0.3- 0.5) because in this phase they endure the later preformed heat shock better than bacteria harvested in the logarithmic phase. Before pelleting the bacteria by centrifuging the culture for 10 min at 4 °C and 1000 x *g* the culture was kept on ice for 10 min. The supernatant was discarded and the cell pellet resuspended in ice cold TFB1 buffer (Table 8). After 90 min on ice the suspension was centrifuged as described previously. This time the bacterial pellet was re-suspended in 1.5 ml cold TFB2 (Table 8). 100 µl aliquots of the 1.5 ml bacterial suspension were then pipetted in pre-chilled reaction tubes, which were immediately flash frozen in liquid nitrogen and later transferred to – 80 °C for storage. For the process of transformation one aliquot of chemical competent cells was thawed on ice, mixed with 1-100 ng of the DNA, which is intended to be transformed and kept on ice for 15 min. The following heat shock of 45 °C for 45 seconds let to permeability of the bacterial cell wall and thereby enabled the DNA uptake. After the heat shock the bacteria suspension was briefly chilled on ice before 900 µl LB or SOC- medium was added. To grow and recover from the heat shock the bacteria were incubated for the following 1-2 h, shaking at 37 °C before they were either plated onto selective media or transferred to a liquid culture containing antibiotics.

2.1.3.2. Preparation and transformation of electro-competent *Yersinia* by electroporation

Electrical pulses create pores that allow genetic material to permeate the bacterial membrane. For electroporation it is important to have a salt free bacterial solution in order to avoid a short circuit. Consequently preparation of electro-competent bacteria involves several washing steps. The first step to make electro-competent *Yersinia* was to prepare an overnight culture, which functions as an inoculation culture the next day. On the following day the overnight culture was diluted 1:50 with LB and the bacteria were grown in a shaking incubator at 27 °C until the culture reached an OD_{600} of 0.6. Subsequently the bacteria were

pelleted by centrifugation at 10600 x *g* , 4 °C. The supernatant was discarded and the pellet was washed twice with 20 ml ice cold autoclaved Millipore water. The third time the bacterial pellet was washed with 10 ml ice cold Millipore water containing 10 % glycerol. Finally the bacteria pellet was resuspended in 600 µl of the 10 % glycerol containing water. 60 µl of the bacterial suspension was aliquoted in pre-chilled reaction tubes. These aliquots were immediately flash frozen in liquid nitrogen and later transferred to -80 °C for storage. For electroporation the cells were thawed on ice and 10 - 1000 ng of salt free DNA was added. After incubation of DNA and bacteria for 10 min on ice the mixture was transferred to pre-chilled electroporation cuvettes with 1 mm electrode gap (PeqLab Biotechnologie GmBH, Germany). Before transformation of the bacteria with the Gene Pulser II electroporator (Biorad, USA), the cuvette was dried from the outside and the bacterial mixture was checked for air bubbles before the cuvette was placed in the cuvette chamber and the electric pulse with the Puls controller Plus (Biorad, USA). The following settings were adjusted at the Electroporator: 50 µF, 1.8 V and 100 Ω (low range). Immediately after the electric pulse the cuvette was placed on ice and 940 µl LB or SOC medium was added. To grow and recover from the treatment, the cells were first grown shaking at 27 °C for at least 1 h before they were either plated onto selective media or transferred to a liquid culture containing antibiotics. Only successfully transformed bacteria were able to grow under the selective conditions.

2.1.4. *Yersinia* Infection

For *Yersinia* infection experiments the cell medium was always changed to antibiotic free medium. One day before the infection experiment, *Yersinia* cultures were grown overnight at 27 °C. The next day 2 ml of this starting culture was used to inoculate 40 ml of fresh LB medium. This culture was incubated 90 min at 37 °C to induce activation of the *Yersinia* type III secretion machinery and Yop expression. After 90min the bacteria were pelleted by centrifugation (10 min, 6000 x *g*, 4 °C) and resuspended in 1 ml ice-cold PBS containing 1 mM $MgCl_2$ and $CaCl_2$. The optical density of bacterial suspension was determined photometrically (Ultrospec 3100 pro, GE Healthcare, Germany) at OD_{600} and adjusted to OD_{600}= 0.36. Cells were then infected by adding this bacteria solution dropwise to the media of the eukaryotic cells. The multiplicity-of-infection (MOI) was 50:1 and the infection time 90 minutes. Exceptional infection times were used for example when preforming the RT-PCR experiments. In that case the primary human macrophages were infected 90 minutes and 6 h (Berneking et al. 2016).

2.1.5. Translocation assay

The Translocation assay was employed to analyze the effector proteins, which were translocated during *Yersinia* infection in the cytoplasm of the host cell. At least one day before infection, the eukaryotic cells (e.g. HEK293) were seeded in antibiotic free media to be adherent and confluent at the time the experiment was performed. Additionally overnight pre-cultures of the *Yersinia* strains were started one day prior the experiment. The next day the *Yersinia* were prepared for infection (section 2.1.4) and given to the eukaryontic cells in an MOI of 50-100. After an infection time of 90 min the cells were washed three times with ice cold PBS on the cell culture dish before 60 µl of a Proteinase K solution (500 µg/ml in PBS) was added to achieve cell lysis. After a brief incubation time of 30 seconds, the solution was removed but cells remained untreated for another 20 min to ensure protein degradation. To finally stop the Proteinase K reaction 60 µl of a 200 mM PMSF stock solution (end concentration of 4 mM) was added. Next, to permeabilize and precipitate cell membranes and to solubilize membrane proteins Digitonin was used. 50 µl of a 1 % Digitonin-PBS solution was given to the cells, which were subsequently scraped and transferred from the 6 well to a 1.5 ml reaction tube. During the incubation time from 20 min at room temperature the tube was briefly vortexed to achieve a homogenous solution. With the following centrifugation for 10 min at 10000 x *g* at 4°C the membranes and DNA were pelleted and the supernatant contained the desired cell cytoplasm and the translocated effector proteins. Immunoblotting analysis employing specific antibodies was used to identify the translocated effectors (Section V, 2.1.5., Figure 12).

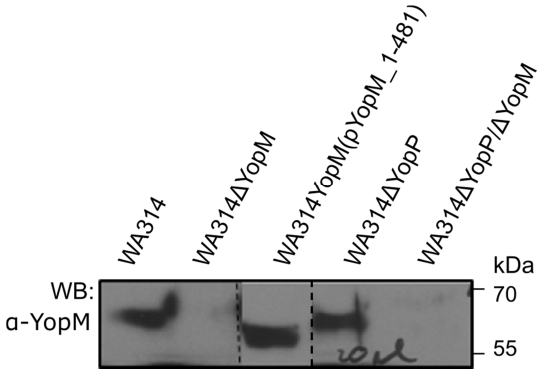

Figure 12: Western blot analysis of the translocated effector YopM in *Yersinia*-infected HEK293 cells.

HEK293 cells were infected with the indicated strains either translocating full length YopM (WA314, WA314ΔYopP), C-terminal truncated YopM (WA314ΔYopM(pYopM_1-481) or no YopM (WA314ΔYopM, WA314ΔYopP/YopM). After 90 min of infection the translocation assay was performed including Proteinase K and Digitonin treatment to analyze the bacterial translocated proteins. Obtained Lysate was subjected to Western blot analysis with the indicated antibodies.

2.1.6. Released protein assay

This method induces the release of bacterial proteins in the media without cell contact. To achieve this situation the bacteria were grown under Calcium-deficient conditions in the presence of EGTA and Glucose (Heesemann et al. 1986). Four milliliter of LB was inoculated 1 to 20 with an overnight *Yersinia* culture and incubated for 1.5 h at 37 °C. The release of proteins was then induced by adding 0.5 mM $MgCl_2$, 0.5 mM EGTA and Glucose to a final concentration of 0.2 %. After incubation for 2 h at 37 °C the optical density of the cultures was determined (OD_{600}). To precipitate comparable amounts of released proteins, the OD measurement was used to adjust the volume of the culture that in the end the equal amount of bacteria was transferred to 1.5 ml reaction tubes. The bacteria were then pelleted by centrifugation at 4900 x *g* for 10 min at 4 °C. The supernatant containing the released proteins was transferred to a new reaction tube. To precipitate the proteins one-tenth of their volume of Trichlor-acetic-acid (TCA) (100 %) was added to a final concentration of 10 %. The solution was kept on ice for 1h or overnight at -20 °C. Subsequently the proteins were pelleted by centrifuging for 30 min, at 20800 x *g* at 4 °C. The pelleted proteins were then washed 1 time with ice cold acetone, before they were resuspended in 4 x sample buffer. After incubating the sample 5 min at 95 °C the probes were ready to be loaded onto SDS-PAGE-gel for Coomassie staining or Western blot analysis (Section V, 2.1.6., Figure 13).

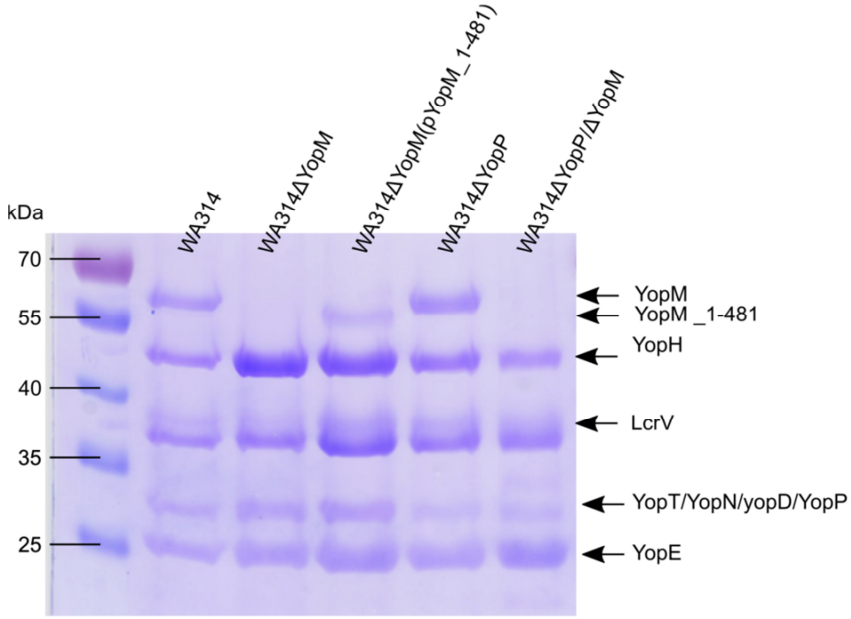

Figure 13: Released protein assay.
Released protein assay was performed with the indicated *Yersinia* strains. The TCA precipitated proteins were boiled in sample buffer and subjected to SDS page. Released proteins are visualized by Commassie staining

2.2. Molecular biology techniques

2.2.1. Working with DNA

2.2.1.1. Isolation of plasmid DNA

Plasmid DNA was isolated from 5 ml bacterial cultures using different Miniprep Kits. Either the Plasmid Miniprep Kit II, peqGOLD (peqlab) or the ZR Plasmid Miniprep-Classic Kit (Zymo Research, USA) was employed following the manufacturer's instructions. To obtain higher amounts of pure plasmid DNA for transfection of mammalian cells the Plasmid Midi Kit (Qiagen, USA) was used. Plasmid DNA preparation was preformed as mentioned in the protocol. To achieve higher purity of the plasmid DNA an additional ethanol precipitation was carried out after the standard preparation. The Plasmid DNA pellet from the preparation was solved in 400µl H_2O and transferred to a small 1.5 ml reaction tube. One-tenth volume 3 M sodiumacetate and two volumes of ethanol (100 %) were added. Precipitated DNA was pelleted by centrifugation at room temperature and washed one time with two volumes 70 % ethanol. The air dried DNA pellet was then solved in 50 µl ddH_20. Purity and concentration was determined with the NanoDrop® ND-1000 spectrophotometer (Peqlab, Germany). For transfection of cells the end-concentration was adjusted to approximately 2 µg/µl.

2.2.1.2. Determination of DNA concentration

The NanoDrop® ND-1000 spectrophotometer (Peqlab, Germany) was used to determine DNA concentrations in solutions. It´s measurement of DNA concentrations is based on the absorptions-maximum of nucleic acids at 260 nm, which is caused by the aromatic ring structure of the bases. For determination of DNA concentrations the spectrophotometer was used according the manufacturer's instructions. Before applying a sample on the fiber optic cable the spectrophotometer was first blanked with the solution the DNA was solved in (mostly ddH_2O). Using the ND-1000 V 3.1.0 software, the concentration and the purity of the sample were displayed. Concentration of potential contaminations such like proteins or phenol was determined at 280 nm. The ratio of the absorption OD_{260}/OD_{280} represents the purity of the DNA solution and should be between 1.8 and 2.

2.2.1.3. Polymerase chain reaction

The polymerase chain reaction (PCR) is a common technique for multiplying certain pieces of DNA by choosing oligonucleotides flanking the region of interest, which is then copied millions of times through a thermostable *Taq*-DNA polymerase (Mullis et al. 1986). Amplification of the gene of interest is based on thermal cycling. The first step at 95 °C induces denaturation of the double stranded DNA. In the next thermal step the primers anneal to their complementary sequence in the single stranded DNA, consequently the temperature is dependent on the melting temperature of the primer and should be 3-5 °C

below. At 72 °C the *Taq* polymerase is activated and extends the DNA sequence from the primer onwards. Dependent on the Polymerase used the optimal extension temperature can vary. For generation of PCR-products in this study mostly the *5 Prime Extender Systems* (5 PRIME GmbH, Germany) was used. This polymerase mix provides better proofreading than the single *Taq* polymerase and is suitable for amplification of long PCR products. A typical composition of a PCR reaction mix and a typical PCR amplification program is depicted in the Table 18 and Table 19. PCR amplification was performed in gradient thermocyclers (Eppendorf, Germany). At the end of reaction the PCR-products were analyzed by agarose gel electrophoresis. Subsequently products can be isolated and purified from the gel and used for downstream applications e.g. subcloning by employing the gel extraction and purification *Nucleo Spin Extract II* Kit (Macherey-Nagel, Germany) according to the manufacturer's instructions. Through introduction of enzymatic restriction site sequences at the 5'-end of the oligonucleotide sequences (primer), PCR is also suitable for generating DNA fragments that can be digested with the respective endonucleases followed by subcloning them into expression vectors.

A typical PCR reaction setup is depicted in the following tables:

Table 18: PCR reaction mix

Reaction composition	Concentration	Amount
DNA template	50-100 ng/µl	1 µl
PCR buffer	10x	5 µl
forward primer	10 pmol/µl	1 µl
reverse primer	10 pmol/µl	1 µl
dNTPs	10 mM	1 µl
Taq polymerase	10 units/µl	0.3 µl
ddH_2O		*ad* 50 µl

Table 19: PCR program

PCR program	Temperature	Time	Cycles
Initial denaturation	95 °C	5 min	1
Denaturation	95 °C	30 s	30-35
Annealing	40-72 °C (Tm - 3-5 °C)	30 s	
Extension	72 °C	1 kb DNA/45-60 s	
Final elongation	72 °C	10 min	1
Storage	8 °C	forever	1

2.2.1.4. Agarose-gel-electrophoresis

The agarose gel electrophoresis is a method to separate mixed population of DNA and proteins in a matrix of agarose. Mainly the agarose gel-electrophoresis is used to separate DNA by fragment length. The negative charged phosphate residues of the DNA lead to a fractionation towards the positive pole when applying an electric field. Depending on their size and conformation the fragments travel through the matrix with different speed. The percentage of the agarose (1-2 %) matrix and the applied voltage (8 V/cm) also determine the running speed of the DNA fragments within the gel. The percentage of agarose matrix and applied voltage was choosen depending on the average size of the DNA fragment pool and the dimension of the used gel. To prepare the agarose gel the appropriate amount of agarose was solved in adequate volume of 1xTAE buffer and heated in the microwave (800 W) until the agarose was completely solved. When cooled down the nuclear acid staining solution RedSAFE (Intron Biotechnology, Korea) was added according to the manufacturer's instructions and the mixture was poured into the agarose tray. A comb was added to create wells for the samples. Once solid, the gel was transferred to an electrophoresis chamber and covered with 1xTAE buffer. Prior to sample loading the DNA was mixed with Orange DNA loading dye (Fermentas, USA). The containing glycerol allows the descent of the DNA probes into the wells and the different dyes make it possible to follow the movement of the DNA. As weight size marker the 1 kb DNA-Ladder GeneRuler (Thermo Fisher Scientific, USA) was added to each DNA separation and was used to determine the DNA fragment size. After running the DNA separation at a Voltage of 8/cm the DNA fragments in the gel matrix were visualized by UV light on a Transilluminator (BioRad, Germany). Excitation of the DNA bound RedSAFE dye (Intron Biotechnology, Korea) led to emission of fluorescence and thereby visualization of the DNA fragments.

2.2.1.5. Restriction digest of DNA

Restriction endonucleases are enzymes that cleave the sugar-phosphate backbone of DNA within a stretch of few bases. These bases are unique for each enzyme and are called recognition sequences. The specificity of the enzymes made the restriction enzyme digestion a common technique used for molecular cloning. By employing primers, which contain specific endonuclease restriction sites, PCR can be used to generate fragments for sub cloning into expression vectors. For that purpose vector and PCR fragments were digested with FastDigest® or NEB restriction endonucleases according to the manufacturer's recommendations. The digested DNA fragments were separated on agarose gels (section 2.2.1.4) and the desired bands were purified from the gel using the DNA/PCR clean up kit „Nucleo Spin Extract II"(Macherey-Nagel, Germany). Subsequently, purified vector and PCR fragments were subjected to ligation (section 2.2.1.6).

2.2.1.6. Ligation

In the ligation reaction a T4 DNA ligase catalyzes the formation of a phosphodiester bond between 5'-phosphate and 3'-hydroxyl termini in duplex DNA or RNA.

Ligation reactions with T4 DNA Ligase (Roche Diagnostics, Swiss) were performed at 16 °C overnight or for 1 h at room temperature. The reaction was performed in the supplied T4 DNA ligation buffer using a molar ratio of at least 1:3 (vector: insert) and 50- 100 ng vector-DNA.

$$ng_{(Insert)} = \frac{ng_{(Vector)} \times kb_{(Insert)}}{kb_{(Vector)} \times \text{molar ratio}_{(Vector/Insert)}}$$

Up to 5µl of the ligation solution was used to transform in chemical competent bacteria (section 2.1.3.)

2.2.1.7. Generation of expression vectors used in this study

2.2.1.7.1. for eukaryontic expression

For expression in eukaryotic cells, YopM constructs were amplified via PCR from virulence plasmid pYVa127/90 (accession NC_004564.1) and cloned into pCS2+MT (XB-VEC-12442480) via the restriction sites *NcoI* and *XbaI* resulting in N-terminally myc-tagged YopM (myc-YopM). For the expression of GST-YopM, YopM was derived from the myc-YopM construct via restriction sites *BamHI* and *NotI* and ligated into the pEBG-2T vector (Dettori et al. 2009). HA-DDX3 constructs were amplified from human cDNA (accession NM_001356) and subsequently cloned into the pCDNA3.1 (+) vector (Invitrogen/Life technologies, Thermo Fisher Scientific, USA) using the restriction sites *HindIII* and *BamHI* resulting in the constructs DDX3-HA, DDX3_1-418-HA and DDX3_418-662-HA. HA-tags where introduced by employing suitable reverse primers (Table 15).

2.2.1.7.2. for bacterial expression

For construction of the mutant *Yersinia* strain translocating a C-terminal truncated YopM, the *Yersinia* WA314ΔYopM strain was recomplemented with the bacterial expression vector pACYC184 harboring the amino acid sequence of Yop_1-481. The YopM_1-481 was cloned via the restriction sites *HindIII* and *XbaI* into the modified pACYC184 vector (Hentschke et al. 2010). The new expression plasmid lacked the C-terminal CBP-SPB-tag and only contained the sequence of YopM_1-481. The purified plasmid was transformed into electro competent *Yersinia* (WA314ΔYopM) (Section V, 2.1.3.2) giving rise to a new strain named WA314ΔYopM(pYopM_1-481) (Table 11). Released protein- (Section V, 2.1.6, Figure 13)

and translocation- assay (Section V, 2.1.5, Figure 12) were performed to ensure functionality of the new strain.

2.2.1.8. DNA sequencing

To revise cloning or PCR-products, probes were given to Seqlab (Göttingen, Germany) to be sequenced with the suitable primer. Sequences provided were compared to sequences stored in the NCBI-database (www.ncbi.nlm.nih.gov) or analyzed with the help of the programs serial cloner (http://serialbasics.free.fr/Serial_Cloner.html) or *CLC Genomics Workbench* (CLC bio; Denmark).

2.2.2. Gene transcription analysis

2.2.2.1. Real Time (RT)-PCR

As the conventional end point PCR (section 2.2.1.3), the real time (RT)-PCR reaction is based on thermal cycling including denaturation, primer annealing and elongation. In contrast to the conventional PCR, in which the amount of target DNA can only be determined after the PCR reaction, the amplifying progress within the RT-PCR is monitored as it occurs. This is enabled by a fluorescence reaction induced within each amplifying process. The thereby emitted fluorescence is directly detected and recorded by the RT-PCR instrument. The higher the starting copy number of the nucleic acid target within a sample, the sooner a significant increase in fluorescence is observed. In general two main chemicals exist to evoke the fluorescence reaction during the RT-PCR amplification process. One is the technique based on a chemical known as SYBR dye. The SYBR dye detects PCR products by binding to double-stranded DNA and thereby emits. The second technique is based on the 5´-3´exonuclease activity of the *Taq* polymerase. In this approach an oligonucleotide probe, non-extendable at the 3' end, fluorescence labeled at the 5'-end and designed to hybridize within the target sequence, is introduced into the polymerase chain reaction assay (Khare & Eckert 2002). In detail the probes contain a fluorescent reporter dye on the 5' end and a quencher dye on the 3'-end. While the probe is intact, the proximity of the quencher dye reduces the fluorescence emitted by the reporter dye by fluorescence resonance energy transfer (FRET). The probe anneals as the primers to its complementary sequence in the single stranded DNA, but in contrast to the primer, the probe is not extended by the *Taq* polymerase due to its missing hydroxyl group. When the polymerase reaches the probe, it recognizes it as double stranded DNA and cleaves it with its 5' - 3' exonuclease activity, which results in the release of mono- and oligonucleotides and leads to the separation of quencher and dye. With separation of quencher and fluorescent dye (reporter dye) the fluorophore can be excited by light and emits the fluorescence. Each PCR cycle leads to

cleavage of more probes and therefore to an increase in fluorescence if the desired DNA or RNA fragment is still present. Thus the fluorescence intensity detected by the PCR instrument is proportional to the amount of amplicon produced. The principles, of how the two different dyes work are illustrated in the following Figure (Section V; 2.2.2.1., Figure 14).

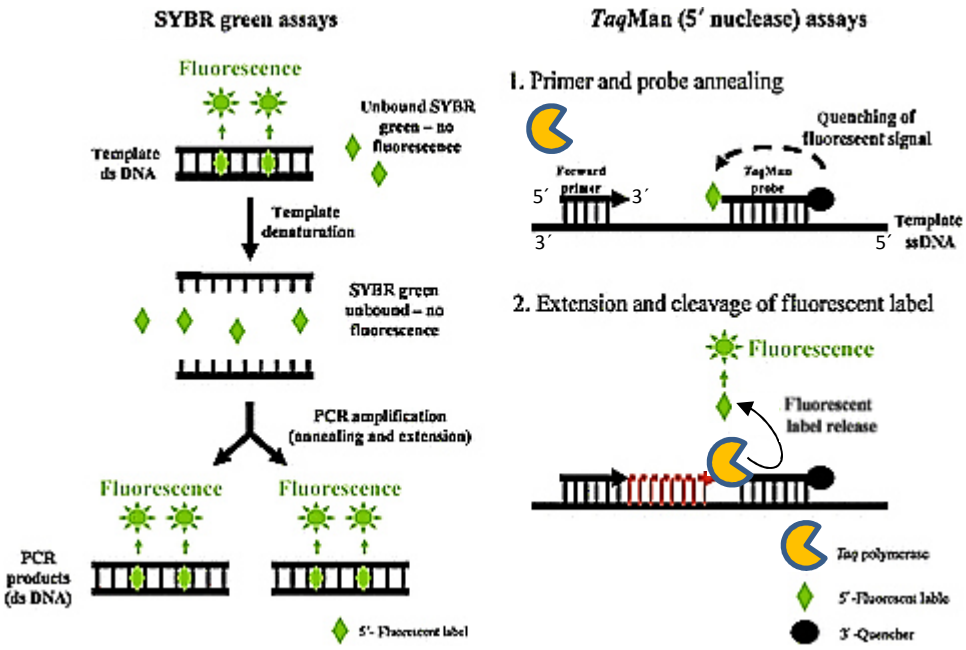

Figure 14: RT-PCR principles based on SYBR green and TaqMan.
On the left side the principles of the SYBR green dye is illustrated. SYBR green binds to double-stranded DNA and emits a fluorescent signal. In its unbound state, SYBR green does not emit fluorescence. Template amplification is therefore measured in each cycle by the corresponding increase in fluorescence. On the right side the principles of the TaqMan assay is depicted. During annealing, the TaqMan probe and primers bind to the template. When the TaqMan probe is intact energy is transferred between the quencher and the reporter; as a result, no fluorescent signal is detected. As the new strand is synthesized by Taq polymerase, the 5`- exonuclease activity of the enzyme cleaves the labeled 5`-nucleotide of the probe, releasing the reporter from the probe. Once it is no longer in close proximity, the fluorescent signal from the probe is detected and template amplification is recorded by the corresponding increase in fluorescence (Smith & Osborn 2009 modified).

In our experimental setup we monitored the fluorescence emitted during amplification with the Light Cycler 480 (Roche Life Science) We employed the TaqMan method and purchased TaqMan-primer probe mixes from Life Technologies (Carlsbad, Californien; USA) to analyze the gene expression from IL-10 (Hs00961622_m1), IL-6 (Hs00985639_m1), TNF (Hs01113624_g1) and IL-1β (Hs00174097_m1) in *Yersinia* infected macrophages. As reference genes to normalize RT-PCR measurements between different samples, we monitored the amplification of GAPDH, TATA-box binding protein (TBP) and beta-2-microglobulin (B2M) within each sample employing the respective suitable primer probe mix (GAPDH (Hs02758991_g1), TBP (Hs00427620_m1), B2M (Hs00187842_m1)). To assess the gene expression in the *Yersinia* infected macrophages we analyzed the RT-PCR data

according to manufacturer's instruction (Roche LightCycler 480 software; Software release 1.5.1.62). To determine the absolute transcription of the mentioned genes within the *Yersinia* infected macrophages, we employed external standards and normalized the absolute gene expression to the corresponding gene expression in uninfected/mock (negative control) or in wild type (positive control) infected cells. The RT-PCR reaction was performed in 96 well plates (Roche Diagnostics, Swiss). Prior to RT-PCR we infected primary human macrophages with different *Yersinia* strains (WA314, WA314ΔYopM, WA314ΔYopM(pYopM_1-481), WA314ΔYopM(pYopM), WA314ΔYopP; WA314ΔYopP/YopM; WA-C) for 1.5 and 6 h and isolated RNA from these infected macrophages with the RNeasy Mini Kit (Qiagen, Germany) according manufacturer's instructions including DNase treatment. 500 ng- 2 µg of the isolated RNA was reverse transcribed using iScript cDNA Synthesis Kit (Biorad, USA) following the manufacturer's instruction. 2 µl- 0.5 µl of this mixture was subjected to each RT-PCR reaction. Next to the primer and probe mix the TaqMan Fast Advanced Master mix (Applied Biosystems, USA) was used containing the Taq-polymerase, reaction buffer and dNTPs. Each 15 µl reaction contained approximately 50 ng c-DNA template, 1x TaqMan Fast Advanced Master Mix and 1x TaqMan Assay containing the gene specific primer and probe. Mastermixes were prepared for each gene when pipetting the 96 well plates. In order to determine the absolute gene transcription in the infected cells at least two dilutions of the standard were run for each gene analyzed on the plate, including the reference genes. The program run on the Light cycler 480 to amplify the genes of interest is depicted in the following table.

Table 20: RT-PCR program run on the Light Cycler 480

PCR program	temperature	time	cycles
Initial denaturation	95 °C	10 min	1
Polymerase activation and Denaturation Annealing and Extension	95 °C 60 °C	15 s 1 min	40-45
Cooling of the instrument	37 °C	10 min	

.

2.3. Biochemical methods

2.3.1. Pulldown and Immunoprecpitation-experiments

2.3.1.1. GST-pulldown experiments

For GST-pulldown experiments in mammalian cell lines, HEK293 cells were either transfected with GST-myc-YopM expressing vectors (Section VI, 1.2, Figure 17) or with plasmids expressing GST and Hemagglutinin (HA) tagged RSK1 (GST-HA-RSK1) (Section VI, 2.1, Figure 21D; Section VI, 2.2, Figure 23). Transfection was carried out with the Calcium phosphate method (Section V, 2.4.2.1.) in a 100 mm dish. 48 h after transfection, when the cells were confluent, they were harvested in 1 ml PBS supplemented with protease inhibitor cocktail (Roche, Swiss). Then the cells were pelleted by centrifugation for 5 min at 1000 x *g* at room temperature and resuspendet in 1 ml PBS containing 1% Triton X-100 (Sigma Aldrich, USA) and protease inhibitor. To ensure cell lysis the solution was subjected to three consecutive cycles of freeze and thaw. In the following total protein within the lysates was determined using Biorad Protein Assay (Biorad Laboratories GmBH, Germany). Lysates containing the same total protein amounts were incubated rotating overnight at 4 °C with 20 µl Gluthathione Sepharose^{TM} 4B (Ge Healthcare, Germany). The next day the beads were washed in batch. The glutathione beads were sedimented by centrifugation for 5 min at 500 x *g* and 4 °C. Supernatant was discarded or kept to analyze the binding-affinity to the beads. In total eight successive washing steps were carried out, each with 1 ml of cold lysis buffer (PBS + 1 % Triton X-100). To elute the bound proteins, the sepharose was boiled 5 min in 60-100 µl 2x SDS-Buffer. Proteins in the eluate and lysates were separated by SDS-PAGE and further analyzed by Western blotting employing the desired antibodies.

2.3.1.2. Immunoprecipitation of endogenous DDX3

HEK293 cells were transfected with myc-YopM. After 48 h the cells were harvested and lysed as described previously (Section V, 2.3.1.1). In this case the lysis-buffer contained 1 % NP 40 instead of TritonX-100. Cell lysates were 2-3 h pre-incubated with 1 µg polyclonal rabbit anti-DDX3 antibody (Bethyl laboratories, USA) rotating at 4 °C. In the following 20 µl Protein A/G Plus-Agarose (Santa Cruz Biotechnology, USA) was added and the samples were incubated for another 2-3 h or overnight rotating at 4 °C. In batch purification of the A/G Plus-Agarose was carried out including eight washing steps with 1 ml PBS containing 1 %NP 40 to reduce unspecific bound proteins. Sedimentation of the A/G Plus-Agarose between the washing-steps was achieved by centrifugation for 5 min at 1000 x *g*. All centrifugation steps were carried out at 4 °C. After the final washing step the sedimented A/G Plus-Agarose beads were boiled in 2x SDS buffer to achieve elution of the attached proteins. For immunoprecepitation of endogenous DDX3 in *Yersinia* infection experiments (Section VI, 1.2,

Figure 18A), the MultiMACS™ Protein G Kit (Miltenyi Biotec GmbH, Germany) was used. HEK293 cells were infected (Section V, 2.1.4.) with *Yersinia* strains translocating YopM. After 90 min the cells were washed 1-2 times with 5 ml TBS (Section V, 1.6, Table 8) on the petri dish and then harvested in 1 ml of the µMac Lysis-Buffer included in the MultiMACS ™ Protein G Kit. Cell lysis was performed according to the manufacturer's instruction. Lysed cells were centifugated for 10 min at 13.000 x *g* at 4 C°. The supernatant, containing the protein, was then incubated with 20 µl (2 µg) monoclonal mouse anti-DDX3 antibody (Santa Cruz Biotechnology, USA) rotating at 4 C°. After 30 min, 50 µl magnetic µMacs Protein G MicroBeads (Miltenyi Biotec GmBH, Germany) were given to the mixture and the mixure was incubated for approximately 2 h, rotating at 4 °C. Immunpurification was performed with the µColumns and µMacs™ Separator (Miltenyi Biotec) according to manufacturer´s instruction. For eluting the proteins from the beads, 20 - 40 µl of hot SDS-buffer was given to the columns. The eluates were immunoblotted and analyzed using the indicated antibodies.

2.3.1.3. Immunoprecipitation of flag-tagged DDX3 and PKN

HEK293 cells were transfected with myc-YopM expression vectors and co transfected with plasmids either expressing DDX3-flag or PKN-flag to investigate the complex formation between YopM, RSK, PKN and DDX3. 48 h post transfection, cell lysates were prepared as described above (Section V, 2.3.1.1). PBS containing 1 % Triton X-100 supplemented protease inhibitor (Complete, Roche, Swiss) was used as lysisbuffer. 20 µl Flag-sepharose (Anti-Flag® M2 Affinity Gel, Sigma Aldrich) was added to the clearified lysates and incubated overnight, rotating at 4°C. In batch washing of the sepahose was carried out eight times in total. Each washing step was carried out with 1 ml of PBS containing 1 % Triton X-100 and the sepharose was sedimented by centrifugation for 5 min at 1000 x *g* at 4 °C. After the last wahing step, the Flag-Sepharose pellet was suspended in 2x SDS-buffer, boiled and loaded onto a SDS-PAGE gel. Lysates and precipitates were analyzed by Western blotting with specific antibodies.

2.3.1.4. Tandem affinity purification

In principle the method of tandem affinity purification is used to subtract a tagged protein of interest together with its interacting proteins from complex solutions such like cell lysates. The difference to ordinary immunoprecipitations is that the protein of interest is double tagged and thereby can be successively affinity purified employing both tags. Within this process, the contaminations within the final eluate are reduced to a minimum. For the tandem affinity purification often a Streptavidin (SBP)– and Calmodulin- binding protein (CBP) sequence are fused to the protein of interest. Such tags, comprising of two different binding proteins are often called tandem affinity purification (TAP)-tags. In our experimental approach the Steptavidin sepharose was employed for the first step of purification. In general

it is directly added to the crude cell lysates. After an incubation of several hours the elution from the Streptavidin sepharose is achieved with Biotin. Obtained eluates are subsequently incubated with Calmodulin sepharose. Excess of Calcium leads to eluation of the proteins in this second step (Rigaut et al. 1999). This second elution should be highly pure and only contain the protein of interest and its interacting proteins. To identify the unknown interacting partners, the eluate can be subjected to SDS-PAGE followed by Comassie/Silver staining and mass-spectrometry analysis of visible bands. In this study a C-terminal SBP-CBP tagged YopM and YopE were purified from cell lysates of WA314ΔYopM(pYopM-SBP-CBP) or WA314ΔYopE(pYopE-SBP-CBP) infected mouse macrophages (J774A.1) in the previously described manner. In total four 100 mm culture dishes of J774A.1 cells (approximately 4×10^6 cells) were infected with the mentioned *Yersinia* strains WA314ΔYopM(pYopM-SBP-CBP) or WA314ΔYopE(pYopE-SBP-CBP) for 90 min (Section V, 2.4.1). The Tandem Affinity purification of the translocated C-terminal SBP-CBP-tagged YopM and YopE was performed with the Interplay™ Tandem Affinity Purification kit (Stratagene, USA). 90 min after infection the cells were washed three times with PBS on plate before they were harvested in 10 ml of the lysis buffer supplied with the Interplay™ Tandem Affinity Purification kit (Stratagene, USA). Cell lysis was achieved by three successive cycles of freeze and thaw. The next steps were performed as suggested by the manufacturers and as described by Moritz Hentschke (Hentschke et al., 2010). Only the final elution from the Calmodulin sepharose was not performed with the provided buffer, instead the sepharose beads were boiled in 60 - 100 µl 2 x SDS-loading buffer. The eluated proteins were then separated by SDS-PAGE and the gel was immunoblotted. Specific RSK, PKN and DDX3 antibodies were applied to investigate if these proteins interact with YopM or YopE.

2.3.2. Determination of protein concentration

The spectroscopic analytical method of Bradford was used to determine concentration of solubilized proteins using the BioRad Protein-Assay-Kit. Water and Bradford reagent were mixed in a 5:1 ratio and 1 - 2 µl of sample was added to 1 ml Bradford mix. The absorbance at 595 nm was measured after 10 min against a blank value in a photometer (Ultrospec 3100 pro, GE Healthcare) and analyzed using a protein standard curve based on different concentrations of BSA (1 - 20 µg/ml).

2.3.3. SDS-Polyacrylamid-Gel-Electrophorese (SDS-PAGE)

The SDS-PAGE is an analytical method used to separate proteins by size. The technique is based upon the principle that a charged molecule will migrate in an electric field towards an electrode with opposite charge (Laemmli 1970). To ensure separation by size only, the samples are treated with sodium dodecyl sulfate (SDS) containing sample buffer. The SDS

denatures proteins and imparts a negative charge to the now linearized proteins. The size separation itself is accomplished by a polyacrylamide gel, which works like a molecular net through which smaller proteins can pass more easily. The gel is composited of two different parts. The upper part, the stacking gel, consists of a Tris-HCl buffer system (pH 6.8) with 4 % Acrylamide. The following part, the resolving gel, is another Tris-HCl-buffer system with a higher pH value (pH 8.8) and a higher Acrylamid percentage (7.5 - 16 %). Under current flow, chloride ions (Cl^-), negatively charged proteins and glycinat ions travel toward the anode. To stack the samples the proteins are carried between Cl^- (leading ions) and dipolar glycinat-ions (following ions) to the edge of the upper part. At a pH of 6.8 the glycinat (within the running buffer) prevails in its uncharged form, which leads to a voltage rise. As a consequence the travel of the charged proteins towards the anode is accelerated until they reach the Cl^- ions on the edge of the upper gel. There the potential falls and the proteins are stacked. The pH shift from the upper part (pH 6.8) to the lower part of the gel (pH 8.8) leads glycinat ions. Glycinat now prevail in its charged form and travels towards the anode. Reasoned by their size the glucinat ions are now transported faster trough the fine meshed gel than the proteins and as a consequence the proteins are now separated by their size.
The PageRuler Prestained Protein Ladder (Thermo Scientific, USA) was applied on each gel as a size reference. The SDS-PAGE gel was prepared as indicated in the following table (Table 21). Buffer compositions of the stacking-, resolving- and SDS-sample buffer are described in Table 8: Buffer (Section V, 1.6). Gels were run at 80 V during stacking and 120 - 150 V during separation in SDS-PAGE electrophoresis cells (Biorad, Germany) filled with SDS-running buffer (Section V, 1.6, Table 8: Buffer).

Table 21: Composition of a 10% Acrylamid SDS-PAGE mini gel

Component/buffer	10 % Resolving gel		4 % Stacking gel	
ddH_2O	4.2	ml	1.55	ml
Resolving Buffer pH 8.8	2.5	ml	-	
Stacking Buffer pH 6.8	-		625	µl
Acrylamid 30 %	3.3	ml	325	µl
APS (10 mg/ml)	50	µl	12.5	µl
TEMED	5	µl	2.5	µl

2.3.4. Coomassie staining

For the fixation and visualization of the proteins the stacking gel was discarded and the resolving gel incubated in a Coomassie staining solution (Section V, 1.6, Table 8: Buffer). After 1 h the gel was destained in an acetic acid based Coomassie destain solution (Section V, 1.6, Table 8: Buffer) either overnight or at least 2 h until the proteins were clearly visible as single blue bands. For documentation, the gel was either scanned or dried in the Gel dryer 543 (Biorad, Germany) for 30 min.

2.3.5. Western blot analysis

In Western blot analysis proteins are electrophoretically transferred from a native or denaturating Polyacrylamide gel electrophoresis to a Polyvinylidendifluorid (PVDF) membrane (Immobilon, Millipore, Germany). For the transfer the semi-dry blotting system OWLHEP-1 (Thermo Scientific, USA) was used. In this apparatus the reassembly of the blotting “sandwich“ started with three, in transfer-buffer (Section V, 1.6, Table 8) soaked, filter-papers (Whatman, 190 g/m2, Hartenstein, Germany). These three filter-papers were placed on the cathode. The SDS-gel was placed on top followed by a methanol activated PVDF-membrane. Terminal, three in transfer-buffer soaked filter-papers were stacked on top of the PVDF-membrane. The blotting apparatus was closed and the protein transfer was performed with amperage of 1.2 mA /cm^2 for 1-1.5 h. The typical setup to transfer proteins separated with a mini-gel (Mini-Protean II Electrophoresis systeme) was 125 mA (constant) for 1.15 h. After protein transfer the sandwich was dismounted and the membrane incubated in a 5 % milk-TBS solution containing 0.3 - 0.5% Tween (Merck Millipore, USA) to block free protein-binding domains. After at least 1 h the membranes were incubated for 3 - 4 h at room temperature with the desired first antibody either in a TBS-Tween or a TBS-Tween-milk solution (Section V, 1.12, Table 16). If this step was carried out overnight, the membranes were incubated at 4 °C. To remove all unspecific bound first anti-body, three washing steps with TBS-solution containing 0.3 - 0.5 % Tween were carried out (each at least 10 min). In the following the membranes were incubated for 1 - 2 h in the suitable secondary antibody solution (Section V, 1.12, Table 16) at room temperature. To remove excess secondary antibody the membrane was again washed three times for at least 10 min with TBS containing 0.3 - 0.5 % Tween. Next, the membranes were ready to be developed. For this purpose either SuperSignal West Pico or SuperSignal West Femto Maximum Sensitivity Substrate (Thermo Scientific, USA) was used according to the manufacturer´s suggestions. Both solutions enable detection of antigen by oxidizing luminol in the presence of horseradish peroxidase (HRP) and peroxide. This reaction produces a prolonged chemiluminescence, which can be visualized on X-ray films (Super RX, Fuji medical X-ray film, Japan). These were developed with the Curix 60 (Agfa, Belgium).

A general overview of first and secondary antibodies used in this study and their employed working dilutions are given in in Table 16 (Section V 1.12).

2.4. Cell culture and cell biological methods

2.4.1. Cultivation of eukaryotic cells

HEK293 cells (ATCC# CRL-11268) were grown in DMEM with 10 % FCS containing 100 µg/ml Penicillin and 100 µg/ml Streptomycin (all from Gibco®). J774A.1 (ATCC# TIB-67) cells were grown in RPMI1640 (Invitrogen, GIBCO® Darmstadt, Germany) supplemented with 10 % FCS, 100 µg/ml Penicillin and 100 µg/ml Streptomycin and additional 2 mM Glutamine. All cell lines were cultured in a humidified 5 % CO_2 atmosphere at 37 °C and passaged every 48 hours. Human peripheral blood monocytes were isolated from buffy coats as described from Kopp and colleagues (Kopp *et al.* 2006). Cells were cultured in RPMI1640 containing 20 % autologous serum. The medium was changes every three days until the cells were differentiated into macrophages after 2 weeks. Then the cells were used for experiments such like *Yersinia* infections. Whenever cells were infected with *Yersinia,* the growth medium was changed to an antibiotic free version before preforming the infection experiment. When the phosphorylation status of RSK was analyzed, the cells were serum starved for a total time of 2 - 4 h before harvesting.

2.4.2. Preparing cyro-stocks for long time storage of cells

Eukaryotic cells were stored in liquid nitrogen at 196 °C. To prepare a cryo-stock, 4×10^6 cells were suspended in 1.5 ml FCS with 10 % (v/v) Dimethyl sulfoxid (DMSO) and transferred to a cryo-vial. The cryo-vial was set in an isopropanol filled cryo-container (Mr. Frosty) and frozen over night at -80 °C. The next day the cells were transferred to be stored in liquid nitrogen.

2.4.3. Cell treatment

2.4.3.1. Leptomycin B treatment

Cells were serum starved for approximately 30 min and then incubated with 25 nM Leptomycin B (LMB) (Sigma-Aldrich, USA) for 3-4 h.

2.4.4. Transfection and siRNA treatment

2.4.4.1. Transfection of HEK293 cells

To achieve transient expression of proteins in eukaryontic cells different transfection methods are known. HEK293 cell were either transfected employing the calcium phosphate method or with polyethylenimine (PEI), linear (Polysience Inc, Pennsylvania, USA) following the manufacturer's instructions. The calcium phosphate transfection method is based on the formation of calcium phosphate DNA precipitates, which are endocytosed by the eukaryotic cells. The method was first described 1973 and from there on further modified (Graham & Van Der Eb 1973). We used sterile filtered HEPES solution and 2.5 M calcium chloride solution (Section V, 1.6, Table 8). The DNA (1 - 1.5 µg for 6 well transfection and 2 - 5 µg DNA for 100 x mm dishes) was directly mixed with a calcium chloride solution, incubated 5 min at room temperature and then added dropwise to the HEPES buffer. Aeration of the phosphate buffer while adding the DNA-$CaCl_2$ solution by vortexing the HEPES solution (Table 8) helped to ensure that the formed precipitates are as fine as possible, which is important to facilitate adherence of the precipitates to the cell surface and their endocytosis. Before adding the mixed solution dropwise to the cells, the solution was incubated 20 min at room temperature to allow forming of the Calcium phosphate DNA precipitates. After 20 min of incubation at room temperature, the formed precipitates are added dropwise to the cells. At the timepoint of the infection the confluency of the cells should be approximately 25-45 %. 24 -48 h after transfection the cells in general expressed the proteins encoded on the transfected expression vectors. To ensure successful transfection a vector expressing GFP was employed as a control. .

2.4.4.2. SiRNA based knockdown

Small interfering RNAs (siRNAs) are short, 20-25 nucleotide long double-stranded RNA molecules, which play a role in a variety of cellular processes. Most notably, the siRNA is involved in the RNA interference (RNAi) pathway where the siRNA interferes with the expression of a specific gene, by hybridizing to complementary mRNA molecules. An RNase III nuclease named Dicer catalyzes the first step of the RNA interference pathway. It not only processes long double stranded RNA in siRNAs, it also initiates formation of the RNA-induced silencing complex (RISC). Within this RISC complex, the double stranded RNA undergoes strand separation. The RISC complex, guided by its bound single stranded siRNA, pairs with the complementary mRNA target. Nucleases within the activated RISC degrade the targeted mRNA. RISC then departs, its RNA guide intact, to mediate additional cycles of target recognition and cleavage. As a consequence of this action the fragmented target mRNA is reduced within the cell, which is accompanied by a reduction of the corresponding protein .This described process can be used to directly reduce the amounts of

certain proteins within the cell by introducing artificial siRNAs. The siRNA used to silence DDX3 expression was purchased from Thermo Scientific (D-006874-02, target sequence ACAUUGAGCUUACUCGUUA, Section V, 1.8, Table 9 :siRNA sequence). As control, an unspecific siRNA collection (Dharmacon, USA) was used. Both unspecific and specific DDX3 siRNA were used as suggested by the manufacturer. RNAi transfection was carried out with Lipofectamine® RNAiMax (Life Technologies, USA) according to the manufacturer's instruction (reverse setup). DDX3 specific knockdown in HEK293 cells was achieved after 24-48h. In case the transfection was performed with the calcium phosphate method (Section V, 2.4.4.1) the siRNA transfection was performed 24 h after DNA transfection and cells were then analyzed after another 24h (Section VI, 3.2., Figure 26A, D). If transfection was carried out with PEI (Section V, 2.4.4.1), siNT/siCtrl- and siDDX3-treatment of HEK293 cells was carried out 16-24 h before transfection of the DNA. In that case cells were usually harvested 16-24 h after the DNA transfection (Section VI, Figure 27B, C). The DDX3 knockdown efficiency was controlled by analyzing the presence of DDX3 within the lysates of siNT/siCtrl and siDDX3 transfected cells by Western blotting (Section V, 2.3.5.) employing a specific DDX3 antibody. Corresponding actin signals in the Western blot analysis served as loading control. Respected DDX3 knockdown efficiency was calculated using ImageJ. Each DDX3 signal was refered to the corresponding actin signal.

2.4.3. Digitonin based cell fractionation

In order to separate the cytoplasm and nuclei of cells, a Digitonin based assay was employed to permeablize the cell membrane to effectively release the content of the cytosol. Digitonin is a steroidal saponin obtained from the seeds of the foxglove plant *Digitalis purpurea.* It binds to and forms pores in membranes by complexing with membrane cholesterol and other β-hydroxysterols (Mooney 1988). The extent of binding to and permeabilization of membranes therefore depends on the accessibility of the membrane and its sterol composition (Schulz 1990). For our purpose of separating the cytosolic and nuclear fraction of eukaryontic cells we used a Digitonin (Sigma Aldrich, USA) concentration of 130 µg/ml. Before the fractionation HEK293 or other cells were washed two times with TBS (Section V, 1.6, Table 8) on the culture dish before harvested in 200-500 µl TBS containing protease and phosphatase inhibitors (Complete and Phosstop, Roche Diagnostics, Swiss). Cells were then pelleted by centrifugation for 5 min, with 1000 x *g*, at 4 °C. The supernatant was discarded and the cell pellet was resuspended in TBS containing 1.3 % Digitonin and the mentioned protease and phosphatase-inhibitors. In the following the cells were kept on ice and membrane permeabilization was checked occasionally under the Microscope (Microscop SZX12, Olympus). When the majority of the cells (> 98 %) appeared to be lysed, which was mostly the case after 15-20 minutes, the nuclei were sedimented by another

centrifugation step (10 min; 2000 x *g*, 4 °C). The supernatant comprising of the cell cytoplasm was collected separately and the pellet, containing the nuclei, was resuspended in TBS containing 0.5 % NP40 (Sigma Aldrich, USA) and the mentioned Protease - and Phosphatase-inhibitors. Although the NP40 facilitates nuclei lysis, the sample was sonified with an Amplitude of 12 V for approximately 10 seconds on ice to break the nuclear membrane. Purity of nuclear (N)- and cytosolic (C)- fractions were determined by Western blot analysis applying the fraction specific antibodies. Lamin A/C is a nuclear marker, which shouldn´t be detected in the cytosol, whereas GAPDH as a cytosolic marker should only be found in the cytosolic fraction. The workflow of the Digitionin based cell fractionation is schematically illustrated in Figure 15 (Section V, 2.4.3.).

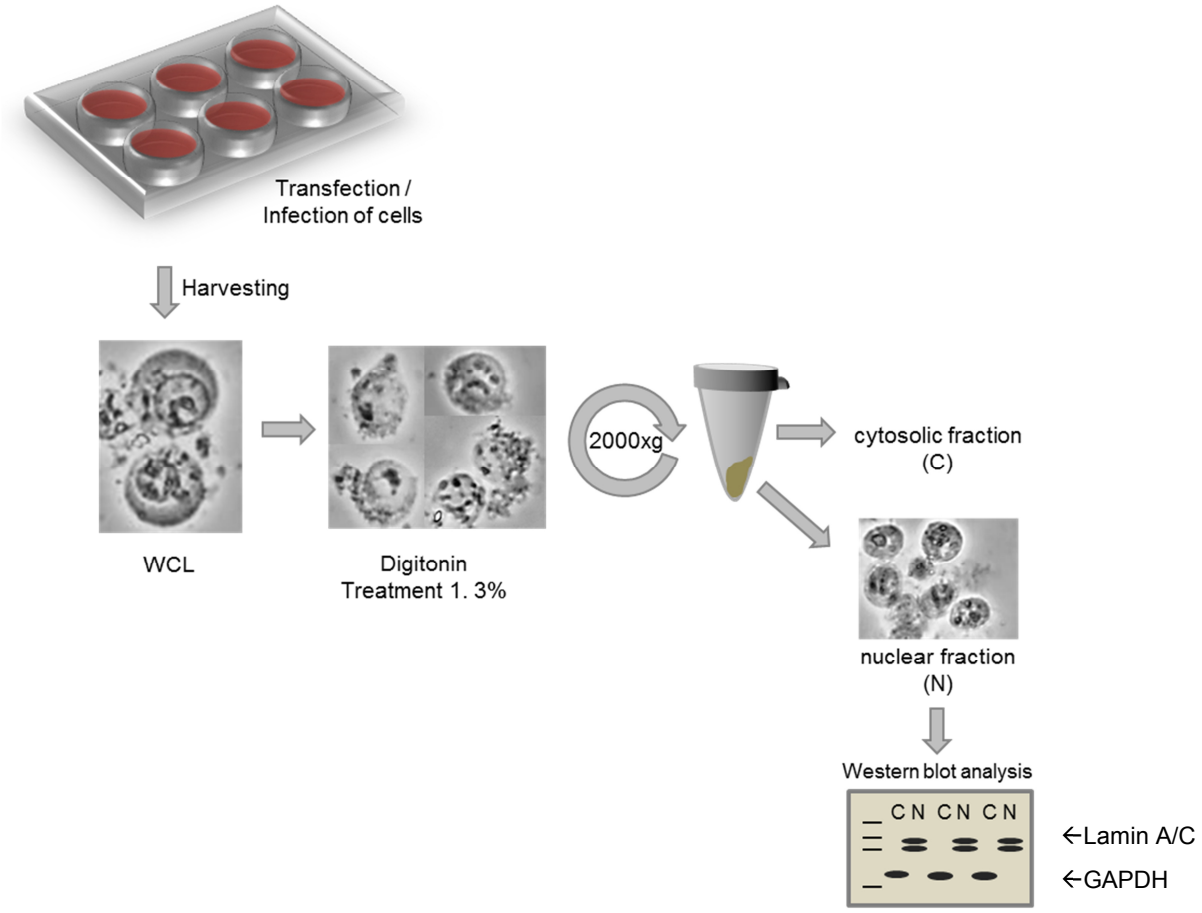

Figure 15: Schematic workflow of the Digitonin based cell lysis.
Infected or transfected cells were washed on the plate before harvested in TBS. The intact cells in the whole cell lysate (WCL) were pelleted and subsequently suspended in TBS containing 1.3 % Digitionin. Digitonin treatment leads to permeabilization of the cellular membrane. Examples of HEK293 cells with disrupted membranes, after incubation with Digitonin are exemplary depicted (middle). Centrifugation sediments the nuclei and the supernatant contains the cytoplasmic fraction. Resuspended nuclei (right side) are sonified to break the nuclear membrane.Purity of both fractions is controlled by Western blot analysis employing specific antibodies. LAMIN A/C served as a control for the nuclear fraction, whereas GAPDH can only be found in the cytosol of cells.

2.5. Statistical methods

For quantification of protein band intensity, films were scanned with a CanonScan 4400F (Canon, Tokio, Japan) with a resolution of 300-500 dpi and signals were analyzed using the ImageJ analysis software Version 1.43u (National Institute of Health, NIH). For further statistical analysis, either to evaluate the nuclear YopM distribution (Section VI, 3.2, Figure 26C) or the expression of IL-10, IL-6, tnf and IL-1β (Section VI, 5), One-way ANOVA, Two-way ANOVA, or t-tests were performed together with the Bonferroni´s multiple comparisons test by employing the GraphPad Prism 5 software (GraphPad Software, USA)

VI Results

1. YopM from *Y. enterocolitica* WA313 interacts with the DEAD-box helicase 3 (DDX3)

1.2 YopM and DDX3 associate in infection and transfection experiments

YopM has been described as one of the key regulators to establish *Yersinia* virulence in vivo (Kerschen et al. 2004; Leung et al. 1990). One approach to enlighten its physiological role is to search for novel eukaryotic interacting proteins. This approach was pursued by Dr. Moritz Hentschke, when he identified several eukaryotic proteins binding to YopM. He affinity purified a tagged YopM from lysates of *Yersinia* infected J774A.1 cells. To achieve bacterial translocation of the tagged YopM he recomplemented the *Y. enterocolitica* serotype O:8 strain WA314(WA314ΔYopM), defective in YopM, with a bacterial expression vector encoding full length YopM fused to a streptavidin-(SBP) and calmodulin- binding peptide (CBP) sequence. This gave rise to a new strain named WA314ΔYopM(pYopM-SBP-CBP) (Hentschke et al. 2010). The resulting SPB-CBP tagged YopM was shown to be translocated into the host cytoplasm and could be affinity precipitated from cell lysates of WA314ΔYopM(pYopM-SBP-CBP) infected J774A.1 cells (Section V; 2.3.1.4). The YopM-SBP-CBP precipitates were separated by SDS-PAGE and visible comassie stained bands were subsequently analyzed by peptide mass fingerprinting. In addition to YopM-SBP-CBP itself and the well-known interaction partners of YopM, RSK1 and PKN2, and their respective isoforms (RSK2, PKN1) (Hentschke et al. 2010), a protein named DEAD-box helicase 3 (DDX3) was identified in the precipitates (Berneking et al. 2016). To confirm the association of YopM and DDX3 we infected J774A.1 cells with WA314ΔYopM(pYopM-SBP-CBP) and a *Yersinia* strain translocating untagged YopM (WA314ΔYopM(pYopM)) as well as a strain translocation a SBP-CBP-tagged YopE (WA314ΔYopE(pYopE-SBP-CBP). The latter stains served as controls to exclude unspecific binding of YopM to the streptavidin/calmodulin sepharose or unspecific binding of cellular proteins to the SBP-CBP tag. Lysates of the infected cells and eluates of each purification step were analyzed by Western blotting for the presence of DDX3. DDX3 co-precipitated with YopM-SBP-CBP, but was not detectable in precipitates from WA314ΔYopM(pYopM), or WA314ΔYopE(pYopE-SBP-CBP) infected cells. In addition to endogenous DDX3, RSK1 and PKN co-immunoprecipitated with YopM-SBP-CBP (Section VI, 1.2., Figure 16). Missing Western blot signals for RSK1 and PKN in the biotin- and Ca^{2+}-eluates from WA314ΔYopM(pYopM) or WA314ΔYopE(pYopE-SBP-CBP) infected cells confirmed the specificity of the affinity precipitation approach.

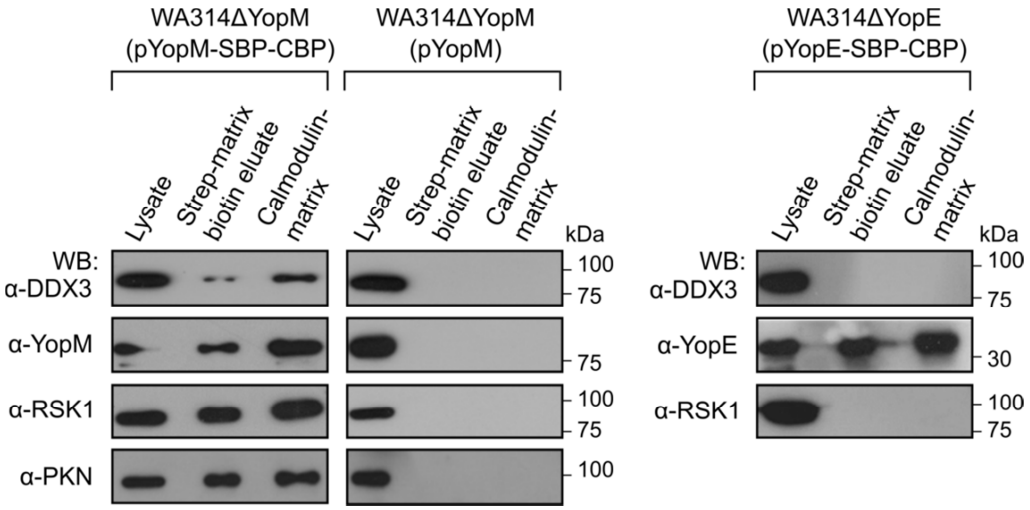

Figure 16: Western blot analysis of Tandem Affinity purified YopM-SPB-CBP confirmed interaction with DDX3, RSK1 and PKN in J774A.1 cells.

J774A.1 cells were infected with WA314ΔYopM(pYopM-SBP-CBP), WA314ΔYopM(pYopM) or WA314ΔYopE(pYopE-SBP-CBP). Proteins eluting from streptavidin-sepharose (biotin elution) and calmodulin-sepharose (boiling in sample buffer) were analyzed by Western blot using indicated antibodies.

To further confirm the interaction of DDX3 and YopM we performed GST-pulldown experiments in GST-myc-YopM- and GST- expressing HEK293 cells. Endogenous DDX3 co-precipitated with GST-myc-YopM but not with GST alone, excluding unspecific binding of DDX3 on the glutathione sepharose beads (Section VI, 1.2., Figure 17).

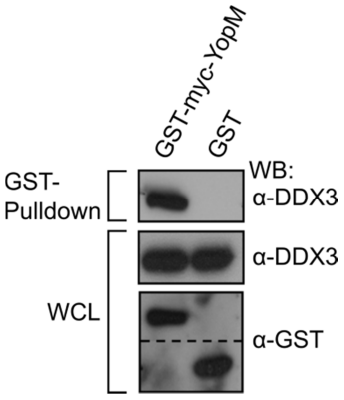

Figure 17: GST–myc-YopM pulldown co-precipitates endogenous DDX3.

GST-myc-YopM or GST expressing HEK293 cells were lysed and GST precipitation was carried out with glutathione sepharose beads. Precepitates were then analyzed by Western blotting using indicated antibodies. Input of GST–myc-YopM and DDX3 was determined by blotting 2.5 % of the whole cell lysates (WCL).

Vice versa, both transfected and bacterially translocated YopM co-immunoprecipitated with endogenous DDX3 in HEK293 cells (Figure 18). Taken together, these experiments show that YopM and DDX3 associate in the *Yersinia* infected host cells. Both proteins show interaction not only if YopM is artificially overexpressed by transfection (Section VI, 1.2., Figure 17, Figure 18A), but also in *Yersinia* infected cells that harbour bacterially translocated "lifelike" amounts of YopM (Section VI, 1.2., Figure 16, Figure 18B).

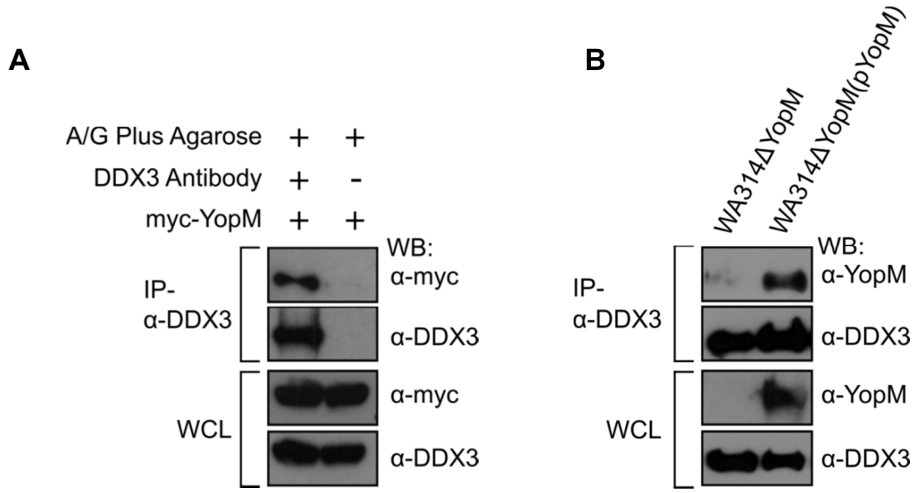

Figure 18: Myc-YopM overexpressed by transfection and bacterially translocated YopM co-immunoprecipitate with endogenous DDX3.
A) Endogenous DDX3 was immunoprecipitated in HEK293 cells expressing myc-YopM. Precipitates and whole cell lysates (WCL) were analyzed by Western blot using indicated antibodies. **B)** Bacterially translocated YopM co-immunoprecipitates with endogenous DDX3. Endogenous DDX3 was immunoprecipitated in HEK293 cells infected with WA314ΔYopM(pYopM) or WA314ΔYopM for 90 min. Precipitates and WCL were analyzed by Western blot analysis using indicated antibodies.

1.3. The LRR-region of YopM and the N-terminal region of DDX3 mediate the association between YopM and DDX3

YopM belongs to the group of Leucine rich repeat (LRR) proteins. The different isoforms of YopM have a conserved N-terminus with two α-helices and a conserved but unstructured C-terminus (Boland et al. 1998). The YopM from *Y. enterocolitica* WA314 consists of 20 LRRs. A schematic overview of full length YopM together with the truncated versions applied in this study is shown in Figure 19A (Section VI, 1.3). To decode the regions of YopM that mediate interaction with DDX3 truncated myc-tagged versions of YopM, that either lack the C-terminus (myc-YopM_1-481) or additionally the first 34 aa of the N-terminus (myc-YopM_34-481), were expressed in HEK293 cells. Endogenous DDX3 co-immunioprecipitated with all three myc-tagged YopM versions (Section VI, 1.3, Figure 19B). Conversely, flag-DDX3 precipitated both YopM deletion constructs (Section VI, 1.3, Figure 19C). Thus, we showed that the LRR region and the two N-terminal α-helices of YopM are sufficient for binding to DDX3.

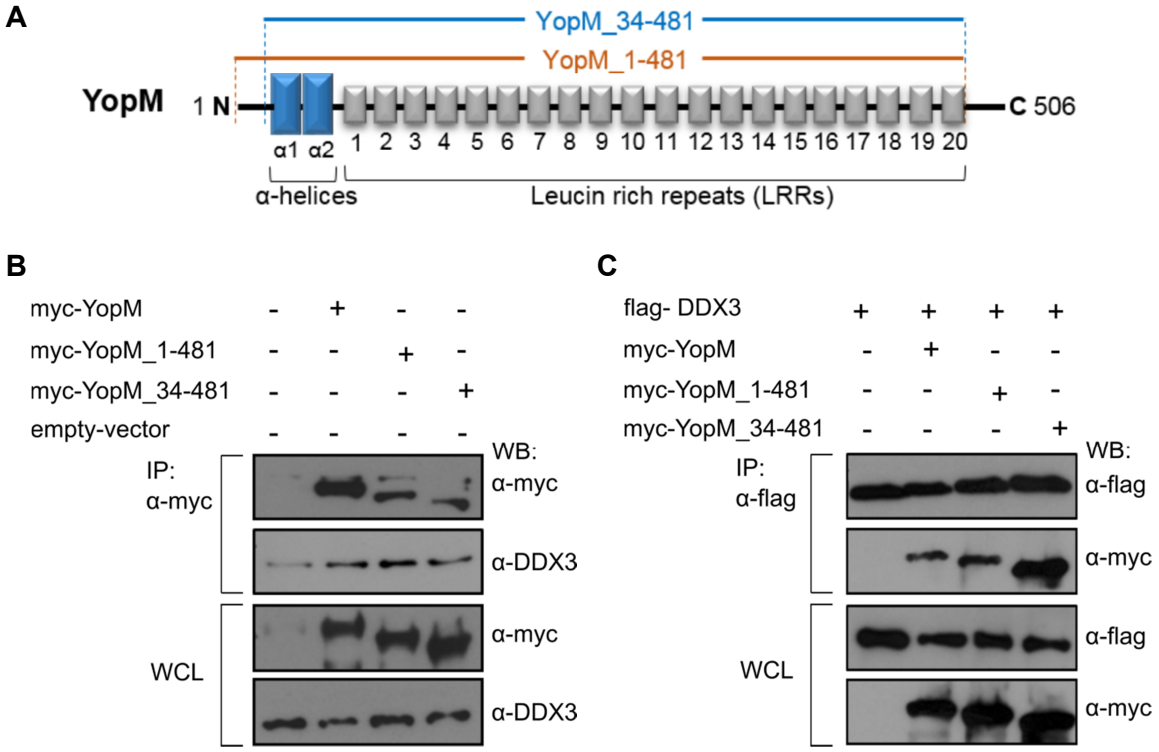

Figure 19: C and N- terminally truncated YopM binds to DDX3.
A) Schematic overview of YopM from *Y. enterocolitica* WA314. The N-terminal blue rectangles in the YopM represent the α-helices α1 and α2. Boxes numbered 1 to 20 represent the Leucine rich repeats (LRRs) of YopM. YopM_34-481 and YopM_1-481 are the truncated versions of YopM used in this study. B and C) Neither the N- nor the C-terminus of YopM facilitate binding to DDX3. **B)** Myc-YopM and truncated versions expressed in HEK293 cells were immunoprecipitated and analyzed for the presence of endogenous DDX3. Precipitates and whole cell lysates (WCL) were analyzed by Western blot using indicated antibodies. C) HEK293 cells were first transfected with vectors expressing truncated versions of myc-YopM. Endogenous DDX3 was precipitated and precipitates were analyzed by Western blot analysis using the indicated antibodies.

Next, we wanted to experimentally elucidate the DDX3 regions, which mediate binding to YopM. For this purpose HEK293 cells were cotransfected with vectors expressing GST-myc-YopM and either full length DDX3 (DDX3_1-662-HA) or truncated versions thereof (DDX3_1-418-HA, DDX3_418-662-HA). GST-pulldowns demonstrated that YopM associates only with full length DDX3 and the C-terminal truncated version of it. N-terminal truncated DDX3 (DDX3_418-662-HA) could not be precipitated by GST-myc-YopM (Section VI, 1.3., Figure 20B), which indicates that the N-terminal region of DDX3 facilitates its association with YopM.

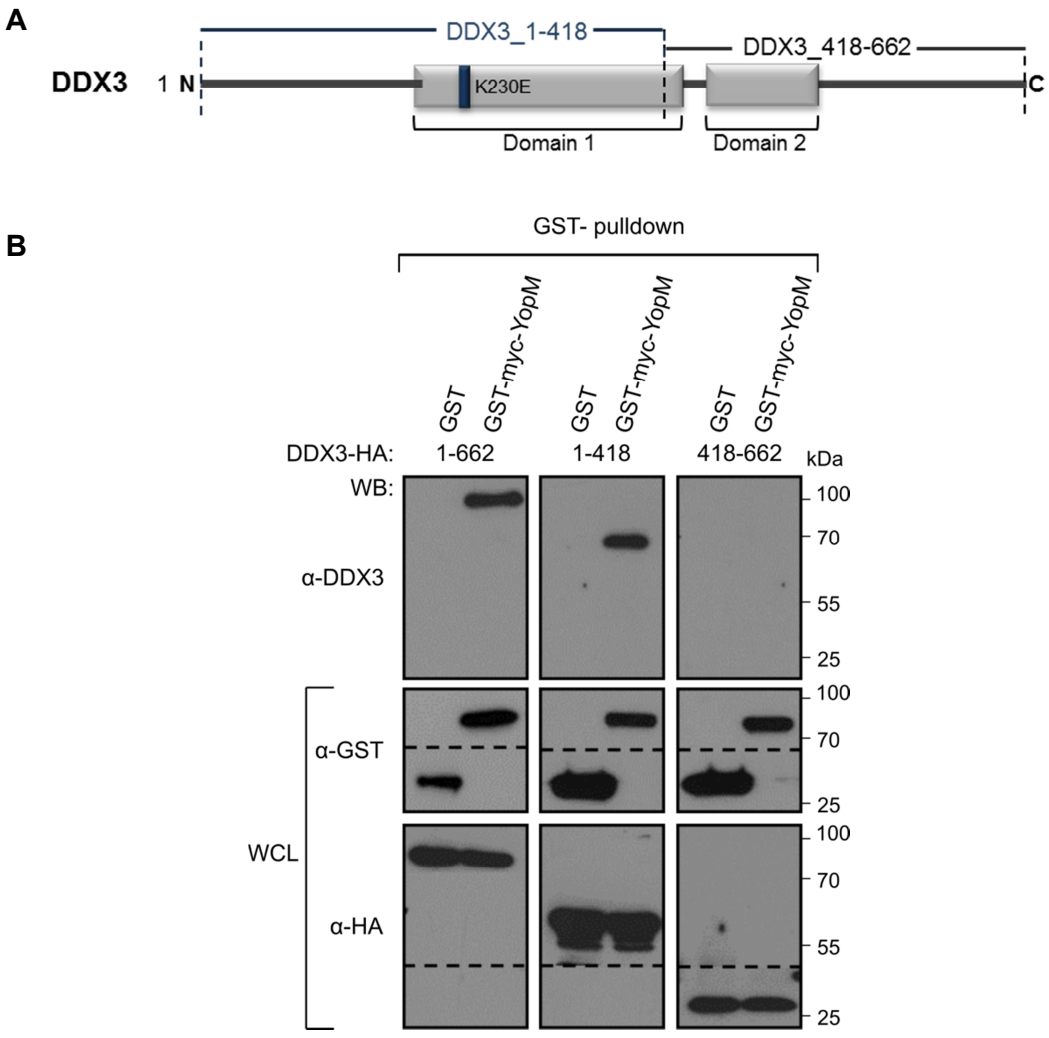

Figure 20: The N-terminus of DDX3 is important for binding toYopM.
A) Schematic representation of DDX3. The gray rectangles in the DDX3 scheme correspond to the two helicase core domains (1 and 2). Truncated constructs used in GST-pulldown and immunoprecipitation are marked by amino acid numbers and brackets. **B)** GST-YopM Pulldown of transfected DDX3 constructs. GST-myc-YopM, GST and indicated HA-tagged DDX3 constructs were co-expressed in HEK293 cells and proteins co-precipitated by glutathione sepharose beads or in whole cell lysate (WCL) were detected by Western blot analysis using the indicated antibodies.

Taken together, we could narrow down the interaction surface of YopM and DDX3 to YopM´s amino acid region 34-481, encompassing the two α-helices and the LLRs and the N-terminus of DDX3.

2. Complex formation of YopM and its eukaryotic interaction partners RSK, PKN and DDX3

2.1. YopM forms a ternary complex with RSK and either DDX3 or PKN

Previous studies demonstrated that YopM forms a protein complex with the two cellular seronine threonine kinases RSK and PKN (McDonald et al. 2003; Hentschke et al. 2010; Höfling et al. 2014). Studies have shown that both kinases normally do not interact within eukaryotic cells. Only in the presence of YopM, RSK1/RSK2 could be co-immunoprecipitated with PKN1/PKN2 (Hentschke et al. 2010). Therefore, it was proposed that YopM functions as a mediator, which brings together different isforms of PKN and RSK in a triple complex. Immunoprecipitations of myc-YopM expressed in HEK293 cells revealed an interaction of YopM with RSK1, PKN and DDX3 (Section VI, 2.1., Figure 21) as observed in WA314ΔYopM(pYopM-SBP-CBP) infected J774A.1 cells (Section VI, 1.2., Figure 16). We next asked whether DDX3 is part of the complex formed between YopM, RSK1 and PKN. To answer this question experimentally we co-transfected myc-YopM expressing HEK293 cells with vectors expressing DDX3-flag, PKN-flag or GST-HA-RSK1 (Section VI, 2.1.,Figure 21B ,C, D). Subsequent flag-immunoprecipitation and GST-HA-RSK1-pulldown experiments showed that neither of the three proteins DDX3, RSK1 or PKN1 interact with each other in the absence of YopM (Section VI, 2.1, Figure 21). Interestingly, in the presence of YopM, DDX3-flag immunoprecipitated RSK1 but not PKN (Section VI, 2.1, Figure 21B). Vice versa, RSK1 but no DDX3 was detectable in the PKN1-flag-immunoprecipitates when YopM was present (Section VI, 2.1, Figure 21C). The GST-HA-RSK1-pulldown experiment served as a positiv control. In GST-HA-RSK1 and myc-YopM co-transfected cells the GST-HA-RSK1 co-precipitated YopM, DDX3 and PKN (Section VI, 2.1, Figure 21D). As a consequence of these experiments we conclude that YopM at least induces the formation of two ternary complexes within the infected host cells. These complexes comprise either YopM, DDX3, RSK1 or YopM, RSK1 and PKN1.

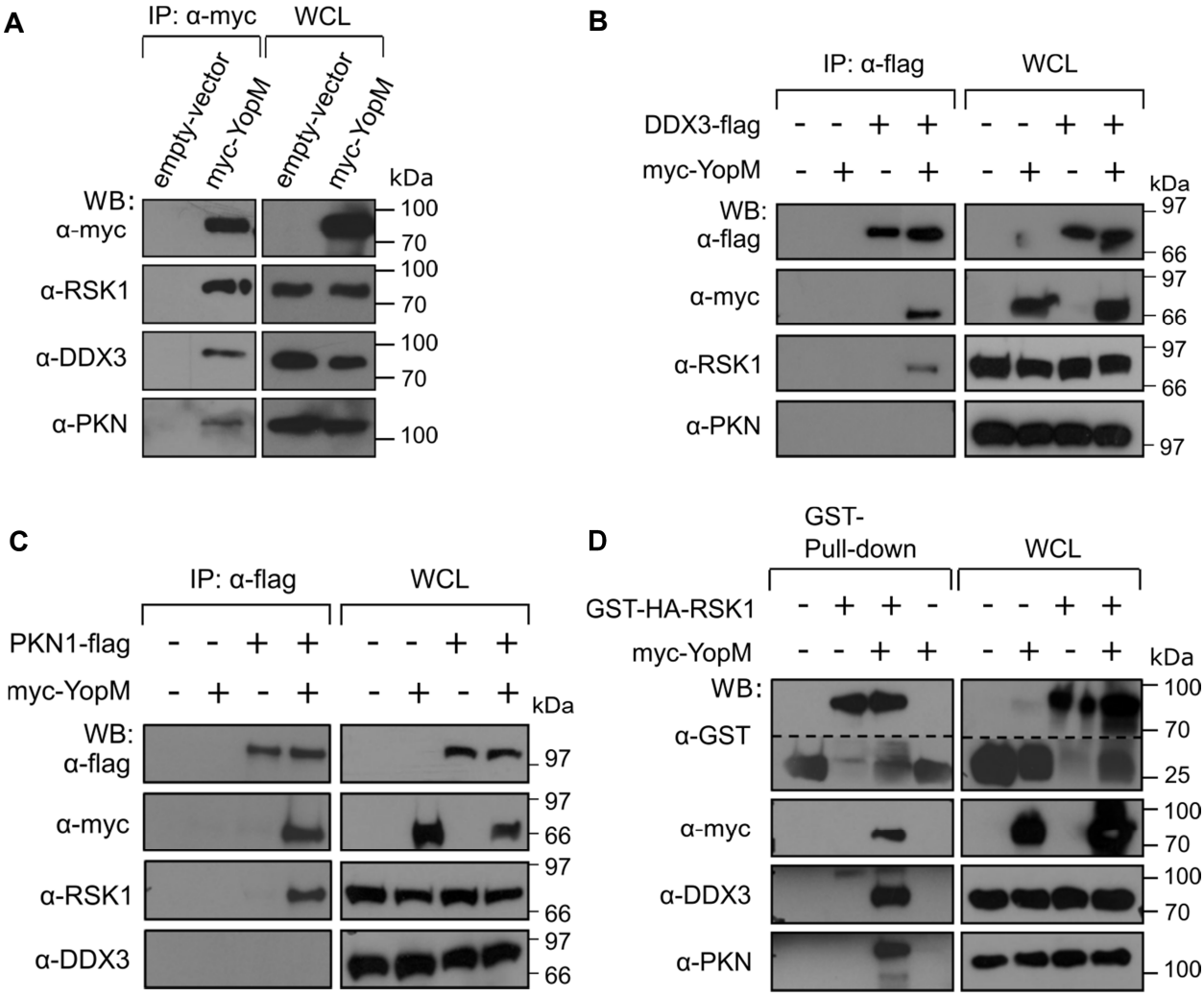

Figure 21: In the presence of YopM the two protein complexes YopM, RSK1, PKN1 and YopM, RSK1, DDX3 are formed.

A) HEK293 cells expressing myc-YopM or an empty vector (pCS2+MT) were lyzed and the lysates were subjected to anti—myc-immunoprecipitation. Corresponding precipitates were analyzed for the presence of RSK1, PKN and DDX3 in Western blot analysis employing the specific antibodies. HEK293 cells expressing myc-YopM were cotransfected with vectors expressing either **B)** DDX3-flag, **C)** PKN1-flag or **D)** GST-HA-RSK1 were lyzed and the lysates were subjected to anti-flag **(B and C)** or anti-GST immunoprecepitation. Precipitates and whole cell lysates (WCL) were analyzed by Western blot using indicated antibodies.

2.2. The protein complexes YopM, RSK1, PKN and YopM, RSK1, DDX3 are formed in the cytosol and nucleus of host cells

YopM and its eukaryotic interaction partners RSK, PKN and DDX3 are known to be present in the cytoplasm and nucleus of eukaryotic cells (Frödin & Gammeltoft 1999; Schröder 2010; Skrzypek et al. 2003; Benabdillah et al. 2004; Mukai et al. 1996; Mukai 2003). First we investigated the cellular distribution of YopM and DDX3. Immunofluorescence staining of myc-YopM in HeLa cells visualized a nuclear (N), nuclear-cytosolic (NC) or cytosolic (C) distribution of YopM (Section VI, 2.2., Figure 22A). In fact; when myc-YopM expressing

HEK293 cells were separated in cytosolic (C) and nuclear (N) fractions, the specific myc-YopM Western blot signal appeared to be more intensive in the cytosolic- (C) than in the nuclear- (N) fraction (Section VI, 2.2., Figure 22B). Although DDX3 was described as a protein shuttling between the cytosol and the nucleus (Owsianka & Patel 1999; Yedavalli et al. 2004; Lai et al. 2008; Schröder et al. 2008) the immunofluorescence staining of endogenous DDX3 in HeLa cells conveyed the impression of a predominantly cytosolic localization of DDX3 (Section VI, 2.2., Figure 22C) similar to YopM.

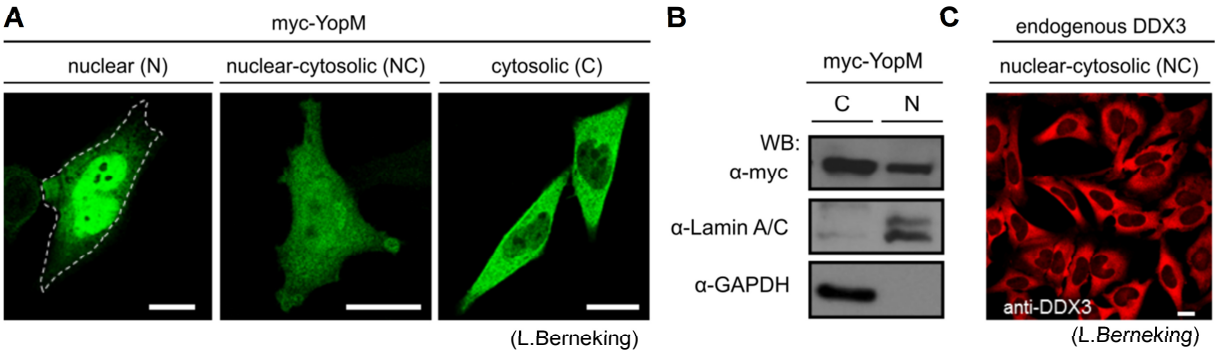

Figure 22: Localization of YopM and DDX3 within the cell.
A) HeLa cells transfected with myc-YopM expressing vectors were immunostained and analyzed by fluorescence microscopy. Representative cells with a nuclear (N), nuclear-cytosolic (NC) and cytosolic (C) myc-YopM distribution are depicted. This experiment was performed in cooperation with Laura Berneking. Scale bar, 20 µm **B)** HEK293 cells transfected with myc-YopM expressing vectors were fractionated in cytosol (C) and nucleus (N) and analyzed by Western blotting with the indicated antibodies. Purity of the cell fractions was controlled with specific antibodies against marker proteins. Lamin A/C is a nuclear protein whereas GAPDH exists in the cytoplasm. C) Staining of endogenous DDX3 in HeLa cells showed a primary cytosolic localization. Scale bar, 20 µm.

Regardless the apparent predominant cytoplasmatic localization of YopM and DDX3 we next asked, whether both complexes (YopM, RSK1, PKN/YopM, RSK1, DDX3) are also formed in the nucleus. GST-HA-RSK1-pulldown experiments, in either the cytosolic- (C) or nuclear- (N) fraction of GST-HA-RSK1 expressing HEK293 cells showed that PKN as well as DDX3 co-precipitate with RSK1, if myc-YopM is present (Section VI, 2.2, Figure 23). Therefore, it is likely that both ternary complexes comprising of (YopM, RSK1, PKN and YopM, RSK1 and DDX3) are formed in the cytoplasm and nucleus of *Y. enterocolitica* WA314 infected cells.

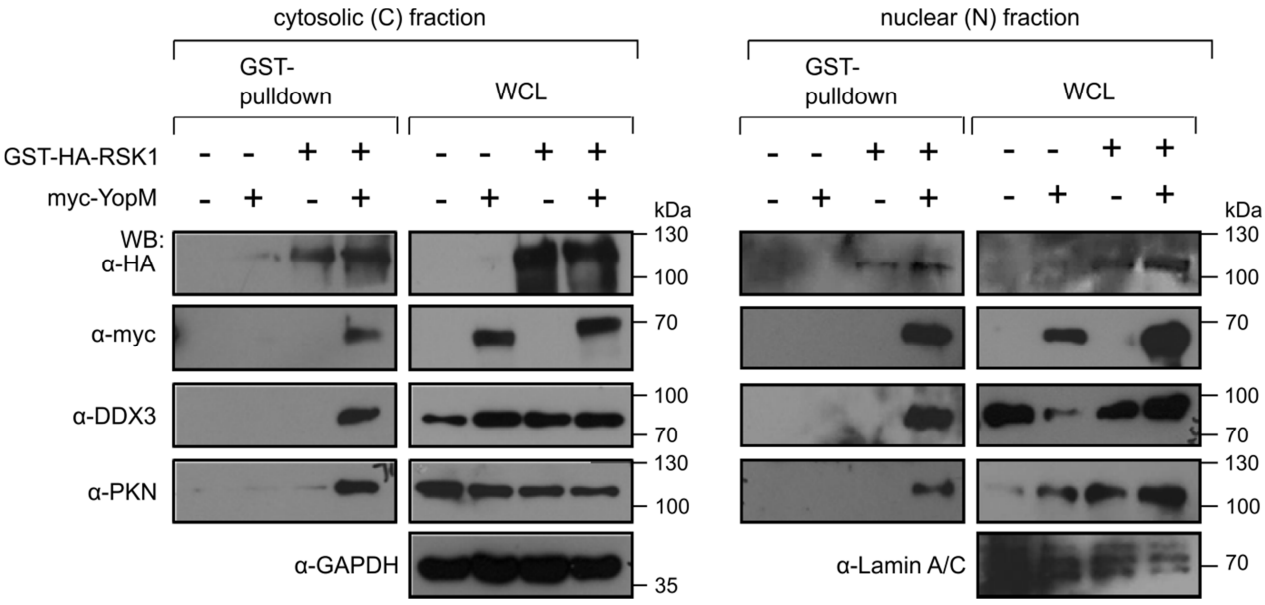

Figure 23: Complexes of YopM, RSK1 and either PKN or DDX3 are formed in the cytosol and nucleus of eukaryotic cells.

HEK293 cells were co-transfected with GST-HA-RSK1- and myc-YopM- expressing vectors. 48 h after transfection the cells were separated in cytosolic- (C) and nuclear- (N) fractions.Two perecent of the cytosolic- and nuclear- fractions, here referred to as whole cell lysates (WCL), were immunoblotted and analyzed with the indicated antibodies to confirm presences of the respective proteins in both lyzed cell compartments. Equal amounts of the lysates (WCL) from the corresponding fractions were subjected to GST-HA-RSK1 pulldown experiments.

3. DDX3 mediates nuclear export of YopM via CRM1

3.1. Nuclear export protein CRM1 co-precipitates with YopM and RSK1 via DDX3

Although YopM´s cytosolic and nuclear presence was shown in several studies, neither a nuclear importin nor exportin for YopM had been identified so far. Moreover, the molecular mechanisms regulating the nuclear-cytosolic shuttling of YopM and YopMs putative nuclear activity are still unclear (Skrzypek et al. 1998; Benabdillah et al. 2004). Because YopM´s interaction with the eukaryotic proteins RSK and PKN was proposed to contribute to *Yersinia*'s virulence (Leung et al. 1990; Skrzypek & Straley 1996; LaRock & Cookson 2012; Chung et al. 2014; Hentschke et al. 2010; McDonald et al. 2003) we searched for DDX3 cellular functions, which might be affected by YopM. DDX3 is a nuclear-cytoplasmic shuttling protein that binds to the exportin chromosome region maintenance 1 (CRM1). Further it is a target of multiple virus manipulations (Yedavalli et al. 2004; Schröder et al. 2008). The human immunodeficiency virus (HIV) employs the DDX3/CRM1 mediated export pathway to transport its unspliced and partially spliced mRNA from the nucleus in the cytosol. The HIV viral RNA-binding protein Rev interacts with DDX3, which itself interacts with CRM1, together this protein formation achieves the nuclear export of the mRNA (Yedavalli et al. 2004). Given

these facts, we postulated that DDX3 might also mediate the nuclear export of YopM, similar to the export of the viral RNA-binding protein Rev. First; we confirmed the cellular interaction of DDX3 and CRM1. HEK293 cells were transfected with a flag-DDX3 expressing vector and cell lysates were subjected to anti-flag immunoprecipitation. We found that CRM1 co-immunoprecipitates with flag-DDX3 (Section VI, 3.1, Figure 24A). Secondly, we investigated the interaction of endogenous DDX3 and CRM1 in infection experiments (Section VI, 3.1, Figure 24B). HEK293 cells were either left uninfected or were infected with WA-C(pTTSS) or WA-C(pTTSS+YopM) for 1.5 h. WA-C(pTTSS) is a strain only harbouring the genes of the TTSS on its pYV. Therefore it forms the needle but doesn't´possess any effectors to deliver in the host cytoplasm. The strain WA-C(pTTSS+YopM) has in addition to all genes of the translocation machinery the YopM gene encoded on its virulence plasmid. Thus, WA-C(pTTSS+YopM) is employed to investigate the YopM effects within infection experiments whereas WA-C(pTTSS) serves as a negative control. Cell lysates of the infected cells were subjected to immunoprecipitation of endogenous DDX3. In DDX3 precipitates of uninfected and WA-C(pTTSS) infected cells no specific PKN, RSK1 or CRM1 signal was detectable. On the contrary, in WA-C(pTTSS+YopM) infected cells YopM, RSK1 and CRM1 but not PKN precipitated with endogenous DDX3 (Section VI, 3.3, Figure 24B). Consequently, YopM and/or RSK1 might enhance the association of DDX3 and CRM1 resulting in a detectable CRM1 Western blot signal in the precipitates, whereas the amounts of CRM1 co-precipitated with endogenous DDX3 in uninfected and WA-C(pTTSS) infected cells may be to small to be detected in Western blot analysis. Taken into account this findings we hypothesized that a quadruple complex of YopM, RSK1, DDX3 and CRM1 might exist in the infected cell in addition to the already described complexes YopM, RSK1, PKN and YopM, RSK1, DDX3.

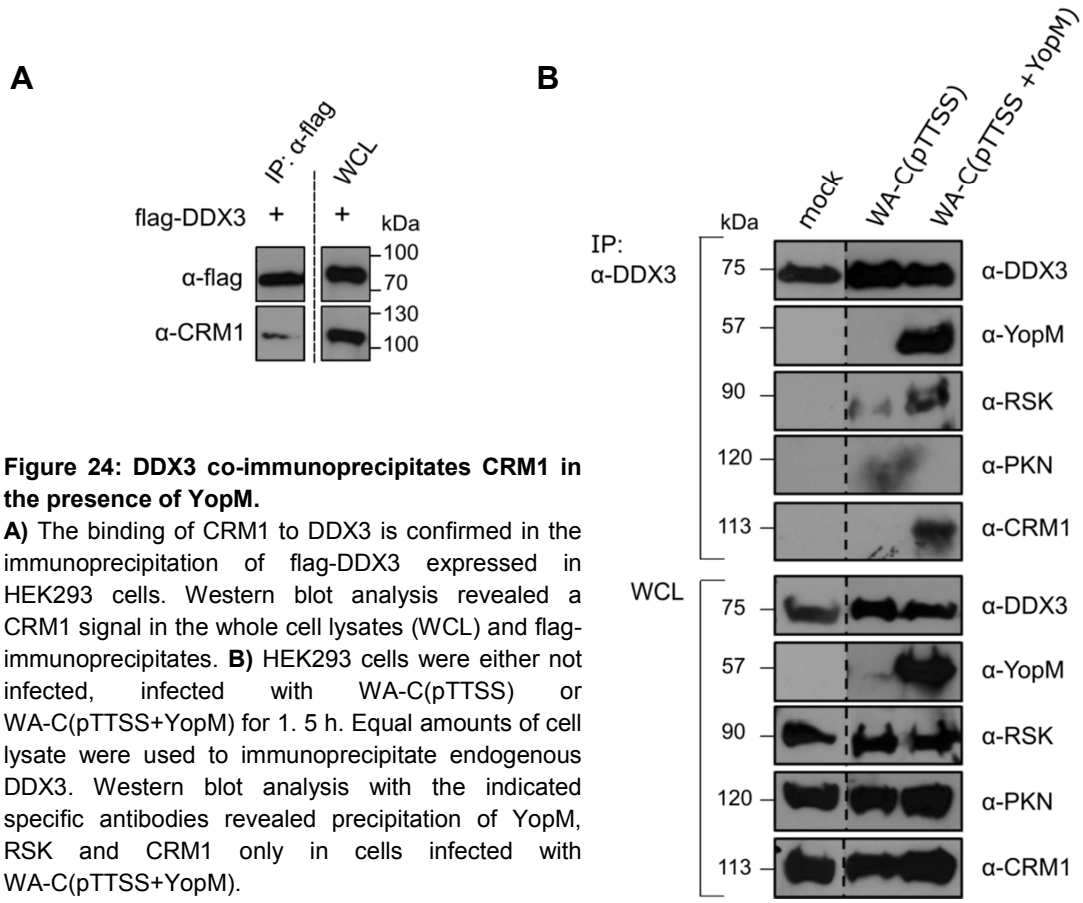

Figure 24: DDX3 co-immunoprecipitates CRM1 in the presence of YopM.
A) The binding of CRM1 to DDX3 is confirmed in the immunoprecipitation of flag-DDX3 expressed in HEK293 cells. Western blot analysis revealed a CRM1 signal in the whole cell lysates (WCL) and flag-immunoprecipitates. **B)** HEK293 cells were either not infected, infected with WA-C(pTTSS) or WA-C(pTTSS+YopM) for 1. 5 h. Equal amounts of cell lysate were used to immunoprecipitate endogenous DDX3. Western blot analysis with the indicated specific antibodies revealed precipitation of YopM, RSK and CRM1 only in cells infected with WA-C(pTTSS+YopM).

3.2. Abrogation of the DDX3/CRM1 mediated nuclear export results in the nuclear accumulation of YopM

After proving the interaction of DDX3, CRM1 and YopM we next asked whether CRM1 mediated DDX3 nuclear export pathway is usurped by YopM to exit the nucleus. Several studies documented that the CRM1 inhibitor Leptomycin B (LMB) abrogates the nuclear export of DDX3 (Yedavalli et al. 2004; Schröder et al. 2008). First we affirmed this proposed inhibitory effect of LMB towards the CRM1 mediated nuclear export of DDX3 in our experimental setting. Immunofluorescence staining of DDX3 in HeLa cells visualized a nuclear accumulation of DDX3 in cells treated with LMB compared to non-treated control cells (Section VI, 3.2, Figure 25). Thus, we could demonstrate that LMB causes a strong nuclear accumulation of DDX3 as described (Yedavalli et al. 2004; Schröder et al. 2008).

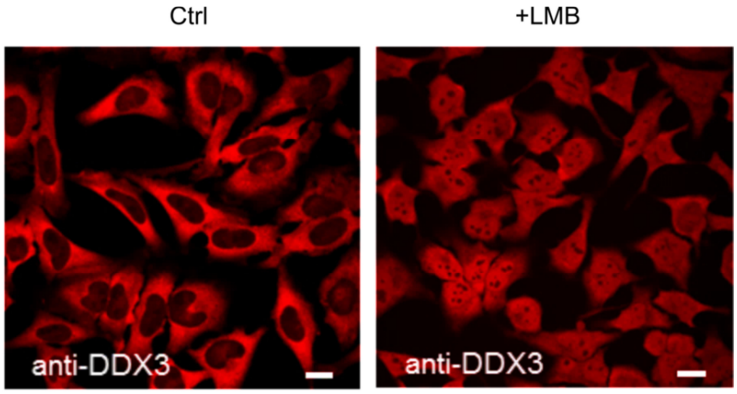

(L.Berneking)

Figure 25: Inhibition of CRM1 leads to nuclear accumulation of DDX3.
HeLa cells were not treated (Ctrl) or treated with 25 nM Leptomycin B (+ LMB) for 4 h and subjected to immunofluorescence staining with α-DDX3 antibody. DDX3 shows a clear shift from the cytosol to nucleus upon the LMB treatment. This experiment was performed in cooperation with Laura Berneking. Scale bar 20µm.

To test whether YopM employs the CRM1 mediated DDX3 nuclear export pathway to shuttle from the nucleus into the cytosol, we first analyzed nuclear and cytosolic distribution of myc-YopM in cells not treated and treated with LMB. For this purpose HEK293 cells were transfected with myc-YopM and exposed to the CRM1 inhibitor LMB prior to fractionation in a cytosol and nucleus. Intensities of myc-specific Western blot signals were determined with ImageJ quantification tool. Total cellular myc-YopM amounts were defined as the sum of corresponding cytosolic- and nuclear myc signals. The percentage of nuclear myc-YopM (% of total) in non-treated control (Ctrl) cells was 9 % and increased to 31 % upon LMB treatment (Section VI, 3.2., Figure 26A, left panels). Thus, YopM's nuclear export is diminished when the CRM1 mediated nuclear export pathway is blocked by LMB treatment. To directly attribute the nuclear export of YopM to its interaction with DDX3 we employed siRNA technology to silence DDX3 expression. HEK293 cells were transfected with myc–YopM expression vectors prior to siRNA transfection and cell fractionation. Quantification of nuclear myc-YopM signals revealed an increase from 10% to 26% upon treatment of cells with DDX3 specific siRNA (siDDX3) (Section VI, 3.2., Figure 26A, right panels). To ensure that YopM shows the same behaviour under more physiological conditions, similar experiments were performed in *Yersinina* infected cells. HEK293 cells were either treated with LMB or DDX3 specific siRNA prior to infection with WA-C(pTTSS+YopM) (Section VI, 3.2., Figure 26B). Cells were fractionated and Western blot analysis was performed employing YopM specific antibodies as well as α-GAPDH and α-LAMIN A/C antibody to obtain a calibration signal for cytosolic and nuclear protein amounts in the respective fractions. ImageJ analysis of the Western blot signal intensities and calculation of the relative

cytosolic and nuclear amounts of YopM revealed abundance of YopM in the cytosolic (C) fraction of untreated or siCtrl treated cells. LMB- or siDDX3-treatment significantly increased the relative amount of nuclear (N) YopM. The YopM/Lamin ratio increased almost 2-fold when cells were treated with LMB compared to untreated cells. A distinct 7-fold increase could be observed in the YopM/Lamin ratio between siCtrl and siDDX3 treated cells. Corresponding to the nuclear YopM enrichments, reductions of cytosolic YopM could be observed in the YopM/GAPDH ratio (Section VI, 3.2., Figure 26B). Quantification of the nuclear YopM Western blot signals documented a significant nuclear enrichment of YopM under the DDX3 knockdown condition and at least a tendency of increased YopM under the LMB treatment condition (Section VI, 3.2., Figure 26C). Thus, bacterially translocated YopM accumulates in the nucleus similar to vector-expressed myc-YopM when the DDX3/CRM1 mediated nuclear export pathway is blocked either by LMB- or siDDX3-treatment. These experiments indicate that YopM's nuclear export is dependent on its interaction with DDX3 and that the CRM1 mediated export of DDX3 is one major mechanism by which YopM exits the nucleus.

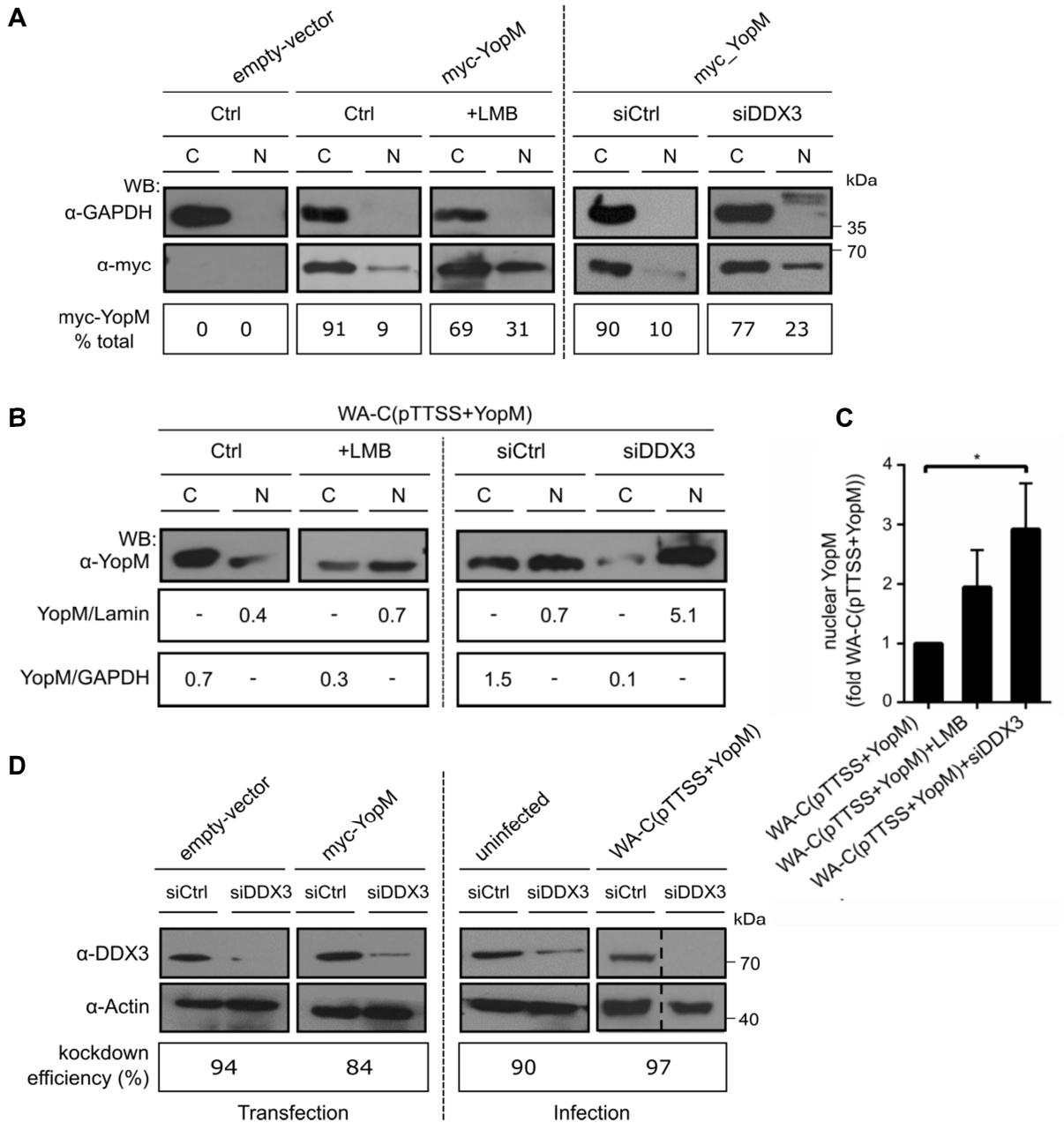

Figure 26: Leptomycin B- or DDX3 siRNA-treatment results in increased nuclear levels of YopM.

A) Myc-YopM expressing HEK293 cells were not treated (control) or treated with 25 nM Leptomycin B (+ LMB) for 4 h (left panel) or were transfected with DDX3 specific (siDDX3) or non-targeting RNA (siCtrl) (right panel). Cells were fractionated in cytosol (C) and nucleus (N) and each fraction was analyzed by Western blot with the indicated antibodies. GAPDH served as a control for clear separation of the fractions. Band intensities of myc-YopM were quantified with ImageJ and the percentage of nuclear and cytosolic YopM was calculated based on the total YopM within the cells. Total YopM was defined as the sum of cytosolic and nuclear myc-YopM Western blot signal intesities. **B)** Before infection with WA-C(pTTSS +YopM) HEK293 cells were either treated with siRNA (non-targeting (siCtrl) or DDX3 specific siRNA (siDDX3)) for 24 h or with LMB for 3-4 h. Cells were fractionated in cytosol (C) and nucleus (N) and each fraction was analyzed by Western blot with the indicated antibodies. Ratio of YopM vs. Lamin or YopM vs. GAPDH was calculated based on the signal intensities of the Western Blot signals, which were determined with ImageJ. The YopM/GAPDH ratio was defined as the cytosolic YopM amount whereas the YopM/Lamin ratio represented the nuclear YopM **C)** Before infection with Yersinia WA-C(pTTSS+YopM) HEK293 cells were not treated or treated with either 25 nM LMB for 4 h or DDX3 specific siRNA for 24 h. 90 min after infecteion the cells were fractionated into cytosol (C) and nucleus (N). Fractions were

subjected to immunoblotting with anti-YopM antibody. Band intensities of YopM signals were determined by ImageJ. The graph depicts the average value of band intensities determined from nuclear YopM Western blot signals in comparison to the nuclear YopM signal intensitiy determined in non treated WA-C(pTTSS+YopM) infected cells. The graph summarizes the values of four different experiments of WA-C(pTTSS+YopM) infected and WA-C(pTTSS+YopM) infected and LMB treated cells. The nuclear YopM signal intensity in infected and with DDX3 specific siRNA treated cells is obtained from three different experiments. Each bar represents mean ± SEM, Bonferroni's multiple comparisons test, *p<0.05. **D)** Western blot analysis of DDX3 in lysates of siCtrl and siDDX3 treated myc-YopM expressing or WA-C(pTTSS+YopM) infected HEK293 cells. Knockdown efficiency was determined using ImageJ. The actin Western blot signal served as a loading control.

3.3. The DDX3/CRM1-mediated nuclear-cytosolic shuttling of YopM is independent of YopM´s interaction with RSK

The C-terminus of YopM is known to mediate the binding to RSK (McCoy et al. 2010). We transfected HEK293 cells with vectors expressing either a C-terminal or C- and N-terminally truncated version of YopM (myc-YopM_1-481 and myc.YopM_34-481). Immunoprecipitation of myc-YopM (full length) confirmed YopMs interaction with RSK1, PKN and DDX3 (Section VI, 3.3., Figure 27A). In contrast the immunoprecipitation of myc-YopM_1-481 and myc-YopM_31-481 showed only a PKN and DDX3 signal in the corresponding Western blot analysis (Section VI, 3.3., Figure 27A). We hereby affirmed that the C-terminus of YopM from *Y. enterocolitica* WA314 mediates the binding to RSK1, as it already has been described for other YopM isoforms (McCoy et al. 2010; Höfling et al. 2014; McPhee et al. 2010). Considering our previous findings, that YopM exits the nucleus via a DDX3/CRIM1 dependent mechanism, we now asked whether this process is RSK1 dependent. For this purpose myc-YopM_1-481 expressing HEK293 cells were treated with LMB, siCtrl or siDDX3 and fractionated in cytosol and nucleus. Nuclear (N) and cytosolic (C) YopM was determined in western blot analysis and signal intensity was defined by ImageJ. The percentage of nuclear myc-YopM_1-481 (% of total) in not LMB treated control (Ctrl) cells was 2 % and increased to 27 % upon LMB treatment (+ LMB) (Section VI, 3.3., Figure 27B, left panel). Under siDDX3 knockdown conditions (siDDX3) the percentage of nuclear YopM_1-481 (% of total) was 32 % which was 10 % higher than in the corresponding control (siCtrl) where the nuclear YopM was 22 % of the total cellular YopM (Section VI, 3.3., Figure 27B; right panel). Thus, the C-terminal truncated version of YopM, unable to bind RSK1, accumulates in the nucleus like full length YopM (Section VI, 3.2., Figure 26A-C) when the DDX3/CRM1 mediated nuclear export is blocked. As a consequence, it can be concluded that YopM's DDX3/CRM1 mediated export occurs independent of its association with RSK1.

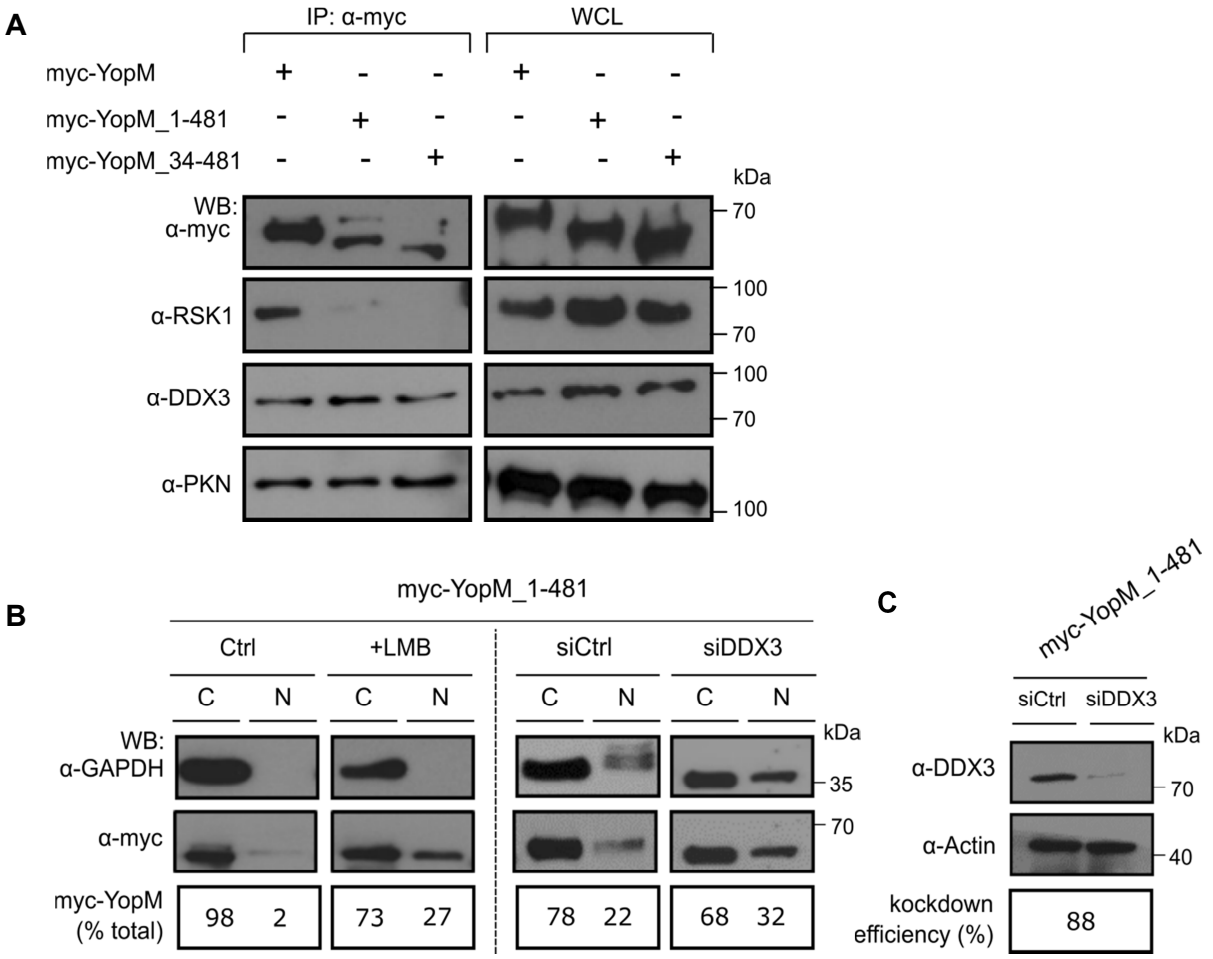

Figure 27: C-terminally truncated YopM fails to associate with RSK1 but is enriched in the nucleus upon treatment with LMB or DDX3 specific siRNA.

A) Indicated myc-YopM constructs were expressed in HEK293 cells for 48 h. Anti-myc immunoprecipitates and whole cell lysates (WCL) were analyzed by Western blotting with the indicated antibodies. In contrast to the truncated myc-YopM (YopM_1-481 and 34-48), full length YopM immunoprecipitated endogenous RSK1. **B)** Myc-YopM_1-481 expressing HEK293 cells were not treated (control, Ctrl) or treated with 25nM LMB (+ LMB) or were transfected with non-targeting (siCtrl) or DDX3 specific (siDDX3) siRNA for 16-24 h. Cells were fractionated in cytosol (C) and nucleus (N) and each fraction was analyzed by Western blot with the indicated antibodies. Cytosolic marker GAPDH served as a control for clear separation of the fractions. Band intensities of myc-YopM were quantified with Image J. **C)** Western blot analysis of DDX3 in lysates of siCtrl- and siDDX3-treated myc-YopM_1-481 expressing HEK293 cells. Knockdown efficiency was calculated using ImageJ. The actin western blot signal served as a loading control.

4. Nucleoplasmatic shuttling of YopM controls the phosphorylation status of RSK1

Previous studies in our laboratory showed that YopM induces a long lasting activation of RSK (Hentschke et al. 2010). RSK1 and its other isoforms are phosphorylated on different serine and threonine residues by several kinases within the ERK/MAPK cascade. The phosphorylation of RSK is a sequential process in which two phosphorylation sites are crucial. One is the serine residue 380 (Ser-380), which provides a docking site for 3'-

phosphoinositide-dependent kinase-1 (PDK1). The second is the serine residue 221 (Ser-221), which is phosphorylated upon docking of PDK1 to RSK and is the last phosphorylation step to fully activate RSK (Anjum & Blenis 2008; Frödin & Gammeltoft 1999; Romeo et al. 2012) (or schematic overview of RSK activation Section VI, 2.1., Figure 5). We first investigated the phosphorylation of RSK1 at Ser-380 and Ser-221 in the presence of YopM in our experimental conditions. HEK293 cells were transfected with myc-YopM expressing vectors or the empty control vector. Lysates of the transfected cells were analyzed for RSK1 phosphorylation by immunoblotting and employing the phospho-RSK specific antibodies α-pS380 and α-pS221. No phosphorylation on residue Ser-380 could be observed and phosphorylation at Ser-221 was only detectable in myc-YopM transfected cells. In addition to the phospho-specific antibodies, an antibody specific for RSK1 was applied in order to determine the total RSK1 quantities in the lysates (Section VI, 4, Figure 28A, left panels). The ratio of phosphorylated vs. total RSK1 was calculated by dividing the respective Western blot signal intensities which were determined with ImageJ. The phospho-Ser-221/RSK1 ratio was almost 2-fold increase in the myc-YopM expressing cells when compared to this ratio in the not YopM expressing control cells (empty-vector). Thus, we confirmed YopM dependent phosphorylation of RSK1 on Ser-221 in the presence of transfected myc-YopM. Next, we investigated the RSK1 phosphorylation in the presence of bacterially injected YopM. HEK293 cells were infected for 1.5 h with different *Y. enterocolitica* strains either translocating YopM (WA-C(pTTSS+YopM) and WA314ΔYopM(pYopM)) or not (WA314ΔYopM and WA-C(pTTSS)). Western blot signals on Ser-380 could only be detected in whole cell lysates of WA314ΔYopM(pYopM) and WA-C(pTTSS+YopM) infected cells. Ser-221 phosphorylation was also enhanced in the cells infected with *Yersinia* strains translocating YopM, when compared to the phospho Ser-221 Western blot signals detected in uninfected or WA314ΔYopM and WA-C(pTTSS) infected cells (Section VI, 4, Figure 28B; left panel). The phospho Ser-221 and Ser-380 vs. endogenous RSK1 ratio reflects the blot signals. The ratio of pS221 and pS380 to RSK1 was 13-times enhanced in lysates of WA314ΔYopM(pYopM) infected cells compared to WA314ΔYopM infected cells (Section VI, 4., Figure 28B; right panel). Thus, we confirmed that YopM enhances the phosphorylation of RSK1 in HEK293 cells regardless if it is artificially expressed or translocated during *Yersinia* infections.

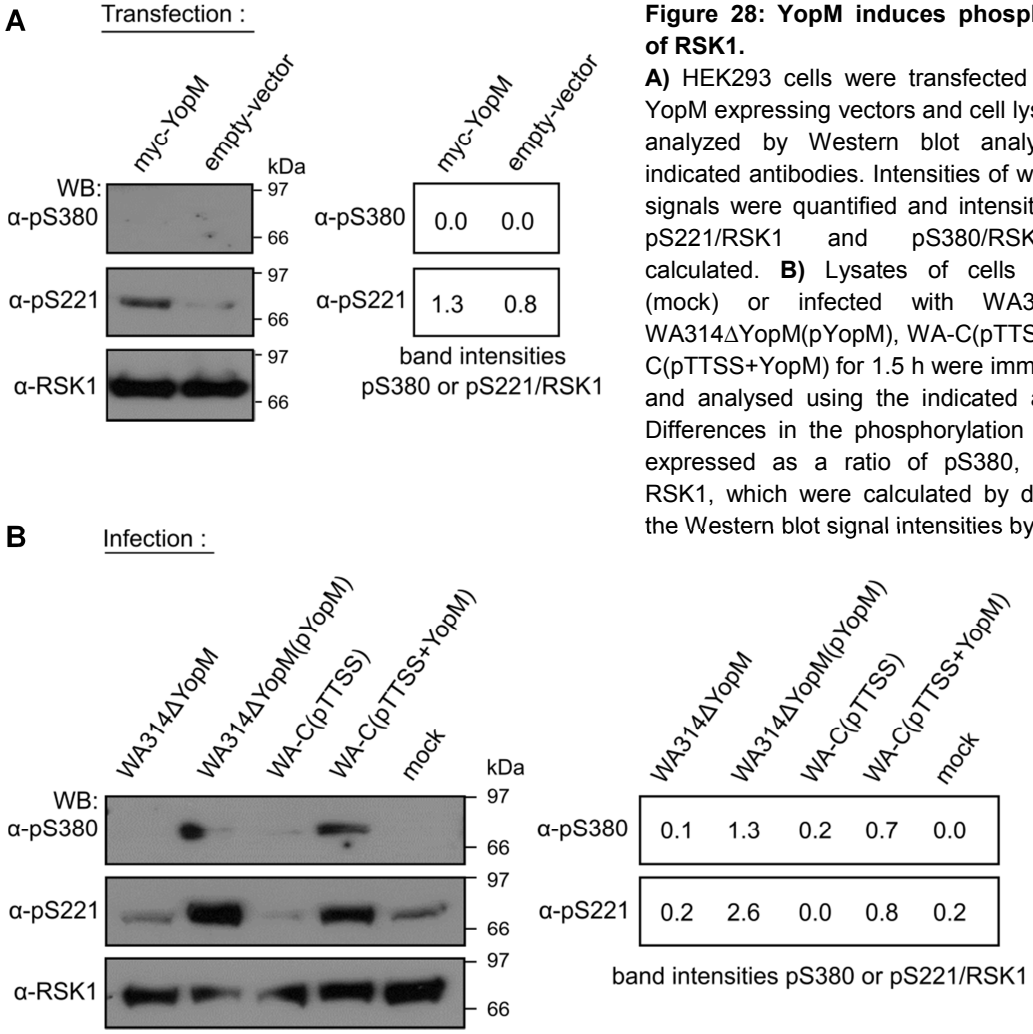

Figure 28: YopM induces phosphorylation of RSK1.
A) HEK293 cells were transfected with myc-YopM expressing vectors and cell lysates were analyzed by Western blot analysis using indicated antibodies. Intensities of western blot signals were quantified and intensity ratios of pS221/RSK1 and pS380/RSK1 were calculated. **B)** Lysates of cells uninfected (mock) or infected with WA314ΔYopM, WA314ΔYopM(pYopM), WA-C(pTTSS) or WA-C(pTTSS+YopM) for 1.5 h were immunoblottes and analysed using the indicated antibodies. Differences in the phosphorylation status are expressed as a ratio of pS380, pS221 vs RSK1, which were calculated by determining the Western blot signal intensities by ImageJ.

In this context we further asked whether nuclear YopM might affect the phosphorylation status of RSK specifically in the nucleus. To answer that question we preformed *Yersinia* infection experiments, fractionated the cells and analyzed the phosphorylation status of nuclear and cytosolic RSK1 with the phospo-specific antibodies. Only in the cytosolic fraction of WA-C(pTTSS+YopM) infected cells phosphorylation on RSK1 could be detected. Neither in uninfected nor in WA-C(pTTSS+YopM) infected cells a strong pS221 or pS380 signal appeared in the corresponding Western blot analysis (Section VI, 4, Figure 29A). Remarkably the cytosolic and nuclear RSK1 distribution was not altered whether the cells were left uninfected or were infected with WA-C(pTTSS) or WA-C(pTTSS+YopM) (Section VI, 4, Figure 29A, bottom panel). The same was observed in HEK293 cells either transfected with myc-YopM expressing vectors or the corresponding empty-vector control. RSK1 distribution remained similar regardless the transfected plasmid. Moreover, only in the

myc -YopM expressing HEK293 cells, cytosolic RSK1 phosphorylation on Ser-221 could be detected (Section 3, 4, Figure 29B, left panel). Next, we overexpressed RSK1 in HEK293 cells by transfecting them with an HA-RSK1 expression vector. This greater RSK1 amounts led to prevailing nuclear RSK1 in cells transfected with only HA-RSK1 or co-transfected with myc-YopM. The additional RSK resulted in already detectable RSK1/HA-RSK1 phosphorylation on Ser-380 and Ser-221 in the nuclear fraction of empty vector co-transfected control cells (Section VI, 4, Figure 29B, middle panel). The presence of myc-YopM further enhanced the phosphorylation status of RSK1/HA-RSK1 on both serine residues (S380 and S221) and led to detectable RSK1 phosphorylation in the nuclear fraction but also in the cytosol (Section VI, 4, Figure 29B, middle panel). Quantification of Western blot signal intensities revealed a 23-fold increased pS221/RSK1 ratio in the cytosol and a 3.5-fold increased pS221/RSK1 ratio in the nucleus when comparing the ratios determined in the HA-RSK1/myc-YopM expressing cells with the ratio in the HA-RSK1 expressing cells. The pS380/RSK1 ratio in HA-RSK1/myc-YopM co-expressing cells was 0.9-fold increased in the cytoplasm and 5 fold increase in the nucleus when comparing these ratios with the ratios determined in only HA-RSK1 expressing cells (Section VI, 3, Figure 29B; right panel). The relative distribution of cytosolic and nuclear RSK1/HA-RSK1 remained again unchanged regardless whether YopM was present or not (Section VI, 3, Figure 29B; bottom panel). As metioned before, overexpression of HA-RSK1 induced a re-distribution of cytosolic and nuclear RSK1. Nuclear RSK1/RSK-HA levels were higher than the cytosolic levels (Section VI, 3, Figure 29B, middle panel), which is opposite to the distribution of endogenous RSK1 (Section VI, 3, Figure 29B, right panel). We therefore concluded that quantities of endogenous nuclear RSK1 might be too low to detect the phosphorylated portions of RSK1 by Western blot analysis. In this regard we can state that YopM induces phosphorylation of RSK1 in the cytosol and nucleus of cells without altering the RSK1 distribution in the respective compartment.

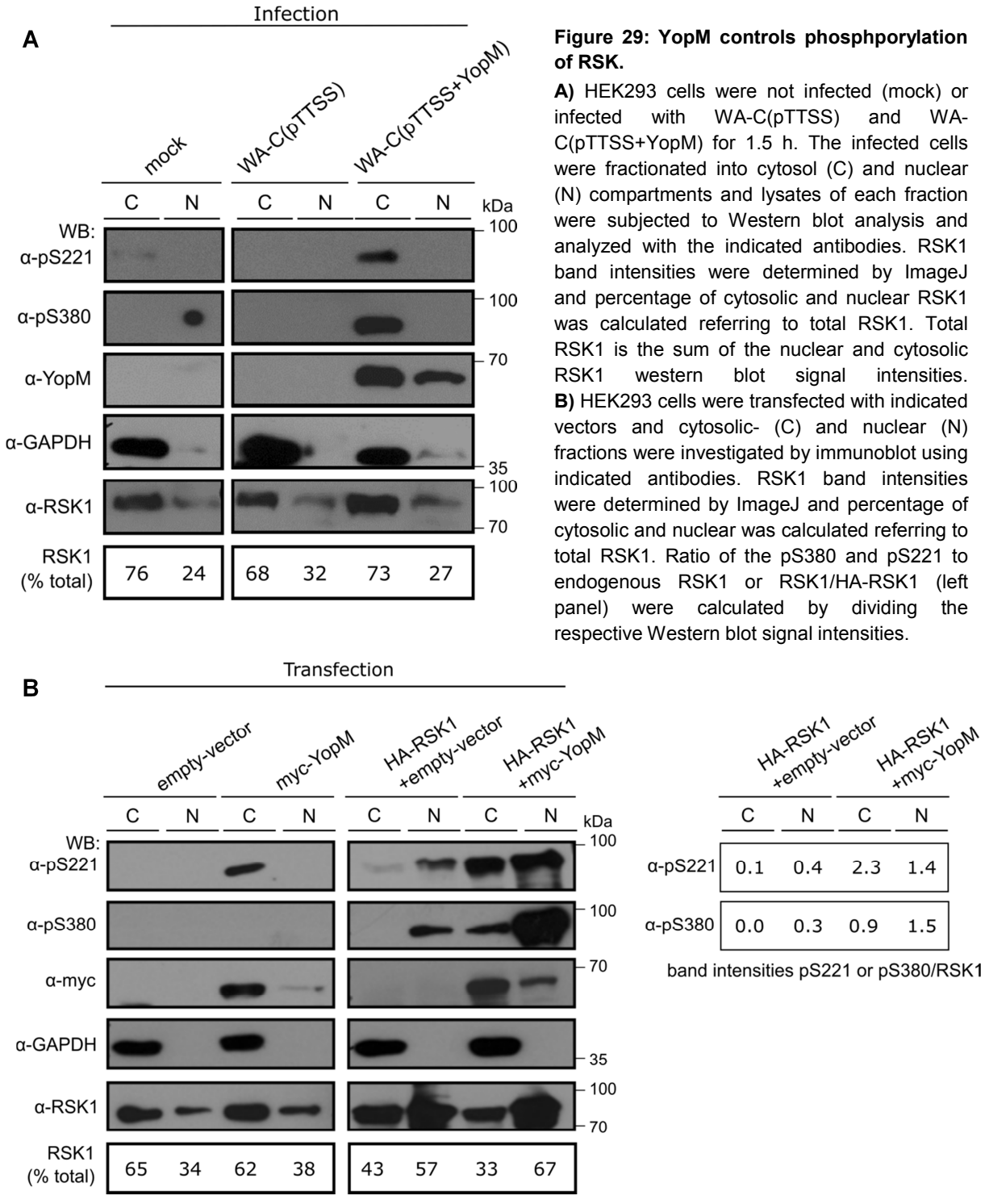

Figure 29: YopM controls phosphporylation of RSK.

A) HEK293 cells were not infected (mock) or infected with WA-C(pTTSS) and WA-C(pTTSS+YopM) for 1.5 h. The infected cells were fractionated into cytosol (C) and nuclear (N) compartments and lysates of each fraction were subjected to Western blot analysis and analyzed with the indicated antibodies. RSK1 band intensities were determined by ImageJ and percentage of cytosolic and nuclear RSK1 was calculated referring to total RSK1. Total RSK1 is the sum of the nuclear and cytosolic RSK1 western blot signal intensities. **B)** HEK293 cells were transfected with indicated vectors and cytosolic- (C) and nuclear (N) fractions were investigated by immunoblot using indicated antibodies. RSK1 band intensities were determined by ImageJ and percentage of cytosolic and nuclear was calculated referring to total RSK1. Ratio of the pS380 and pS221 to endogenous RSK1 or RSK1/HA-RSK1 (left panel) were calculated by dividing the respective Western blot signal intensities.

4.1. LMB or DDX3 kockdown leads to enhanced phosphorylation of nuclear RSK1

We demonstrated that blockage of the DDX3/CRM1 mediated nuclear export, either via LMB or DDX3 knockdown enriches nuclear YopM (Section VI, 3.2.). Since we showed that YopM induces phosphorylation of cytosolic and nuclear RSK (Section VI, 4.) we now asked, whether this RSK phosphorylation is influenced by the nucleo-cytosolic shuttling of YopM. To answer this question, we treated HEK293 cells with LMB or specific DDX3 siRNA, infected them with WA-C(pTTSS) or WA-C(pTTSS +YopM), preformed cell fractionation an analyzed the fraction with by Western blot analysis (Section VI, 4.1, Figure 30A). The ratio of pS221/RSK1 was 3-fold enriched in the nucleus of LMB treated cells compared to the ratio determined in the nuclear fraction of WA-C(pTTSS +YopM) infected but not LMB treated control cells (Ctrl) (Section VI, 4.1, Figure 30A left and middle panel). Cells infected with WA-C(pTTSS) in combination with LMB treatment showed no nuclear RSK1 phosphorylation (Section VI, 4.1, Figure 30A, right panel WB and right panel pS380,pS221/RSK1 ratio). Similarly, DDX3 knockdown increased nuclear RSK1 phosphorylation on Ser-221 and Ser-380 in WA-C(pTTSS+YopM) infected cells when compared with the phoyphorylation of these residues in siCtrl and WA-C(pTTSS+YopM) infected cells (Section VI, 4.1, Figure 30B, left panel, WB). Quantification revealed a 2-fold and 5-fold increased ratio of pS221/RSK1 or pS380/RSK1, within the nuclear fraction of siDDX3 treated cells in comparision to the ratios determined in siCtrl treated cells. No phospho-specific RSK1 signals could be detected in the nuclear fraction of siDDX3 transfected and WA-C(pTTSS) infected cells (Section VI, 4.1, Figure 30B, righth panel, WB). Neither the presence or absence of YopM nor the LMB- or siDDX3-treatment did alter the overall nuclear distribution of RSK1 between the cytosol and the nucleus (Section VI, 4.1, Figure 30A, B, last two bottom panels) The observed increase of nuclear YopM upon abrogation of the DDX3/CRM1 mediated nuclear export (Section VI, 3.2) led to the hypothesis that the enhancement of phosphorylated nuclear RSK1 directly correlates with the nuclear YopM level. Thus, the nucleo-cytosolic shuttling of YopM could serve the purpose to adjust and sustain the phosphorylation level of nuclear RSK. Because phosphorylated nuclear RSK itself is known to interfere with transcriptional regulators by phosphorylating them, it can be hypothesized that YopM mediates it´s immunoregulatory functions by controlling nuclear RSK phosphorylation.

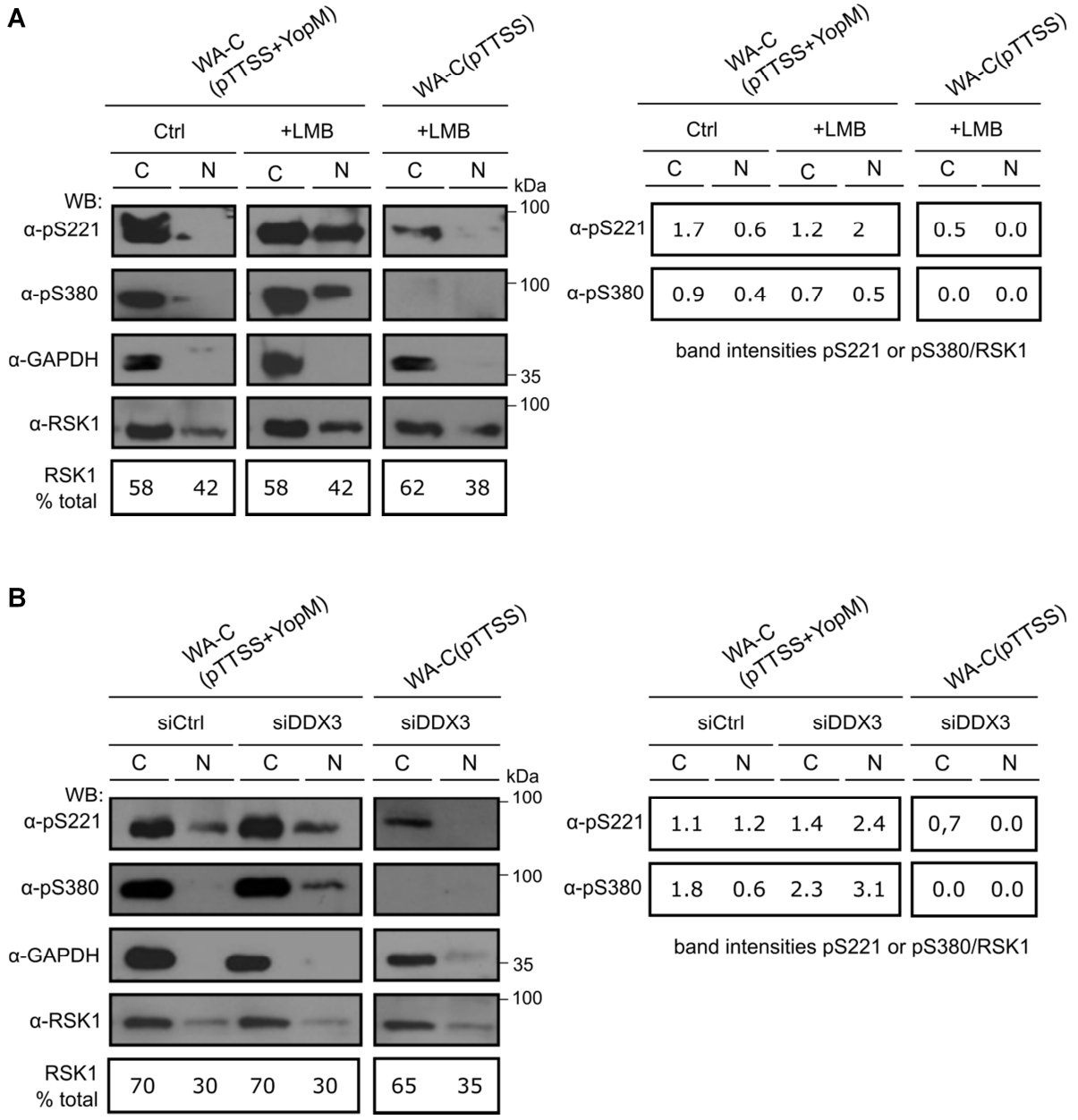

Figure 30: Leptomycin B treatment and DDX3 knockdown induces nuclear RSK phosphorylation.
A and B) HEK293 cells were not treated (Ctrl) or treated with 25 nM LMB for 4 h (+ LMB). **B)** HEK293 cells were treated with control siRNA (siCtrl) or DDX3 specific siRNA (siRNA No. 3) for 24 h. Cells were then infected with *Yersinia* WA-C(pTTSS+YopM) or WA-C(pTTSS) for 1.5 h. Afterwards the infected cells were fractionated into cytosolic (C) and nuclear (N) compartments and fractions were investigated by immunoblot using indicated antibodies. Intensities of the pS221- pS380- and RSK1 protein bands were quantified by ImageJ. Intensity ratios of pS221/RSK1 and pS380/RSK1 were calculated by dividing the respective Western blot signal intensities. RSK1 total is the sum of cytosolic and nuclear RSK1 signal intensities. RSK1 % total indicates the nuclear or cytosolic percentage of it.

4.2. C-terminally truncated YopM is not able to stimulate RSK phosphorylation.

To investigate whether direct interaction of RSK and YopM is essential to mediate the hyperphosphorylation of RSK, we performed cell fractionations with HEK293 cells expressing C-terminal truncated myc-YopM. HEK293 cells were transfected with an empty vector control or either myc-YopM-, myc-YopM_1-481 or myc-YopM_34-481- expressing vectors. Cell fractionation was performed and cellular fractionations were analyzed with α-pS221 and α-pS380 antbodies. Expression of myc-YopM_1-481 or myc-YopM_34-481 did not lead to enhanced RSK1-phosphorylation. The phosphorylation of RSK in cells expressing the truncated YopM was similar to the phospho Ser-221 or phospho Ser-380 western blot singnals detected in the empty vector transfected control cells (Section VI, 4.2, Figure 31). A basal phosphorylation on Ser-221 but not on Ser-380 could be detected in the cytosolic fractions of the empty vector transfected control cells and in the cells which were transfected with myc-YopM_1-481 or myc-YopM_34-481- expressing vectors. The phospho-RSK1 western blot signals in myc-YopM expressing HEK293 cells were the most intensive. Again the distribution of nuclear and cytosolic RSK1 was not affected by myc-YopM or the truncated myc-YopM. Therfore we can conclude that the direct interaction of YopM and RSK is needed to induce phosphorylation of RSK.

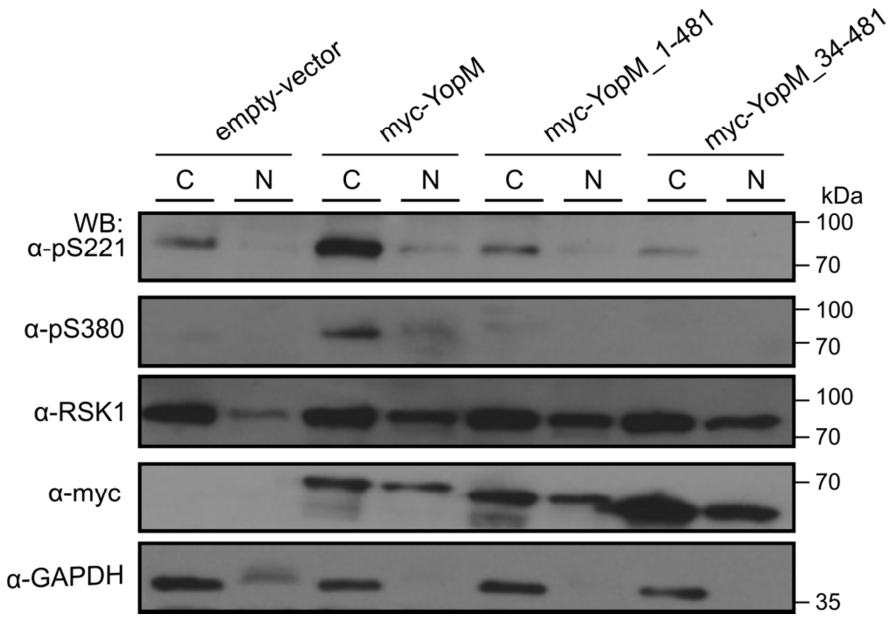

Figure 31: YopM_1-481 mutant is not able to stimulate phosphorylation of RSK.
Indicated myc-YopM constructs were expressed in HEK293 cells for 48h. Cells were harvested and separated in cytosolic (C) and nuclear (N) fractions. These were analyzed by Western blotting using the indicated antibodies.

5. Immunoregulatory effects of YopM

5.1. YopM increases IL-10 expression in *Yersinia* infected primary human macrophages

IL-10 protein was already found to be YopM dependent elevated in the sera of *Yersinia* infected mice (McPhee et al. 2010). RNAseq analysis revealed decreased levels of IL-10 mRNA in WA314ΔYopM infected vs. wild type infected macrophages. To confirm and further analyze the YopM effect on IL-10 expression we performed quantitative real time (RT)-PCR. To this end primary macrophages were either left uninfected (mock) or were infected with WA314 or WA314ΔYopM for 1.5 or 6 h. Total RNA was isolated and IL-10 mRNA levels were analyzed by RT-PCR (Section V, 2.2.2.1). Donor specific analysis of the IL-10 transcription revealed variable IL-10 transcription levels in the *Yersinia* infected macrophages derived of three different donors (Section VI, 5.1, Figure 32; left three graphs). However the IL-10 expression in WA314 infected cells was increased in each donor in comparison to IL-10 transcripts in uninfected (mock) or WA314ΔYopM infected cells. Moreover, the analysis revealed that the IL-10 transcription does not chance significantly between 1.5 h and 6 h of infection. On this basis, we chose to investigate the IL-10 expression in infected macrophages derived from four additional human donors at the 6 h time point. The RT-PCR analysis of the IL-10 expression in macrophages, normalized to the IL-10 expression level in uninfected cells (mock), confirmed the impression that YopM enhances IL-10 transcription in *Yersinia* infected primary human macrophages. IL-10 mRNA levels were about 3 times reduced in mock and WA314ΔYopM infected cells in comparison to the IL-10 level in wild type (WA314) infected primary human macrophages (Section VI, 5.1.,Figure 32, right graph). Thus, we could confirm the YopM dependent transcriptional upregulation of IL-10 in primary human macrophages as indicated by the RNAseq analysis.

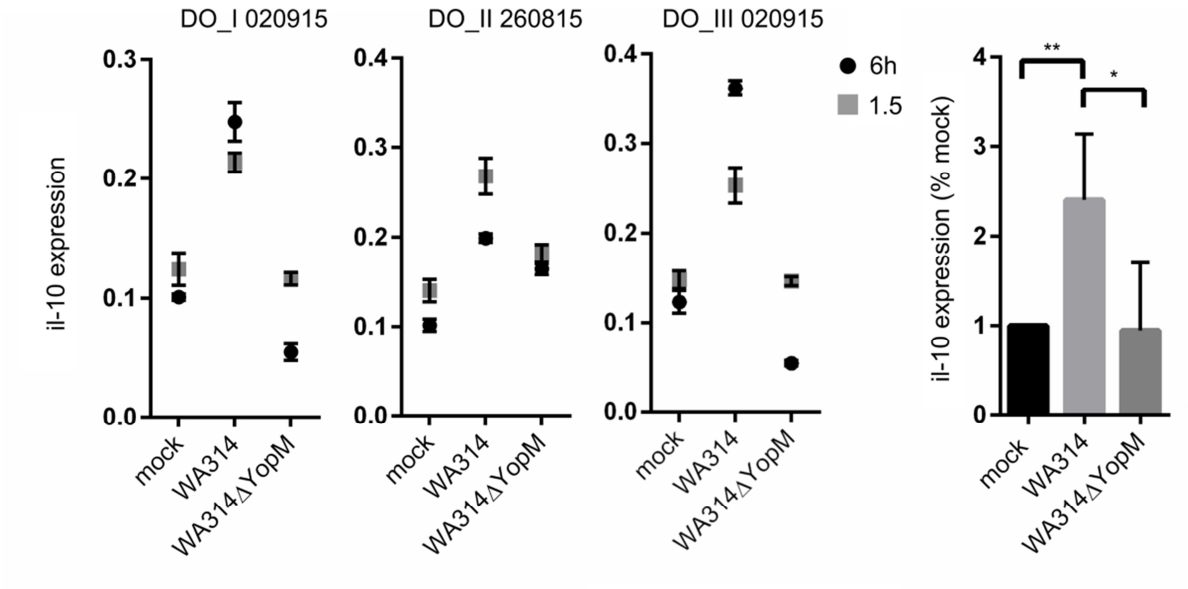

Figure 32: YopM enhances the transcription of IL-10 in infected primary macrophages.
Total RNA of primary macrophages from three different donors (sample names of the donors are indicated above the graphs) was isolated. Cells were either untreated (mock) or infected with WA314 or WA314ΔYopM for 6 h or 1.5 h. Isolated RNA was reversed transcribed and RT-PCR was performed with human IL-10 specific primer. IL-10 expression was normalized to three housekeeper genes (GAPDH, TBP, B2M). The left graph summarizes the gene transcription within the macrophages infected with WA314 or WA314ΔYopM normalized to the IL-10 transcription in uninfected cells (mock) after 6 h of infection. Each bar in graph represents mean ± SD of values from all 7 donors. Statistical analysis was performed with ordinary One-way ANOVA analysis, Bonferroni´s multiple comparison, **p<0.01, *p<0.05.

5.1.2. C-terminally truncated YopM induces an attenuated RSK phosphorylation and fails to reduce IL-10 expression in primary human macrophages

We could demonstrate that YopM affects the phosphorylation of RSK (Section VI, 4.1.) Because RSK itself is an established regulator of gene transcription we assumed that YopM's effect on nuclear RSK phosphorylation could result in the inhibition or stimulation of cytokine transcription. This was further supported by the finding that blockage of nuclear export of YopM by LMB- or siDDX3-treatment led to enhanced nuclear RSK phosphorylation (Section VI, 4.2). Moreover, it was already shown that some immunoregulatory proteins, i.e. IL-10, are regulated in dependence of YopM's interaction with RSK (McPhee et al. 2010; McPhee et al. 2012). To now investigate whether the transcriptional effects of *Y. enterocolitica* YopM are dependent on it´s RSK interaction we recomplemented the *Y. enterocolitica* serotype O:8 strain WA314, defective in YopM (WA314ΔYopM), with a bacterial expression vector encoding YopM_1-481, giving rise to a the new strain WA314ΔYopM(pYopM_1-481). We confirmed the functionality of the new strain in terms of effector secretion and translocation by performing released protein and translocation assays (Section V, 2.1.5, and 2.1.6). Additionally we investigated the effect of this strain on RSK1 phosphorylation by infecting primary human macrophages with it and the following strains

Y. enterocolitica WA314ΔYopM and WA314ΔYopM(pYopM). The YopM lacking WA314ΔYopM mutant strain served as a negative control. WA314ΔYopM(pYopM) orginate from a WA314ΔYopM strain which was recomplemented with a full length YopM expressing vector. This strain was employed as a positive control. Human primary macrophages were infected with the above mentioned strains for 6 h. Cells were fractionated and analyzed by immunoblot with the phospo-specific antibodies α-pS221 and α-pS380. Macrophages infected with WA314ΔYopM(pYopM_1-481) showed reduces phospho-RSK singnals in the Western blot compared to the signals detectable in WA314ΔYopM(pYopM) infected cells. In the cells infected with WA314ΔYopM no phosphorylation was detectable on any of the investigated RSK phosphorylation sites (Section VI, 5.1.2, Figure 33A). Thus, YopMs interaction with RSK is also required in primary human macrophages to induce RSK phosphorylation (Section VI, 4.2.). We performed quantitative RT-PCR analysis with mRNA isolated from the primary human macrophages of three different donors which were infected with the wild type strain and the mentioned mutant strains. Similar to the phosphorylation level of RSK, IL-10 expression was significantly increased in WA314ΔYopM(pYopM) infected macrophages compared to the IL-10 transcripts determined in macrophages infected with a YopM (WA314ΔYopM) or WA314ΔYopM(pYopM_1-481) (Section VI, 5.1.2., Figure 33B). Given these results we can conclude that the direct interaction of YopM and RSK is important to elevate the transcription of the anti-inflammatory cytokine IL-10 during *Yersinia* infection. Further it is likely that this process correlates with the phosphorylation status of RSK which, as we showed, can be controlled by YopM via its DDX3 dependent nucleocytoplasmic shuttling.

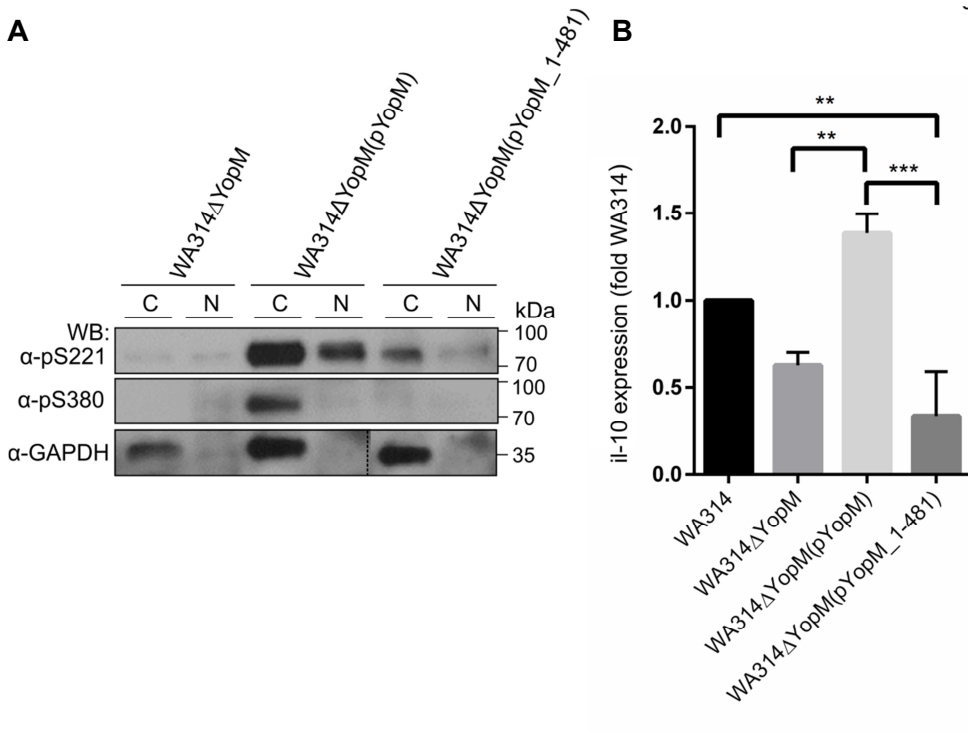

Figure 33: Full length YopM in contrast to its C-terminally truncated version induces hyperphosphorylation of RSK1 and enhances IL-10 expression in primary human macrophages.
A) Primary human macrophages were infected with *Yersinia* WA314ΔYopM, WA314ΔYopM(pYopM) or WA314ΔYopM(pYopM_1-481). Cells were fractionated in cytosol (C) and nucleus (N). Fractions were subjected to Western blot analysis using the indicated antibodies. **B)** Macrophages derived from three donors were infected with WA314, WA314ΔYopM, WA314ΔYopM(pYopM) or WA314ΔYopM(pYopM1-481) for 6 h. mRNA was isolated and subjected to RT-PCR with IL-10 specific primers. Bars in graph represents mean ± SD of values from all 3 donors for WA314, WA314ΔYopM(pYopM1-481) and WA314ΔYopM(pYopM) infected cells. Statistical analysis was performed with ordinary One-way ANOVA analysis, Bonferroni´s multiple comparison, **p<0.01 ***p<0.001.

5.1.3. YopM enhances TNF transcription in *Yersinia* infected human macrophages dependent on its interaction with RSK

Primary human macrophages derived from five different human donors were not treated (mock) or infected with WA314 or WA314ΔYopM for 6 h. RNA isolates of these infection experiments were subjected to quantitative RT-PCR. As for IL-10 the TNF transcription varied among the donors (Section VI, Figure 34, five left graphs). Nevertheless a general trend of attenuated TNF transcription could be observed in uninfected and WA314ΔYopM infected cells compared to the TNF transcription determined in WA314 infected cells. This is also reflected in the right graph which includes each TNF transcription determined within the RNA isolates of the infected macrophages (Section VI, 5.1.3, Figure 34, right graph).

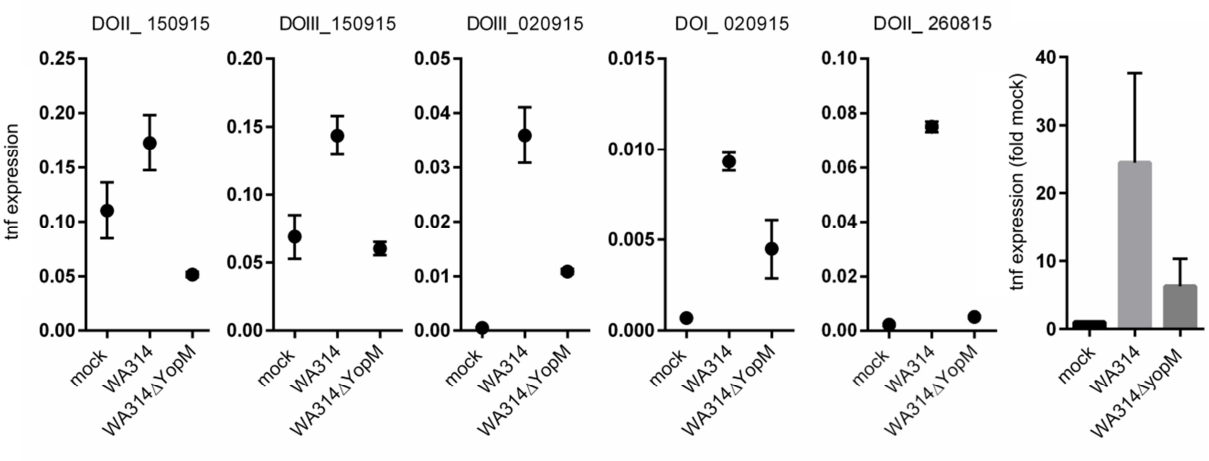

Figure 34: YopM enhances the transcription of TNF in *Yersinia* infected primary macrophages.
Total RNA of primary macrophages derived from five donors (sample name of the donor is indicated above the graph) was isolated after infection with the *Yersinia* strains WA314 and WA314ΔYopM for 6 h. One subset of cells was left untreated (mock) as a negative control. Isolated RNA was reversed transcribed and RT-PCR was performed with primer specific for human TNF. The amplification of the three housekeeper genes (GAPDH, TBP, B2M) was performed to standardize the amount of sample RNA added to the reaction. The left graphs represent the absolute TNF expression within *Yersinia* infected macrophages. Within each graph the expressions within macrophages derived from one donor are depicted. The right graph summarizes the gene transcription normalized to the TNF transcription in uninfected cells (mock). Each bar, represents mean ± SD of values from 5 donors.

We additionally infected macrophages with WA314ΔYopM(pYopM_1-481) or WA314 ΔYopM(pYopM) to investigate whether the increase of TNF transcription induced by YopM is RSK dependent. RT-PCR analysis of TNF in WA314ΔYopM(pYopM_1-481) infected macrophages revealed that YopM_1-481 does not enhance the TNF expression in primary human macrophages. The level of TNF transcripts was similar to the levels determined in WA314ΔYopM infected cells (Section VI, 5.1.3., Figure 35). Therefore it is likely that the interaction of YopM and RSK is required to enhance TNF transcription.

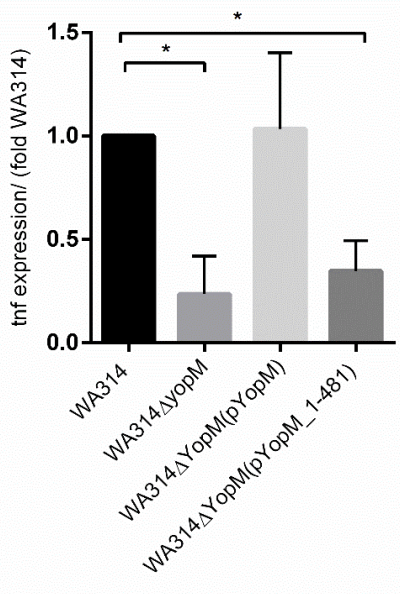

Figure 35: Interaction of YopM with RSK is mandatory to enhance TNF transcription in primary human macrophages.
Macrophages derived from three different donors were infected with WA314, WA314ΔYopM, WA314ΔYopM (pYopM1-481) or WA314ΔYop(pYopM) for 6 h. RNA was isolated and subjected to RT-PCR with TNF specific primers. Each bar in graph except WA314ΔYopM represents mean ± SEM of values from 3 donors (DO2_150915, DO3_150915, DO1_201015). Bar WA314ΔYopM represents mean of two donors DO2_150915, DO3_150915); *p<0.05 analyzed with paired t-test.

5.1.4. YopM induces IL-6 and IL-1β transcription in *Yersinia* infected primary human macrophages independent of its RSK interaction

Macrophages of three different human donors were not treated (mock) or infected with WA314 or WA314ΔYopM for 6 h. RNA isolates of these infected cells were analyzed by RT-PCR for the expression of IL-6 or IL-1β. The analysis revealed a similar expression pattern for IL-6- and IL-1β among the donor specific analysis. Mock infected cells showed the lowest IL-6 or IL-1β expression, whereas in *Yersinia* wild type infected cells the IL-6- and IL-1β transcription levels reached a maximum. The absence of YopM resulted in an attenuated transcription of both genes when compared to the IL-6 and IL-1β expression determined in wild type (WA314) infected cells (Section VI, 5.1.4., Figure 36A, B; left 3 graphs). This trend is also reflected in the right graph which summarizes the IL-6 and IL-1β transcription determined in the RNA isolates of macrophages derived from each different donor (Section VI, 5.1.3, Figure 34, right graph). In summary we can state that the IL-6 and IL-1β expression in primary human macrophages is YopM dependently upregulated in the context of infection.

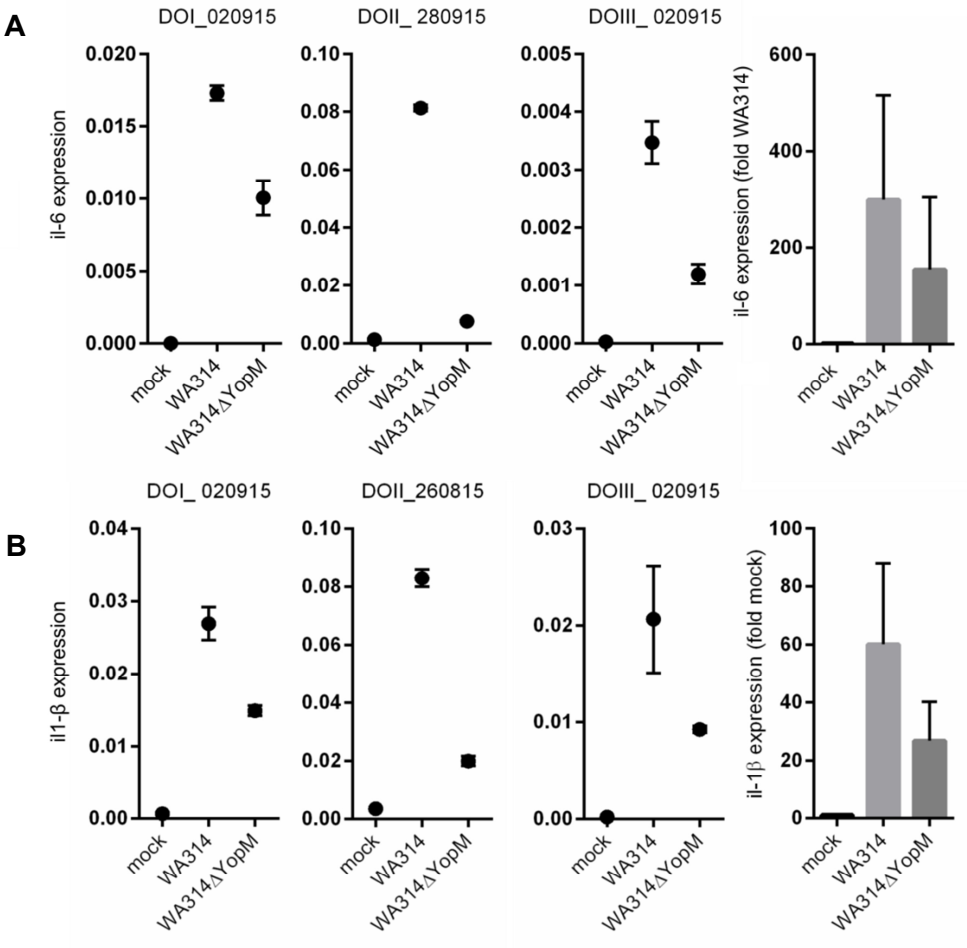

Figure 36: YopM enhances the transcription of IL-6 and IL-1β in *Yersinia* infected primary macrophages. Total RNA of primary macrophages derived from three donors was isolated after infection with *Yersinia* WA314 or WA314ΔYopM for 6 h. One subset of cells were left untreated (mock) as a negative control. Isolated RNA was reversed transcribed and RT-PCR was performed with primers specific for human **(A** IL-6 or **(B** IL-1β. Gene

expression was normalized to three housekeeper genes (GAPDH, TBP, B2M). Left graph summarizes the gene transcription within normalized to the IL-6 and IL-β transcription in uninfected cells (mock): Each bar in the graphs srepresents mean ±SD (left three graphs), ± SEM (right graph) of values from 3 donors.

Further we investigated if this process is dependent on the interaction of YopM and RSK. Next to infecting the human macrophages with wild type *Yersinia* strain (WA314) we treated them with the *Yersinia* strain translocating C-terminally truncated YopM (WA314ΔYopM(pYopM-1-481)), full length YopM (WA314ΔYopM(pYopM)) or the strain lacking YopM (WA314ΔYopM). Quantitative RT-PCR analysis of IL-6 expression showed no significant difference in the IL-6 transcription. C-terminal truncated YopM induces the same IL-6 transcription as full length YopM (Section VI, 5.1.4, Figure 37; right graph). Only the lack of YopM results in attenuated IL-6 expression. Similar observation could be made for the IL-1β expression (Section VI, 5.1.4, Figure 37, left graph). The attenuated IL-6 or IL-1β transcription in WA314ΔYopM infected macrophages confirms the earlier results that the expression of both cytokines indeed is enhanced in the presence of YopM but in contrast to the IL-10 transcription (Section VI, 5.1.2. Figure 33B), the IL-6 and IL-1β expression seems not to be dependent on YopMs interaction with RSK1.

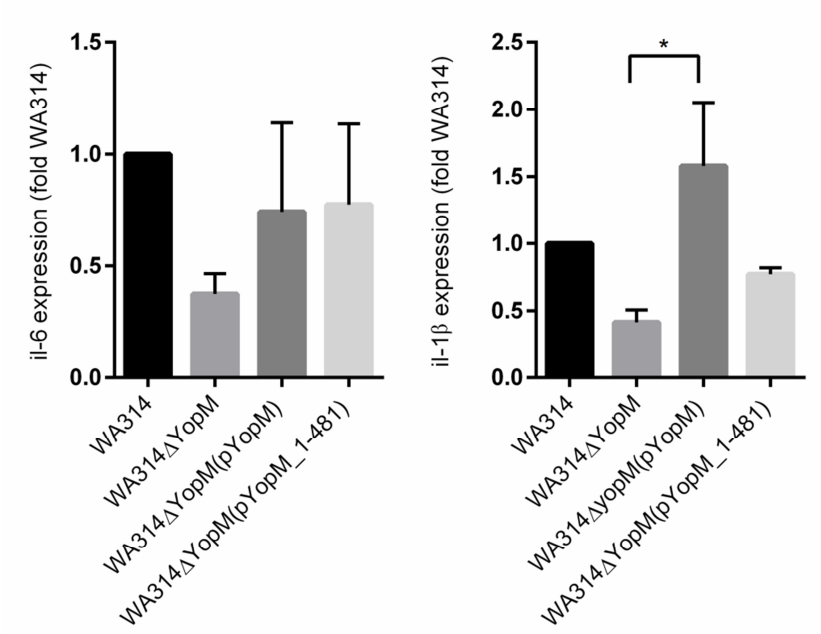

Figure 37: IL-6 and IL-1β transcription is not dependent on interaction of YopM with RSK1.
Determination of IL-6 (left graph) and IL-1β (right graph) transcription in Yersinia infected macrophages via RT-PCR. Total RNA was isolated from primary macrophages derived from 4 (il-6) or 3 (il-1β) different donors. Cells of each donor were either untreated (mock) or infected with WA314, WA314ΔYopM, WA314ΔYopM(pYopM) or WA314ΔYopM(pYopM-1-481) for 6 h. Isolated RNA was reversed transcribed and RT-PCR was performed with human IL-6 and IL-1β specific primers. Expression was normalized to three housekeeper genes (GAPDH, TBP, B2M). Each bar in graph represents mean ± SEM of values from all donors. Statistical analysis was performed with ordinary One-way ANOVA analysis, Bonferroni´s multiple comparison; *p<0.05.

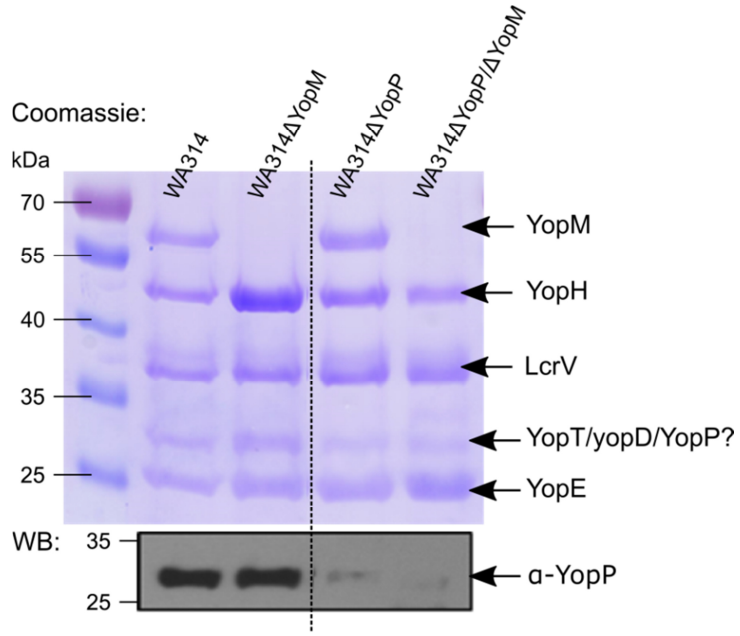

Figure 38: Released protein assays of *Yersinia enterocolitica* WA314 mutant strains.
Yersinia strains were grown at 27°C. Temperature shift to 37°C and chelation of calcium ions induced the release of bacterial proteins into the medium without cell contact. Proteins in the media were precipitated by TCA and resuspended in SB buffer before loading on SDS PAGE gel. The separated released proteins in the SDS PAGE gel were made visible by Coomassie staining (upper part). To detect YopP the gel was immunoblotted and analyzed with specific antibodies (bottom part).

5.2. Immunoregulatory effects of YopM and YopP

Besides YopM, YopP/YopJ is the other *Yersinia* outer protein known to interfere with the host cell immune response through manipulating the release of cytokines. It acts by inhibiting NF-κB- and MAPK- signaling simultaneously (Ruckdeschel et al. 1998; Ruckdeschel et al. 1997; Viboud & Bliska 2005; Orth et al. 1999). A recently published paper demonstrated that cytokines in *Yersinis pestis* infected bone marrow derived macrophages (BMDM) are produced and expressed differently, when YopP, YopM or both effectors are not translocated during infection (Ratner et al. 2016). In this context we were interested to find out whether the presence or absence of YopP alters the IL-10-, TNF-, IL-6- or IL-1β expression in primary human macrophages. Next to that we wanted to investigate if the enhanced cytokine expression which we attributed to YopM (Section VI, 5) is chanced by YopP. To answer that questions we infected primary human macrophages with two additional Yersinia strains which either lacked YopP (WA314ΔYopP) or YopP and YopM (WA314ΔYopP/YopM). Prior to RT-PCR analysis we performed released protein assays to ensure similar secretion of the effector proteins by the different *Yersinia* strains. We preformed the assay whith every strain we used to investigate the effects of YopM and YopP on cytokine expression. The Coomassie blue stained SDS-PAGE gel of the released proteins from *Yersinia* WA314 and WA314ΔYopP revealed similar amounts of secreted YopM (Section VI, 5.2., Figure 38). To detect the released YopP the SDS-PAGE gel was immunoblotted. Two bands in the Western blot analysis with similar signal intensity indicated that the WA314 and the WA314ΔYopM strain secrete equal amounts of YopP. The other secreted *Y.* proteins visible in the Coomassie stained gel were also secreted in equally in all investigated WA314 strains.

5.2.1. Absence of YopP changes YopMs stimulatory effect on IL-10 expression to an inhibitory effect

To analyze the interplay of YopM and YopP on IL-10 transcription we infected primary human macrophages with WA314, WA314ΔYopM, WA314ΔYopP, WA314ΔYopP/YopM and WA-C for 1.5 and 6 h. WA-C infections were preformed to investigate the IL-10 expression in primary human macrophages when almost none of the *Yersinia* defence mecanisms are active. WA-C interacts with the host cells via Invasin but lacks the virulence plasmid and as a consequence all encoded proteins *e.g*. YadA, TTSS and all effector Yops. From the obtained RT-PCR data we conclude that YopP, in contrast to YopM, reduces the IL-10 expression in the infected macrophages after 1.5 and 6 h (Section VI, 5.2.1., Figure 39). Thus, one could assume that YopM regulates the IL-10 transcription antagonistic of YopP. However, when YopP alone or YopP and YopM were both missing we observed an enhanced IL-10 expression which reverse indicates a downregulation of the IL-10 transcription. The IL-10 transcription in WA314ΔYopP/YopM infected cells was similar in magnitude as the IL-10 expression in WA-C infected cells (Section VI, 5.2.1., Figure 39). From these data we can state that YopM and YopP seem to influence each other in the IL-10 transcriptional regulation. In the presence of YopP, YopM has stimulatory effect on IL-10 expression compared to the IL-10 expression determined in WA314 infected macrophages. However, the IL-10 expression in the WA314ΔYopP and WA314YopP/YopM infected macrophages indicates that YopM has rather no major stimulatory effects on the IL-10 expression but rather tends to also inhibit IL-10 expression when YopP is not present. Although the dimensions were slightly increased at the 6 h time points the overall expression patterns were not changed at 6 h vs. 1.5 h of infection.

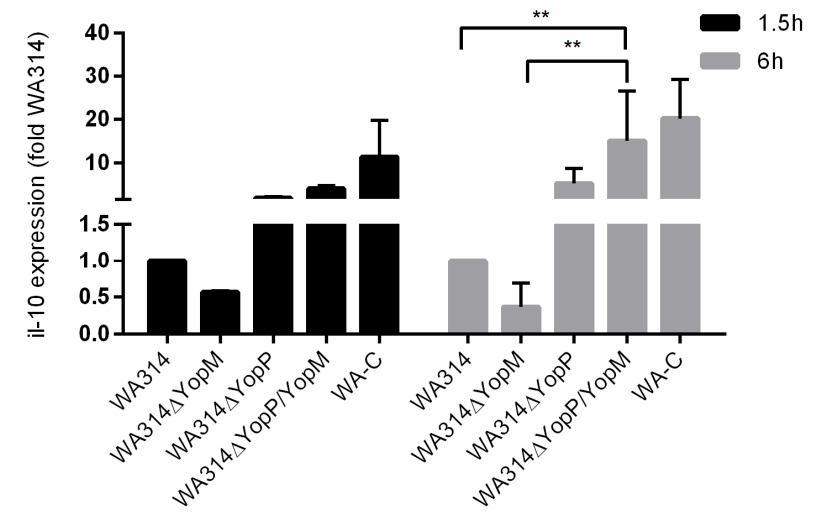

Figure 39: YopM inhibits IL-10 expression in primary human macrophages infected with a YopP deficient strain.
Primary human macrophages were infected with Yersinia WA314, WA314ΔYopP, WA314ΔYopP/YopM or WA-C for 6h. mRNA of two donors infected with WA314ΔYopM were analyzed by RT-PCR for IL- 10 expression. IL-10 expression analysis was performed as described in methods and IL-10 RT-PCR results were normalized to reference genes and to the IL-10 mRNA level determined in WA314 infected cells of the respected donors (DOI_020915, DOII_260815; DOIII_020915). Bars in the graph represent mean ± SEM of values from all 3 donors, except the graph of il-10 expresssion in WA314ΔYopM infected primary macrophages, which represent mean ± SEM of values from 2 donors. Statistical analysis was performed with one sided t-test, *p<0.05*.

5.3. YopM and YopP regulate expression of IL-10 and NF- κB targeted genes TNF, IL-6 and IL-1β

YopP/YopJ is well known to block the NF-κB dependent expression of inflammatory cytokines in *Yersinia* infected macrophages. Interestingly, IL-10 was shown to inhibit the expression of NF-κB- and endotoxin-inducible cytokines such as TNF, IL-1β and IL-6 in mononuclear phagocytes (Donnelly et al. 1999). Motivated by these findings we investigated whether TNF, IL-6 and IL-1β expression is regulated by YopM and YopP in *Yersinia* infected human macrophages. Additionally we analyzed how the expression of TNF, IL-6 and IL-1β might be altered in macrophages when YopM acts in the absence of YopP, i.e. when cells were infected not only with WA314ΔYopM but also with WA314ΔYopP and WA314ΔYopP/YopM.

5.3.1. TNF expression in primary human macrophages is mainly controlled by YopP

Primary human macrophages derived from three human donors were infected with WA314, WA314ΔYopM, WA314ΔYopP or WA314ΔYopP/YopM for 1.5 and 6 h and the isolated mRNAs were subjected to quantitative real time PCR. If comparing the TNF transcription in WA314ΔYopP- and WA314ΔYopM infected macrophages, with the TNF transcription

determined in WA314 infected macrophages, it can be concluded that YopM enhances the TNF expression in the cells whereas YopP reduces it. However, similarly as already seen for IL-10 expression, led the absence of YopP and YopP/YopM to no more activatory effect of YopM on the TNF expression. After 1.5 h of infection the TNF expression was similar in WA314ΔYopP and WA314ΔYopP/YopM infected cells. Only a tendency of activation by YopM at 6 h of infection could be observed in macrophages infected with these strains (Section VI, 5.3.1; Figure 40). This data suggests that YopP is the main regulator of TNF transcription within the first 1.5 h of infection where YopM has no stimulatory effect in the absence of YopP. Only in later time points of infection YopM could potentially act as an antagonist of YopP.

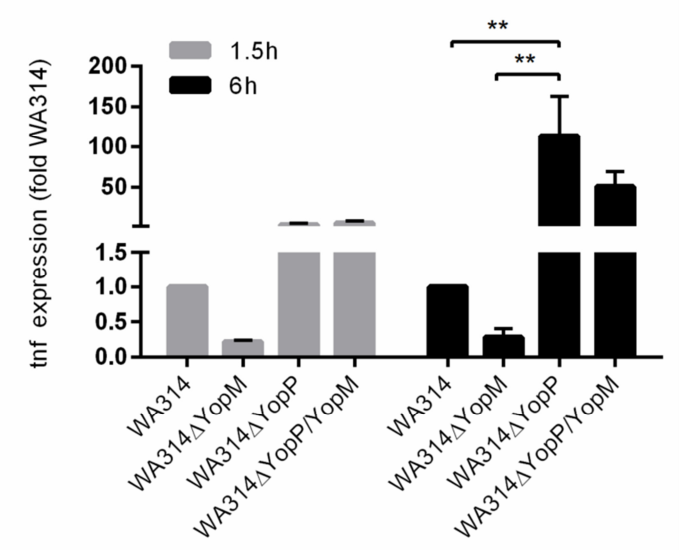

Figure 40: TNF expression in primary human Macrophages after 1.5 h and 6 h of infection.
Macrophages derived from three different donors were infected with WA314, WA314ΔYopM, WA314ΔYopP or WA314ΔYopP/(YopM) for 1.5 and 6 h. TNF expression analysis was performed as described previously. Each bar in graph represents mean ± SEM of values from three donors, analyzed with two way ANOVA , Bonferroni's multiple comparisons test; ** p<0.001.

5.3.2. YopMs stimulating effects on the transcription of the pro-inflammatory cytokines IL-6 and IL-1β is reversed to a inhibitory effect in the absence of YopP

Quantitative RT-PCR analysis of the IL-6 expression in macrophages revealed an attenuated transcription of IL-6 in WA314ΔYopM infected cells compared to the transcription determined in WA314 infected cells. Thus, it can be concluded that YopM is able to increases the expression of IL-6. After 1.5h of infection the IL-6 expression in the absence of YopP and YopP/YopM appeared almost similar, indicating that YopM has no more stimulatory effect on the IL-6 expression. Instead it rather seemed to suppress IL-6 expression even further. This tendency was clearly visible after 6h of infection. The IL-6 transcription in WA314ΔYopM/YopP infected cells is 8-fold increased compared to the IL-6 expression in WA314ΔYopP infected cells (Section VI, 5.3.2, Figure 41). Because the lack of both

effectors, YopM and YopP, results in the highest IL-6 expression it can be speculated that YopP and YopM synergistically repress the IL-6 transcription in the context of infection. Further the data hints towards the facts that YopM can reverse its function in the absence of YopP and acts as a suppressor of pro-inflammatory cytokine transcription

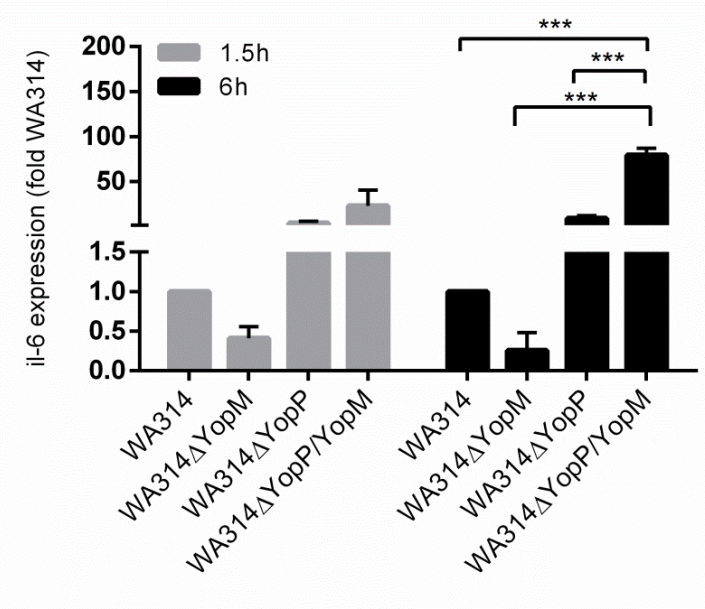

Figure 41: IL-6 expression is increased when YopP and YopM are missing.
Total RNA of primary macrophages derived from 2 different donors was isolated. Cells of each donor were infected with WA314, WA314ΔYopM, WA314, WA314ΔYopP or WA314ΔYopP/YopM for 1.5 h or 6 h. Isolated RNA was reversed transcribed and RT-PCR was performed with human IL-6 specific primers. IL-6 expression was normalized to three housekeeper genes (GAPDH, TBP, B2M). Each bar in graph represents mean ± SD of values from all donors (3 x 1.5 h; 2 x 6 h) Statistical analysis was performed with One-way ANOVA analysis, Bonferroni´s multiple comparison, ***p<0.0001

Next to IL-6 we analyzed the IL-1β transcription in primary human macrophages infected with the mentioned *Yersinia* strains for 1.5 and 6 h. IL-1β transcription was YopM dependently upregulated when comparing the IL-1β transcription levels in WA314 and WA314ΔYopM infected macrophages as already observed for the transcription of IL-10, TNF and IL-6. Absence of YopP indicated an enhanced expression of IL-1β which reverse hint to a downregulatory effect of YopP on the IL-1β expression. This effect was even more pronounced after 6h of infection. The IL-1β expression in WA314ΔYopP infected cells was about 80-fold increased in comparison to the expression determinded in WA314ΔYopM infected cells. Additional the IL-1β expression in the absence of YopM/YopP was 2-fold enhanced in comparison to the IL-1β expression determined in WA314ΔYopP infected macrophages (Section VI, 5.3.2., Figure 42). Given these results we can conclude that IL-1β is regulated similar to IL-6 and that YopM's stimulating effect on IL-1β transcription is reversed in the absence of YopP.

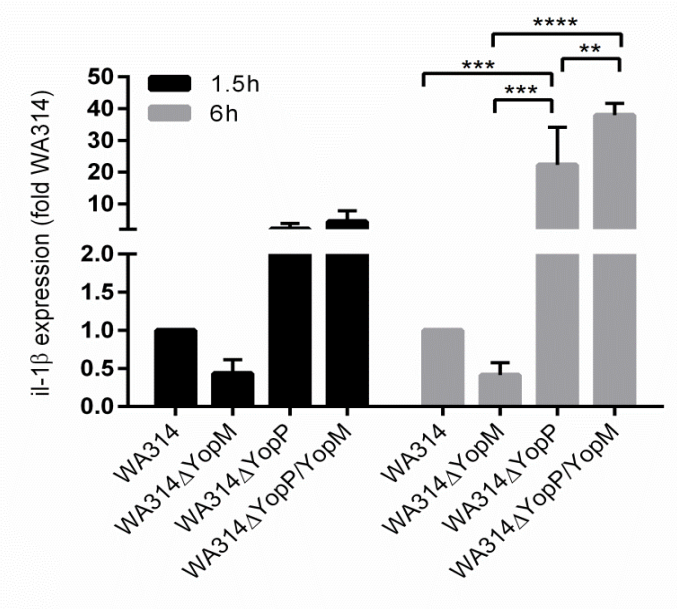

Figure 42: IL-1β expression is repressed when YopP and YopM are missing.

Total RNA of primary macrophages derived from 3 different donors was isolated. Cells of each donor were infected with WA314 or WA314ΔYopM WA314 WA314ΔYopP and WA314ΔYopP/YopM. for 1.5 h and 6 h. Isolated RNA was reversed transcribed and RT-PCR was performed with human IL-1β specific primer. The expression was normalized to the expression of three housekeeper genes (GAPDH, TBP, B2M). Each bar in graph represents mean ± SD of values from all Statistical analysis was performed with One-way ANOVA analysis, Bonferroni´s multiple comparison, ** p<0.001.
, ***p<0.0001, ****p<0.00001

VII Discussion

1. *Y. enterocolitica* YopM and its interaction partners

1.1. Interaction of *Y. enterocolitica* YopM and DEAD box helicase 3 (DDX3)

In this thesis the new identified association of YopM and DDX3 was verified and biochemically characterized (Section VI, 1 and 2). Interaction studies showed that the core region of YopM (aa 34-481) consisting of the LRR region and the two N-terminal α-helices that initiate LRR folding, facilitates YopM´s binding to DDX3 (Section VI, 1.3., Figure 19). The core region of *Y. enterocolitica* WA314 was recently crystallized in our group. This data provided evidence that YopM binds to DDX3 in a 2:1 complex in which the LRR regions of the YopM dimer create an interface to which DDX3 associates (Rumm 2014; Berneking et al. 2016). The LRR region of bacterial leucine rich repeat proteins, such like YopM, is commonly known to facilitate binding to eukaryotic proteins within the host (Kobe & Deisenhofer 1994). Often this interaction is connected to physiological functions which favor bacterial survival. For example, *Listeria monocytogenes* uses its leucine rich repeat containing protein Internalin to enter epithelial cells via interaction with E-Cadherin (Schubert et al. 2002; Mengaud et al. 1996). Additionally, YopM from *Y. pestis* was found to interact with α-Thrombin via its LRRs 4–9 and 6–9 which affected the lethallity of *Y. pestis* (Hines et al. 2001; Skrzypek & Straley 1996). Within our studies and this dissertation work we could attribute the nucleo-cytosolic shuttling of YopM from *Y. enterocolitica* WA414 to its interaction with DDX3. Further we could provide evidence that the thereby controlled phosphorylation of RSK affects the IL-10 and TNF expression in *Y. enterocolitica* WA314 infected primary human macrophages (Section VI, 5.1.2., 5.1.3.). Nevertheless, YopM could subvert other functions of DDX3 to successful establish *Yersinia* infection. One such function may be inferred by the interaction sites of DDX3 and YopM. The interaction site of DDX3 which mediated its binding to YopM was clarified by GST-pulldown experiments in HEK293 cells cotransfected with vectors expressing GST-myc-YopM and either full length DDX3_1-662-HA, DDX3_1-418-HA or DDX3_418-662-HA. It was demonstrated that the N-terminal region of DDX3, aa 1-418, is mandatory for the interaction of both proteins (Section VI, 1.2., 1.3, Figure 20). The interaction region was further narrowed down by pull down experiments with recombinant purified GST-YopM and His-tagged truncated versions of DDX3 to the unstructured N-terminal region from amino acid 101 to 168 of DDX3 (Rumm 2014; Berneking et al. 2016). Thus, YopM of *Y. enterocolitica* occupies N-terminal regions of DDX3 similar to the poxvirus, which was shown to interact with aa 1-139 of DDX3 and to thereby block the stimulatory effect of DDX3 on INF-β promoter induction (Schröder et al. 2008). It would be interesting to investigate, if YopM´s interaction with DDX3 could also lead to attenuated

INF-β production and therefore would contribute to silence the host immune response in *Yersinia* infection. Whether, YopM subverts other DDX3 functions such as cell cycle control, regulation of apoptosis and innate immune signaling deserves further investigation as well.

1.2. Complex formation of YopM, RSK1, PKN and DDX3

Several publications state a complex formation of YopM with the cellular kinases RSK1 and PKN1 or it´s isoforms (PKN2/RSK2) (Hentschke et al. 2010; Höfling et al. 2014; McDonald et al. 2003; McPhee et al. 2010). We could confirm this interaction with the tandem affinity purification of SBP-CBP tagged *Y. enterocolitica* YopM (Section VI, 1.2, Figure 16) and immunoprecipitations of myc-YopM in HEK293 cells transfected with myc-YopM expressing vectors (Section VI, 1.2., Figure 17). Moreover PKN-flag and GST-HA-RSK immunoprecipitations performed in this study provide evidence that interaction of RSK1 and PKN is mediated by YopM (Section VI, 2.1, Figure 21 C,D) which is in line with the common assumption that YopM brings together RSK and PKN in a complex (McDonald et al. 2003; Hentschke et al. 2010). Furthermore we confirmed by these and additional pulldowns or immunoprecipitation experiments that DDX3 is a new interaction partner of YopM (Section VI, 1.2.) (Rumm 2014; Berneking et al. 2016). However, we could not identify a quadruple complex containing DDX3, YopM, RSK1 and PKN1. Instead we demonstrated that YopM forms at least two different ternary complexes in the cell: YopM, RSK, PKN or YopM, RSK, DDX3 (Section VI, 2.1, Figure 21). YopM from *Y. pseudotuberculosis* was shown to associate with PKN via its LRRs 6 to 15 (McPhee et al. 2010) (McPhee et al. 2010) and studies on YopM from *Y. enterocolitica* 8081 stated that next to the complete LRR region the C-terminus of YopM is important for its association with PKN (Höfling et al. 2014). As far as our data show this is not applicable for the C-terminus of YopM from *Y enterocolitica* WA314. In immunoprecipitations of C-terminal truncated versions of myc-YopM (myc-YopM_1-418 and YopM_34-418) we could detect PKN in the corresponding Western blot analysis (Section VI, 1.3., Figure 19). Additionally this experiment demonstrated that the C-terminus of *Y. enterocolitica* WA314 is mandatory to facilitate the interaction of YopM and RSK as already shown for other YopM isoforms (McCoy et al. 2010; McPhee et al. 2010). On this account we conclude that the N- and C-terminus are dispensable for the interaction of YopM and PKN and more likely only the whole LRR stretch including both α-helices facilitate the binding of YopM from *Y.enterocolitica* and PKN. This was proven in myc-YopM and myc-YopM_1-418 and YopM_34-418 immunoprecipitations (Section VI, 3.3, Figure 27A). As mentioned before this region of YopM from *Y.enterocolitica* is also suspected to mediate the interaction of YopM and DDX3 (Section VI, 1.3., Figure 19) (Berneking et al. 2016). We showed that in PKN1-flag pulldown no DDX3 could be precipitated and vice versa no PKN in DDX3-flag pulldowns (Section VI, 2.1, Figure 21C, D). Thus, it can be assumed that PKN

and DDX3 associate with YopM via the same region. Because of that it is likley that PKN and DDX3 do not exist together in a quadruple complex comprising YopM, RSK, PKN and DDX3. Instead it is more conceivable that both DDX3 and PKN compete for interaction with a complex of YopM and RSK, which leads to the formation of the two ternary complexes YopM, RSK1, PKN and YopM, RSK1, DDX3. GST-HA-RSK1 pulldowns in cytosolic and nuclear fraction indicated that both complexes are simultaneously and ubiquitously present (Section VI, 2.1, Figure 23). Further studies should address the exact principles, which lead to formation of YopM, RSK1, PKN or YopM, RSK1, DDX3. Knockdown experiments of every complex component RSK1, PKN or DDX3 could be performed to address this question in the future. Further co-crystals of the complex would allow drawing conclusions on the functionality of the ternary complexes and could reveal the exact intermolecular organization.

2. Nuclear-cytosolic shuttling of YopM via DDX3 and CRM1

We provide evidence that DDX3 mediates nuclear export of YopM via the CRM1 export pathway (Section VI, 3.) and propose that this export enables the nucleo-cytosolic shuttling of YopM. DDX3 itself was shown to be part of the CRM1 mediated RNA export pathway. It facilitates the nuclear export of Human Immunodeficiency Virus (HIV) -mRNA via the RNA-binding protein Rev of HIV (Yedavalli et al. 2004). We blocked the proposed DDX3/CRM1 nuclear export with LMB- or specific DDX3 siRNA-treatment and could observe an intranuclear accumulation of YopM. Thus, it is likely that YopM utilizes DDX3 to exit the nucleus, similar to the Rev protein of HIV which was demonstrated to interact with DDX3 to export viral mRNA (Yedavalli et al. 2004). A functional ternary complex of CRM1/DDX3 and Rev was proposed. We as well would favor the hypothesis of a functional complex between YopM, DDX3 and CRM1 reasoned by Co-IPs of DDX3 which precipitated YopM and CRM1 (Section VI, 3.1., Figure 24). Nevertheless we cannot exclude the existence of the binary complexes DDX3/CRM1 and DDX3/YopM. Further, it remains uncertain how DDX3 and CRM1 interact in the presence of YopM and how the nucler export is facilitated. Although, our experiments confirmed efficient nuclear arrest of DDX3 when employing LMB (Section VI, 3.2, Figure 25), we could not confine interaction of CRM1 and DDX3 to the N-terminal nuclear export sequence (NES) of DDX3 (aa 1-22) as described in other studies(Lai et al. 2008; Yedavalli et al. 2004). Instead our observations indicate that the N-terminal region of DDX3 is rather occupied by the interaction with YopM (Section VI, 1.3.1.Figure 20) (Rumm 2014; Berneking et al. 2016). This facts lead to the question, “Can CRM1 and YopM simultaneously associate with the N-terminal DDX3 region or do they sterically impede each other?” So far nothing is know about that but alternatively to the N-terminal NES, the C-terminus of DDX3 (aa 260–517) was as well describe to facilitate the interaction between

DDX3 and CRM1 (Yedavalli et al. 2004). This region could facilitate the DDX3 and CRM1 association in the presence of YopM to avoid potential sterically interference in a YopM, DDX3, CRM1 complex. If we consider, that DDX3 and YopM interact via the interface created by a YopM dimer (Rumm 2014; Berneking et al. 2016), it is conceivable that DDX3 binds N-terminal to the created YopM interface and simultaneously interacts with CRM1 via its C-terminal region (aa 260-517). A schematic overview of this hypothetic complex is given in Figure 43 (Section VII, 2). A recent published study, again on the DDX3-, CRM1-, HIV Rev-mediated nuclear export of viral mRNA, state that the CRM1/DDX3 interaction is mediated by the DDX3-N-terminal region (aa 1-182) (Fröhlich et al. 2016). Taken into account that this region encloses the NES of DDX3 (aa 1-22), the finding stands in contrast to the earlier proposed DDX3/CRM1 interacting region within the DDX3, CRM1, HIV Rev complex (Yedavalli et al. 2004). These different reported DDX3/CRM1 interation sites underline the fact that only structural data of a DDX3/CRM1/HIV Rev- or DDX3/CRM1/YopM-co-crystals can resolve the intermolecular organization within these complexes. Further structural data could provide information on the unknown molecular mechanisms which drive the YopM-nuclear-export. Export of a CRM1 associated cargo through the nuclear pore complex (NPC) involves in general a complex formation of CRM1, RanGTP and Ran-binding protein 3 (RanBP3). This multimeric complex, loaded with the export cargo, interacts with a nucleoporin complex (Nup214–Nup88) before the whole multicomplex disassembles in the cytoplasm by a RanGTP/RanGDP hydrolysis driven mechanisms (Lindsay 2001). It is unclear if a complex of YopM, DDX3, CRM1 and RanGTP is exported via association to RanBP3. In theory, simultaneous binding of RSK1 to the C-terminus of YopM, resulting in a YopM, DDX3, CRM1, RSK1 quadruple complex would be possible. Because neither LMB- or siDDX3-treatment led to changes in the cytosolic and nuclear distribution of endogenous RSK (Section VI, 4., Figure 28, Figure 29) we conclude that non phosphorylated RSK is most likely not exported via a YopM, DDX3, CRM1 mediated mechanism. But it also has to be considered, that RSK is described to phosphorylate Ran-binding protein-3 (RanBP3) (Yoon et al. 2008) and therefore could facilitate the nuclear export of YopM, DDX3, CRM1 by an unknown mechanism. Thus, the molecular principles behind the YopM, DDX3, CRM1 nuclear export are an interesting question which should be address in the future. Further, theDDX3/CRM1 mediated nuclear-cytosolic shuttling of YopM implies that bacterial effectors may target eukaryotic nuclear proteins to their advantage like it is known from several viruses (Ariumi et al. 2007; Yedavalli et al. 2004; Ariumi 2014). Since the N-terminal domain of DDX3 was recently shown to be required for HIV- mRNA translation (Fröhlich et al. 2016), it would be interesting to investigate if YopM as well utilizes other functions of DDX3 beneficial for the

bacteria. Moreover, it would be interesting to investigate whether other YopM isoforms associate with DDX3 to favor bacterial survival in the host.

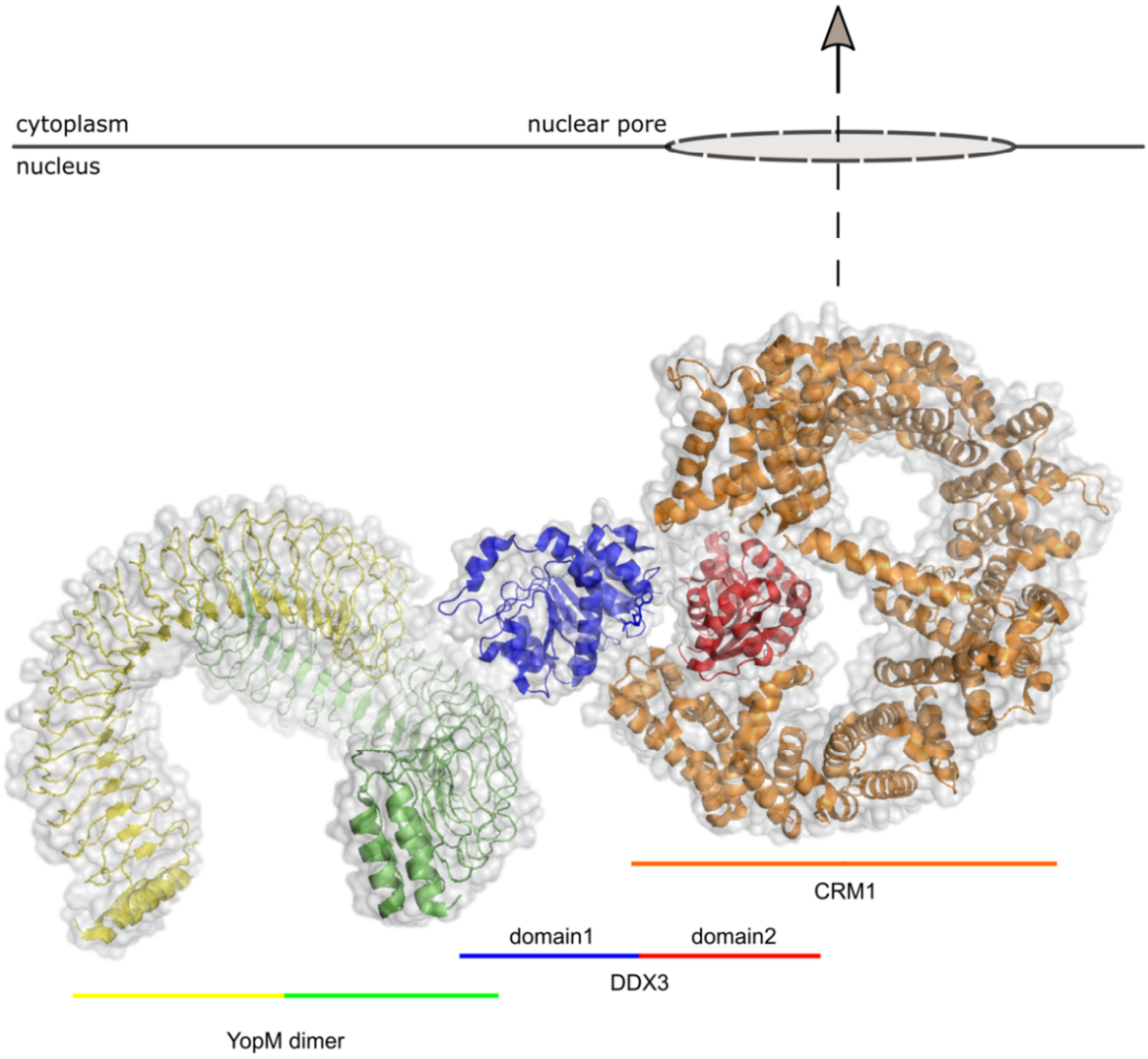

Figure 43: Potential structure of the ternary nuclear export complex comprising YopM, DDX3 and CRM1. Pymol structures of the YopM dimer (PDB code 4OW2 (Berneking et al. 2016) monomers yellow and green), DDX3 (PDB code 2I4I (Högbom et al. 2007) blue and red) and CRM1 (PDB code 4FGV (Monecke et al. 2013) orange) were used to model the hypothetical structure of the YopM, DDX3, CRM1 complex.

3. Consequences of the YopM mediated RSK1 phosphorylation

RSK phosphorylation was shown to be sustained in the presence of YopM (Hentschke et al. 2010; McDonald et al., 2003). We confirmed this RSK activation by determining its phosphorylation status on serine residue 221 and 380 (Section VI, 4., Figure 28,Figure 29,Figure 30,Figure 31). The YopM dependent phosphorylation occured in HEK293 cells (Section VI, 4., Figure 28Figure 29,Figure 30,Figure 31) and in the primary human macrophages (Section VI, 5.1.2., Figure 33A). Additionally, that YopM controls the

phosphorylation status of RSK was shown for YopM from different *Y. enterocolitica* (McDonald et al. 2003; Hentschke et al. 2010; Höfling et al. 2014). Although the induction of RSK phosphorylation seems to be one common feature of YopM, no direct downstream targets of this phosphorylated RSK had been identified so far. It has been suggested that YopM activated RSK, can in turn phosphorylate PKN (McDonald et al. 2003) but further downstream effects of this reaction are as well unknown. By blocking the DDX3/CRM1 mediated nuclear export, which resulted in an increased intranuclear level of YopM, we could show that the nuclear-cytosolic shuttling of YopM correlates with the phosphorylation status of nuclear RSK1 (Section VI, 4.1., Figure 30). With regard to the observed nuclear accumulation of YopM in cells treated with LMB or specific siDDX3 RNA we suggest that enhanced nuclear RSK phosphorylation results from enhanced amounts of nuclear YopM. This was underlined by the fact that the distribution of endogenous RSK remained similar between the nucleus and cytosol under this treatment. YopMs ability to control nuclear RSK phosphorylation Regardless of the exact mechanism, YopMs ability to control nuclear RSK phosphorylation can have impact on RSKs known function to interfere with transcriptional regulation. The cAMP response element–binding protein CREB is one transcription factor known to be targeted by RSK (Bonni et al. 2008). When phosphorylated by RSK it regulates c-fos transcription. C-fos itself is implicated in cell proliferation, differentiation, and development (Chen et al. 1993). Notably, microarray analysis, performed with mRNA from *Y enterocolitica* infected macrophages, indicate that YopM might differentially regulate cell-cycle- and cell-growth-genes but c-fos was not detected within this analysis. RSK further interferes with NF-κB. NF-κB regulates the expression of genes influencing a broad range of biological processes including the innate and adaptive immunity, inflammation and stress responses (Ghoda et al. 1997). Based on this, it was conceivable that the YopM induced nuclear RSK phosphorylation influences cytokine transcription. Indeed we and other could show that YopM influences cytokine transcription and production (Hoffmann et al. 2004; Höfling et al. 2014; Kerschen et al. 2004; Sauvonnet, Garcia-sanz, et al. 2002; Berneking et al. 2016). Only studies with recombinant purified YopM connected this process to the phosphorylation status of RSK so far (Höfling et al. 2014; Rüter et al. 2010). We were able to demonstrate that in *Y. enterocolitica* WA314 infected primary macrophages the IL-10 (Section VI, 5.1.2., Figure 33B) and TNF (Section VI, 5.1.3.,Figure 35) expression is controlled by YopM in a RSK dependent manner. RT-PCR analysis in *Yersinia* infected macrophages under siDDX3 knockdown conditions revealed an increased IL-10 expression in WA314 infected macrophages in comparison to the IL-10 expression determined in siCtrl treated and WA314 infected or uninfected control cells (Berneking et al. 2016). This underlines our hypothesis that cytokine expression is influenced, if by the correlation of

intranuclear YopM and RSK phosphorylation. Next to IL-10 we determined a YopM dependent transcriptional upregulation of TNF (Section VI, 5.1.3., Figure 34), IL-6 and IL-1β (Section VI, 5.1.4., Figure 36) in Y. *enterocolitica* infected human primary macrophages. IL-1β secretion in macrophages infected with *Y. pseudotuberculosis* is downregulated in a YopM and RSK dependent manner (Chung et al. 2014). In this work a mechanism is suggested by which the association of YopM and RSK contributes to YopMs interaction with IQGAP, resulting in caspase-1 deactivation and thereby decreased IL-1β production (Chung et al. 2014). Regardless of our seemingly contradictory finding, that YopM increases IL-1β transcription, it has to be considered, that more than one regulatory process can result in the same phenotype. YopM in association with RSK can manipulate different pathways within the host cell which will result in an attenuated inflammatory response of the host. Moreover, the complexities of cellular processes might often mask regulations evoked by single effectors. Therefore, it remains challenging to attribute the processes induced by the YopM, RSK interaction, to concrete regulatory pathways within the infected cells. Especially the variety of processes regulated by RSK itself leave room for speculations. Nuclear YopM mediated RSK phosphorylation could, next to influencing gene transcription, for example facilitate the export of the hypothetical YopM/DDX3/CRIM1 complex because RSK was shown to regulate activity of the Ran-binding protein 3 (RanBP3) (Yoon et al. 2008) which is important in the CRM1 mediated crossing of the nuclear envelope (Lindsay 2001).

4. Immuregulatory effects mediated by YopM

The recently reported interaction of YopM and caspase-1 and the thereby accompanied inhibition of IL-1β production (LaRock & Cookson 2012; Chung et al. 2014) is the most recent finding which connects YopM to the overall immunosuppressive effects observed in mouse infection experiments (Leung et al. 1990). Caspase-1 assays with recombinant YopM from *Y. enterocolitica* WA314 did not show any inhibition of caspase-1 activity in the presence of YopM (Rumm 2014). But RNAseq analysis of mRNA isolated from *Y. enterocolitica* infected primary human macrophages revealed prominent cytokine associated pathways upregulated by YopM. This finding indicates that YopM from *Y. enterocolitica* might systematically contribute to *Yersinia's* virulence in vivo by manipulation the transcription of diverse cytokines (Berneking et al. 2016). Prominent pathways upregulated by YopM based on the RNAseq data included the JAK-STAT signaling pathway, Toll-like receptor signaling pathway and Cytokine-cytokine receptor interaction (Berneking et al. 2016). All of these pathways contain genes such as tumor necrosis factor (TNF), IL-12, IL-15, IL-18 and IL-10, which were already shown to be transcriptionally regulated by recombinant purified YopM (Höfling et al.

2014; Rüter et al. 2010). The RNAseq data showed that IL-10 was already upregulated by YopM after 1.5h of infection which we could confirm with RT-PCR analysis (Section VI, 5.1./5.2.1. ,Figure 32, 39). We could as well confirm the upregulation of IL-10 expression by YopM after 6h of infection as shown in the RNAseq data generated from mRNA isolated from macrophages uninfected or infected with WA314 and WA314ΔYopM for 6h (Berneking et al. 2016) (Section VI, 5.1./5.2.1. ,Figure 32, 39). Studies on transcriptional regulation in HS60 cells treated with recombinant purified YopM, state a minor effect of YopM on IL-10 transcription (Rüter et al. 2010). This is contradictory to our results. We could observe a 3-fold upregulation of IL-10 mRNA after 6 hours of infection (Section VI, 5.1,Figure 32)(Berneking et al. 2016). This upregulation reflects well the 4-fold increase of IL-10 protein induced by YopM in *Y. pseudotuberculosis* infected mice (McPhee et al. 2010; McPhee et al. 2012). Moreover we could confirm that the induction of IL-10 expression is depended on the C-terminal RSK binding region of YopM (Figure 33), which was already demonstrated for secreted IL-10-protein (McPhee et al. 2010). However, the exact mechanism behind the regulation of IL-10 by RSK remains unclear. Recently, a RSK- and CREB (cAMP response element binding protein) dependent regulation of IL-10 was described in bone marrow derived macrophages exposed to products released by the parasite *S. mansoni.* The parasite induces Toll–like receptor activation and activation of the MEK/ERK/RSK-cascade. The thereby phosphorylated RSK was proposed to enhance CREB phosphorylation which as a consequence induced IL-10 transcription (Sanin et al. 2015). A similar mechanism would be plausible for the YopM- and RSK dependent upregulation of IL-10 expression in *Y. enterocolitica* WA314 infected macrophages or the increased IL-10 protein in the sera of *Y. pseudotuberculosis* infected mice (McPhee et al. 2010). Next to IL-10 the RNAseq- and RT-PCR-data surprisingly revealed a YopM dependent upregulation of TNF transcription after 6h of infection (-3,21 log2-fold (Berneking et al. 2016) (Section VI, 5.1.3., Figure 34). This finding stands in contrast to the common observation that TNF as a major player in the innate immune response is rather known to be downregulated upon *Yersinia* infection (Beuscher et al. 1995; Ruckdeschel et al. 1998; Ruckdeschel et al. 1997). A recent study attributed YopM from *Y. enterocolitica* 8081 to the transcriptional regulation of TNF but unlike us, this work demonstrated a YopM dependent downregulation of the TNF expression in HS60 cells treated with recombinant YopM (Rüter et al. 2010). Considering the IL-10 signaling pathway, it may be possible that the elevated IL-10 level in WA314 infected macrophages influences the TNF expression by complex autocrine mechanisms and feedback regulation, which results in the attenuation of TNF transcripts in the presence of YopM. IL-10 mediated signaling is known to control expression of NF-κB regulated genes via the JAK-STAT pathway including STAT3 and the suppressor of cytokine signaling

3 (SOCS3) (Yoshimura et al. 2007; Johnston & Shea 2003; Donnelly et al. 1999; Riley et al. 1999). The RNAseq analysis revealed that the genes transcripts of both were upregulated in a YopM dependent way. WA314ΔYopM infected macrophages showed compared to wild type infected cells a 1.8- and 3.12 log2- fold transcriptional downregulation of Stat3- and SOCS3- transcripts (Berneking et al. 2016). Thus, the TNF transcription indeed could be regulated by IL-10 trough its impact on JAK-STAT signaling. In addition to TNF we investigated the expression of the NF-κB controlled genes IL-6 and IL-1β. RT-PCR analysis of mRNA isolated from primary human macrophages infected with either *Y. enterocolitca* WA314 or the YopM deficient strain (WA314ΔYopM) indicated a YopM dependent transcriptional upregulation of these cytokines (Section VI, 5.1.4., Figure 36).This again stands in contrast to the common expectations that YopM is suspected to downregulate pro-inflammatory cytokines and leaves us with the question, if IL-1β and IL-6 transcription in *Yersinia* WA314 infected macrophages might also be regulated in an IL-10 dependent manner. There are some evidences that IL-10 and IL-6 influence each other via JAK-STAT--signaling with SOCS3 as a key player in this immunregulation. Further IL-6 was shown to have inflammatory but as well anti-inflammatory properties (Niemand et al. 2003; Johnston & Shea 2003). IL-1β was recently demonstrated to be YopM dependently downregulated in *Y. pestis* or *Y. pseudotuberculosis* infected macrophages as a result of caspase-1 inhibition (Ratner et al. 2016; Schoberle et al. 2016). To exclude involvement of YopM from *Y. enterocolitica* WA314 in this regulation RT-PCR on the pro-IL-1β transcripts in infected macrophages could be performed. However, RT-PCR analysis revealed a suppression of IL-6 and IL-1β expression in WA314ΔYopP and WA314ΔYopP/YopM infected macrophages in comparison to WA314 and WA314ΔYopM infected macrophages, indicating that YopMs stimulatory effect on gene transcription is reversed to an inhibitory one, once YopP is missing. This emphasizes that in the context of infection the translocated effector proteins build a regulatory network to control the host immune response. This to some extent could explain why our studies on IL-10 and TNF expression in *Y. enterocolitica* infected macrophages revealed contradictory results compared to the studies in which cells were treated with recombinant YopM only (Rüter et al. 2010; Höfling et al. 2014). Effects of YopM and YopP on the expression of the immunoregulatory cytokines IL-10, TNF, IL-1β and IL-6 will be discussed in the following paragraphs. If we take together the RNAseq- and RT-PCR-data, we for the first time could provide evidence, that YopM from *Y. enterocolitica* systematically regulates transcription of genes involved in different immunoregulatory pathways. Nevertheless, there are other ways proposed how YopM could contribute to *Yersinia* virulence by interfering with the host immune response. Next to transcriptional regulation of cytokines (Höfling et al. 2014; Rüter et al. 2010; Berneking et al. 2016) and

caspase-1 inhibition (LaRock & Cookson 2012; Chung et al. 2014; Schoberle et al. 2016), YopM could evoke silencing of the host immune response by acting like IpaH4.5. IpaH4.5 is a leucine-rich-repeat containing protein related to YopM which was found in *Shigella flexneri* (Wang et al. 2013). In *Shigella flexneri* infections IpaH4.5 targets Tank binding kinase (TBK-1) to inhibit the Interferon regulatory factor 3 (IRF3), which then results in decreased IFN-β transcription (Zheng et al. 2015). It would be interesting to investigate, if YopM of *Y. enterocolitica* WA314 possesses E3-ubiquitin ligase function such like IpaH4.5 and therefore could block the INF-β induction through polyubiquitination and subsequently degradation of TBK1 (Zheng et al. 2015), or if IFN-β might be rather repressed by the interaction of YopM and DDX3, similar to how the poxvirus K7 interferes with DDX3 to attenuate INF-β production (Schröder et al. 2008).

Taken together, in consideration of YopM´s diverse roles in transcriptional regulation and its inhibitory effect on caspase-1 activation depending on the YopM isoform and host cell type, it can be stated that the processes by which the effector protein YopM could manipulate the host immune response are multifactorial. Investigating downstream targets of YopMs interaction partners, RSK, DDX3 and PKN might help to create an overview of the cellular proteins or pathways manipulated by YopM upon infection. Nevertheless, these potentially YopM-manipulated cellular pathways are often regulated in complex ways by autocrine and paracrine mechanisms resulting in a regulatory network difficult to comprehend. This may impede the task to elucidate the underlying mechanisms behind YopMs immunosuppressive effects in the host with the aim to cause disease. Therefore, it remains a challenging task to elucidate the mechanisms behind YopMs prominent role to essentially contribute to *Yersina* virulence in vivo.

5. Model of YopM´s nuclear-cytosolic shutting and transcriptional IL-10 regulation

From our data we conclude that in the eukaryotic cells at least two ternary complexes can be formed between YopM and its known interaction partners RSK1, PKN and DDX3. One consists of YopM, RSK1, DDX3 and most likely CRM1 at times, the other one of YopM, RSK1, and PKN. Which of these complexes is preferentially formed at what cellular condition remains unclear but we propose that the RSK, PKN, DDX3, CRM1 complex is build whenever YopM exits the nucleus. In this case YopM takes advantage of the DDX3/CRM1 mediated nuclear export but how it exactly crosses the nuclear envelope remains still unknown. Nevertheless we were able to identify a nuclear export principle of YopM which similar as the nuclear import had been elusive for a long time. Still neither any definite

nuclear localization sequence (NLS) nor any importin had been identified which could elucidate the mechanisms behind YopMs nuclear entry (Benabdillah et al., 2004; Scharnert et al., 2013; Elzbieta Skrzypek et al., 1998, 2003). Anyhow, with the knowledge that YopM leads to hyperphosphorylation of RSK in the complex of YopM, RSK, PKN (Hentschke et al. 2010; McDonald et al. 2003; Berneking et al. 2016) we could provide evidence by blocking the nuclear export of YopM via LMB treatment or DDX3 knockdown that the nuclear level of YopM is able to control nuclear RSK phosphorylation. RT-PCR analysis showed that YopM enhances IL-10 expression dependent on its interaction with RSK. Thus we conclude that nuclear YopM can control the phosphorylation status of nuclear RSK and thereby most likley as well controls RSKs ability to gene transcription by activating transcription factors such as NF-κB or CREB. Since IL-10 was not only found to be enriced on the transcriptional level in a YopM dependent manner but also in the sera of infected mice (McPhee et al. 2010; McPhee et al. 2012) we assume that the produced IL-10 can lead to feedback regulations. IL-10-signaling could influence the regulation of the NFκ-B regulated genes IL-6, IL-1β and TNF, the expression of which was affected by YopM in *Y. enterocolitica* WA314 infected primary human macrophages.

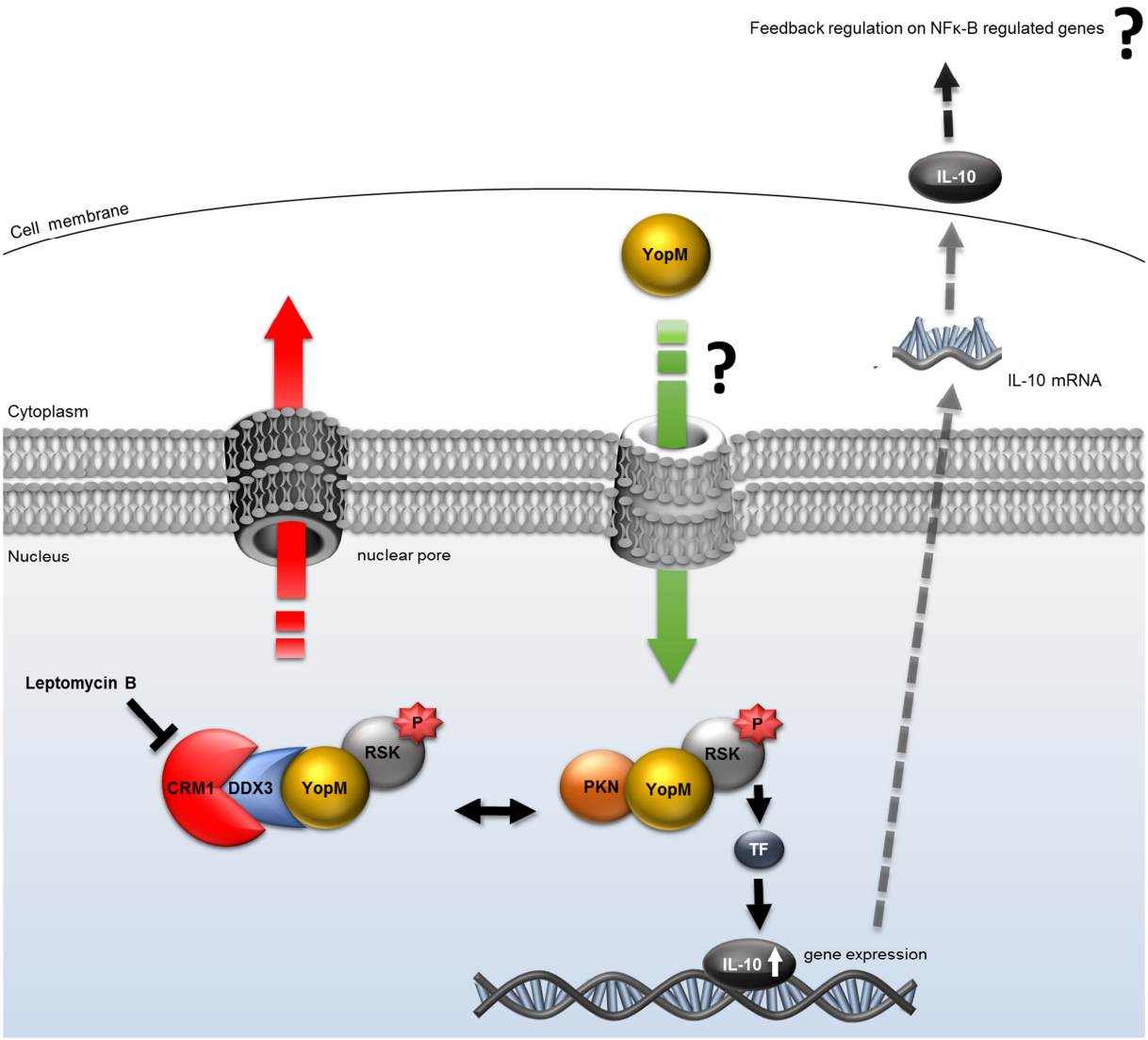

Figure 44: Model of YopMs nuclear-cytoplasmatic shutting and transcriptional IL-10 regulation

6. Interplay between YopM and YopP in *Yersinia* inflammatory response

Recent studies demonstrate that YopM and YopJ synergistically manipulate cytokine production upon infection with *Y. pseudotuberculosis* or *Y. pestis* in bone marrow derived macrophages (BMDM) (Ratner et al. 2016; Schoberle et al. 2016). Our RT-PCR analysis of IL-10-, IL-6-, IL-1β and TNF transcripts in primary human macrophages infected with WA314, WA314ΔYopM, WA314ΔYopP or WA314ΔYopP/YopM revealed that *Y. enterocolitica* effectors YopM and YopP can have opposite and concordant effects on cytokine gene transcription (Section VI, 5.2.). We provide evidence that in contrast to YopM, YopP inhibits IL-10 transcription in *Y. enterocolitica* WA314 infected macrophages (Section VI, 5.2.1., Figure 39). Based on findings that YopM induces IL-10 transcription (Figure 32) we expected decreased amounts of IL-10 mRNA in cells infected with WA314ΔYopM/YopP compared to

cells infected with WA314ΔYopP. But surprisingly we observed that infection with WA314ΔYopM/YopP leads to further increased IL-10 transcription compared to transcription levels determined in WA314ΔYopP infected cells. This hints towards the fact, that in the absence of YopP, YopM rather reduces than increases IL-10 expression (Section VI, 5.2.1, Figure 39). Taking into account that IL-10 is an anti-inflammatory cytokine (Gru 2005) and known to suppress immunity in the context of general bacterial infection (Boonstra et al. 2006; de Waal Malefyt et al. 1991*), Yersinia* would benefit from increased IL-10 production during infection to dampen the host immune response. Thus, it might be possible that other *Yersinia* effector proteins increase the IL-10 transcription if YopM and YopP, both known to regulate cytokine production in the host, are not active for whatever reason. This hypothesis is supported by a study, which states that in the absence of YopM, YopJ promotes virulence of *Y. pseudotuberculosis* in infected mice (Schoberle et al. 2016). By this, the study gives evidences, that the effector proteins are likely to functionally replace each other to sustain bacterial host survival. IL-10 is not only regulated by pathogens to favour their survival, it also can be produced by the infected host itself to prevent exaggerated inflammatory responses which could cause autoimmune pathologies (Hawrylowicz & O'Garra 2005) (Li & He 2004). This regulation may contibute to the enriched IL-10 expression in cells infected with the plasmidless strain WA-C, which is known to be recognized and internalised by macrophages and thus could lead to a exaggerated immune response. In general YopP/YopJ is known to inhibt the NF-κB mediated transcription of proinflammatory cytokines such as TNF, IL-1β and IL-6 in infected macrophages (Ruckdeschel et al. 1997; Monack et al. 1997; Schesser et al. 1998; Orth et al. 1999; Denecker et al. 2002). We confirmed YopP dependent decrease of TNF transcripts in infected primary human macrophages after 1.5 and 6 h of infection (Section VI, 5.3., Figure 40). On the transcriptional level our data indicate that YopM, in contrast to YopP, upregulates TNF expression in primary human macrophages. When both effectors, YopM and YopP, were lacking (WA314ΔYopM/YopP) TNF transcription was decreased in comparison to the TNF expression determined in WA314ΔYopP infected macrophages after 6 h of infection. After 1.5 h of infection no such different expression levels could be observed (Section VI, 5.3., Figure 40). This hints towards the possibility that TNF is likely to be regulated only by YopP in the early phase of infection. At later time points YopMs positive effect on TNF transcription might result in decreased TNF expression in WA314ΔYopM/YopP infected macrophages. Thus, we can state that in the time course of infection genes are differently regulated by the *Yersinia* effectors. Moreover YopM seems to be able to regulate transcription of some cytokines in the opposite direction as YopP. IL-6 and IL-1β expression is induced by YopM as well whereas YopP represses their transcription (Section VI, 5.3.1.,Figure 41,Figure 42). One can conclude from the significant difference in

IL-6 expression between the WA314ΔYopM and WA314ΔYopM/YopP infected macrophages that YopM at later time points contributes greatly to IL-6 repression (Section VI, 5.3.1., Figure 41). Transcriptional analysis of IL-6 expression in *Y. pestis* infected peritoneal macrophages did indicate a mainly YopJ dependent downregulation of IL-6 after two hours of infection (Ratner et al. 2016). Elevated IL-6 levels have also been reported in the sera of *Y. pestis* ΔYopM infected mice compared to IL-6 protein detected in wild type *Y. pestis* infections after 16 h whereas no significant difference could be observed after 1 h (Uittenbogaard et al. 2012). Consequently it is likely that IL-6 expression is downregulated by YopM at later time points of infection. IL-1β protein has been reported to be YopM dependently downregulated in the sera of bone marrow derived macrophages (BMDM) (Ratner et al. 2016; Schoberle et al. 2016). This stands in contrast to our findings, where absence of only YopM led to upregulation of IL-1β in *Y. enterocolitica* WA314 infected primary macrophages (Section VI, 5.1.1., Figure 37B, 5.3.1., Figure 42). Infection with the WA314ΔYopP strain revealed a YopP induced downregulation of IL-1β (Section VI, 5.3.1., Figure 42) which is again opposite to the IL-1β levels detected in the serum of *Yersinis pestis* ΔYopP infected BMDM (Ratner et al. 2016). We observed the highest IL-1β expression in primary macrophages infected with *Y.* enterocolitica WA314ΔYopP/YopM (Section VI, 5.3.1., Figure 42) were most IL-1β was as well detected in the sera of *Y. pestis* infected BMDM (Ratner et al. 2016). Thus, the opposite effects on IL-1β transcription in infected macrophages from YopM or YopJ/P alone, from either *Y. pestis* or *Y. enterocolitica,* seem to result in the same enhanced IL-1β expression when both effectors are missing (Section VI, 5.3.1., Figure 42) (Ratner et al. 2016). This leads to the question whether the other translocated Yops take over the immunoregulatory activities in the absence of YopP and YopM, or if the observed elevated IL-1β -transcription /-secretion is the standard immune reaction of the infected cell to defend the bacteria. However, the different regulation of IL-1β in *Y. pestis* or *Y. enterocolitica* infected macrophages, when either YopM or YopP are lacking, might be explained by different IL-1β regulation. In contrast to YopM of *Y. enterocolitica*, YopM of *Y.pestis* or *Y. pseudotuberculosis* had been shown to repress caspase-1 activation and thereby IL-1β production (Chung et al. 2014; LaRock & Cookson 2012). Irrespective of the speculations that the high transcription level of IL-6 or IL-1β in WA314ΔYopP/YopM infected cells might be explained by the host cell immune response to fight the bacteria, it can be stated that YopMs stimulatory effects on cytokine expression can as well be reversed resulting in an inhibitory effect, if YopP is missing. In summary, we can state that YopM regulates gene expression differently in the presence or absence of YopP. Infections with mutant strains, either lacking YopM or YopP or both effectors, indicated that the YopM mediated increased IL-10, IL-6, IL-1β and TNF expression is opposed regulated when YopP is lacking. For IL-10, IL-6 and IL-1β

YopM´s stimulating effects are reversed to downregulating effects when YopP is not present. This hints towards the fact that in the sum YopM and YopP more effectively manipulate host immune response than each effector by itself. TNF expression in WA314ΔYopP/YopM infected primary macrophages compared to WA314ΔYopP infected macrophages showed that in contrast to the other investigated cytokines, TNF might be different regulated in later time points of infection. Regardless of the underlying mechanism or the regulation of explicit cytokines, it can be stated that most likely only the sum of effectors and their interplay can tightly regulate the host cell immune response to successful establish virulence. Since only infection with *Y. pestis* strains lacking both effectors YopP and YopM lead to attenuated virulence in vivo and either YopM or YopP lacking mutant strains led to comparable virulence as infections with the wild type stain (Ratner et al. 2016) it can be assumed that YopM and YopP mainly contribute to virulence of *Yersinia*. Thus, investigating their interplay in the infected host could elucidate *Yersinia's* immunoregulatory mechanism caused by the translocated effectors to silence the host immune response and is an interesting question to investigate in the future.

VIII References

Aepfelbacher, M., 2004. Modulation of Rho GTPases by type III secretion system translocated effectors of Yersinia. *Reviews of physiology, biochemistry and pharmacology*, 152, pp.65–77.

Aepfelbacher, M. & Heesemann, J., 2001. Modulation of Rho GTPases and the actin cytoskeleton by Yersinia outer proteins (Yops). *Int J Med Microbiol*, 291(4), pp.269–276.

Akira, S. & Takeda, K., 2004. Toll-like receptor signalling. *Nature reviews. Immunology*, 4(7), pp.499–511.

Andersson, K. et al., 1996. YopH of Yersinia pseudotuberculosis interrupts early phosphotyrosine signalling associated with phagocytosis. *Molecular microbiology*, 20(5), pp.1057–69.

Andor, A. et al., 2001. YopE of Yersinia, a GAP for Rho GTPases, selectively modulates Rac-dependent actin structures in endothelial cells. *Cellular Microbiology*, 3(5), pp.301–310.

Andrade, A. et al., 2004. The vaccinia virus-stimulated mitogen-activated protein kinase (MAPK) pathway is required for virus multiplication. *The Biochemical journal*, 381, pp.437–446.

Anjum, R. et al., 2005. The tumor suppressor DAP kinase is a target of RSK-mediated survival signaling. *Current Biology*, 15(19), pp.1762–1767.

Anjum, R. & Blenis, J., 2008. The RSK family of kinases: emerging roles in cellular signalling. *Nature reviews. Molecular cell biology*, 9(10), pp.747–58.

Ariumi, Y. et al., 2007. DDX3 DEAD-box RNA helicase is required for hepatitis C virus RNA replication. *Journal of virology*, 81(24), pp.13922–13926.

Ariumi, Y., 2014. Multiple functions of DDX3 RNA helicase in gene regulation, tumorigenesis, and viral infection. *Frontiers in Genetics*, 5(DEC), pp.1–10.

Auerbuch, V. & Isberg, R.R., 2007. Growth of Yersinia pseudotuberculosis in mice occurs independently of Toll-like receptor 2 expression and induction of interleukin-10. *Infection and immunity*, 75(7), pp.3561–70.

Autenrieth, I. & Flrschlng, R., 1996. Penetration of M cells and destruction of Peyer ' s patches by Yersinia enterocolitica : an uItrastructural and histological study. , 44(June 1995), pp.285–294.

Autenrieth, I.B. et al., 1994. Immune responses to Yersinia enterocolitica in susceptible BALB/c and resistant C57BL/6 mice: An essential role for gamma interferon. *Infection and Immunity*, 62(6), pp.2590–2599.

Autenrieth, I.B. & Heesemann, J., 1992. In vivo neutralization of tumor necrosis factor-alpha

and interferon-gamma abrogates resistance to Yersinia enterocolitica infection in mice. *Medical microbiology and immunology*, 181(6), pp.333–338.

Barbieri, J.T., Riese, M.J. & Aktories, K., 2002. Bacterial toxins that modify the actin cytoskeleton. *Annual review of cell and developmental biology*, 18, pp.315–344.

Barz, C. et al., 2000. The Yersinia Ser/Thr protein kinase YpkA/YopO directly interacts with the small GTPases RhoA and Rac-1. *FEBS Letters*, 482(1-2), pp.139–143.

Bella, J. et al., 2008. The leucine-rich repeat structure. *Cellular and Molecular Life Sciences*, 65(15), pp.2307–2333.

Benabdillah, R. et al., 2004. Identification of a nuclear targeting signal in YopM from Yersinia spp. *Microbial Pathogenesis*, 36(5), pp.247–261.

Bergsbaken, T., Fink, S.L. & Cookson, B.T., 2009. Pyroptosis: host cell death and inflammation. *Nat Rev Microbiol*, 7(2), pp.99–109.

Berlato, C. et al., 2002. Involvement of suppressor of cytokine signaling-3 as a mediator of the inhibitory effects of IL-10 on lipopolysaccharide-induced macrophage activation. *Journal of immunology (Baltimore, Md. : 1950)*, 168, pp.6404–6411.

Berneking, L. et al., 2016. Immunosuppressive Yersinia Effector YopM Binds DEAD Box Helicase DDX3 to Control Ribosomal S6 Kinase in the Nucleus of Host Cells. *PLoS pathogens*, Jun 14;12((doi: 10.1371/journal.ppat.1005660. eCollection 2016.).

Beuscher, H.U. et al., 1995. Bacterial evasion of host immune defense: Yersinia enterocolitica encodes a suppressor for tumor necrosis factor alpha expression. *Infection and Immunity*, 63(4), pp.1270–1277.

Bibel, D. & Chen, T., 1976. Diagnosis of plaque: an analysis of the Yersin-Kitasato controversy. *Bacteriological reviews*, 40(3), pp.633–651.

Bjørbæk, C., Zhao, Y. & Moller, D.E., 1995. Divergent functional roles for p90rsk kinase domains. *Journal of Biological Chemistry*, 270(32), pp.18848–18852.

Black, D.S. & Bliska, J.B., 2000. The RhoGAP activity of the Yersinia pseudotuberculosis cytotoxin YopE is required for antiphagocytic function and virulence. *Molecular Microbiology*, 37(3), pp.515–527.

Bliska, J.B. & Falkow, S., 1992. Bacterial resistance to complement killing mediated by the Ail protein of Yersinia enterocolitica. *Proceedings of the National Academy of Sciences of the United States of America*, 89(April), pp.3561–3565.

Bliska, J.B., Galan, J.E. & Falkow, S., 1993. Signal transduction in the mammalian cell during bacterial attachement and entry. *Cell*, 73(M), pp.903–920.

Bohn, E. & Autenrieth, I.B., 1996. IL-12 is essential for resistance against Yersinia enterocolitica by triggering IFN-gamma production in NK cells and CD4+ T cells. *Journal of immunology (Baltimore, Md. : 1950)*, 156(4), pp.1458–1468.

Bol, G.M., Xie, M. & Raman, V., 2015. DDX3, a potential target for cancer treatment. *Molecular cancer*, 14(1), p.188.

Boland, A. & Cornelis, G.R., 1998. Role of YopP in suppression of tumor necrosis factor alpha release by macrophages during Yersinia infection. *Infection and immunity*, 66(5), pp.1878–84.

Boland, A., Havaux, S. & Cornelis, G.R., 1998. Heterogeneity of the Yersinia YopM protein. *Microbial pathogenesis*, 25(6), pp.343–8.

Bonni, A. et al., 2008. Cell Survival Promoted by the Ras-MAPK Signaling Pathway by Transcription-Dependent and -Independent Mechanisms. , 1358(1999), pp.1–6.

Botlagunta, M. et al., 2008. Oncogenic role of DDX3 in breast cancer biogenesis. *Oncogene*, 27(28), pp.3912–3922.

Bottone, E.J., 1997. Yersinia enterocolitica: The charisma continues. *Clinical Microbiology Reviews*, 10(2), pp.257–276.

Brubaker, R.R., 2003. Interleukin-10 and inhibition of innate immunity to Yersiniae: Roles of Yops and LcrV (V antigen). *Infection and Immunity*, 71(7), pp.3673–3681.

Calautti, E. et al., 2002. Fyn tyrosine kinase is a downstream mediator of Rho/PRK2 function in keratinocyte cell-cell adhesion. *Journal of Cell Biology*, 156(1), pp.137–148.

Carniel, E., Guilvout, I. & Prentice, M., 1996. Characterization of a large chromosomal “high-pathogenicity island” in biotype 1B Yersinia enterocolitica. *Journal of bacteriology*, 178(23), pp.6743–51.

Caruthers, J.M. & McKay, D.B., 2002. Helicase structure and mechanism. *Current Opinion in Structural Biology*, 12(1), pp.123–133.

Chao, C.H. et al., 2006. DDX3, a DEAD box RNA helicase with tumor growth-suppressive property and transcriptional regulation activity of the p21waf1/cip1 promoter, is a candidate tumor suppressor. *Cancer Research*, 66(13), pp.6579–6588.

Chen, R.H. et al., 1996. Phosphorylation of c-Fos at the C-terminus enhances its transforming activity. *Oncogene*, 12(7), pp.1493–1502.

Chen, R.H., Abate, C. & Blenis, J., 1993. Phosphorylation of the c-Fos transrepression domain by mitogen-activated protein kinase and 90-kDa ribosomal S6 kinase. *Proceedings of the National Academy of Sciences of the United States of America*, 90(December), pp.10952–10956.

Chen, R.H., Sarnecki, C. & Blenis, J., 1992. Nuclear localization and regulation of erk- and rsk-encoded protein kinases. *Molecular and cellular biology*, 12(3), pp.915–927.

Chung, L.K. et al., 2014. IQGAP1 is important for activation of caspase-1 in macrophages and is targeted by Yersinia pestis type III effector YopM. *mBio*, 5(4), pp.e01402–14.

Clark, D.E.. C. et al., 2005. The serine/threonine protein kinase, p90 ribosomal S6 kinase, is

an important regulator of prostate cancer cell proliferation. *Cancer Research*, 65(8), pp.3108–3116.

Clark, M.A., Hirst, B.H. & Jepson, M. a., 1998. M-cell surface Beta-1 integrin expression and invasin-mediated targeting of Yersinia pseudotuberculosis to mouse Peyer's patch M cells. *Infection and Immunity*, 66(3), pp.1237–1243.

Cornelis, G.R., 2002. The Yersinia Ysc-Yop "type III" weaponry. *Nature reviews. Molecular cell biology*, 3(10), pp.742–752.

Cornelis, G.R., 2002. Yersinia type III secretion: send in the effectors. *The Journal of Cell Biology*, 158(3), pp.401–408.

Cornelis, G.R., 2002. Yersinia type III secretion: Send in the effectors. *Journal of Cell Biology*, 158(3), pp.401–408.

Cornelis, G.R. & Wolf-Watz, H., 1997. The Yersinia Yop virulon: a bacterial system for subverting eukaryotic cells. *Molecular microbiology*, 23(5), pp.861–7.

Cover, T.L. & Aber, R.C., 1989. Yersinia enterocolitica. *The New England journal of medicine*, 321(1), pp.16–24.

Dalby, K.N. et al., 1998. Identification of regulatory phosphorylation sites in mitogen-activated protein kinase (MAPK)-activated protein kinase-1a/p90(rsk) that are inducible by MAPK. *Journal of Biological Chemistry*, 273(3), pp.1496–1505.

Denecker, G. et al., 2002. Effect of low- and high-virulence Yersinia enterocolitica strains on the inflammatory response of human umbilical vein endothelial cells. *Infection and immunity*, 70(7), pp.3510–20.

Dettori, R. et al., 2009. Regulation of the interaction between protein kinase C-related protein kinase 2 (PRK2) and its upstream kinase, 3-phosphoinositide-dependent protein kinase 1 (PDK1). *Journal of Biological Chemistry*, 284(44), pp.30318–30327.

Dewoody, R.S., Merritt, P.M. & Marketon, M.M., 2013. Regulation of the Yersinia type III secretion system: traffic control. *Frontiers in cellular and infection microbiology*, 3(February), p.4.

Ditton, H.J. et al., 2004. The AZFa gene DBY (DDX3Y) is widely transcribed but the protein is limited to the male germ cells by translation control. *Human Molecular Genetics*, 13(19), pp.2333–2341.

Dong, L.Q. et al., 2000. Phosphorylation of protein kinase N by phosphoinositide-dependent protein kinase-1 mediates insulin signals to the actin cytoskeleton. *Proceedings of the National Academy of Sciences of the United States of America*, 97(10), pp.5089–94.

Donnelly, R.P., Dickensheets, H. & Finbloom, D.S., 1999. The interleukin-10 signal transduction pathway and regulation of gene expression in mononuclear phagocytes. *Journal of interferon & cytokine research : the official journal of the International Society*

for Interferon and Cytokine Research, 19(6), pp.563–573.

Dukuzumuremyi, J.M. et al., 2000. The Yersinia protein kinase A is a host factor inducible RhoA/Rac-binding virulence factor. *The Journal of biological chemistry*, 275(45), pp.35281–90.

Dümmler, B.A. et al., 2005. Functional characterization of human RSK4, a new 90-kDa ribosomal S6 kinase, reveals constitutive activation in most cell types. *Journal of Biological Chemistry*, 280(14), pp.13304–13314.

Erikson, E. & Maller, J.L., 1985. A protein kinase from Xenopus eggs specific for ribosomal protein S6. *Proceedings of the National Academy of Sciences of the United States of America*, 82(3), pp.742–6.

Etienne-Manneville, S. & Hall, A., 2002. Rho GTPases in cell biology. *Nature*, 420(6916), pp.629–635.

Evdokimov, A.G. et al., 2002. Crystal structure of the Yersinia pestis GTPase activator YopE. *Protein science : a publication of the Protein Society*, 11, pp.401–408.

Evdokimov, A.G. et al., 2000. Overproduction, purification, crystallization and preliminary X-ray diffraction analysis of YopM, an essential virulence factor extruded by the plague bacterium Yersinia pestis. *Acta Crystallographica Section D BIOLOGICAL CRYSTALLOGRAPHY*, 56(12), pp.1676–1679.

Evdokimov, A.G. et al., 2001. Unusual molecular architecture of the Yersinia pestis cytotoxin YopM: a leucine-rich repeat protein with the shortest repeating unit. *Journal of molecular biology*, 312(4), pp.807–21.

Felek, S. & Krukonis, E.S., 2008. The Yersinia pestis Ail protein mediates binding and Yop-delivery to host cells required for plague virulence. *Infect Immun*.

Forman, S. et al., 2008. yadBC of Yersinia pestis, a new virulence determinant for bubonic plague. *Infection and Immunity*, 76(2), pp.578–587.

Frödin, M. & Gammeltoft, S., 1999. Role and regulation of 90 kDa ribosomal S6 kinase (RSK) in signal transduction. *Molecular and Cellular Endocrinology*, 151(1-2), pp.65–77.

Fröhlich, A. et al., 2016. DEAD-box RNA helicase DDX3 connects CRM1-dependent nuclear export and translation of the HIV-1 unspliced mRNA through its N-terminal domain. *Biochimica et Biophysica Acta - Gene Regulatory Mechanisms*, 1859(5), pp.719–730.

Gabrielli, B. et al., 1984. Phosphorylation of ribosomal protein S6 and a peptide analogue of S6 by a protease-activated kinase isolated from rat liver. *FEBS Letters*, 175(2), pp.219–226.

Galyov, E.E. et al., 1993. A secreted protein kinase of Yersinia pseudotuberculosis is an indispensable virulence determinant. *Nature*, 361(6414), pp.730–732.

Geissler, R., Golbik, R.P. & Behrens, S.E., 2012. The DEAD-box helicase DDX3 supports

the assembly of functional 80S ribosomes. *Nucleic Acids Research*, 40(11), pp.4998–5011.

Ghoda, L., Lin, X. & Greene, W.C., 1997. The 90-kDa ribosomal S6 kinase (pp90(rsk)) phosphorylates the N-terminal regulatory domain of I??B?? and stimulates its degradation in vitro. *Journal of Biological Chemistry*, 272(34), pp.21281–21288.

Ginty, D.D., Bonni, A. & Greenberg, M.E., 1994. Nerve growth factor activates a Ras-dependent protein kinase that stimulates c-fos transcription via phosphorylation of CREB. *Cell*, 77(5), pp.713–725.

Graham, F.L. et al., 1977. Characteristics of a human cell line transformed by DNA from human adenovirus type 5. *Journal of General Virology*, 36(1), pp.59–72.

Graham, F.L. & Van Der Eb, A.J., 1973. Transformation of rat cells by DNA of human adenovirus 5. *Virology*, 54(2), pp.536–539.

Grahek-Ogden, D. et al., 2007. Outbreak of Yersinia enterocolitica serogroup O:9 infection and processed pork, Norway. *Emerging Infectious Diseases*, 13(5), pp.754–756.

Grant, S.G.N. et al., 1990. Differential plasmid rescue from transgenic mouse DNAs into Escherichia coli methylation-restriction mutants. *Proceedings of the National Academy of Sciences of the United States of America*, 87(12), pp.4645–4649.

Grosdent, N. et al., 2002. Role of Yops and adhesins in resistance of Yersinia enterocolitica to phagocytosis. *Infection and Immunity*, 70(8), pp.4165–4176.

Gru, G., 2005. New insights into the molecular mechanism of interleukin-10- mediated immunosuppression. *Journal of Leukocyte Biology*, 77(January), pp.3–15.

Guan, K.L. & Dixon, J.E., 1990. Protein tyrosine phosphatase activity of an essential virulence determinant in Yersinia. *Science (New York, N.Y.)*, 249(4968), pp.553–6.

Håkansson, S. et al., 1996. The Yersinia YpkA Ser/Thr kinase is translocated and subsequently targeted to the inner surface of the HeLa cell plasma membrane. *Molecular microbiology*, 20(3), pp.593–603.

Hawrylowicz, C.M. & O'Garra, a, 2005. Potential role of interleukin-10-secreting regulatory T cells in allergy and asthma. *Nature reviews. Immunology*, 5(4), pp.271–83.

Heesemann, J. et al., 1993. Virulence of Yersinia enterocolitica is closely associated with siderophore production, expression of an iron-repressible outer membrane polypeptide of 65,000 Da and pesticin sensitivity. *Molecular microbiology*, 8(2), pp.397–408.

Heesemann, J., Algermissen, B. & Laufs, R., 1984. Genetically manipulated virulence of Yersinia enterocolitica. *Infection and Immunity*, 46(1), pp.105–110.

Heesemann, J. & Laufs, R., 1983. Construction of a mobilizable Yersinia enterocolitica virulence plasmid. *Journal of Bacteriology*, 155(2), pp.761–767.

Heise, T. & Dersch, P., 2006. Identification of a domain in Yersinia virulence factor YadA that

is crucial for extracellular matrix-specific cell adhesion and uptake. *Proceedings of the National Academy of Sciences of the United States of America*, 103(9), pp.3375–80.

Hentschke, M. et al., 2010. Yersinia virulence factor YopM induces sustained RSK activation by interfering with dephosphorylation. *PloS one*, 5(10), p.e13165.

Heroven, A.K. & Dersch, P., 2014. Coregulation of host-adapted metabolism and virulence by pathogenic yersiniae. *Frontiers in cellular and infection microbiology*, 4(October), p.146.

Hetzer, C. et al., 2007. Recruitment and activation of RSK2 by HIV-1 Tat. *PLoS ONE*, 2(1).

Hines, J. et al., 2001. Structure-function analysis of Yersinia pestis YopM's interaction with alpha-thrombin to rule on its significance in systemic plague and to model YopM's mechanism of binding host proteins. *Microbial pathogenesis*, 30(4), pp.193–209.

Hoffmann, R. et al., 2004. Transcriptional responses of murine macrophages to infection with Yersinia enterocolitica. *Cellular Microbiology*, 6(4), pp.377–390.

Höfling, S. et al., 2014. Manipulation of pro-inflammatory cytokine production by the bacterial cell-penetrating effector protein YopM is independent of its interaction with host cell kinases RSK1 and PRK2. *Virulence*, 5(6), pp.1–11.

Högbom, M. et al., 2007. Crystal structure of conserved domains 1 and 2 of the human DEAD-box helicase DDX3X in complex with the mononucleotide AMP. *Journal of molecular biology*, 372(1), pp.150–9.

Imada, K. & Leonard, W.J., 2000. The Jak-STAT pathway. *Molecular Immunology*, 37(1-2), pp.1–11.

Isberg, R.R. & Barnes, P., 2001. Subversion of integrins by enteropathogenic Yersinia. *Journal of cell science*, 114(Pt 1), pp.21–28.

Isberg, R.R., Voorhis, D.L. & Falkow, S., 1987. Identification of invasin: a protein that allows enteric bacteria to penetrate cultured mammalian cells. *Cell*, 50(5), pp.769–778.

Jacobi, C.A. et al., 1998. In vitro and in vivo expression studies of yopE from Yersinia enterocolitica using the gfp reporter gene. *Molecular Microbiology*, 30(4), pp.865–882.

Jalava, K. et al., 2006. An outbreak of gastrointestinal illness and erythema nodosum from grated carrots contaminated with *Yersinia pseudotuberculosis*. *The Journal of infectious diseases*, 194(9), pp.1209–1216.

Jenkins, B.J., 2014. Transcriptional Regulation of Pattern Recognition Receptors by JAK/STAT Signaling, and the Implications for Disease Pathogenesis. *Journal of interferon & cytokine research : the official journal of the International Society for Interferon and Cytokine Research*, 00(00), pp.1–9.

Johnston, J.A. & Shea, J.J.O., 2003. Matching SOCS with function. , 4(6), pp.507–509.

Jones, S.W. et al., 1988. A Xenopus ribosomal protein S6 kinase has two apparent kinase

domains that are each similar to distinct protein kinases. *Proceedings of the National Academy of Sciences of the United States of America*, 85(10), pp.3377–81.

Juris, S.J. et al., 2000. A distinctive role for the Yersinia protein kinase: actin binding, kinase activation, and cytoskeleton disruption. *Proceedings of the National Academy of Sciences of the United States of America*, 97(17), pp.9431–6.

Kayser, F.H. et al., 2001. *Medizinische Mikrobiologie* 10th ed., Thieme.

Kerschen, E.J. et al., 2004. The plague virulence protein YopM targets the innate immune response by causing a global depletion of NK cells. *Infection and immunity*, 72(8), pp.4589–602.

Khare, V. & Eckert, K.A., 2002. The proofreading 3′→5′ exonuclease activity of DNA polymerases: a kinetic barrier to translesion DNA synthesis. *Mutation Research/Fundamental and Molecular Mechanisms of Mutagenesis*, 510(1-2), pp.45–54.

Kim, H.M. et al., 2007. Crystal Structure of the TLR4-MD-2 Complex with Bound Endotoxin Antagonist Eritoran. *Cell*, 130(5), pp.906–917.

Kobe, B. & Deisenhofer, J., 1995. Proteins with leucine-rich repeats. *Current Opinion in Structural Biology*, 5(3), pp.409–416.

Kobe, B. & Deisenhofer, J., 1994. The leucine-rich repeat: A versatile binding motif. *Trends in Biochemical Sciences*, 19(10), pp.415–421.

Koch-Nolte, F. et al., 2005. Use of genetic immunization to raise antibodies recognizing toxin-related cell surface ADP-ribosyltransferases in native conformation. In *Cellular Immunology*. pp. 66–71.

Koornhof, H., Smego, R.J. & Nicol, M., 1999. Yersiniosis. II: The pathogenesis of Yersinia infections. *European journal of clinical microbiology & infectious diseases*, 18(2), pp.87–112.

Kopp, P. et al., 2006. The kinesin KIF1C and microtubule plus ends regulate podosome dynamics in macrophages. *Molecular biology of the cell*, 17(6), pp.2811–2823.

Kuang, E. et al., 2008. Activation of p90 ribosomal S6 kinase by ORF45 of Kaposi's sarcoma-associated herpesvirus and its role in viral lytic replication. *Journal of virology*, 82(4), pp.1838–1850.

Laemmli, U.K., 1970. Cleavage of structural proteins during the assembly of the head of bacteriophage T4. *Nature*, 227(5259), pp.680–685.

Lai, M.-C., Lee, Y.-H.W. & Tarn, W.-Y., 2008. The DEAD-box RNA helicase DDX3 associates with export messenger ribonucleoproteins as well as tip-associated protein and participates in translational control. *Molecular biology of the cell*, 19(9), pp.3847–3858.

Lamkanfi, M. & Dixit, V.M., 2011. Modulation of inflammasome pathways by bacterial and viral pathogens. *Journal of immunology (Baltimore, Md. : 1950)*, 187(2), pp.597–602.

LaRock, C.N. & Cookson, B.T., 2012. The Yersinia Virulence Effector YopM Binds Caspase-1 to Arrest Inflammasome Assembly and Processing. *Cell Host & Microbe*, 12(6), pp.799–805.

Laskowski-Arce, M.A. & Orth, K., 2007. The elusive activity of the Yersinia protein kinase A kinase domain is revealed. *Trends in Microbiology*, 15(10), pp.437–440.

Lee, C.S. et al., 2008. Human DDX3 functions in translation and interacts with the translation initiation factor eIF3. *Nucleic Acids Research*, 36(14), pp.4708–4718.

Lee, S.J. et al., 2000. Protein kinase C-related kinase 2 phosphorylates the protein synthesis initiation factor eIF4E in starfish oocytes. *Developmental biology*.

Leung, K.Y., Reisner, B.S. & Straley, S.C., 1990. YopM inhibits platelet aggregation and is necessary for virulence of Yersinia pestis in mice. *Infection and Immunity*, 58(10), pp.3262–3271.

Li, M.C. & He, S.H., 2004. IL-10 and its related cytokines for treatment of inflammatory bowel disease. *World Journal of Gastroenterology*, 10(5), pp.620–625.

Lilo, S., Zheng, Y. & Bliska, J.B., 2008. Caspase-1 activation in macrophages infected with Yersinia pestis KIM requires the type III secretion system effector Yopj. *Infection and Immunity*, 76(9), pp.3911–3923.

Linder, P., 2006. Dead-box proteins: a family affair--active and passive players in RNP-remodeling. *Nucleic acids research*, 34(15), pp.4168–80.

Lindsay, M., 2001. RanBP3 is a cofactor for Crm1-mediated nuclear protein export. *J. Cell Biol.*, 153(7), pp.1391–1402.

Maesaki, R. et al., 1999. The structural basis of Rho effector recognition revealed by the crystal structure of human RhoA complexed with the effector domain of PKN/PRK1. *Molecular cell*, 4(5), pp.793–803.

Marra, A. & Isberg, R.R., 1997. Invasin-dependent and invasin-independent pathways for translocation of Yersinia pseudotuberculosis across the Peyer's patch intestinal epithelium. *Infection and Immunity*, 65(8), pp.3412–3421.

McCoy, M.W. et al., 2010. The C-terminal tail of Yersinia pseudotuberculosis YopM is critical for interacting with RSK1 and for virulence. *Infection and Immunity*, 78(6), pp.2584–2598.

McDonald, C. et al., 2003. The yersinia virulence factor YopM forms a novel protein complex with two cellular kinases. *The Journal of biological chemistry*, 278(20), pp.18514–23.

McPhee, J.B. et al., 2012. Interleukin-10 induction is an important virulence function of the Yersinia pseudotuberculosis type III effector YopM. *Infection and Immunity*, 80(7),

pp.2519–2527.

McPhee, J.B., Mena, P. & Bliska, J.B., 2010. Delineation of regions of the Yersinia YopM protein required for interaction with the RSK1 and PRK2 host kinases and their requirement for interleukin-10 production and virulence. *Infection and immunity*, 78(8), pp.3529–39.

Mengaud, J. et al., 1996. Antibodies to the leucine-rich repeat region of internalin block entry of Listeria monocytogenes into cells expressing E-cadherin. *Infection and Immunity*, 64(12), pp.5430–5433.

Michiels, T. & Cornelis, G.R., 1991. Secretion of hybrid proteins by the Yersinia Yop export system. *Journal of Bacteriology*, 173(5), pp.1677–1685.

Mikula, K.M., Kolodziejczyk, R. & Goldman, A., 2012. Yersinia infection tools-characterization of structure and function of adhesins. *Frontiers in cellular and infection microbiology*, 2, p.169.

Miller, V.L. et al., 2001. Identification of regions of Ail required for the invasion and serum resistance phenotypes. *Molecular Microbiology*, 41(5), pp.1053–1062.

Miller, V.L., Bliska, J.B. & Falkow, S., 1990. Nucleotide sequence of the Yersinia enterocolitica ail gene and characterization of the Ail protein product. *Journal of bacteriology*, 172(2), pp.1062–1069.

Moffatt, B.A. & Studier, F.W., 1987. T7 lysozyme inhibits transcription by T7 RNA polymerase. *Cell*, 49(2), pp.221–227.

Monack, D.M. et al., 1997. Yersinia signals macrophages to undergo apoptosis and YopJ is necessary for this cell death. *Proceedings of the National Academy of Sciences of the United States of America*, 94(19), pp.10385–10390.

Mooney, R.A., 1988. [18] Use of digitonin-permeabilized adipocytes for cAMP studies. In *Initiation and Termination of Cyclic Nucleotide Action*. pp. 193–202.

Mota, L.J. & Cornelis, G.R., 2005. The bacterial injection kit: type III secretion systems. *Annals of medicine*, 37, pp.234–249.

Mukai, H., 2003. The structure and function of PKN, a protein kinase having a catalytic domain homologous to that of PKC. *Journal of Biochemistry*, 133(1), pp.17–27.

Mukai, H. et al., 1996. Translocation of PKN from the cytosol to the nucleus induced by stresses. *Proceedings of the National Academy of Sciences of the United States of America*, 93(19), pp.10195–9.

Mukai, H. & Ono, Y., 1994. A novel protein kinase with leucine zipper-like sequences: its catalytic domain is highly homologous to that of protein kinase C. *Biochemical and biophysical research communications*, 199(2), pp.897–904.

Mullis, K. et al., 1986. Specific enzymatic amplification of DNA in vitro: The polymerase chain

reaction. *Cold Spring Harbor Symposia on Quantitative Biology*, 51(1), pp.263–273.

Murray, P.J., 2006. Understanding and exploiting the endogenous interleukin-10/STAT3-mediated anti-inflammatory response. *Current Opinion in Pharmacology*, 6(II), pp.379–386.

Nakajima, R. & Brubaker, R.R., 1993. Association between virulence of Yersinia pestis and suppression of gamma interferon and tumor necrosis factor alpha. *Infection and Immunity*, 61(1), pp.23–31.

Nakajima, T. et al., 1996. The signal-dependent coactivator CBP is a nuclear target for pp90(RSK). *Cell*, 86(3), pp.465–474.

Niemand, C. et al., 2003. Activation of STAT3 by IL-6 and IL-10 in primary human macrophages is differentially modulated by suppressor of cytokine signaling 3. *Journal of immunology (Baltimore, Md. : 1950)*, 170(6), pp.3263–3272.

Oberhettinger, P. et al., 2011. The sequence of the pYV virulence plasmid from Yersinia enterocolitica strain WA-314 biogroup 1B serotype O:8. *Plasmid*, 65(1), pp.20–24.

Orth, K. et al., 2000. Disruption of signaling by Yersinia effector YopJ, a ubiquitin-like protein protease. *Science*, 290(5496), pp.1594–7.

Orth, K. et al., 1999. Inhibition of the mitogen-activated protein kinase kinase superfamily by a Yersinia effector. *Science*, 285(5435), pp.1920–3.

Owsianka, a M. & Patel, a H., 1999. Hepatitis C virus core protein interacts with a human DEAD box protein DDX3. *Virology*, 257, pp.330–340.

Paczosa, M.K. et al., 2014. Yersinia pseudotuberculosis uses ail and yada to circumvent neutrophils by directing yop translocation during lung infection. *Cellular Microbiology*, 16(2), pp.247–268.

Von Pawel-Rammingen, U. et al., 2000. GAP activity of the Yersinia YopE cytotoxin specifically targets the Rho pathway: A mechanism for disruption of actin microfilament structure. *Molecular Microbiology*, 36, pp.737–748.

Pearce, L.R., Komander, D. & Alessi, D.R., 2010. The nuts and bolts of AGC protein kinases. *Nature reviews. Molecular cell biology*, 11(1), pp.9–22.

Pepe, J.C. et al., 1995. Pathogenesis of defined invasion mutants of Yersinia enterocolitica in a BALB/c mouse model of infection. *Infection and Immunity*, 63(12), pp.4837–4848.

Perry, R.D. & Fetherston, J.D., 1997. Yersinia pestis - Etiologic agent of plague. *Clinical Microbiology Reviews*, 10(1), pp.35–66.

Persson, C. et al., 1999. Localization of the Yersinia PTPase to focal complexes is an important virulence mechanism. *Molecular Microbiology*, 33(4), pp.828–838.

Phan, J. et al., 2003. High-Resolution Structure of the Yersinia pestis Protein Tyrosine Phosphatase YopH in Complex with a Phosphotyrosyl Mimetic-Containing Hexapeptide.

Biochemistry, 42(45), pp.13113–13121.

Philip, N.H. et al., 2014. Caspase-8 mediates caspase-1 processing and innate immune defense in response to bacterial blockade of NF-kappaB and MAPK signaling. *Proc Natl Acad Sci U S A*, 111(20), pp.7385–7390.

Pierson, D.E. & Falkow, S., 1993. The ail gene of Yersinia enterocolitica has a role in the ability of the organism to survive serum killing. *Infection and Immunity*, 61(5), pp.1846–1852.

Pouliot, K. et al., 2007. Evaluation of the role of LcrV/TLR2-mediated immunomodulation in the virulence of Yersinia pestis. *Infect. Immun.*, pp.IAI.01644–06+.

Prehna, G. et al., 2006. Yersinia virulence depends on mimicry of host Rho-family nucleotide dissociation inhibitors. *Cell*, 126(5), pp.869–80.

Pujol, C. & Bliska, J.B., 2005. Turning Yersinia pathogenesis outside in: subversion of macrophage function by intracellular yersiniae. *Clinical immunology (Orlando, Fla.)*, 114(3), pp.216–26.

Ratner, D. et al., 2016. Manipulation of IL-1β and IL-18 production by Yersinia pestis effectors YopJ and YopM and redundant impact on virulence. *Journal of Biological Chemistry*, 1(2), p.jbc.M115.697698.

Rayment, I., Smith, C. & Yount, R.G., 1996. The active site of myosin. *Annual review of physiology*, 58, pp.671–702.

Reithmeier-Rost, D. et al., 2007. The weak interaction of LcrV and TLR2 does not contribute to the virulence of Yersinia pestis. *Microbes and infection / Institut Pasteur*, 9(8), pp.997–1002.

Revell, P.A. & Miller, V.L., 2000. A chromosomally encoded regulator is required for expression of the Yersinia enterocolitica inv gene and for virulence. *Molecular Microbiology*, 35(3), pp.677–685.

Revell, P.A. & Miller, V.L., 2001. Yersinia virulence: More than a plasmid. *FEMS Microbiology Letters*, 205(2), pp.159–164.

Richards, S. a et al., 2001. Characterization of regulatory events associated with membrane targeting of p90 ribosomal S6 kinase 1. *Molecular and cellular biology*, 21(21), pp.7470–7480.

Rigaut, G. et al., 1999. A generic protein purification method for protein complex characterization and proteome exploration. *Nature biotechnology*, 17(10), pp.1030–1032.

Riley, J.K. et al., 1999. Interleukin-10 receptor signaling through the JAK-STAT pathway. Requirement for two distinct receptor-derived signals for anti-inflammatory action. *Journal of Biological Chemistry*, 274(23), pp.16513–16521.

Rocak, S. & Linder, P., 2004. DEAD-box proteins: the driving forces behind RNA metabolism. *Nature reviews. Molecular cell biology*, 5(3), pp.232–241.

Romeo, Y., Zhang, X. & Roux, P.P., 2012. Regulation and function of the RSK family of protein kinases. *Biochemical Journal*, 441(2), pp.553–569.

Roppenser, B. et al., 2009. Yersinia Enterocolitica Differentially Modulates RhoG Activity in Host Cells. *Journal of Cell Science*, 122(5), pp.696–705.

Roux, P.P., Richards, S.A. & Blenis, J., 2003. Phosphorylation of p90 Ribosomal S6 Kinase (RSK) Regulates Extracellular Signal-Regulated Kinase Docking and RSK Activity Phosphorylation of p90 Ribosomal S6 Kinase (RSK) Regulates Extracellular Signal-Regulated Kinase Docking and RSK Activity. , 23(14), pp.4796–4804.

Ruckdeschel, K. et al., 2004. Signaling of apoptosis through TLRs critically involves toll/IL-1 receptor domain-containing adapter inducing IFN-beta, but not MyD88, in bacteria-infected murine macrophages. *Journal of immunology (Baltimore, Md.: 1950)*, 173, pp.3320–3328.

Ruckdeschel, K. et al., 1998. Yersinia enterocolitica impairs activation of transcription factor NF-kappaB: involvement in the induction of programmed cell death and in the suppression of the macrophage tumor necrosis factor alpha production. *The Journal of experimental medicine*, 187(7), pp.1069–1079.

Ruckdeschel, K. et al., 1997. Yersinia enterocolitica promotes deactivation of macrophage mitogen-activated protein kinases extracellular signal-regulated kinase-1/2, p38, and c-Jun NH2-terminal kinase. Correlation with its inhibitory effect on tumor necrosis factor-alpha production. *The Journal of biological chemistry*, 272(25), pp.15920–15927.

Ruckdeschel, K. et al., 2001. Yersinia outer protein P of Yersinia enterocolitica simultaneously blocks the nuclear factor-kappa B pathway and exploits lipopolysaccharide signaling to trigger apoptosis in macrophages. *Journal of immunology (Baltimore, Md : 1950)*, 166(3), pp.1823–1831.

Rumm, A., 2014. *Biochemische und strukturelle Charakterisierung von YopM aus Yersinia enterocolitica WA-314 und dessen Wirts-Zielstrukturen*.

Rüter, C. et al., 2010. A newly identified bacterial cell-penetrating peptide that reduces the transcription of pro-inflammatory cytokines. *Journal of cell science*, 123(Pt 13), pp.2190–2198.

Sahoo, M. et al., 2011. Role of the Inflammasome, IL-1?, and IL-18 in Bacterial Infections. *The Scientific World JOURNAL*, 11, pp.2037–2050.

Sanin, D.E., Prendergast, C.T. & Adrian, P., 2015. IL-10 Production in Macrophages Is Regulated by a TLR-Driven CREB-Mediated Mechanism That Is Linked to Genes Involved in Cell Metabolism.

Sauvonnet, N., Garcia-sanz, J.A., et al., 2002. Regulation of mRNA Expression in Macrophages after Yersinia enterocolitica Infection. *Journal of Biological Chemistry*, 277(28), pp.25133–25142.

Sauvonnet, N., Lambermont, I., et al., 2002. YopH prevents monocyte chemoattractant protein 1 expression in macrophages and T-cell proliferation through inactivation of the phosphatidylinositol 3-kinase pathway. *Molecular Microbiology*, 45(3), pp.805–815.

Saxena, M. & Yeretssian, G., 2014. NOD-like receptors: Master regulators of inflammation and cancer. *Frontiers in Immunology*, 5(JUL), pp.1–16.

Scharnert, J. et al., 2013. Autonomous translocation and intracellular trafficking of the cell-penetrating and immune-suppressive effector protein YopM. *Cellular and Molecular Life Sciences*, 70(24), pp.4809–4823.

Scheffzek, K., Ahmadian, M.R. & Wittinghofer, A., 1998. GTPase-activating proteins: Helping hands to complement an active site. *Trends in Biochemical Sciences*, 23(7), pp.257–262.

Schesser, K. et al., 1998. The yopJ locus is required for Yersinia-mediated inhibition of NF-kappaB activation and cytokine expression: YopJ contains a eukaryotic SH2-like domain that is essential for its repressive activity. *Molecular microbiology*, 28(6), pp.1067–79.

Schoberle, T.J. et al., 2016. Uncovering an Important Role for YopJ in the Inhibition of Caspase-1 in Activated Macrophages and Promoting *Yersinia pseudotuberculosis* Virulence. *Infection and Immunity*, (January), pp.IAI.00843–15.

Schotte, P. et al., 2004. Targeting Rac1 by the Yersinia effector protein YopE inhibits caspase-1-mediated maturation and release of interleukin-1?? *Journal of Biological Chemistry*, 279(24), pp.25134–25142.

Schröder, M., 2010. Human DEAD-box protein 3 has multiple functions in gene regulation and cell cycle control and is a prime target for viral manipulation. *Biochemical Pharmacology*, 79(3), pp.297–306.

Schröder, M., Baran, M. & Bowie, A.G., 2008. Viral targeting of DEAD box protein 3 reveals its role in TBK1/IKKε-mediated IRF activation. *The EMBO Journal*, 27(15), pp.2147–2157.

Schubert, W.D. et al., 2002. Structure of internalin, a major invasion protein of Listeria monocytogenes, in complex with its human receptor E-cadherin. *Cell*, 111(6), pp.825–836.

Schulte, R. et al., 2000. Translocation of Yersinia enterocolitica across reconstituted intestinal epithelial monolayers is triggered by Yersinia invasin binding to ??1 integrins apically expressed on M-like cells. *Cellular Microbiology*, 2(2), pp.173–185.

Schulz, I., 1990. Permeabilizing cells: some methods and applications for the study of

intracellular processes. *Methods in enzymology*, 192(1986), pp.280–300.

Shahbazian, D. et al., 2006. The mTOR/PI3K and MAPK pathways converge on eIF4B to control its phosphorylation and activity. *The EMBO journal*, 25(12), pp.2781–91.

Shao, F. et al., 2002. A Yersinia Effector and a Pseudomonas Avirulence Protein Define a Family of Cysteine Proteases Functioning in Bacterial Pathogenesis. *Cell*, 109(5), pp.575–588.

Shao, F. et al., 2003. Biochemical characterization of the Yersinia YopT protease: cleavage site and recognition elements in Rho GTPases. *Proceedings of the National Academy of Sciences of the United States of America*, 100(3), pp.904–909.

Shibata, H. et al., 1996. Characterization of the interaction between RhoA and the amino-terminal region of PKN. *FEBS Letters*, 385(3), pp.221–224.

Shih, J.-W. et al., 2012. Critical roles of RNA helicase DDX3 and its interactions with eIF4E/PABP1 in stress granule assembly and stress response. *The Biochemical journal*, 441(1), pp.119–29.

Simonet, M. & Falkow, S., 1992. Invasin expression in Yersinia pseudotuberculosis. *Infection and Immunity*, 60(10), pp.4414–4417.

Sing, A. et al., 2005. A hypervariable N-terminal region of Yersinia LcrV determines Toll-like receptor 2-mediated IL-10 induction and mouse virulence. *Proceedings of the National Academy of Sciences of the United States of America*, 102(44), pp.16049–16054.

Singleton, M.R., Dillingham, M.S. & Wigley, D.B., 2007. Structure and mechanism of helicases and nucleic acid translocases. *Annual review of biochemistry*, 76, pp.23–50.

Skrzypek, E. et al., 2003. Application of a Saccharomyces cerevisiae model to study requirements for trafficking of Yersinia pestis YopM in eucaryotic cells. *Infection and Immunity*, 71(2), pp.937–947.

Skrzypek, E., Cowan, C. & Straley, S.C., 1998. Targeting of the Yersinia pestis YopM protein into HeLa cells and intracellular trafficking to the nucleus. *Molecular Microbiology*, 30(5), pp.1051–1065.

Skrzypek, E. & Straley, S.C., 1996. Interaction between Yersinia pestis YopM protein and human alpha-thrombin. *Thrombosis research*, 84(1), pp.33–43.

Smith, C.J. & Osborn, A.M., 2009. Advantages and limitations of quantitative PCR (Q-PCR)-based approaches in microbial ecology. *FEMS Microbiology Ecology*, 67(1), pp.6–20.

Soto-Rifo, R. et al., 2012. DEAD-box protein DDX3 associates with eIF4F to promote translation of selected mRNAs. *The EMBO journal*, 31(18), pp.3745–56.

Soulat, D. et al., 2008. The DEAD-box helicase DDX3X is a critical component of the TANK-binding kinase 1-dependent innate immune response. *The EMBO journal*, 27(15), pp.2135–2146.

Stark, G.R. & Darnell, J.E., 2012. The JAK-STAT pathway at twenty. *Immunity*, 36(4), pp.503–14.

Straley, S.C. et al., 1993. Yops of Yersinia spp. pathogenic for humans. *Infection and Immunity*, 61(8), pp.3105–3110.

Straley, S.C. & Perry, R.D., 1995. Environmental modulation of gene expression and pathogenesis in Yersinia. *Trends in Microbiology*, 3(8), pp.310–317.

Street, M. & Wt, L., 2006. The extracellular signal-regulated kinase : Multiple substrates regulate diverse cellular functions The extracellular signal-regulated kinase : Multiple substrates regulate diverse cellular functions. *Online*, 24(773557635), pp.21–44.

Sun, J.P. et al., 2003. Crystal structure of the Yersinia protein-tyrosine phosphatase YopH complexed with a specific small molecule inhibitor. *Journal of Biological Chemistry*, 278(35), pp.33392–33399.

Sun, M. et al., 2013. DDX3 regulates DNA damage-induced apoptosis and p53 stabilization. *Biochimica et Biophysica Acta - Molecular Cell Research*, 1833(6), pp.1489–1497.

Sweet, M.J. & Hume, D.A., 1996. Endotoxin signal transduction in macrophages. *Journal of leukocyte biology*, 60(1), pp.8–26.

Takahashi, M. et al., 1999. Characterization of a novel giant scaffolding protein, CG-NAP, that anchors multiple signaling enzymes to centrosome and the Golgi apparatus. *Journal of Biological Chemistry*, 274(24), pp.17267–17274.

Takahashi, M. et al., 1998. Proteolytic activation of PKN by caspase-3 or related protease during apoptosis. *Proceedings of the National Academy of Sciences*, 95(20), pp.11566–11571.

Taylor, R.G., Walker, D.C. & McInnes, R.R., 1993. E. coli host strains significantly affect the quality of small scale plasmid DNA preparations used for sequencing. *Nucleic acids research*, 21(7), pp.1677–1678.

Toyotome, T. et al., 2001. Shigella Protein IpaH9.8 Is Secreted from Bacteria within Mammalian Cells and Transported to the Nucleus. *Journal of Biological Chemistry*, 276(34), pp.32071–32079.

Trasak, C. et al., 2007. Yersinia protein kinase YopO is activated by a novel G-actin binding process. *Journal of Biological Chemistry*, 282(4), pp.2268–2277.

Trülzsch, K. et al., 2003. Analysis of chaperone-dependent Yop secretion/translocation and effector function using a mini-virulence plasmid of Yersinia enterocolitica. *International journal of medical microbiology : IJMM*, 293(2-3), pp.167–77.

Trülzsch, K. et al., 2004. Contribution of the major secreted Yops of Yersinia enterocolitica O:8 to pathogenicity in the mouse infection model. *Infection and Immunity*, 72(9), pp.5227–5234.

Tsang, T.M. et al., 2013. Ail proteins of Yersinia pestis and Y. pseudotuberculosis have different cell binding and invasion activities. *PLoS ONE*, 8(12).

Tsang, T.M., Felek, S. & Krukonis, E.S., 2010. Ail binding to fibronectin facilitates Yersinia pestis binding to host cells and yop delivery. *Infection and Immunity*, 78(8), pp.3358–3368.

Uff, S. et al., 2002. Crystal structure of the platelet glycoprotein Ib (alpha) N-terminal domain reveals an unmasking mechanism for receptor activation. *The Journal of biological chemistry*, 277(38), pp.35657–63.

Uittenbogaard, A.M. et al., 2012. Toward a molecular pathogenic pathway for Yersinia pestis YopM. *Frontiers in cellular and infection microbiology*, 2(December), p.155.

Viboud, G.I. & Bliska, J.B., 2005. *YERSINIA* OUTER PROTEINS: Role in Modulation of Host Cell Signaling Responses and Pathogenesis. *Annual Review of Microbiology*, 59(1), pp.69–89.

Vincent, S. & Settleman, J., 1997. The PRK2 kinase is a potential effector target of both Rho and Rac GTPases and regulates actin cytoskeletal organization. *Molecular and cellular biology*, 17(4), pp.2247–2256.

Walker, J.E. et al., 1982. Distantly related sequences in the alpha- and beta-subunits of ATP synthase, myosin, kinases and other ATP-requiring enzymes and a common nucleotide binding fold. *The EMBO Journal*, 1(8), pp.945–951.

Wang, F. et al., 2013. Shigella flexneri T3SS effector IpaH4.5 modulates the host inflammatory response via interaction with NF-κB p65 protein. *Cellular Microbiology*, 15(3), pp.474–485.

Wang, H., Kim, S. & Ryu, W.-S., 2009. DDX3 DEAD-Box RNA helicase inhibits hepatitis B virus reverse transcription by incorporation into nucleocapsids. *Journal of virology*, 83(11), pp.5815–5824.

Weng, D. et al., 2014. Caspase-8 and RIP kinases regulate bacteria-induced innate immune responses and cell death. *Proceedings of the National Academy of Sciences of the United States of America*, 111(20), pp.7391–6.

Williams, L. et al., 2004. Signal transducer and activator of transcription 3 is the dominant mediator of the anti-inflammatory effects of IL-10 in human macrophages. *The Journal of Immunology*, 172(1), pp.567–576.

Wölke, S., Ackermann, N. & Heesemann, J., 2011. The Yersinia enterocolitica type 3 secretion system (T3SS) as toolbox for studying the cell biological effects of bacterial Rho GTPase modulating T3SS effector proteins. *Cellular microbiology*, 13(9), pp.1339–57.

Xing, J., Ginty, D.D. & Greenberg, M.E., 1996. Coupling of the RAS-MAPK pathway to gene

activation by RSK2, a growth factor-regulated CREB kinase. *Science (New York, N.Y.)*, 273(5277), pp.959–963.

Yang, X. et al., 2004. ATF4 is a substrate of RSK2 and an essential regulator of osteoblast biology: Implication for Coffin-Lowry syndrome. *Cell*, 117(3), pp.387–398.

Yao, T. et al., 1999. Suppression of T and B lymphocyte activation by a Yersinia pseudotuberculosis virulence factor, yopH. *The Journal of experimental medicine*, 190(9), pp.1343–50.

Yedavalli, V. et al., 2004. Requirement of DDX3 DEAD Box RNA Helicase for HIV-1 Rev-RRE Export Function. , 119, pp.381–392.

Yoon, S.O. et al., 2008. Ran-Binding Protein 3 Phosphorylation Links the Ras and PI3-Kinase Pathways to Nucleocytoplasmic Transport. *Molecular Cell*, 29(3), pp.362–375.

Yoshimura, A., Naka, T. & Kubo, M., 2007. REVIEWS SOCS proteins , cytokine signalling and immune regulation. , 7(June), pp.454–465.

Zeniou, M. et al., 2002. Expression analysis of RSK gene family members: the RSK2 gene, mutated in Coffin-Lowry syndrome, is prominently expressed in brain structures essential for cognitive function and learning. *Human molecular genetics*, 11(23), pp.2929–2940.

Zhang, Y. et al., 2005. Inhibition of MAPK and NF-kappa B pathways is necessary for rapid apoptosis in macrophages infected with Yersinia. *Journal of immunology (Baltimore, Md. : 1950)*, 174(12), pp.7939–7949.

Zheng, Z. et al., 2015. Bacterial E3 Ubiquitin Ligase IpaH4.5 of Shigella flexneri Targets TBK1 To Dampen the Host Antibacterial Response. *The Journal of Immunology*.

Zumbihl, R. et al., 1999. The cytotoxin YopT of Yersinia enterocolitica induces modification and cellular redistribution of the small GTP-binding protein RhoA. *Journal of Biological Chemistry*, 274(41), pp.29289–29293.

IX List of Tables

X List of Figures

XI List of Abbreviations

°C	degree celsius
µF	microfarrad
µg	microgram
µl	microliter
µm	micrometer
µM	micromolar
A	Adenine
aa	amino acid
ad	add
Ail	Attachment invasion locus
Amp	Ampicillin
ANOVA	Analysis of variance
APS	Ammonium persulfate
ATP	Adenosinetriphosphate
BAD	Bcl-2-associated death promoter protein
bp	base pair
BSA	Bovine Serum Albumin
C	Cytosine
ca.	circa
$CaCl_2$	Calcium cloride
CBP	Calmodulin-Binding Peptide /Protein
Cdc42	Cell division cycle 42 GTP binding protein
cDNA	copy DNA
cm	centimeter
CPP	cell penetrating peptide
CREB	cAMP response element binding protein
CRM1	exportin chromosome region maintenance 1
CTKD	C-terminal kinase domain
DAMPs	danger-associated molecular patterns
dd	double distilled
ddH_2O	distilled water
DDX3	DEAD box helicase 3
DMSO	Dimethyl sulfoxide
DNA	Deoxyribonucleic acid
dNTP	Deoxyribonucleotide triphosphate (dATP, dCTP, dGTP, dTTP)
E. coli	*Escherichia coli*
EDTA	Ethylenediamine tetra-acetic acid
ERK	extracellular signal-regulated kinase
et al.	and others (lat.: „et alteri“)
FAE	the follicle-associated epithelium
Fak	focal adhesion kinase
FCS	Fetal calf serum
FD	fast digest
Flag	peptide sequence DYKDDDDK
FyB	Fyn-binding protein
G	Guanine,
g	gram
g	relative centrifugal force
GAP	GTPase activating protein
GDI	GDP (Guanosine diphosphate) dissociation inhibitors
GDP	Guanosine diphosphate
GEF	guanine nucleotide exchange factor
GFP	Green fluorescent protein
GST	Glutathione-S-transferase
GTP	Guanosine 5'-Triphosphate
h	hour
HA	Hemagglutinin, peptide sequence YPYDVPDYA
HPI	High Pathogenicity Island

HRP	Horseradish peroxidase
IF	Immunofluorescence
IFN	interferon
IKBα	NF-kappa-B inhibitor alpha
IKK	inhibitor of nuclear factor kappa-B kinase
IL	interleukin
IP	Immunoprecipitation
IPTG	Isopropyl β-D-1-thiogalactopyranoside
IQGAP1	IQ Motif Containing GTPase Activating Protein 1
IRAK 1/4	Interleukin-1 receptor-associated kinase 1/4
IRF3	Interferon regulatory factor 3
JAK	Janus kinase
Kan	Kanamycin
kbp	kilo base pairs
kDa	kilo Dalton
KIM	kinase interaction motif
L	liter
LB	Lysogeny broth (Luria-Bertani)
LRRs	leucine-rich-repeats
M	molar
mA	Milli Ampere
MACS	Magnetic Cell Sorting System
MAPK	mitogen activated protein kinase
MAPKK	mitogen activated protein kinase (MAPK) kinase
MCS	Multiple Cloning Site
mg	milligram
min	minute
ml	millilitre
mM	millimolar
mRNA	messenger-RNA
mRNPs	messenger ribonucleoprotein particles
MW	Molecular Weight
Myd88-	Myeloid differentiation primary response gene 88
NF-κB	nuclear factor 'kappa-light-chain-enhancer' of activated B-cells
ng	nanogram
NLRP3	nucleotide-binding domain, leucine-rich-containing family, pyrin domain-containing-3
NLRs	NOD-like receptors
nM	Nanomolar
nt	non-targeting, neurotransmitter
NTKD	N- terminal kinase domain
OD	Optical density
PAGE	Polyacrylamide gel electrophoresis
PAMPs	pathogen-associated molecular patterns
PBS	Phosphate buffered saline
PBST	PBS with Tween-20
PCR	Polymerase chain reaction
PDK	3′-phosphoinositide-dependent kinase
PEI	polyethylenimine
PKN/PRK	Protein Kinase C-Related Kinase
pM	Pikomolar
pmol	Pikomol
PP	Peyer’s patches
PRRs	Pattern recognition receptors
pYV	Yersinia virulence plasmid
Rab	Ras-associated binding
Rac	Ras-related C3 botulinum toxin substrate
Rap1	Ras-related protein 1
RhoA	Ras homolog gene family, member A
RISC	the RNA-induced silencing complex
RLH	RIG-like helicases

RLRs	RIG-I- like receptors
RNA	Ribonucleic acid
ROS	reactive oxygen species
RSK	ribosomal S6 Kinase
RT	room temperature
RT-PCR	Real time PCR
s	second
SBE	signal transducer and activator of transcription (STAT)-binding elements
SBP	Streptavidin-Binding-Peptide / Protein
SD	Standard deviation
SDS	Sodium dodecylsulfate
SEM	Standard error of the mean
ser	serine
SH3	Src-homology 3 domain
siRNA	small interfering RNA
SOCS3	Suppressor of Cytokine Signaling-3
SRE	serum response element
STAT	signal transducer and activator of transcription
T	Thymine
TAE	Tris-acetate-EDTA
TAP	tip associated protein; tandem affinity purification
Taq	*Thermus aquaticus*
TBK1	Tank binding kinase 1
TBS	Tris buffered saline
TBST	TBS with Tween-20
TGF-β	tumor growth factor- β
thr	threonine
TIR	Toll-Interleukin 1 Receptor
TIRAP	Toll-Interleukin 1 Receptor (TIR) Domain Containing Adaptor Protei
TLR	toll like receptor
TNF	tumor necrosis factor
TRAF6	TNF (tumor necrosis factor)receptor associated factor 6
TRIF	Toll/IL-1R domain-containing adapter inducing interferon-β
Tris	Tris-(hydroxymethyl)-aminomethane
TTSS	type three secretion system
U	Uracil
UV	Ultraviolet
V	Volt
Yops	*Yersinia* outer proteins/ *Yersinia* effector proteine
Ω	Ohm

XII Acknowledgements

First, I want to thank everybody from the lab and friends & family, who supported me at all times by providing advices on any kind of problem I encountered or decisions I had to make during my PhD studies. Further, I thank everybody who helped to accomplish this dissertation, either by proofreading or working on the same project and thereby contributed to publish part of this work.

In particular, my thanks goes to Prof. Dr. Martin Aepfelbacher for continuously supporting me in my project and driving for driving it with critical thoughts, questions and discussions in new directions.

Next, I would like to thank Prof. Wolfgang Streit for being my second thesis reviewer and evaluating my disputation. I am especially gratefully to Prof. Dr. Kehr for taking over the guidance of the disputation.

Furthermore, I want to thank PD Dr. Moritz Hentschke, who first evoked my interest on *Yersinia* and passed on his knowledge including different molecular techniques, which were really helpful when challenging new experimental questions. I also thank his laboratory members Anja and Cristina for providing me a warm welcome at the UKE and helping me in word and deed whenever I had a question. I am further grateful, to all past and still present lab members of the Aepfelbacher group for making the lab transfer as easy as possible by quickly introducing me in in the lab practices and of course also supporting me and answering every question I had, even I asked the hundredth time how to order something in the CS system, or annoyed everyone; because I once again lost my pipette or tweezers somewhere in the huge lab. In regards to that I especially thank Franzi and Theresa for their patience because; I guess, I asked them at least 99 times of the 100 about the CS or where to find things and occupied their PC almost as often. Moreover I thank Andi and Manuel for being the calm anchor within the bunch of chickens and Andi additional for his help on YopM cloning, Liane for not only keeping the lab clean and tidy, but also being always ready to support at any time either in organization or expertise, Kirsten for keeping up a good morning spirit (“der Herbst , der Herbst der Herbst ist da …..”☺), Claudia for blotting advices and extensive editorial help and Laura for being a companion in the “YopM- life “ including the ups and downs within the project. I further thank all the “Newbies”, Maren, Aileen, Indra and Jane for bringing new fun and new ideas into the group and partially into the YopM project. In general; I thank the whole department of medical Microbiology, Virology and Hygiene for creating such a nice working environment and additionally for the fun outside the lab including festival visits, Kneipen-quartett-evenings, diverse work and non-work- related

travels, weddings…etc. In particular I would like to thank Kerstin for helping me through any kind of transformation I had to go through and actually generating some of them☺. In regards to that also a huge thanks to Linda and the-Verbindungsbahn-crew for taking care of me. You made thinks a lot easier, not only for my parents. Markos and Kerstin, your soups definitely eased the biggest concerne of my Dad that I will starve within seconds after the operations. Last but not least I thank Marc and my parents for just being the way they are.

XIII Publications

Parts of the content presented here have been published:

Berneking, Laura, Marie Schnapp, Andreas Rumm, Claudia Trasak, Klaus Ruckdeschel, Malik Alawi, Adam Grundhoff

"Immunosuppressive *Yersinia* Effector YopM Binds DEAD-Box Helicase DDX3 to Control Ribosomal S6 Kinase in the Nucleus of Host Cells."

PLoS Pathogens 2016, 12(6):e1005660.doi: 10.1371/journal.ppat.1005660

Posters with parts of the dissertation:

- **2012**
  - **3rd national *Yersinia* Meeting, Tübingen ,2012**
  - **64. DGHM Jahrestagung, Hamburg, 2012**

[1]Moritz Hentschke, [1]Andreas Rumm, [1]Marie Schnapp, [1]Claudia Trasak, [1]Markus Perbandt, [2]Alexey Kikhney and [1]Martin Aepfelbacher

"*Yersinia* enterocolitica YopM interacts with a DEAD-box helicase"

[1)]Institute for Medical Microbiologie, Virology and Hygiene ; University medical center Hamburg Eppendorf (UKE); [2)] EMBL c/o DESY, Hamburg

- **2015**
  - **Annual meeting of the American Society for Biochemistry and Molecular Microbiology (ASBMB), Boston, USA**
  - **1st Center for Structural and System Biology (CSSB) international Symposium, Hamburg**
  - **67. DGHM Jahrestagung, Münster**

[1]Laura Berneking, [1]Marie Schnapp, [1]Claudia Trasak [1,2]Markus Perbandt, [3]Alexey Kikhney, [3]Dmitry Svergun, [4]Friedrich Buck, [2]Cristian Betzel, [1]Moritz Hentschke and [1]Martin Aepfelbacher

"Nuclear export of *Yersinia* effector YopM is mediated by DEAD box helicase DDX3 and regulates phosphorylation of nuclear ribosomal S6 kinase 1"

[1)]Institute for Medical Microbiologie, Virology and Hygiene and [4)]Clinical Chemistry, ; University medical center Hamburg Eppendorf (UKE); Department of Biochemistry [3)] EMBL c/o DESY, Hamburg

- **2016**
  - **Annual meeting of the American Society for Microbiology (ASM), Boston,USA**

[1]Laura Berneking, [1]Marie Schnapp, [1]Claudia Trasak, [2]Malik Alawi,[2]Adam Grundhoff, [3]Alexey G Kikhney, [1,4]Markus Perbandt, [4]Cristian Betzel, [3]Dmitry Svergun, [1]Moritz Hentschke and [1]Martin Aepfelbacher

"MO-649: Immunsuppressive *Yersinia* effector YopM binds DEAD-box helicase DDX3 to control ribosomal S6 kinase in the nucleus of host cells"

[1)]Institute for Medical Microbiologie, Virology and Hygiene, University medical center Hamburg Eppendorf (UKE); Heinrich-Pette-Institut (HPI), Hamburg, Germany 3)European Molecular Biology Laboratory (EMBL), Hamburg, Germany, 4) Institute of Biochemistry and molecular Biology, University of Hamburg, Germany

XIV Declaration on oath

I hereby declare, on oath, that I have written the present dissertation on my own and have not used other than the acknowledged resources and aids.

Hamburg, August 2016

_____

Marie Schnapp